BIOMECHANICS AND FUNCTION OF THE FEMALE RAT URETHRA IN STRESS URINARY INCONTINENCE INDUCED BY BIRTH TRAUMA

by

Rachelle Prantil-Baun

B.S., Syracuse University, 2000

M.S., University of Pittsburgh, 2004

Submitted to the Graduate Faculty of

School of Engineering in partial fulfillment

of the requirements for the degree of

Doctor of Philosophy

University of Pittsburgh

2007

UNIVERSITY OF PITTSBURGH

SCHOOL OF ENGINEERING

This dissertation was presented

by

Rachelle Prantil-Baun

It was defended on

July 12, 2007

and approved by

William C. de Groat, Ph.D., Department of Pharmacology

Naoki Yoshimura, Ph.D., Departments of Urology and Pharmacology

Michael B. Chancellor, M.D., Department of Urology

Richard Debski, Ph.D., Department of Bioengineering

Harvey S. Borovetz, Ph.D., Department of Bioengineering

Dissertation Director: David A. Vorp, Ph.D., Departments of Bioengineering and Surgery

BIOMECHANICS AND FUNCTION OF THE FEMALE RAT URETHRA IN STRESS URINARY INCONTINENCE INDUCED BY BIRTH TRAUMA

Rachelle Prantil-Baun, M.S.

University of Pittsburgh, 2007

Stress urinary incontinence (SUI) is common in women after vaginal delivery (VD) in childbirth or pelvic trauma, and may be associated with altered biomechanical or functional properties of the urethra. The goal of this dissertation was to identify biomechanical and functional changes in the urethra in a rat model of VD, as well as to understand the role of longitudinal smooth muscle in the healthy urethra.

Female rat urethras were isolated in a rat model of SUI induced by VD. Controls were urethras isolated from normal rats. Our established ex vivo urethral testing system was utilized for biomechanical and pharmacological assessments. In this system, outer diameter was measured via a laser micrometer, and recorded along with applied intraluminal pressure to a computer. Urethral thickness was assessed histologically.

Biomechancial properties of the urethra were markedly altered by VD for the baseline, passive (via calcium chelation), and active (stimulation via adrenergic and muscarinic receptors) states, most notably in the proximal urethra. Additionally, contractile responses to phenylephrine and bethanechol increased in the proximal urethra in VD rats compared to controls. There were also changes in the VD mid urethral segment. Functional and biomechanical parameters indicated that basal activity was increased for VD compared to controls in the middle segment, as well as adrenergic active biomechanical properties at low strains. VD impaired the basal tone distally compared to controls, but this was the only difference observed.

VD urethras had evidence of altered collagen and elastin. Additionally, there was a lack of PGP 9.5, tyrosine hydroxylase, and vesicular acetylcholine transferase in the urethras of the VD group. This suggests that VD has mechanically damaging effects on urethral innervation.

Finally, the role of the longitudinal smooth muscle in the urethra was further clarified via a modified urethral testing system. Circumferential and longitudinal testing of baseline, active, and passive urethral properties and function supported the idea that the role of longitudinally-oriented components of the urethra was to lengthen or shorten to enable the circumferential muscle to fully contract and shorten as required.

In summary, this dissertation has provided evidence of damaged muscular, neural, and matrix components of the urethra associated with VD. The combination of these changes may contribute to SUI induced by VD.

TABLE OF CONTENTS

LIST OF TABLES

LIST OF FIGURES

PREFACE

Almost seven years ago, I entered engineering graduate school as a young and inexperienced, smart and determined, unconfident and nervous student. I was not sure what I was going to accomplish at graduate school or how far I was going to go. Overall, this journey has changed me both personally and professionally. My father once told me that getting your Ph.D. is only 10% intelligence and 90% guts. Of course, my father was right. Still, even with courage, it helps to be surrounded by supporting mentors and researchers that have both outstanding careers and character. It is these people that have made all of the difference in my academic career.

First, I would like to thank my academic and research advisors at Syracuse University, Karen Hiiemae, Ph.D., and Jeremy L. Gilbert, Ph.D. They were the first to believe in me and my abilities as a scientist and engineer. They loved their research so much that they served as an inspiration for me. I would also like to thank the Dean Lori Hunter, Ph.D, my mentor in the Academic Excellence Workshop (AEW). She encouraged me to shoot for the stars.

At the University of Pittsburgh, I have been blessed with the opportunity to work with world renowned scientists and doctors. First, I would like to thank Dr. Naoki Yoshimura. Working in the urology research laboratory for a year has taught me how a lab should truly be run. Never have I worked in such a friendly, knowledgeable, and efficient environment. I would also like to thank Dr. Michael Chancellor. He is one of the most well known and ground-breaking urologists, and he has always been there to successfully bridge the bench top to the

clinic. Dr. William de Groat has been a pivotal person in my scientific development. Working with him has been an honor, and it was an opportunity of a lifetime. He has always motivated me to think outside of the box, and for this, I cannot thank him enough. Dr. de Groat, Dr. Chancellor and Dr. Yoshimura are wonderful people. The amount of joy that people (including myself) have working for them speaks volumes. They are what makes Pittsburgh urological research a truly exciting experience.

If only I could think of one thing that Vickie Erickson was not good at. I send my deepest appreciation for all of your knowledge, which encompasses biology, chemistry, neuroscience, computers, life and so much more. Vickie, you have always been there for me through thick and thin, and I will miss you. I would also like to thank the members of my committee, they have also been very important to the success of my thesis, Richard E. Debski, Ph.D. and Harvey S. Borovetz, Ph.D. The biomechanical expertise that you provided was essential. I would also like to thank my advisor, David Vorp, Ph.D. for providing me with the remarkable opportunity to work with urology and pharmacology for my thesis project.

There have been so many people in the last seven years that have played a role in my success. I would like to thank Stephanie Kute, Ph.D. and Ron Jankowski, Ph.D. for guiding me through my first year in the lab. I would also like to thank Donna Haworth, Robert Dulabon, Scott Vanepps, Timothy Maul, Dr. Minoru Miyazato, Dr. Yasuhiro Kaiho, and Dr. Kazumasa Torimoto. All of you are great researchers and it has been a pleasure working with all of you. I would also like to thank my mom and dad for their everlasting support. I am so lucky to have parents like you.

Last, but certainly not least, I would like to send my deepest gratitude to my husband, Matt Baun. Matt, you have been there in every way possible. From staying with me during those

late experiments to brainstorming with me for new design ideas, you have made this experience worth it. I am very anxious for us to take the next step in our lives.

1.0 INTRODUCTION

Stress urinary incontinence (SUI), which is defined as involuntary loss of urine secondary to an increase in abdominal pressure (during events such as sneezing, coughing, laughing or other stress conditions), in the absence of bladder contractions, is very common in 33.9% of women over the age of 40 [1, 2]. This condition is embarrassing and may lead to social isolation. Unfortunately, there are few effective non-surgical and pharmacological therapies. Although the etiology of SUI seems to be multi-factorial, vaginal child birth has been demonstrated to have a major impact on the development of SUI [3]. Thus, the study examining the effects of simulated birth trauma on urethral function in animals could lead to our better understanding of the pathophysiology of the urethral continence mechanisms underlying SUI and the development of better treatment modalities of SUI.

1.1 LOWER URINARY TRACT: ANATOMY AND PHYSIOLOGY

There are two major components of the lower urinary tract: the bladder and the urethra (Figure 1.1), which work together to store and periodically release urine, otherwise known as voiding or micturition. The bladder and the urethra have opposing function. Essentially, the bladder acts as a reservoir for storing urine and as a pump for expelling it during voiding. The urethra remains closed during bladder filling and provides a tight mucosal seal to maintain continence.

During micturition, the urethra dilates in a controlled manner to provide a conduit for the urinary stream. Furthermore, the bladder and urethra must coordinate to prevent leakage during bladder filling by generating urethral pressures exceeding that of bladder (a.k.a. intravesical) pressure [4]. The following sections describe, in detail, the innervation, anatomical structure, and reflex control of the bladder and the urethra.

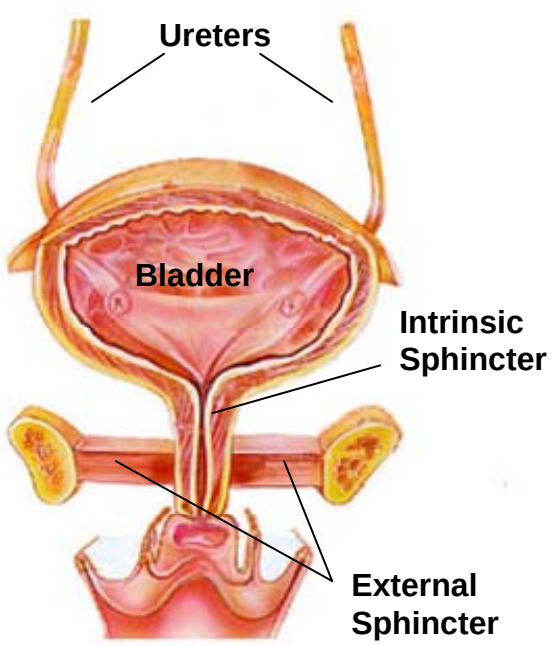

Figure 1.1 A depiction of the lower urinary tract anatomy

1.1.1 Urinary Bladder

The bladder is mainly comprised of smooth muscle cells, arranged cirumferentially (middle layer) and longitudinally (outer layer). The bladder has a water tight lining consisting of several layers of epithelial cells, known as transitional epithelium [5]. The bladder cans anatomically be divided into 2 separate segments: the detrusor, or bladder body, and the trigone, or bladder base. The detrusor is primarily responsible for the contraction that expels urine from the body during micutrition. The trigone functionally continues to the bladder neck and urethra to serve as a continence unit of the bladder base, contracting and closing the outlet.

The bladder is innervated by two kinds of autonomic nerves; namely parasympathetic and sympathetic nerves (**Figure 1.4**). Parasympathetic (cholinergic) efferent input emerges from the

sacral segment of the spinal cord and is carried through the pelvic nerve. Sympathetic (noradrenergic) efferent input is mainly carried through the hypogasteric nerve which arises from the inferior mesenteric ganglion where sympathetic preganglionic nerves originating from the thoracic-lumbar region of the spinal cord make synaptic connections [6]. The pelvic and hypogastric nerve also convey afferent activity from the bladder to the spinal cord via small myelinated A-delta fibers and unmyelinated C-fibers [5].

1.1.2 The Urethra

The urethra is comprised of several layers depicted in **Figure 1.2**. The first layer is known as the urothelium, which lines the entire length of the urethra and is continuous with the bladder urothelium. The second layer is the

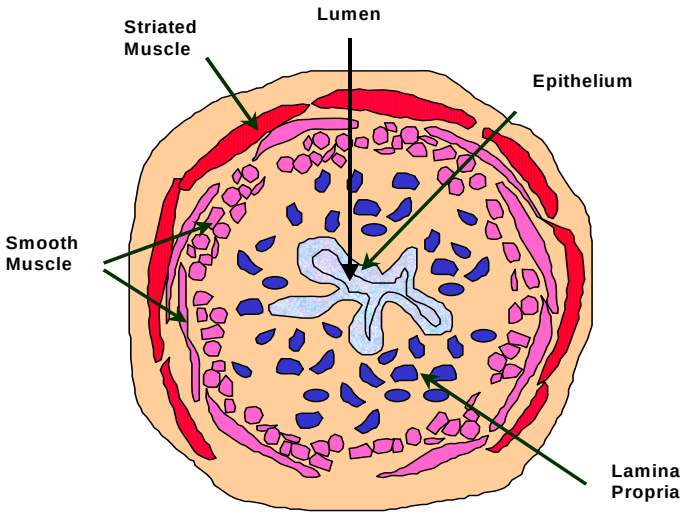

Figure 1.2 A schematic of a urethral cross section

lamina propria, which comprises the submucosal layer. This layer is populated with blood vessels and a small amount of longitudinally arranged elastic fibers. The lamina propria likely fills with blood via its vasculature helping to maintain a mucosal seal along with the high urethral pressures generated by contraction of the smooth and striated muscle [7, 8]. Under the lamina propria follows the smooth muscle layer including both circumferential and longitudinal

orientations. Urethral smooth muscle in both orientations generates a spontaneous intrinsic tone which is highest in the mid urethral segment [7].

The urethral outer layer is composed of striated muscle. During urine storage the striated sphincter is active and becomes activated during increases in abdominal pressure. Although it is commonly thought that the smooth muscle provides involuntary sphincteric support and striated muscle is voluntary, it has been established that circumferentially-arranged smooth and striated sphincter muscles contribute to the the bulk of the permanent luminal closure force, while the role of longitudinal smooth muscle is less clear [9].

The urethra has three types of innervation: sympathetic, parasympathetic, and somatic (**Figure 1.4**). The hypograstric nerve innervates the proximal urethra/bladder neck region and provides sympathetic innervation, which releases norepinephrine to stimulates β-adrenergic receptors to relax trigone smooth muscle and α_1-adrenergic receptors to contract proximal urethral smooth muscle. Parasympathetic innervation, which travels in the pelvic nerve arises from pre-ganglionic neurons in the sacral spinal segments. Parasympathetic pre-ganglionic axons make connections with postganglionic neurons in the pelvic plexus which, in turn, innervate circular and longitudinal smooth muscle. This parasympathetic input is cholinergic, as well as peptidergic and nitrergic [10, 11]. During voiding, parasympathetic input releases acetylcholine which stimulates muscarinic receptors on bladder smooth muscle for contraction, and releases nitric oxide for urethral smooth muscle relaxation [12]. The striated EUS is innervated by somatic motor neurons via the pudendal nerve (from sacral segments, S1-S4) providing voluntary and involuntary control.

1.1.3 Extracellular matrix of the urethra

Collagen is the primary extra cellular matrix component of the urethra, as seen in the histological cross section of the mid urethral segment (**Figure 1.3**). The collagen fibers run circumferentially on a global level, but are randomly oriented locally. Collagen is present in the urethra to provide stiffness and structural support [13].

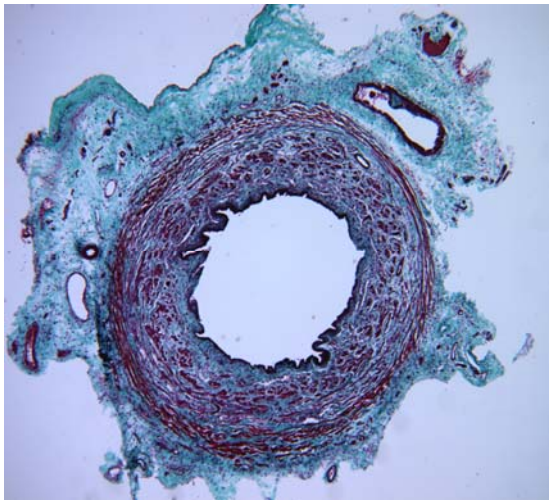

Figure 1.3 Lillie's modified Masson's trichrome stain of the middle segment of a urethra (green=collagen, red=muscle)

On the other hand, elastic fibers (generally called elastin) are less abundant in the urethra, and, subsequently, their role is less clear. Elastic fibers run longitudinally along the urethra suburothelial region. Additionally, elastic fibers are localized around the smooth and striated muscle fibers. One histological study concluded that due to scarcity of elastic fibers in the urethra and the predominately longitudinal orientation, elastic fibers do not play a major contributory factor to urinary incontinence [14]. Another study found elastic fibers in the proximal, middle, and distal urethral segments, populating the submucosa and longitudinal smooth muscle layers. This study confirmed the previous findings that elastic fibers were

longitudinally positioned, running the entire length of the urethra; however, the elastic fibers aid the longitudinal muscle in urethral shortening during voiding and provide passive recoil for the longitudinal muscles returning the urethra to its original length [15].

1.1.4 Storage and micturition reflex mechanisms

Neural control of the bladder and urethra is regulated by involuntary and voluntary central neural mechanisms for both smooth and striated muscle. Urine storage is regulated by two reflexes: the somatic storage reflex and the sympathetic storage reflex. The somatic storage reflex is rapid and is initiated in response to a sudden increase in bladder pressure, activating the striated urethral muscle. The reflex pathway consists of myelinated Aδ afferent nerve fibers in the pelvic nerve which enter the sacral spinal cord and then send signals via the lateral pathway to Onufrowicz's nucleus. Next, the axons from the motor neurons pass along the pudendal nerve and release acetylcholine, stimulating the nicotinic cholinergic receptors for striated muscle contraction.

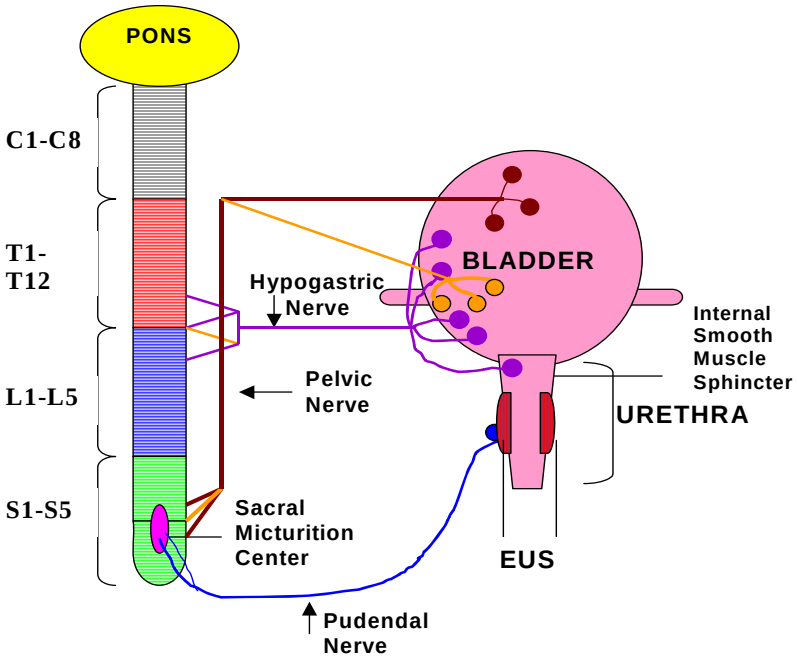

Figure 1.4 A schematic of lower urinary tract innervation

The sympathetic storage reflex is initiated as the bladder distends. Cell bodies in the sacral dorsal root ganglia (DRG) correspond to the bladder stretch receptors sending afferent signals along myelinated Aδ fibers in the pelvic nerve to the spinal cord. Following this path to the upper lumbar cord, efferent sympathetic preganglionic neurons (L1-L3) project fibers along the inferior splanchnic nerve to the inferior mesenteric ganglion (IMG) and proceed along the hypogastric nerve to the pelvic plexus and/or the urethra, where postganglionic nerve terminals release norepinephrine (NE), a non selective adrenergic agonist. This facilitates storage by stimulation of the β3 adrenergic receptors for detrusor relaxation and α_1-adrenergic receptors for urethral smooth muscle contraction. This reflex is relatively slow and has a latency of almost 60 ms in cats [11].

Micturition reflexes are responsible for bladder emptying. There are two types: supraspinal reflex (Aδ fiber bladder afferent to bladder efferent path) and spinal reflex (C-fiber bladder afferent to bladder efferent reflex). The suparaspinal reflex is responsible for mediating micturition under normal conditions and has an action time of 120 ms. Initiated by stretch receptors in the detrusor, the signal traverses the pelvic nerve via Aδ myelinated fibers to reach the spinal cord. These primary afferent fibers send signals along Lissauer's tract in order to contact second order neurons in the dorsal horn of the sacral spinal cord. These neurons project to the neurons in the brain periaqueductal gray which, in turn, activates the neurons in the pontine micturition center (PMC). Neurons in the PMC target directly to the bladder preganglionic neurons located in the lateral band region of the sacral parasympathetic nucleus. The efferent signals are sent along the pelvic nerve to activate pelvic parasympathetic postganglionic neurons in the pelvic plexus resulting in a release of acetylcholine which induces

a bladder contraction by stimulating muscarinic receptors, M_2 and M_3, in detrusor smooth muscle. Parasympathetic postganglionic nerves also release nitric oxide which relaxes urethral smooth muscle.

Another spinal reflex is initiated via unmyelinated C-fibers and organized in the sacral spinal cord. The parasympathetic efferent pathways of this reflex seem to be the same as those of the supraspinal reflex. This reflex is more apparent in animals after spinal cord injury and/or outlet obstruction and has a latency on average of 90 ms.

1.2 NEURO-PHARMACOLOGICAL ASSESSMENT OF THE NORMAL URETHRA

Neuro-pharmacological assessment of the urethra is comprised largely of in vivo studies. Ex vivo studies include urethral strip studies, with few exceptions [16]. For in vivo studies, animal models have been utilized to assess continence and voiding reflex mechanisms. Ex vivo studies have focused on the physiology of the normal urethra, attempting to understand the role of neural and muscular components.

1.2.1 Continence mechanisms of the urethra: in vivo studies

With a micro-tip transducer catheter in the proximal and middle segments of the urethra, the role of bladder-urethral reflexes in the continence mechanisms was studied by Kamo et al.[17]. Intra-urethral pressures were assessed simultaneously with increasing intravesical pressure. It was discovered that abrupt bladder pressure increases induced a middle urethra contraction in the

absence of reflex bladder contractions (i.e. acute spinal cord transection, T8-T9). Additionally, transection of either the pudendal, iliococcygeous/pubococcygeous, or the hypogastric nerves significantly reduced urethral responses that were activated by bladder pressure increases. These results indicated that elevation of intravesical pressures can elicit a pelvic afferent nerve mediated continence reflex in the middle segment of the urethra, which is mediated by activation of sympathetic and somatic nerves. Thus, it was concluded that this type of innervation may contribute to the prevention of SUI via the storage reflex mechanism.

Micro-tip transducer catheter studies were also conducted using a rat model of birth trauma [18]. This experiment revealed in decreased intra-urethral pressures in the middle urethral segment induced by increasing intravesical pressures during sneezing in the birth trauma group. There were no changes in the proximal urethra response.

1.2.2 Continence mechanisms of the urethra: ex vivo studies

Since the urethra has complex innervation and structure, there is much dispute about the role of the muscular and neural components. For example, it has been determined that circular smooth muscle in the proximal urethra is dominated by α1 adrenergic receptors mediated contractions while longitudinal smooth muscle of the proximal urethra is dominated by muscarinic receptor mediated contractions [19]. One study attempted to utilize ex vivo bath studies and histology to assess the influence of muscle type on functional responses in the female rat urethra [10]. Urethras were isolated into circular or longitudinal strips and placed into an ex vivo physiologic bath. Circular strips responded to electrical field stimulation (EFS) of short pulse durations (0.005-0.8 ms) with rapid contractions which were unaffected by alpha or beta adrenergic blocking agents or by muscarinic antagonists and low calcium conditions. Circular contractions

were affected by depolarizing striated muscle relaxants (e.g., succinylcholine) and tetrodotoxin (blocking agent for voltage gated sodium channels), indicating this response is due to striated muscle contraction activated by pudendal nerve stimulation. Responses of longitudinal preparations were less dramatic. EFS induced a relaxation followed by a contraction, although responses were much more attenuated than that of circular preparations. However, both preparations dynamically responded to calcitonin gene-related peptide (cGRP, a sensory activating agent) by significantly relaxing. Other agents, such as substance P (a neuropeptide released by sensory afferents) and 5-hydroxytryptamine (5 HT, a serotinergic agonist), induced a contraction on both circular and longitudinal preparations. These results indicated that tonically active circular muscle may play a role in the maintaining urethra closure; whereas, the striated muscle may be more responsible for rapid contractions, i.e. during sudden changes in abdominal pressure. The longitudinal smooth muscle may be a continuation of bladder smooth muscle, and, if activated simultaneously with the bladder, may create a shortening of the urethra, decreasing urethral resistance during voiding [10].

To further elucidate the role of longitudinal and circular muscle in the urethra, Arner et al. [20] assessed shortening velocity of each orientation of muscle. They observed that tonic contractions were typical of circular smooth muscle, and phasic contractions were common in longitudinal urethral smooth muscle. Additionally, the longitudinal smooth muscle had a larger maximal shortening velocity compared to circular muscle, meaning that longitudinal smooth muscle has a faster rate of tension development in activated muscle.

The striated urethral component is thought to be the most important contributor to maintaining continence [21]. Unfortunately, due to the delicate nature of urethral striated muscle and the complexity of urethral tissue, there have been few ex vivo studies. Most methods rely

upon anatomical characterization with histological methods [7]. Pharmacological and physiological experiments have confirmed that striated muscle receives pudendal innervation. Striated muscle has been characterized with electrical field stimulation (EFS) by a rapid contraction in response to neural stimulation, which can be abolished with tetrodotoxin, a voltage gated sodium channel blocker. Finally, there is controversial evidence that nitrergic mechanisms are present in urethral striated muscle. Garcia-Pascual A. et al. [22] isolated female sheep urethras, dissected mucosal and smooth muscle layers from the tissue, and pretreated the muscle strips with D-tubocurarine to induce a blockade of nicotinic receptors at the neuromuscular junction. Results for these functional studies showed that nitric oxide synthase inhibitors (NOSi) have an effect on EFS on the striated urethral sphincter. Ng-nitro-L-arginine, a NOSi, had a weak effect on contractile responses, but N omega propyl-L-arginine, a neuronal NOSi, had a potent effect on the striated musculature. Additionally, neuronal nitric oxide synthase (nNOS) was distinguished on intramural nerves and striated fibers.

1.2.3 Spontaneous myogenic tone

The regulation of smooth muscle contraction is achieved with two primary methods: agonists binding to receptors or an influx of Ca^{+2} through voltage/receptor operated calcium channels. Briefly, these actions, in conjunction with other steps detailed in Figure 1.5, lead to elevated intracellular calcium, which interacts with calmodulin activating myosin light chain (MLC) kinase. MLC kinase phosphorylates the light chain of myosin and cross-bridge cycling occurs with actin; thereby, initiating smooth muscle cell shortening [23].

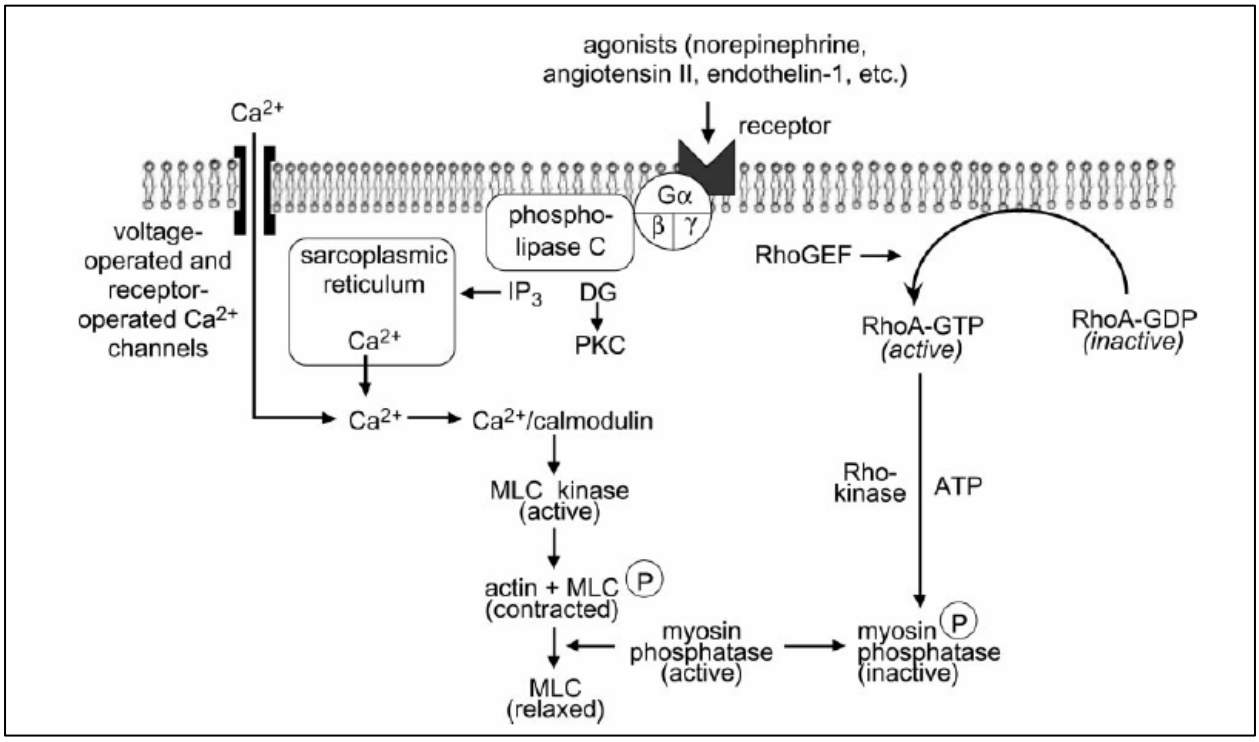

Figure 1.5 A depiction of the mechanism involved with the regulation of smooth muscle contraction [23]. Briefly, an agonist binds to a receptor which increased phospholipase C activity through coupling with a G protein. This event produces two second messengers: diacylglycerol (DG) and inositol 1,4,5-triphosphate (IP_3). IP_3 binds to receptors on the sarcoplasmic reticulum, releasing activator calcium. Activator calcium binds to calmodulin activating MLC kinase which phophorylates the light chain of myosin. Actin and myosin form cross bridges, producing a smooth muscle contraction.

Many smooth muscles exhibit spontaneous contractile activity (i.e., in the absence of ion or agonist stimulation), which is comprised of two types, slow waves and spikes [24]. Lower urinary tract smooth muscle exhibits spontaneous myogenic activity during the filling phase. More specifically, this type of tone contributes significantly to urethral closure pressures during the storage phase. The role of this spontaneous activity appears to be to permit the individual muscle bundles to adjust their length in response to filling [25].

Spontaneous tone in the urethra may be calcium dependent resulting from a sustained elevation of intracellular calcium brought on by ion pumps or channels in the cell membrane [25,

26]. Additionally, studies performed on female pig proximal urethra suggest that Rho-GTPase and ROK are obligatory for generating urethral tone [26]. This was made obvious by complete smooth muscle relaxation in the presence of a ROK inhibitor, Y-27632, and inhibition of urethral tone with Toxin B from C. difficile. ROK and Rho-GTPases act to inhibit myosin phosphatase which promotes smooth muscle relaxation (Figure 1.5).

Another source of spontaneous activity in the urethra may be interstitial cells of Cajal (ICC's). These cells have been localized in rabbit urethral smooth muscle [27]. These cells were branched, non-contractile, and thin, not spindle shaped as smooth muscle cells. ICC's had many mitochondria, intermediate filaments, and stain positive for vimentin. ICC's are also strongly dependent on intracellular calcium, indicated by the abolished activity in calcium free solutions [28]. Furthermore, calcium regulation via ryanodine receptors and IP_3 sensitive stores contribute to spontaneous activity generated by ICC's. Additionally, ICC's are thought to mediate neuronal nitric oxide response. Still, this has yet to be proven for cholinergic transmission [28].

1.3 STRESS URINARY INCONTINENCE

SUI is the involuntary leakage of urine on effort, exertion, sneezing or coughing. This definition describes a symptom rather than a diagnosis and suggests an abnormality without an explanation of the cause of incontinence or whether it is treatable [29]. Much of this is due to the lack of knowledge of the pathology of SUI.

In the year 2000, Americans spent millions of dollars trying to cope with this type of urinary dysfunction [30]. SUI is the most common type of urinary incontinence in women. However, the number of sufferers has been underreported, which can be attributed to a diverse number of definitions and diagnoses. Ultimately, this contributes to the limitations of therapies and aid for urinary dysfunction.

1.3.1 Characterization and diagnosis of SUI

Two major contributing factors of SUI are childbirth and pelvic trauma. These factors may cause anatomical changes in the lower urinary tract and pelvic floor. Two common anatomical changes are loss of bladder neck/ proximal urethra support, also known as urethra hypermobility and intrinsic sphincter deficiency (ISD) from neuro-muscular compromise [31].

Much of the damage from childbirth is largely attributed to impaired muscular, neural, and connective tissue components. Muscle damage factors into the loss of bladder neck support, as well as the ability to provide the pressure needed to supersede intravesical pressures during a 'stress' episode. Connective tissue could be frayed during vaginal birth; thus, eliminating support from the anterior vaginal wall and pubic symphysis via the pubo-urethral ligament. Finally, neural damage interrupts the storage reflex mechanisms (discussed in Section 1.1.4) needed for bladder-urethra coordination [29, 31].

ISD and urethral hypermobility are not easily diagnosed. Although it is largely ignored for diagnosing SUI, the gold standard of diagnoses is a combination of functional and structural studies by means of video-urodynamics. Urethral hypermobililty is determined with an imaging technique, such as lateral stress cystography or a Q-tip test. However, ISD is more difficult to

diagnose and requires extensive urodynamics. One technique to identify ISD and urethral hypermobility is urethral pressure profile (UPP). This involves pulling a pressure-sensing catheter through the urethra with a constant speed from bladder orifice to distal urethral meatus. Intra-urethral pressure is measured along the entire length of the urethra. Parameters obtained are maximum urethral pressure (MUP) and maximum urethral closure pressure (MUCP; bladder pressure subtracted from MUP). If MUCP is less than 20 cm H2O, this can be correlated with ISD. Patients are asked to cough during UPP measurement. During the cough, the ratio between intraurethral pressure and intravesical pressure can be determined; thus providing the pressure transmission ratio (PTR; expressed as a percentage). If the PTR is low, urethral hypermobility may be present. Still, the cutoff points for PTR and MUCP are not validated and cannot be applied to individual cases. Therefore, this method is not entirely reliable for diagnosing SUI [32].

1.3.2 Current treatments and therapies for SUI

Patients who suffer from SUI require one of two categories of treatment: non-invasive and surgically invasive therapies [33]. Non invasive therapies are mostly conservative and are the initial treatment of choice. These therapies are commonly lifestyle changes including, weight loss, and appropriate exercises. Patients are taught pelvic floor physiotherapy (i.e. Kegel exercises) or intra vaginal devices, such as cones. Kegel exercises have been effective in up to 65% of the cases [34]. One problem with these exercises is that women tend to perform them incorrectly. To solve this problem, a vaginal cone can be inserted into the vagina while the pelvic floor is contracted to prevent slippage; thereby, making the exercises more effective.

Where conservative management fails to achieve continence, surgery is an alternative. Slings, a piece of material that is placed beneath the urethra for support, are a common invasive solution for patients with SUI. Slings have been composed of autologous (patient's own fascia), cadaveric, or synthetic materials. Placement of slings is mostly at the bladder neck and the mid urethral wall (e.g. tension-free tape). While there has been a high percentage of success with invasive surgery, the results do not last more than two years, and complications of infection, erosion, and damage to other organs may occur [35].

More recent therapies have proven to be successful. Injection of a bulking agent, such as bovine collagen, into the submucosal or periurethral tissues is both effective and minimally invasive. Still, agents that include collagen are only temporary since it degrades over time, and injection therapy is not as effective as surgery [36].

Pharmacotherapies available for SUI are limited. Sympathetic adrenergic input to urethral smooth muscle is abundant, unlike the bladder. There is physiological, pharmacological, and molecular evidence that suggests that α_{1A} adrenergic receptors are responsible for mediating the effects of norepiniphrine on urethral tone and pressure [37]. However, clinical assessment of non selective α adrenergic receptor agonists have proven to have only limited efficacy. This has been attributed to cardiovascular side effects.

A more recent pharmacotherapy of interest is serotonin and norepinephrine reuptake inhibitors. These agents play an important role in the inhibition of the micturition reflex, mediated through 5-hydroxytryptaymine, 5-HT receptors. 5-HT and serotonergic receptors are located in the spinal cord around the lower urinary tract reflex pathways [38]. These receptors are involved in increasing bladder capacity and sphincter muscle activity. This may work through a dual mechanism of norepinephrine action on the urethra and serotonergic mechanisms

[37, 38]. While this drug shows promise, patients discontinue use of these agents (such as Duloxetine) due to nauseous side effects.

1.4 PAST RESEARCH IN SUI: *IN VIVO* STUDIES

Therapies and treatments are lacking for SUI due to the lack of scientific research on the pathology of the lower urinary tract. This is due, in part, to the lack of animal models available, as well as inefficient devices to measure lower urinary tract changes.

1.4.1 In vivo studies

To fully investigate and develop treatments for SUI, an understanding of the normal and patho-physiological control of continence is required. It is important to acknowledge that animal models resemble the human lower urinary tract both anatomically and physiologically. The rat animal model does have certain differences in the lower urinary tract from the human. These differences deal with neurotransmitter mechanisms and coordination of voiding [39]. Pharmacological evidence suggests that adenosine triphosphate (ATP) may be the neurotransmitter responsible for atropine resistant bladder contractions. As for the coordination of voiding, lower urinary tract of the adult rat displays reflex bladder contractions that occur simultaneously with rhythmic contractions of the external urethral sphincter (EUS). Rhythmic contractions of the EUS have been thought to promote voiding by creating a urethral pumping action or by inducing temporary isometric contractions of the bladder [40]. However, this

characteristic of voiding is reminiscent of detrusor sphincter dyssynergia in humans, which is the loss of coordination of the bladder and its outlet, observed following lesions of the spinal cord.

The animal models that have been created to mimic SUI have been produced in the female rat. These models include pudendal nerve crush or transection, vaginal distension or birth trauma, electro cauterization, and urethrolysis [40]. The following sections will discuss each model in detail.

1.4.1.1 Pudendal nerve crush and transection

The pudendal nerve innervates the external urethral striated sphincter muscle, which is thought to be the major contributor to the continence mechanism. Therefore, damage to this nerve disrupts striated sphincter activity [41], producing a model of SUI. Pudendal nerve crush involves pressing the sheath of the pudendal nerve with forceps two times for 30 seconds. This nerve damage causes an increase in urinary frequency and a significant decrease in leak point pressure [42]. Histology of pudendal nerve crush shows less nerve fascicles near the external urethral striated sphincter (EUS).

Pudendal nerve transection is more commonly employed than the nerve crush model. In the transection model, ilium and sacrum bones are separated followed by pudendal nerve isolation bilaterally. A length of 2-3 mm of the nerve is removed in order to prevent regeneration [43]. After 6 weeks post-transection, abnormal urodynamic measurements include a decrease in bladder contraction amplitude and voided volume, an increase in bladder contraction duration and residual urine, and changes in EUS activity [43]. Structural changes after pudendal nerve transection include decreased volume of striated muscle fibers. The smooth muscle volume remained constant [44].

While models involving pudendal nerve injury produce the desired symptoms common to SUI, this model has some limitations. Innervation of the lower urinary tract is complex. Although much of the credit for continence has been given to the EUS, the smooth muscle component of the urethra, which is largely ignored, also contributes to continence. Thus, other types of innervation (e.g., sympathetic or parasympathetic) are ignored in this model. Another problem with this model is variability of volume of the balloon and duration of VD. Such inconsistencies make it difficult to compare results between investigators.

1.4.1.2 Vaginal Distension

Efforts have been made to simulate birth trauma in female animal models in order to assess the mechanically damaging effects on the lower urinary tract. A hallmark study by Lin and colleagues [45] developed a rat model of simulated birth trauma in order to understand the functional, anatomic, and histological effects of vaginal trauma on adjacent structures and urinary continence mechanisms. The bladder was emptied by an intra-urethral catheter. A foley catheter (12F) was inserted into the vagina and the balloon was inflated to 2 ml for 4 hours in virgin female rats. Marked cellular swelling and interstitial edema in the levator ani muscle progressively increased for 24 hours after vaginal distension. After four weeks, muscular necrosis occurred in the urethral wall. Additionally, vaginal distension was correlated with a significant loss in ganglia, as well as c-Fos immunoreactivity in spinal segments, L6-S1, indicating nerve injury.

This group combined simulation of delivery (vaginal distension) with pregnancy (i.e. pregnant rats) to examine the effects of both delivery and pregnancy on the innervation of the lower urinary tract [46]. There were two groups in this study: rats that delivered pups and rats that were vaginally distended post-delivery. In this particular case, vaginal distension (or

ballooning) consisted of a 22F foley catheter filled with 5 ml of distilled water. The catheter was placed intra-vaginally and inflated for 3 hours. This simulated the pressure of a large fetus on the pelvic floor and lower urinary tract during a prolonged second stage of labor. Leak point pressure (LPP) measurements indicated incontinence occurring in 29.2% of the rats and this increased to 58.3% after ballooning, suggesting that injury to the continence mechanism is minor compared to that of a prolonged labor. Immunohistochemical results conveyed a decreased expression of neuronal nitric oxide synthase (nNOS) in the bladder neck/ proximal urethra region, a complete loss of sympathetic post-junctional urethral innervation (as indicated by tyrosine hydroxylase immunohistochemistry) in circular smooth muscle of the outer mid-urethra, and altered sensory nerve fibers, as indicated by CGRP, neuropeptide Y (NPY), and vasoactive intestinal peptide (VIP) immunohistochemistry.

Cannon et al. [47] assessed the effects of vaginal distension on urethral anatomy and function with several versions of this rat model: prolonged vaginal distension, balloon inflation for 1 hour, and intermittent vaginal distension, 5 cycles of balloon inflation for 5 minutes. Four days after vaginal distension, leak point pressures and histological assessment was performed. These results agree with the previous studies in which vaginal distension causes a lower LPP, and, furthermore, prolonged vaginal distension worsened this measure. Histological results indicated severe damage to the skeletal muscle layer. Investigators proposed that this may be due to ischemic injury or pudendal nerve damage.

While this model for SUI helps researchers to isolate mechanical damage from hormonal effects during labor, there are limitations that should be taken into consideration. Rats are quadrupeds and have a lax abdominal wall. Thus, the external pressure in a rat does not result in

similar forces to that of humans. Additionally, the protocol for vaginal distension is different for each study. This makes it difficult to compare results for LPP and histology.

1.4.1.3 Electrocauterization and urethrolysis

Electrocauterization and urethrolysis serves as a model for ISD resulting from pelvic surgery [48, 49]. The animal is anesthetized and surrounding tissues lateral to the middle urethra are cauterized with a fine tip, high temperature cauternary unit. Cauterization was extended from 1 cm from the bladder neck to the mid urethra. Cystometry revealed that the intercontraction intervals for the bladder were not different between the cauterized and control groups. LPP's were significantly lower in the cauterized group compared to that of controls. Finally, histological assessment revealed damage to the striated sphincter in the mid urethra, as well as lack of nerve fibers, as indicated by protein gene product 9.5 (PGP 9.5) staining [48].

1.4.2 Extracellular matrix changes in SUI

Few studies have concentrated on altered components of the extracellular matrix in women with SUI. Furthermore, few studies involving animal models have quantified any change to collagen or elastic fiber components. Falconer et al. [50] assessed the periurethral tissue from biopsies of continent and stress incontinent women. Results indicated an increase in collagen I and III in the tissue from incontinent women. Overall, there was a 30% increase in collagen concentration, as well as an increase in collagen crosslinking, in women with SUI. However, results from various groups are conflicting. Other studies using the same experimental set up have found opposite results [51].

An extensive study using a rat model assessed the effects of childbirth (i.e. simulated birth trauma via vaginal distenstion) on mid urethral extracellular matrix components [52]. Collagen and elastin were quantified from histological cross sections from the middle urethral segment. Results suggested an increase in collagen concentration after vaginal distension, but there was a decrease in the quantity of muscle fibers. Finally, the amount of elastic fibers increased after vaginal distension.

1.5 IMPORTANCE OF BIOMECHANICS IN THE LOWER URINARY TRACT

Due to its organization (recall **Section 1.1.2**), the urethra possesses both active and passive functions that provide it with the ability to open and close during micturition. The smooth and striated muscle components of the urethra provide a sphincter mechanism – i.e., an active urethral closure pressure – to maintain continence. On the other hand, the collagen and elastin within the tissue plays a passive role, keeping the urethra from over-distending during increases in bladder pressure and voiding, and helping the urethra to return to a closed state after voiding. These active and passive traits can be altered in various disease states or with mechanical damage to innervation, and this, in turn, can lead to functional changes in SUI. The ability to properly characterize fundamental mechanical tissue properties can be powerful in understanding normal tissue function, as well as elucidating underlying causes of dysfunction and its pathological progression. Surprisingly, little is known about the normal biomechanical properties of the urethra and the changes that may contribute to SUI. More detailed mechanical

contributions of the urethra are not yet available, and this may be attributed to the lack of appropriate experimental techniques to perform these investigations.

1.5.1 Biomechanical studies of the urethra

Despite the principal mechanical function of the urethra, in particular the generation of controlled resistance for the prevention of urine leakage from the bladder, its biomechanical properties have remained largely unexplored. Few studies attempting to characterize the mechanical behavior of this tissue have been performed to date [53-59]. Furthermore, the anatomical basis for previous physiological studies remains unclear. To date, the mechanical contributions of the various components of the urethra have yet to be clearly defined [13]. Ex vivo experimental systems have assisted in the development of working hypotheses regarding the initiation and progression of vascular diseases [60]. Application of such experimental devices, modified specifically for the study of the urethra, could yield similar success. Such information is essential to adequately address currently unresolved issues pertaining to the consequences of damage to individual structures of the urethra, and ultimately the potential clinical effectiveness of therapeutic strategies to address such damage.

1.5.1.1 In vivo studies

There have been a few studies that have made efforts to understand how the urethra is affected biomechanically by SUI. Urethral dilatation studies were developed utilizing a probe developed for the measurement of intraurethral pressure and cross-sectional area incorporated into a balloon catheter for inflation and deflation. A stress relaxation parameter (i.e., dissipation of energy over time) was used to evaluate women suffering SUI symptoms. The outcome

indicated that women with SUI had an increased stress relaxation parameter for the proximal urethra/bladder neck signifying muscle and connective tissue damage in this portion [58, 59, 61]. Limitations of this study involve the size of balloon catheters and infusion rates used; these could have variable affects on the biomechanical data.

A similar study was performed to evaluate the influence of drugs on urethral resistance to dilatation in healthy females [62]. Measurements were carried out at the bladder neck (proximal urethra), middle urethra, and the external meatus (distal urethra). The effects of adrenergic and muscarinic agonists and antagonists were assessed, as well as pudendal nerve blockade. Results indicated no significant differences in response to any treatments with the exception of the bilateral pudendal nerve blockade. In this case, there was a significant reduction of the stress relaxation parameter at the bladder neck and in the middle urethra.

Yalla et al. [63] employed an animal model for static pressure – urethral outer diameter measurements to evaluate the effects of urethral myotomy and tissue death on urethral stiffness in a canine model. Results showed that compliance increased for damaged or dead urethral tissue compared to controls. Unfortunately, this study was only able to provide qualitative observations, instead of quantitative biomechanical data.

1.5.1.2 Ex vivo studies

There has only been one ex vivo study of an intact urethra (and none in relation SUI). While in vivo studies are practical for identifying the mechanical role of the urethra plus the contribution of surrounding structures (i.e. pelvic floor, anterior vaginal wall, etc.) in maintaining continence, an ex vivo model can more carefully delineate the role of each urethral component on the pathogenic urethra. Mayo and Hinman [54] utilized an ex vivo model to evaluate the mechanical anisotropy of the female dog urethra. A urethral segment was excised and placed

into a bath and static pressure was applied while urethral length was measured. Conclusions suggested that circumferential muscle and connective tissue fibers are more dominant than longitudinal ones, indicating mechanical anisotropy. Although this is the first ex vivo study, the entire organ was not examined, and the in vivo length was not maintained allowing urethral shrinkage once excised.

The modified ex vivo system described by Jankowski et al.[64] was used to assess the pressure and outer diameter relationships of the healthy urethra in a rat model. Incremental compliance and beta stiffness was calculated from pressure and outer diameter recordings, and the histological thickness was assessed for incremental elastic moduli calculations, which is a measure of stiffness, and for derived stress-strain relationships. Due to the heterogeneous nature of the urethra, proximal, middle, and distal segments were assessed separately and compared.

Results indicated a proximal to distal compliance gradient, where the proximal was significantly more compliant than that of the middle and distal segments. This was prevalent at low pressure ranges; on the other hand, high pressure compliance values were similar for all three segments. This study also distinguished a smooth muscle basal tone that was present in the urethra, which was indicated by the significant difference between the baseline (no chemical agents are added to inhibit or activate muscular components; Section1.2.3) and passive (muscular components are inhibited by calcium chelation agents) pressure-diameter curves.

Following this study, efforts were made to characterize the smooth and striated musculature of the middle urethra [65]. Utilizing chemical stimulation of striated and smooth muscle contraction, results demonstrated that the active striated component was one third as effective as the active smooth muscle component for resisting deformation. These results conflict with other studies [66] and require further research.

1.5.2 Hypotheses and specific aims

While efforts have been made to understand the affects of SUI urethra with in vivo and ex vivo strip studies, a more detailed understanding of the pathophysiologic mechanisms employing a controlled experimental environment is needed. Utilizing our current ex-vivo whole mount technique pressure-diameter data will be generated to assess biomechanical changes. The functional aspect of the urethra was studied by pharmacological manipulation in order to understand the physiological effects of SUI induced by vaginal distension (VD) on the smooth muscle instrinsic sphincter. Additionally, the system was modified in order to evaluate the longitudinal component. Finally, both pharmacological and biomechanical data were compared to micro-structural and immunohistochemical analyses. The specific aims and corresponding hypotheses are as follows:

Specific Aim 1: To assess changes in regional biomechanical properties in the baseline and passive states of the female rat urethra in a model of simulated birth trauma in order to identify changes in SUI and correlate these changes to structural changes in muscle, collagen, and elastin.

Hypothesis 1: SUI induced by VD yields measurable changes to the regional biomechanical properties of the urethra, as well as its structural components. More specifically, compared to healthy controls and based on preliminary data, SUI induced by vaginal distension increases compliance (decrease beta stiffness and incremental elastic modulus).

Specific Aim 2: To assess the role of collagen and elastin in a healthy urethra

Hypothesis 2: Elastin will contribute to the distensibility of the urethra, and collagen will contribute to urethral stiffness.

Specific Aim 3: To assess changes to the urethral smooth muscle response to an α_1 adrenergic agonist in SUI induced by VD, and to assess the presence sympathetic nerve fibers of the urethra histologically.

Hypothesis 3: Pathophysiological changes to pharmacologically-induced adrenergic smooth muscle contraction can be identified in SUI compared to healthy controls. SUI induced by VD will cause a decrease in muscular contraction, as well as resistance against increasing intralumenal pressures. This will be reflected by a lack of sympathetic nerve fibers in urethras from VD.

Specific Aim 4: To assess changes to the urethral smooth muscle response to a cholinergic muscarinic agonist in SUI induced by VD, and to further assess the presence cholinergic nerve fibers of the urethra histologically.

Hypothesis 4: Pathophysiological changes to pharmacologically-induced cholinergic muscarinic smooth muscle contraction can be identified in SUI compared to healthy controls. SUI induced by VD will cause a decrease in muscular contraction, as well as resistance against increasing intralumenal pressures. This will be reflected by a lack of cholinergic nerve fibers in urethras from VD.

Additionally, the role of the longitudinal urethral smooth muscle remains controversial. Developing some insight to its coexisting function with urethral circumferential smooth muscle would help to understand the urethras activity in both voiding and storage. Furthermore, this knowledge would help us to better understand how the urethra is damaged in lower urinary tract

disorders. Of course, the tools are limited to study this aspect of the urethra. Therefore, the final aim and hypothesis are:

.

Specific Aim 5: To modify the existing experimental system for evaluation of the role of longitudinally-oriented smooth muscle in pharmacologically induced urethral contraction and relaxation

Hypothesis 5: The biomechanical properties of the longitudinal and circumferential smooth muscle can be assessed simultaneously.

In order to understand the role of the urethra in maintaining urine storage, an analyses of its biomechanical and pharmacological properties will provide insight into the contribution of the various urethral components (i.e., longitudinally- and circumferentially- oriented smooth muscle, extracellular matrix components, and neural components) to normal function and how these components are distorted in SUI caused by birth trauma. Distinguishing the components most influenced, it may help to provide more efficient therapies for SUI.

Table 1.1 (below) details the experiments that were assessed for both the functional and biomechanical experiments, as well as the number of specimens tested. Each experiment was carried out to address each specific aim and hypothesis addressed previously.

Table 1.1 The number of studies performed to address specific aims and hypotheses. Collagen compromised experiments (sodium hydroxide treated) and elastase treated experiments were not performed using VD urethras.

FUNCTIONAL EXPERIMENTS	**CONTROL (N)**	**VD (N)**
Phenylephrine (PE)	8	9
Bethanechol (BE)	7	7
BIOMECHANICAL EXPERIMENTS	**CONTROL (N)**	**VD (N)**
Baseline	8	8
Passive	16	8
Active-PE	8	8
Active-BE	7	7
Collagen compromised	4	0
Elastase treated	4	0
Longitudinal assessment	6	6

2.0 BASELINE AND PASSIVE URETHRAL BIOMECHANICS OF THE FEMALE RAT URETHRA IN SUI

2.1 SIGNIFICANCE OF URETHRAL BIOMECHANICS

While many investigators have attempted to assess the biomechanics of the urethra in general, little knowledge remains about the urethral basal muscle tone and the passive matrix. It has been well established that in female urethras the non-neural component is a significant contributor to the high pressure region of the urethral pressure profile [67]. However, since this study was performed in vivo, it is difficult to distinguish the basal tone in the urethra from that of the the passive matrix. To date, it has not been established whether or not these two components act separately.

Applying techniques and theories in biomechanics can provide insight to the different contributions of each. Performing physiologic ex vivo studies with a female urethra, we could assess the activity of basal tone separately from the passive state. Furthermore, we also assessed the effects of SUI induced by VD on these two components.

2.2 METHODS

2.2.1 Animals

Adult female Sprague-Dawley rats used in this study (200-250 g, approximately 8-12 weeks of age; Harlan; Scottdale, PA) and were housed at the University of Pittsburgh under the supervision of the Department of Laboratory Animal Resources. The policies and procedures of the animal laboratory are in accordance with those detailed in the guide for the 'Care and Use of Laboratory Animals' published by the US Department of Health and Human Services. Procedural protocols were approved by the University of Pittsburgh Institutional Animal Care and Use Committee.

2.2.2 Vaginal distension model

Animals underwent vaginal distension using a protocol developed by Kamo et al. [18]. In short, female rats were anesthetized with halothane (2%) via oxygen gas. A 5 ml 10 Fr Rusch-Foley balloon catheter was inserted into the vagina, and the balloon catheter was inflated with 4 ml of water. Distension was maintained for 2-4 hours. Four days after vaginal distension, rats were then assessed for leak point pressure (LPP) in order to determine if the model was complete (i.e., that animals were truly experiencing true stress urinary incontinence). More specifically, if the rat had an LPP less than 34 cm H_20, the rat model was considered complete [18].

2.2.3 Urethral isolation

An intraluminal catheter (PE 50 Intramedic tubing; Becton Dickinson, 42741, Sparks,MD) was inserted into the urethra, and an incision at the apex of the bladder dome was made. The bladder was ligated with silk suture (4-0), as well as the distal external meatus. The ureters were tied off to prevent leakage and to serve as anatomical landmarks for in vivo length measurement, which were made prior to excision. The maintenance of in vivo length is important since the tissue is anisotropic [54], and it is important to account for animal-to-animal variability; thus, all tests were standardized by keeping each specimen at its own specific in vivo length. For transport, urethral specimens were then placed in cold media 199 (due to its wide use in organ culture) that was previously bubbled for a minimum of 30 minutes with a gas mixture (95% oxygen and 5 % carbon dioxide) in order to prevent anoxia.

2.2.4 Ex vivo system

Experiments were two systems were utilized. Although pressure application and outer diameter measurements remained unchanged, the specimen box was modified for urethral testing, as opposed to its previous use for vascular assessment [64, 68]. The following sections will discuss the development of both systems in detail.

2.2.4.1 Static pressure

Modifications of pressure application were required in order to accommodate the urethral tissue as discussed previously [64]. Several constraints were considered when making alterations. First, the system previously had been used to mimic the arterial environment, in

which high pressures of 100 mmHg or more were applied, as well as the application of pulsatility. For the rat urethra, the maximum pressure experienced is approximately 25 mmHg [69], and flow is not continuous, but intermittent (i.e., during time of voiding). Thus, it would be appropriate to apply hydrostatic pressure and ignore the effects of flow.

In these studies, increases in static pressure were applied and held constant. Since the system was closed, it was appropriate to measure pressure at one location, and this was achieved just proximally to the urethra (Figure 2.1) via a strain gauge transducer (model #: PX272, Baxter Healthcare Co., Deerfield, IL), which output a signal to a pressure monitor (Model #: 90603A, Space Labs Inc.). Static pressure was achieved by clamping off the distal tubing (i.e., the outlflow for the urethra) and by utilizing a hydrostatic pressure reservoir attached to a graduated ring stand. The reservoir was manually displaced to graduations, which were calibrated by a water manometer for intervals of 2 mmHg using the pressure height relation (equation 2.1).

$$p - p_o = \Delta p = \rho g h \qquad \textbf{(2.1)}$$

where g is the gravitational constant and p_o is the previous pressure. The range of intralumenal pressure applied was 0 to 20 mmHg. As for the working fluid, which was cell culture media, the density was taken as $\rho=\rho_{H2O}= 1000\ {}^{kg}\!/_{m^3}$. For an incremental change (Δp) in pressure of 2mmHg, the change in height (h) necessary was calculated from equation 2.1 as 2.7 cm. The applied intraluminal pressure was continuously recorded via computer. *Error propogation analysis of pressure measurements is discussed in detail in Appendix B, subsection B.1.*

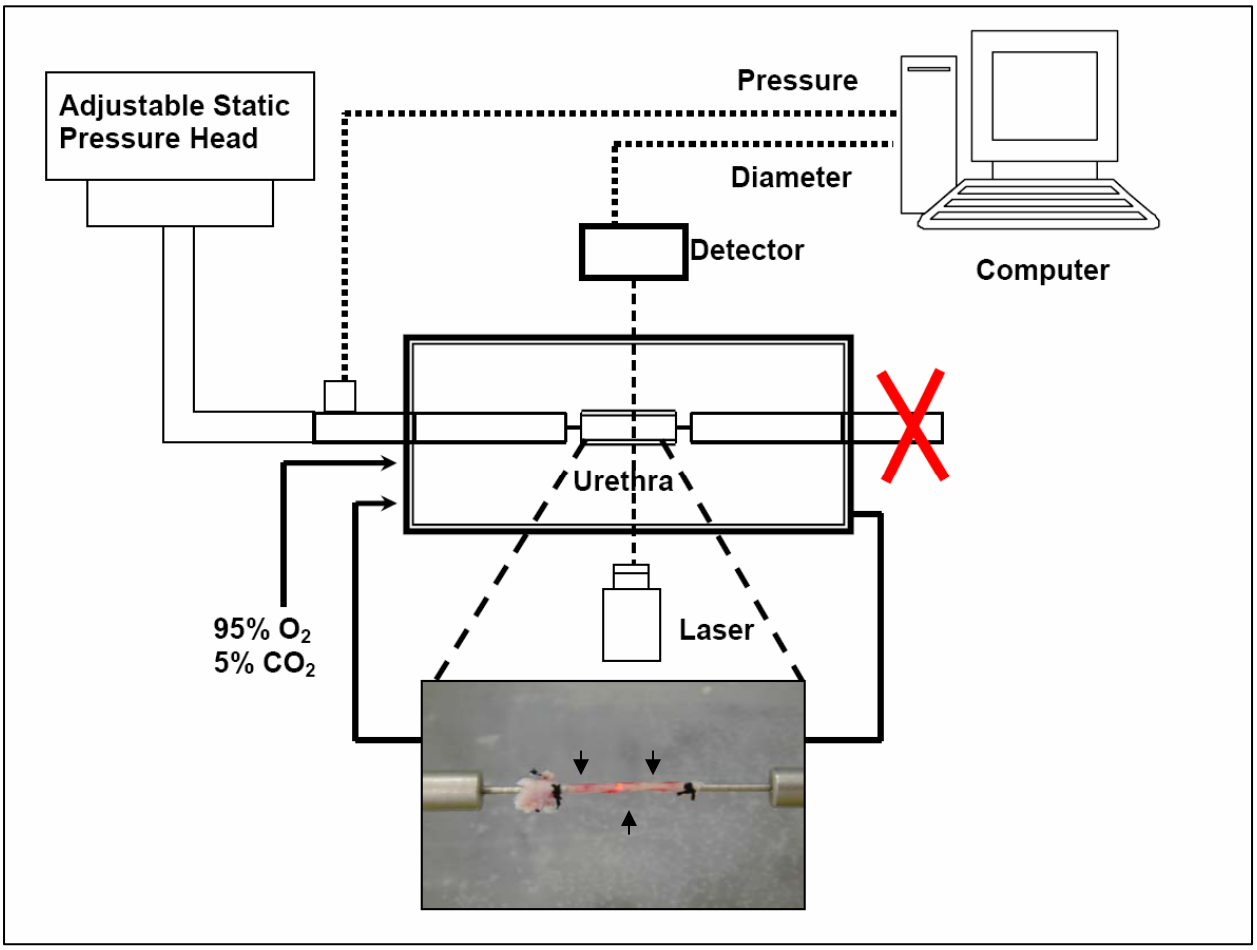

Figure 2.1 A schematic of the urethral testing system; black arrow represent proximal, middle, and distal segments, respectively from left to right.

2.2.4.2 Outer diameter measurement

The outer diameter of the urethra was measured using a helium-neon laser micrometer (laser Model # 162-100, Beta Lasermike, Dayton,OH). The laser emits monochromatic light at 632.8 nm and has a measurement range from .254 to 50 mm (+/- .001 micron accuracy). A urethra is placed in the path of the beam preventing light from reaching the photocell opposite the emission source (Figure 2.1). Using the time interval for a scanning segment and sweep velocity (9800 cm/s), the laser calculates the blocked distance (i.e., the outer diameter). Analog

laser voltages are digitized through a 16 channel A/D converter in order to output the measurement to the computer (Pentium III 266 MHz, Gateway Inc, Irvine, CA) where it continuously records the data [70-72]. The laser micrometer is calibrated with precisely machined tubes of known diameter. *Error propogation analysis of outer diameter measurements is discussed in detail in Appendix B, subsection B.1.*

2.2.4.3 Components of the ex vivo urethral testing system

Due to the small size of the rat urethra, specially fabricated tees with an outer diameter of approximately 1.25 mm were used. Pressure ports were attached to the tees with transparent polyethylene tubing (3/16" inner diameter, McMaster-Carr, #5233k56). Two types of tissue housing chambers were used in these experiments: one originally made for vascular segments, a dynamic vascular testing (DVT) box [68], and another recently made for urethral tissue. Both are composed of plexi-glass with glass windows inserted into the side panels. The glass windows are offset at 5° to minimize diffraction of the laser that scans through the chamber for the purpose of outer diameter measurement [73]. The lid to the housing chamber consisted of plexi-glass with a gas exchange port attached to the top.

The urethral testing box was made to accommodate various methods required in order to assess the urethra. The DVT box has a volumetric capacity of 800 ml. This large volume makes it difficult to wash the specimen for pharmacological testing, and lengthens the time for pharmacological agents to reach equilibrium. To eliminate this problem, the urethral testing box was downsized to a volumetric capacity of 400 ml. Additionally, circulation ports were placed diagonally across from each other (i.e., inlet on the top right and outlet on the bottom left) in order to improve mixing of pharmacological agents in the bath, as well as shortening the time to

reach equilibration. Mixing kinetics were assessed for both the DVT box and the urethral testing box. *A detailed discussion of these evaluations is provided in Appendix B, subsection B.2.*

For the urethral testing box, plugs were made for the box to add versatility to the urethral testing box. One plug was made for the perfusion tee for circumferential measurements. Another plug was made to secure the differential variable reluctance transducer (DVRT; discussed in the following section) so that both circumferential and longitudinal measurements can be made.

2.2.5 Biomechanical Assessment

Biomechanical testing was used to assess urethral function after VD. Biomechanical tests were executed in baseline and passive states. Baseline tone refers to a tissue state in which no attempt was made to either stimulate or eliminate contraction of either muscle component. In the baseline state, basal smooth muscle tone is present and active. Basal tone is commonly stretch-sensitive [74], and may aid the urethra by providing resistance to the increases in intravesical pressure. Passive tone is used to describe the state in which muscular activity is eliminated by calcium and magnesium exclusion.

2.2.5.1 Biomechanical experiments

Urethral specimens were mounted onto the tees of the ex vivo testing system described in **Section 2.2.4** and **Figure 2.1**. First, the tissue was preconditioned, which helped to minimize viscous effects and ensure repeatability [75]. Briefly, preconditioning consisted of 10 cycles of static pressure, ranging from 0 to 8 mmHg. Next, the urethra was subjected to a static pressure-inflation experiment consisting of pressures ranging from 0 to 20 mmHg in increments of 2 mmHg (**Figure 2.2**).

Due to the fact that the tissue is non-homogeous, measurements were taken at three positions along the length of the urethra: proximal, middle and distal segments. These segments were distinguished as a certain percentage of in vivo length: proximal was 30%; middle was 50%, and distal was 70%.

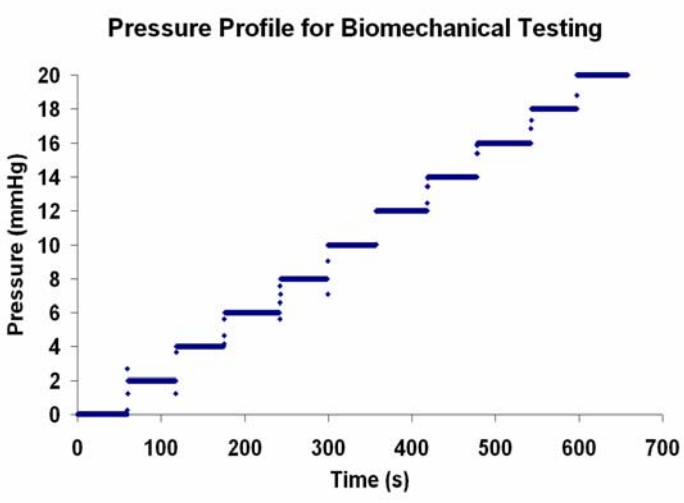

Figure 2.2 Pressure profile for the biomechanical tests

Baseline experiments were performed previous to the passive studies. For the passive state, 3mM ethylenediamine tetraacetic acid (EDTA), a calcium and magnesium chelator, was added to the bath. The incorporation of this agent occurred prior to passive mechanical testing and the tissue was allowed to equilibrate for 30 to 45 minutes in order to ensure that muscle contractions were completely inhibited.

2.2.5.2 Biomechanical parameters

From measured pressure and outer diameter data, we were able to calculate various biomechanical parameters. Compliance (C) is the fractional change in volume that occurs in response to a unit change in pressure, and was calculateded as follows:

$$C = \frac{(D_{max} - D_{min}) / D_{min}}{(P_{max} - P_{min})} \qquad \textbf{(2.2)}$$

Here, D_{max} and D_{min} represent the measured diameters corresponding to the maximum and minimum pressures, P_{max} and P_{min}, used to define the range over which the compliance is calculated. Due to the nonlinearity of the pressure-diameter curve, compliance was evaluated over small pressure ranges with relatively linear portions of the curve; i.e, for the following pressure ranges: 0-6 mmHg (low), 6-12 mmHg (middle), 12-20 mmHg (high). This approach permitted correlations of differences in biomechanical behavior with tissue microstructure [76, 77]. Urethral biomechanical properties were also quantified by calculating for beta stiffness (β), which is a dimensionless parameter that may be utilized to describe the full-range, non-linear pressure-diameter response [78]. This is given by:

$$\beta = \frac{\ln\left(\frac{P}{P_S}\right)}{\left(\frac{D}{D_S} - 1\right)} \qquad \textbf{(2.3)}$$

where P_s and D_s are the same standard pressure and paired corresponding diameter, respectively. We chose P_s to be 10 mmHg, since it is roughly at the mid point of the physiological range.

The incremental elastic modulus, E_{inc}, characterizes tissue stiffness by taking into account the changes in tubular geometry induced by incremental changes in pressure while providing a single constant representing a modulus for both the radial and circumferential directions [79]. This is defined as:

$$E_{inc} = \frac{\Delta P}{\Delta R_o}\left(\frac{2R_i^{\,2}R_o}{R_o^{\,2} - R_i^{\,2}}\right) + \left(\frac{2PR_o^{\,2}}{R_o^{\,2} - R_i^{\,2}}\right) \qquad \textbf{(2.4)}$$

where ΔP and ΔR_o are the incremental changes in transmural pressure (2 mmHg) and outer radius, respectively. R_i, R_o and P are the inner and outer radius and the total pressure at the beginning of the increment, respectively. It should be noted that this method was used to assess the stiffness of baseline and passive states of various pressures.

Circumferential stress-strain curves were generated from pressure-diameter data and the histological thickness. If we assume that urethral specimens are thick-walled, linearly elastic, isotropic cylinders, the circumferential stress (σ_θ) may be estimated by:

$$\sigma_\theta = P\frac{R_i^2}{\left(R_0^2 - R_i^2\right)}\left(1+\frac{R_0^2}{r^2}\right) \qquad \textbf{(2.5)}$$

where r is the radial coordinate through the thickness of the wall (i.e., r =0 at the center of the lumen, $r = R_i$ at the inner wall surface, $r = R_o$ at the outer wall surface, etc.).

Circumferential strain, ε_θ, is defined by:

$$\varepsilon_\theta = \frac{\Delta\overline{R}}{\overline{R}_o} \qquad \textbf{(2.6)}$$

where $\Delta\overline{R}$ is the change in the mean or mid-wall radius ($\overline{R} = \frac{R_o + R_i}{2}$) from its unpressurized value, $\overline{R}_o$.

2.2.5.3 Geometry estimation

Due to the non-uniform nature of the urethra along its length [54], a thickness must be determined for each segment (i.e., proximal, middle, and distal segments) separately in order to calculate R_i from the measured R_o for use in equations 2.4 to 2.6. Thus, after the biomechanical

testing was performed, specimens were fixed under zero transmural pressure in 4% paraformaldehyde overnight, followed by 30% sucrose solution. Specimens were snap frozen in TBS freezing medium (Fisher Scientific Co., #15-183-13) within a cryo-mold. Urethral cross-sections were cut using a cryostat (Thermo Shandon, Waltham, MA) to 15-20 microns at temperatures of -29 to -31°C and stained with Lillie's modified Masson's trichrome stain.

Photographs of the entire urethral cross-section were taken at a magnification of 4x with MagniFire Software (#DP12,Olympus, Dulles, VA) and color digital camera (version 2.1C,DP12, Olympus, Dulles, VA) connected to an Olympus microscope (model BX45, Dulles,VA). The images of each urethral cross-section were then imported in Scion Imaging software (version 0.4.0.3, Scion Corp., Fredrick, MD) where the dimensions of urethral cross-sections were quantified, and 4 to 5 urethral cross section for each segment (proximal, middle, and distal) were averaged for each urethra. Twice the thickness measurement was subtracted from the outer diameter measured by the laser micrometer during the experiment in order to yield the inner diameter for that section. If we assume that the tissue is incompressible and that no length changes occur, then it can be assumed that cross sectional area does not change, regardless of increases in intralumenal pressures. The following relationship for cross-sectional area will then hold:

$$\pi\left(R_o^2 - R_i^2\right)_{Px} = \pi\left(R_o^2 - R_i^2\right)_{Po} \qquad \textbf{(2.7)}$$

Here, R_{oPx} and R_{iPx} are the outer and inner radii, respectively, at any applied pressure (P_x), while R_{oPo} and R_{iPo} are the respective outer and inner radii measured at P_o=0mmHg. Note that everything is known in equation 2.7, except for R_{iPx} , so that for every given measured R_{oPx}, the corresponding value of R_{iPx} can be estimated from:

$$R_{i_{Px}} = \sqrt{R_{o_{Px}}^2 - R_{o_{Po}}^2 + R_{i_{Po}}^2} \quad \textbf{(2.8)}$$

2.2.6 Quantification and assessment of collagen, elastin and muscle of the urethra

After pressure-diameter collection, urethras were re-catheterized and preserved using certain methods depending on the particular endpoint of interest. For histology, specimens were fixed in a picric acid based fixative (e.g. Bouin's or Zamboni's) overnight at 4°C. Finally, tissue that would be used for the biochemical (dye-binding) assay was snap frozen and placed at -80°C overnight, followed by dehydration using a Vacufuge concentrator (#5301, Eppendorf, Westbury, NY).

Post-fixation, tissues undergoing histological analyses were immersed in 30% sucrose solution for a minimum duration of 1 week. Tissue was separated into proximal, middle, and distal portions and embedded with OCT freezing medium (#15-183-13, Fisher Scientific, Waltham, MA) with dry ice or liquid nitrogen.

For microscopy all pictures were captured using MagniFire Software (#DP12,Olympus, Dulles, VA) attached to a color digital camera (version 2.1C, DP12, Olympus, Dulles, VA) connected to an Olympus microscope (model BX45, Dulles,VA). The images of each urethral cross-section were then imported in Scion Imaging software (version 0.4.0.3, Scion Corp., Fredrick, MD). For quantification of positive stain or different structural components, such as collagen and muscle, all pictures were taken at four positions of the urethra clockwise (e.g., 12:00, 3:00, 6:00, and 9:00) at 20x magnification, and elastin was acquired at 40x. Pictures were quantified using NIH imaging software, and calibrated using a ruler. Percent area quantification of muscle, elastin and collagen components was calculated using, equation 2.9:

$$\%A_{stain} = \frac{A_{stain}}{A_{total}} * 100 \quad \textbf{(2.9)}$$

where, A_{stain} is defined as the area of positive stain measured and A_{total} is the total area of the urethral position measured.

2.2.6.1 Histology

Histology was used to study structural changes in muscular and ECM components. Specifically, Lillie's modified Masson's trichrome stain was used to assess changes in collagen and muscle. Elastic fiber arrangement was assessed with Miller's elastic stain, and collagen fiber arrangement was assessed using picrosirius red with polarized light microscopy.

2.2.6.2 Lillie's modified Masson's trichrome stain

Lillie's modified Masson's trichrome stain was used to quantify changes in the amount of muscle and collagen in the proximal, middle, and distal segments of the urethra. In order to intensify the color reaction, the tissue (18 micron thickness) was fixed for 24 hours in Bouin's fixative at room temperature. Slides were washed in running tap water for 10 minutes and placed into Gill's hematoxylin (#23-24565, Fisher Scientific, Waltham, MA) for 30 seconds while heated in the microwave. Slides were washed with running tap water followed by distilled water. Next, slides were placed in dilute ammonium hydroxide solution until sections turned blue. Slides were stained with Celestine blue (#206342, Sigma Aldrich, St. Louis, MO) for 30 seconds. After rinsing slides in running water, slides were stained in Biebrich Scarlet-acid fuschin (#HT151, Sigma Chemical Co., St. Louis, MO) for 15 seconds, and 5% phosphotungstic acid was used for 15 minutes to differentiate between collagen and muscle. Finally, slides were

stained in 2% light green (#L5382, Sigma Aldrich, St. Louis, MO) and rinsed in distilled water. All slides were dehydrated and immersed in xylene for clearing. Slides were coverslipped with Permount (#100496-552, VWR International). Resulting stains are depicted in Figure 1.3, where green represents collagen, purple represents cell nuclei, and red represents muscle fibers.

2.2.6.3 Miller's elastic stain

Miller's elastic stain is commonly used to assess elastic fibers in the lower urinary tract [14]. This stain involved incubating sections (10 micron thickness) in distilled water followed by staining sections in Miller's elastic stain (Victoria blue 4R (#224176, Sigma Aldrich, St. Louis, MO); new fuschsin (#N0638, Sigma Chemical Co., St. Louis, MO); crystal violet (#C3886, Sigma Aldrich, St. Louis, MO); resorcin (#216801, Sigma Aldrich, St. Louis, MO); dextrin (#D2006, Sigma Chemical Co., St. Louis, MO); ferric chloride (#F2877, Sigma Chemical Co., St. Louis, MO); all agents were boiled in hot water, filtered and dissolved in 95% ethanol) for 3-4 hours at room temperature. Sections were differentiated in 95% alcohol, subjected to ascending alcohols for dehydration, and xylene for clearing. Slides were coverslipped with permount.

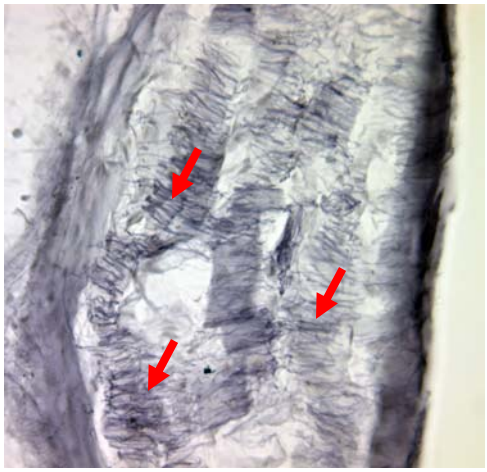

Figure 2.3 Miller's elastic stain of a representative mid urethral segment (40x); Red arrows exemplify elastic fibers (black, dark purple)

Since elastic fibers are extremely small, a magnification of 40x was needed to view this stain (Figure 2.3).

2.2.6.4 Picrosirius red with polarized microscopy

Picrosirius red stains collagen red by reacting with sulphonic acid groups with basic groups present in the collagen molecule. Elongated dye molecules are attached in parallel to the collagen fiber's long axis; thus, birefringency is created [80]. The protocol used for this study was previously established [81]. Briefly, sections were cut at 18 μM thick and fixed in Bouin's fixative for 24 hours at room temperature. Slides were washed in running tap water and rinsed in distilled water. Slides were placed in 0.2% phosphomolybdic acid for 1 minute in order to improve the detail of the collagen fibers followed by staining in PSR (direct red 80; #43665, Standard Fluka) for 1.5 hours. Sections were placed in hydrochloric acid (0.01 N), dehydrated with ascending alcohol solutions, and cleared with xylene.

Polarized microscopy was used to visualize the stained sections using crossed polarizing filters. Tightly packed and highly aligned collagen fibers show polarization colors of longer wavelengths (e.g., orange to red). Less aligned and loose fibers are indicated by green to light yellow colors which are shorter in wavelength [82].

2.2.7 Biochemical quantification of collagen and elastin

Biochemical kits were utilized to quantify any changes in the amount of collagen (Sircol collagen assay, #CLRS1111, Accurate Chemical Co., Westbury, NY) and elastin (Fastin elastin assay, #CLRF2000, Accurate Chemical Co., Westbury, NY).

For the collagen assay, dehydrated urethras were separated into proximal, middle, and distal segments, weighed, and minced into small pieces. Each segment was digested with a solution consisting of pepsin (0.1 mg/ml; #P7000, Sigma Chemical Co.) and hydrochloric acid (0.01 N) for 72 hours at 4°C. Digested solution was transferred to a micro-centrifuge tube (100 µl volume or 50 µl and 50 µl of pepsin/HCl solution). Samples were compared to prepared collagen standards (consisting of bovine collagen I, 1mg/ml, provided by the kit) of 0, 5, 10, 20, 30, 40 and 50 µl of collagen type I. The Sirius red dye reagent (1 ml) was added to the digested solution and standards, which were allowed to bind for 1 hour. Tubes were centrifuged for 10 minutes at 10,000 rpm at room temperature. The supernatant was discarded, and the solid was dissolved in 1 ml of sodium hydroxide solution (alkali reagent). Samples were pipetted into a 96 well plate (i.e., 200 µl in 5 wells for each sample and standard). The absorbance for each well was measured using a microplate reader (EL x 800, Biotech Instruments, Inc.) at a wavelength of 562 nm.

Collagen standard concentrations were plotted versus their respective absorbance readings. This resulted in a linear relationship which allowed calculation of collagen concentration in the proximal, middle, and distal segments from the absorbance measured. Results are reported as percent of dry weight of the urethral segment. Collagen standards were prepared for each urethra.

From previous histological studies, we know that the amount of elastin in the urethra is small [14]. Thus, we assessed the amount of urethral elastin in the entire urethra. After tissue was dehydrated, the dry weight was recorded.

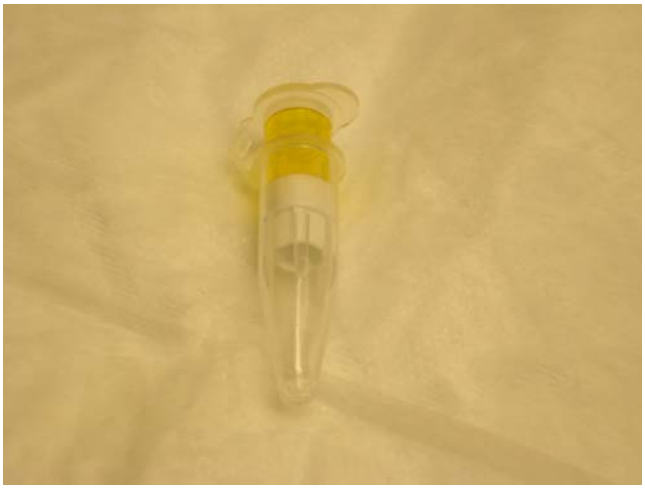

Figure 2.4 The microcon filtering device: the yellow portion is a separate piece, which is a YM 3 filter and the clear portion is a centrifuge tube that collects the filtrate.

Samples were placed into a microcentrifuge tube with 0.25 M oxalic acid (0.2 ml per 0.1 g of tissue wt; #O0376, Sigma Chemical Co., St. Louis, MO). Tubes were heated to 95°C for 1 hour and transferred to ice for approximately 15 minutes. Samples were centrifuged at 3000 rpm for 10 minutes at 4°C. This was repeated until all of the tissue was compacted to the bottom. Next, the supernatant was pipetted into a new microcentrifuge tube and labeled. This process was repeated until the tissue completely dissolved (i.e., 3-4 times). The extracts were concentrated with a microcon filtering device (Figure 2.4; Millipore, #42420). The samples were pipetted into the filter (yellow portion) and centrifuged at 14,000 rpm for 100 minutes. The solid portion left over was collected and transferred to a new microcentrifuge tube with 1 ml of the elastin extraction solution. The extraction process lasted 24 hours at 4°C.

The next day tubes were centrifuged at 12,000 rpm for 10 minutes at 4°C, and the supernatant was discarded. Fastin elastin dye reagent was added to the tubes (1 ml) and 100 µl of 90% of aquaeous ammonium sulfate, which bridges the α-elastin molecule to the dye molecule was added. Dye was allowed to bind with the elastin molecules for 1 hour at room

temperature. It should also be noted that at this time elastin standards were prepared in the same manner with soluble α-elastin, in the following concentrations: 0, 5, 10, 20, 30, 40, 50, 70 μl/ml.

Samples were centrifuged at 12,000 rpm in room temperature, and the supernatant was removed. The solid matter leftover (i.e., elastin) was dissolved in the destaining reagent. Once dissolved, all solutions were transferred to a 96 well plate, in the same manner as described for the collagen assay. The specific wavelength used to measure absorbance was 450 nm. Absorbance values and known elastin standard concentrations were fit to a linear curve in order to assess the concentration of the elastin in the urethral samples.

2.2.8 Statistical analyses

Statistical comparisons, as well as curve fits, were performed with software packages, Sigma Stat (version 2.0, Jandel Scientific, Richmond, CA) and SPSS (version 15.0, SPSS Inc., Chicago, IL). Biomechanical comparisons for the baseline and passive state involved comparing within groups (e.g., proximal vs. middle, middle vs. distal, etc.) and comparing between groups (e.g., control vs. VD). For parametric data, a Student's t test was used to compare compliance and beta stiffness between VD and control groups in both baseline and passive states and between baseline and passive data for controls and VD separately. For nonparametric data, a Mann-Whitney rank sum test was performed. For comparisons within groups but across regions, (i.e., proximal vs. middle, middle vs. distal, etc.), one factor ANOVA with repeated measures was used. For comparisons involving incremental elastic moduli and circumferential stress values at a given pressure, two factor ANOVA with repeated measures was used where group (VD vs. control) was one factor and pressure level (0 to 20mmHg) was the second factor. Post-hoc testing was performed with a Student-Neuman Keuhl's test. For non parametric data, Friedman

Repeated Measures Analysis of Variance on Ranks was performed with a Dunn's pair-wise comparison post-hoc test. Statistical significance was indicated by a p value less than 0.05. All comparisons for histological and biochemical endpoints were made with a student's t test or Mann-Whitney test.

2.3 RESULTS

Nonlinear, sigmoidal shaped pressure-diameter curves were noted for all segments of the control group in the baseline state, and for the middle and distal segments of the VD group (**Figure 2.5**). The proximal segment of the baseline VD specimens exhibited an exponential shape, as did all segments for both VD and control specimens under passive conditions [83].

2.3.1 Baseline and passive biomechanical results

2.3.1.1 Compliance and beta stiffness

In the baseline state, no significant differences in compliance were noted between segments for the control urethras (**Tables 2.1 and 2.2**). However, VD resulted in a significant increase in low pressure compliance, from 0 to 6mmHg, for the proximal segment compared to the middle and distal segments. Similarly, beta stiffness was significantly lower in the proximal segment compared with the middle segment for the VD group. Under passive conditions, a significant proximal-to-distal gradient in low pressure compliance was observed for both control and VD groups (**Table 2.2**). No other segmental differences in compliance or beta stiffness

values were noted. Passive middle pressure compliance was decreased for middle and distal control segments and also for VD proximal segments, compared to their respective baseline values (**Tables 2.1 and 2.2, Figures 2.5-2.6**).

Under baseline conditions, no significant differences between control and VD groups were noted in compliance for any urethral segment (**Table 2.1; Figure 2.6**). However, VD groups exhibited significantly increased beta stiffness (i.e., decreased distensibility for the entire pressure range) for the middle segment under baseline conditions. Under passive conditions, VD urethras had increased low pressure compliance but only in the proximal urethral segment; whereas, in the baseline state, this same comparison was not significant (p=0.055). No significant differences in beta stiffness were noted for any segment between control and VD groups under passive conditions (**Table 2.2; Figures 2.5-2.6** [83]).

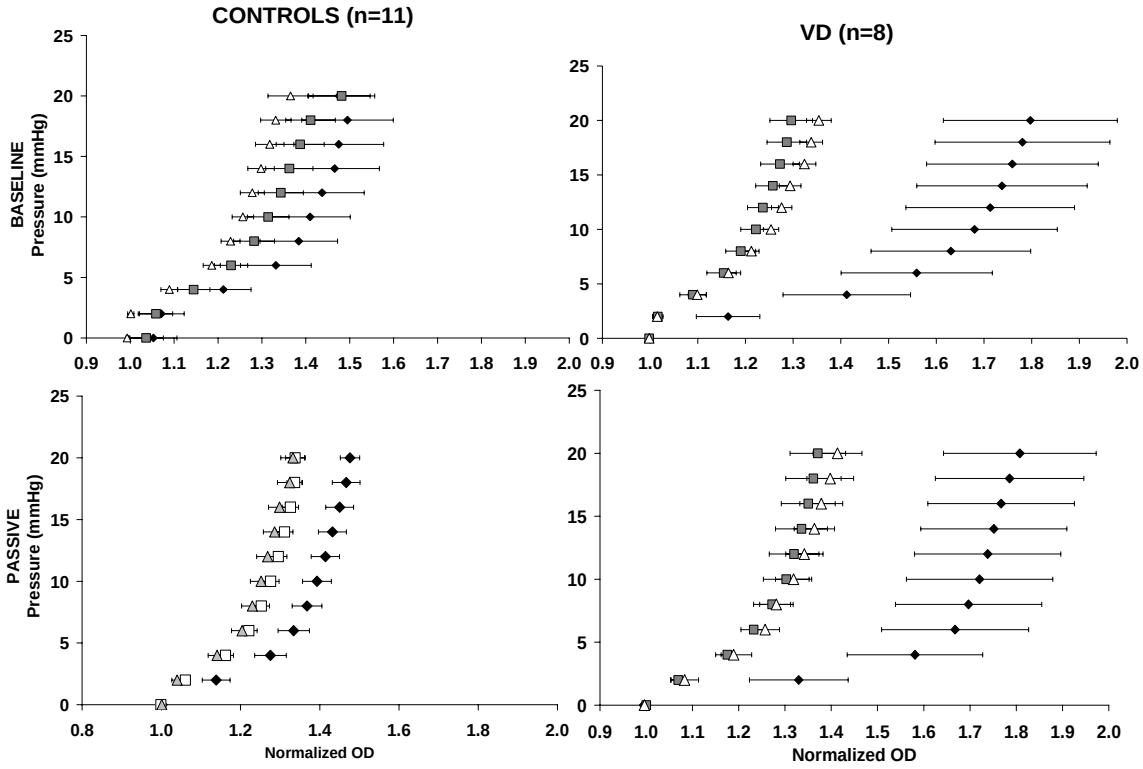

Figure 2.5 Pressure-diameter data for proximal, middle, and distal segments of control (n=8, left) and VD (n=8, right) urethras in the baseline (top) and passive (bottom) conditions

Table 2.1 Compliance and beta stiffness values for control and VD urethras in baseline conditions

Baseline State	CONTROLS (N=11)			VD (N=8)		
Compliance (X100)	Proximal	Middle	Distal	Proximal	Middle	Distal
Low Pressure	4.62 ± 0.60	3.24 ± 0.55	3.19 ±0.38	9.44± 2.43 $^{X\,**}$	2.57 ± 0.29 ^{X}	2.69±0.65 **
Middle Pressure	1.15 ± 0.18	1.64 ± 0.20	1.34 ±0.14	1.77 ± 0.24	1.26 ± 0.21	1.67±0.41
High Pressure	0.69 ± 0.17	0.80 ± 0.15	0.67 ±0.10	1.05 ± 0.41	0.66 ± 0.09	0.74±0.41
Beta Stiffness	7.31 ± 0.90	7.78± 0.80^	7.58 ±0.80	6.80 ± 0.88*	10.44±0.87 *^	9.47±1.08

Table 2.2 Compliance and beta stiffness values for control and VD urethras in passive conditions

Passive State	CONTROLS (N=11)			VD (N=8)		
Compliance (X100)	Proximal	Middle	Distal	Proximal	Middle	Distal
Low Pressure	5.87±0.74 $^{*\wedge +}$	3.70 ± 0.36^	3.37 ± 0.45 $^{+}$	11.51±1.91 $^{*o\#}$	3.48 ± 0.40 ^{o}	3.74 ± 0.54 $^{\#}$
Middle Pressure	1.03 ± 0.14	0.98 ± 0.12	0.90 ± 0.06	0.83 ± 0.16	1.02 ± 0.27	1.03 ± 0.26
High Pressure	0.69 ± 0.14	0.62 ± 0.05	0.48 ± 0.05	0.42 ± 0.07	0.49 ± 0.06	0.66 ± 0.11
Beta Stiffness	10.00 ± 0.86	10.65 ± 0.69	10.69 ± 0.76	9.58 ± 1.21	12.81±1.47	11.45± 1.47

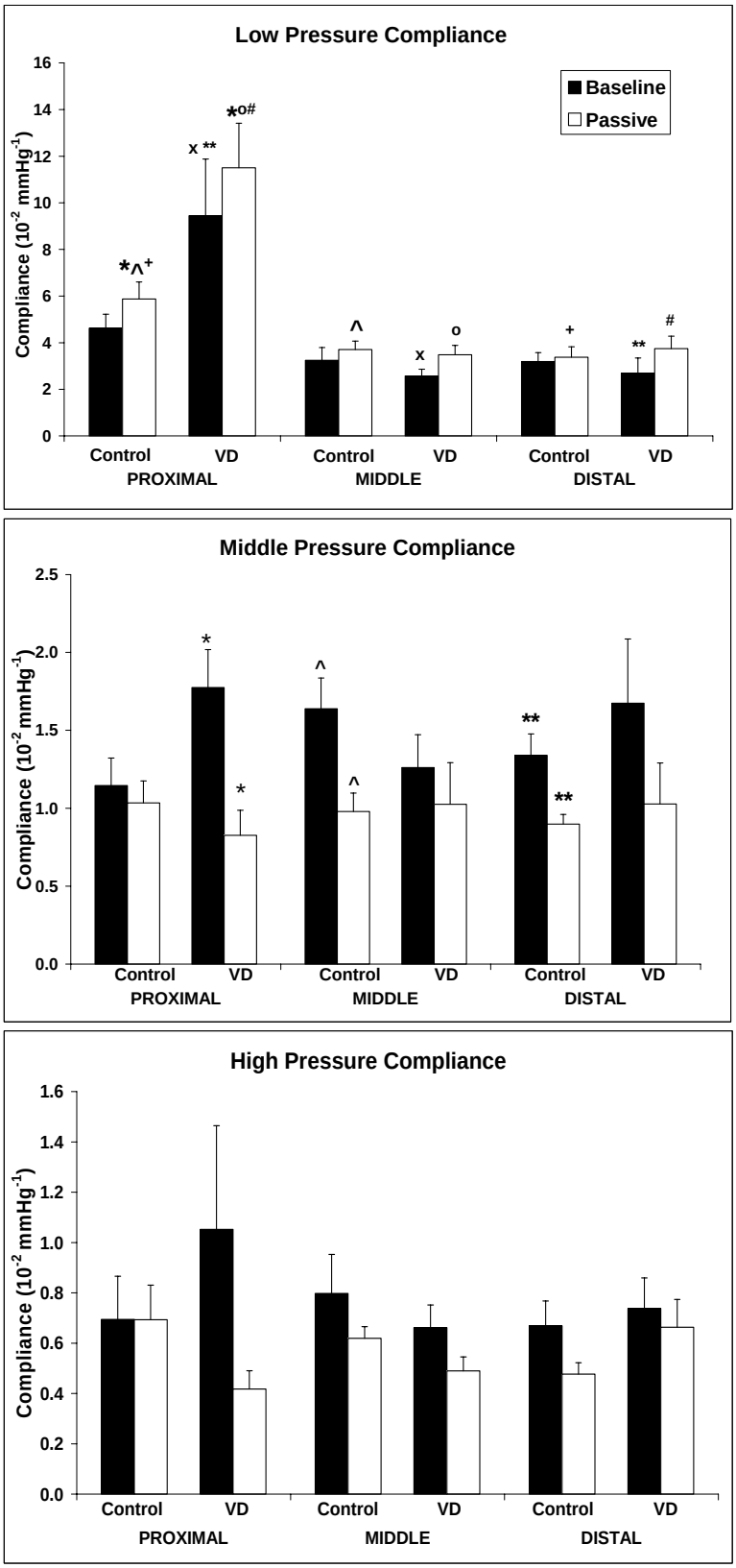

Figure 2.6 Baseline and passive compliance values in control (n=11) and VD (n=8) groups for low (top), middle (middle), and high (bottom) pressure ranges. Significant differences between groups indicated by *,+, O, ^,#,.**

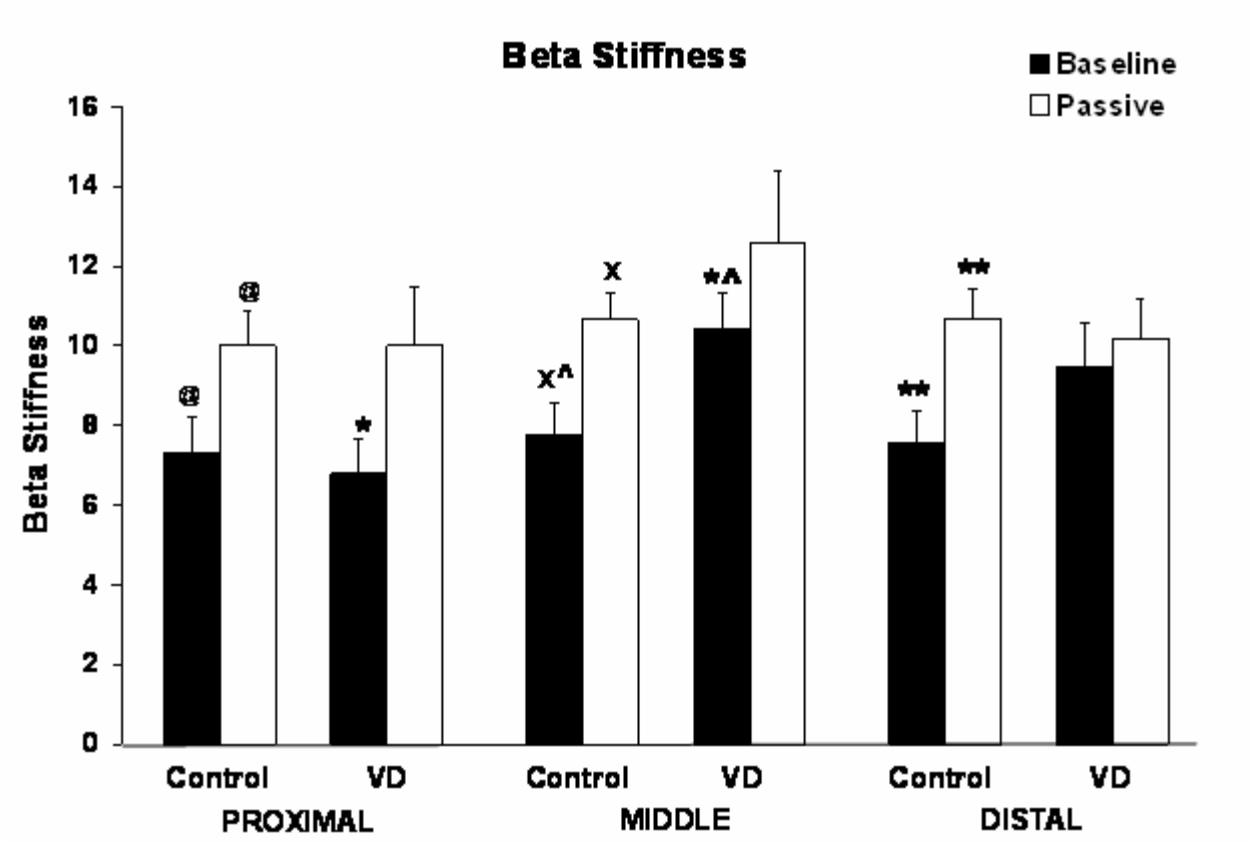

Figure 2.7 Beta stiffness values for control (n=11) and VD (n=8) urethras in both the baseline and passive states. Significanct differences between groups indicated by @,*,X,^, .**

2.3.1.2 Circumferential stress-strain response and incremental elastic moduli

Control circumferential stress-strain response at baseline exhibited exponential behavior which revealed the same compliance gradient as seen in the pressure diameter data, i.e. proximal segments more compliant than middle urethral segments, and middle segments more compliant than distal segments (**Figure 2.7**). This gradient was collapsed in control passive tissue. For VD urethras, the proximal urethra was clearly more compliant than middle and distal portions in both baseline and passive states.

Due to spontaneous basal urethral smooth muscle contractions in the baseline state, negative E_{inc} values were generated for pressures ranging from 0 to 4 mmHg; therefore, E_{inc} values are reported for 6 to 20 mmHg only. With only a few exceptions, E_{inc} (i.e, incremental elastic moduli or stiffness values for each step of pressure) for both the control and VD urethras increased with increasing pressure in both baseline and passive states (**Figure 2.9**).

In the baseline state, data trends suggest that the peak value of E_{inc} for the proximal segment was higher compared to that for middle and distal segments in both control and VD urethras, though these differences were not significant (**Table 2.3**). A similar trend of peak E_{inc} values for proximal urethras was noted for VD urethras in the passive state (**Figure 2.8**).

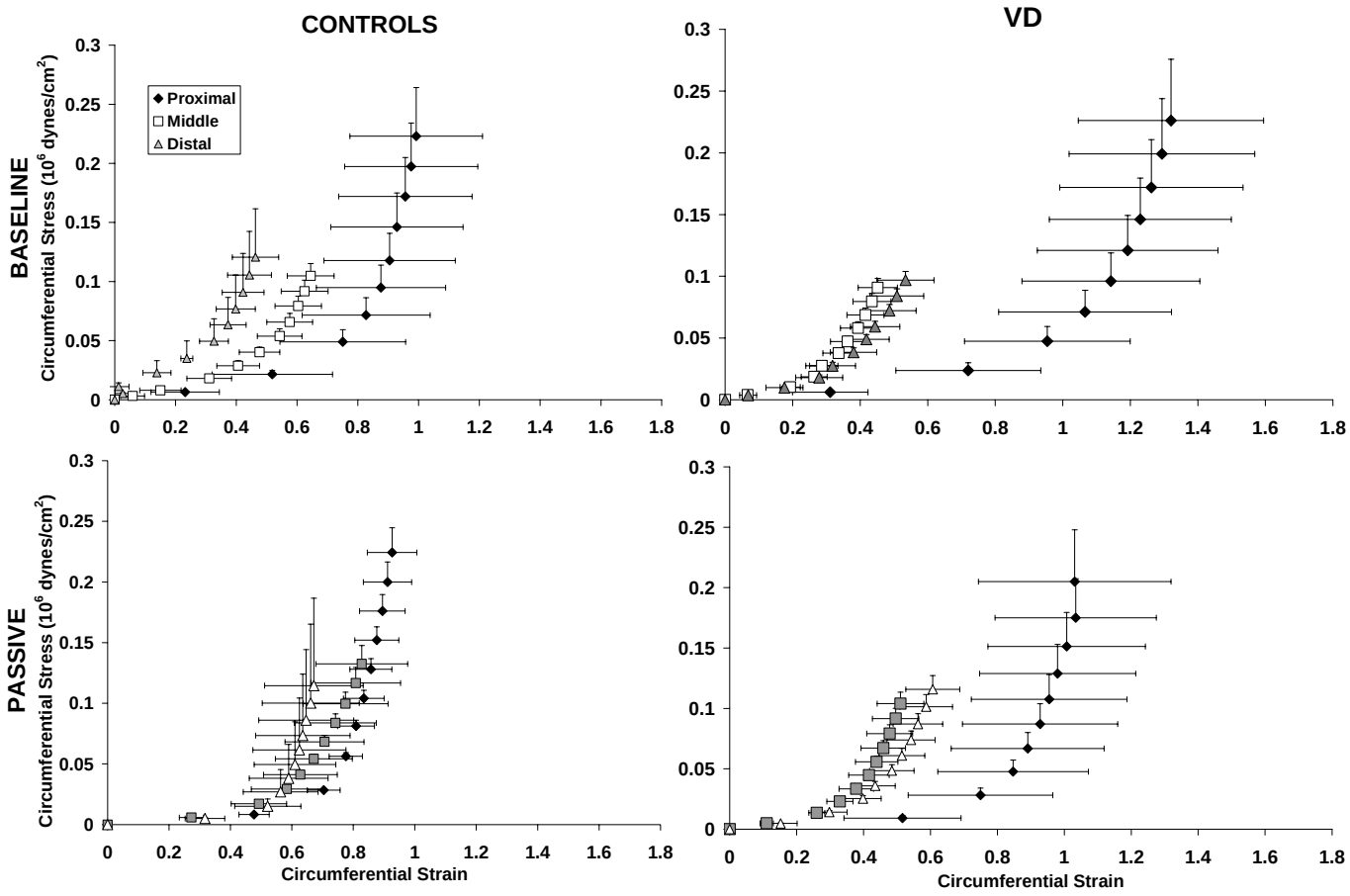

Figure 2.8 Circumferential stress-strain response for control (n=8, left) and VD (n=8, right) urethras in the baseline (top) and passive (bottom) conditions

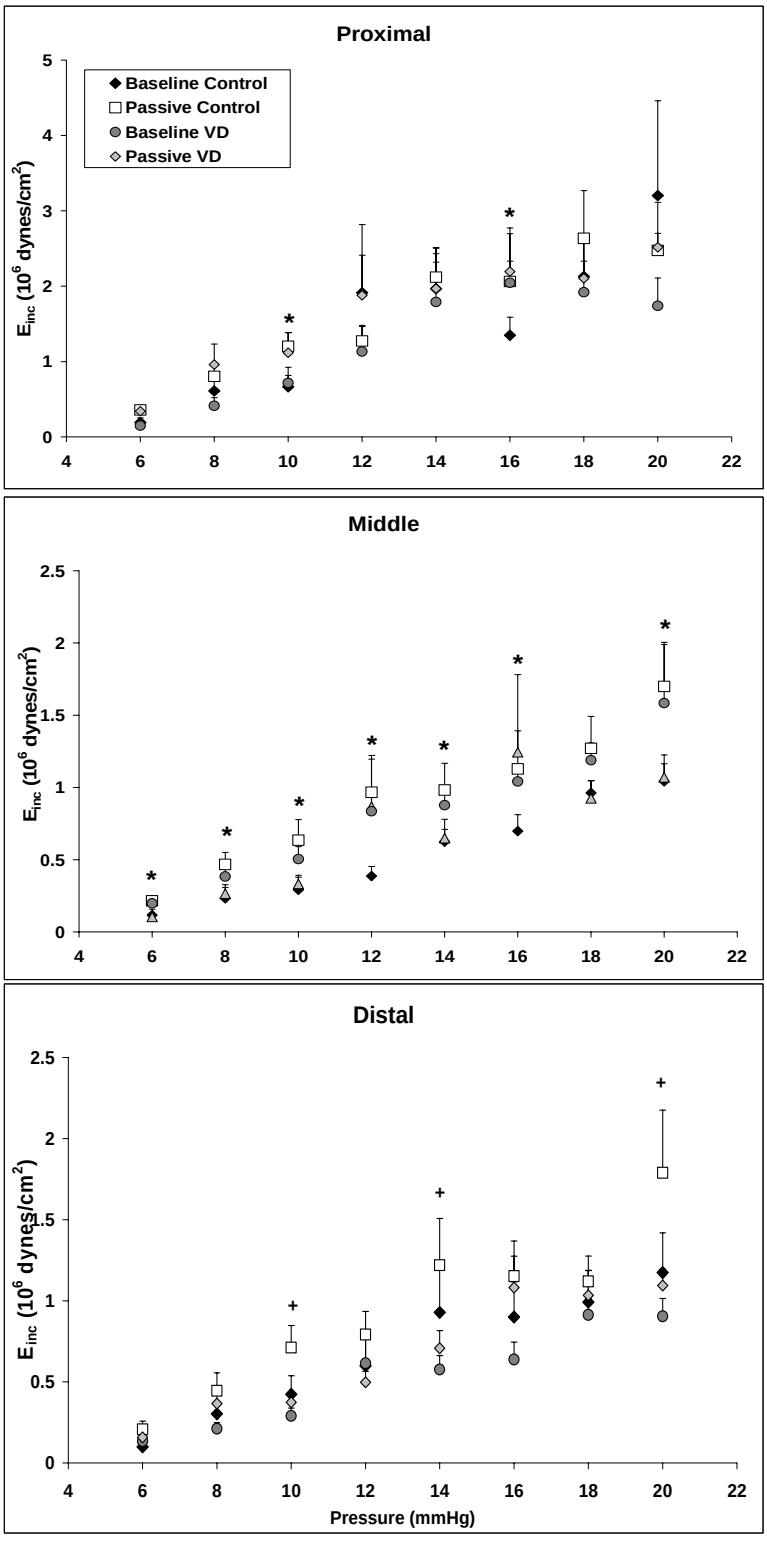

Figure 2.9 Incremental elastic moduli values for proximal (top), middle (center), and distal (bottom) urethral segments of control (n=8) and VD (n=8). *represents a significant difference ($p<0.05$) between baseline and controls at the indicated pressure; + represents significance between control and VD within that particular segment at the indicated pressure.

Table 2.3 Peak incremental elastic moduli (Einc) values for control and VD groups in both baseline and passive states. In the passive state, peak Einc values for control distal segments were significantly higher than for VD distal segments (*p<0.05).

	BASELINE			PASSIVE		
	Proximal	Middle	Distal	Proximal	Middle	Distal
Control (N=8)	3.20±1.26	1.04±0.12	1.17±0.24	2.63±0.63	1.70±0.29	1.79±0.39*
VD (N=8)	2.04±0.73	1.24±0.54	0.90±0.10	2.52±0.60	1.58±0.42	1.09±0.10*

2.3.2 Histological Results

2.3.2.1 Collagen and muscle quantification

Using Masson's trichrome stain, collagen resulted in a green color, and dark red represented muscle (both striated and smooth; **Figure 2.10**). The largest portion of muscle was located in the middle portion of the urethral sphincter. Qualitatively, the control urethras (n=5) had oriented circular muscle compared to VD urethras (n=5). In VD middle urethras, the outer muscle layer had muscle fibers that were broken while control circular muscle was uninterrupted.

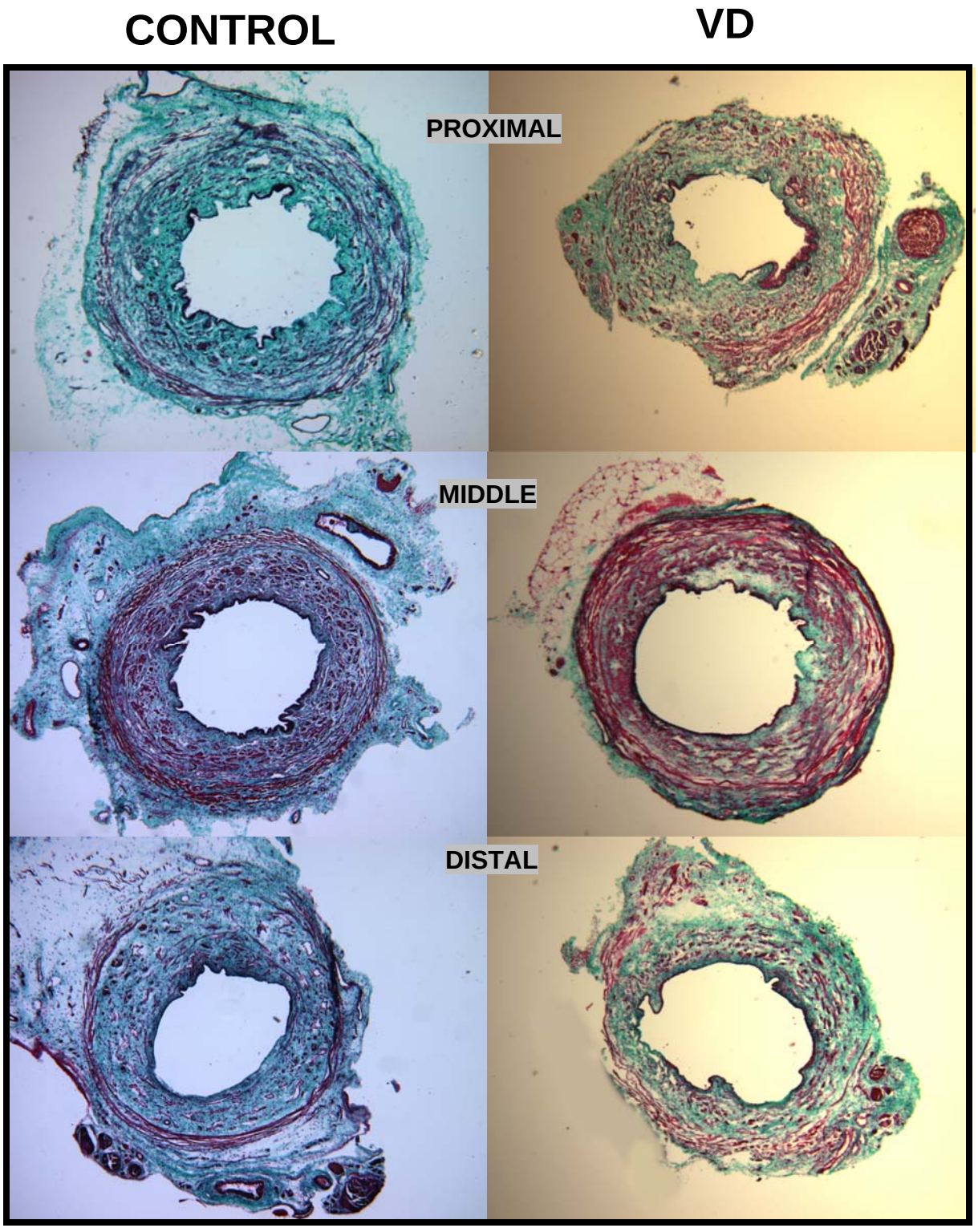

Figure 2.10 Masson trichrome stain for representative sections of controls (left) and VD (right) at the proximal (top), middle (center), and distal (bottom) portions. Green represents collagen and red represents muscle. Images were acquired at 4 x.

Quantification of muscle and collagen separately revealed that urethral tissue is largely made of collagen (on average: 70% collagen and 25% muscle). Proximal (72 ± 4%) and distal segments (78 ± 3%) had a larger amount of collagen than middle portions (67 ± 1%) in the cross sectional area of control urethras. Compared to controls, VD urethras had less muscle per cross sectional area in proximal (24 ± 4% vs. 18 ± 3%), middle (26 ± 4% vs. 20 ± 4%), and distal (18 ± 3% vs. 15 ± 2%) segments. However, these differences were not statistically significant ($p=0.12$). The collagen for VD middle (75 ± 3%) segments was significantly higher compare to that of controls ($p<0.05$; **Figure 2.11**).

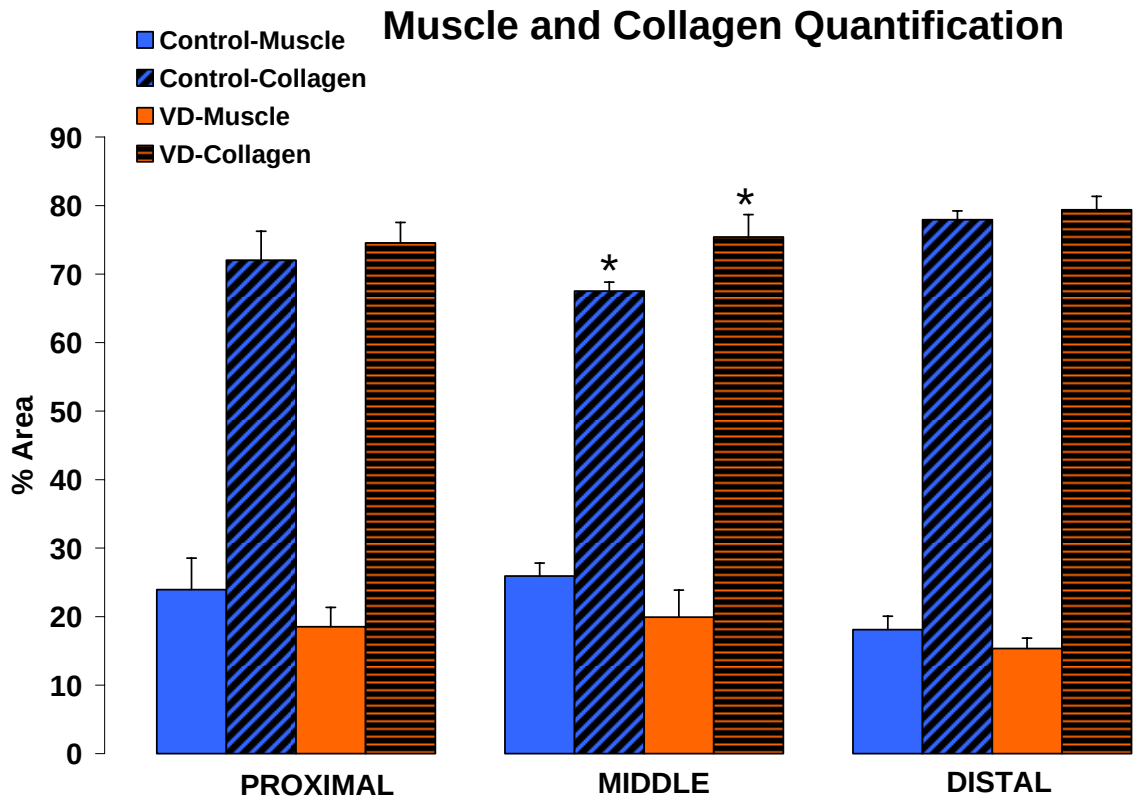

Figure 2.11 Quantified collagen and muscle components of the urethra comparing control (n=5) and VD (n=5) urethras. Significant differences between groups indicated by *p<0.05.

2.3.2.2 Polarized Microscopy

Polarized microscopy with picrosirius red staining was performed to estimate any changes in collagen fiber thickness and orientation via color changes (**Figure 2.12**). For example, colors of shorter wavelengths (light yellow to dark yellowish-green) represent collagen fibers that are thinner and less organized. On the other hand, colors ranging from orange to red represent collagen fibers that are thick and highly oriented [82].

In control urethras, the proximal portion showed the most organized collagen appearing primarily red in color. The middle portion also revealed much organization (primarily red) with the exception of the dorsal portion of the urethra where the color was yellow. Finally, the distal portion seemed to vary from specimen to specimen, but overall the there was less organization in this part of the urethra compared to proximal and middle regions.

VD urethras exhibited different characteristics compared to that of controls. VD proximal segments had an increased presence of thin and loose fibers as indicated by the green-light yellow colors. However, the largest changes were found in the middle region of the VD middle urethra. Light yellow was found throughout the entire smooth muscle region. Finally, the distal region was slightly affected by VD, but, as stated previously, it was consistent that the distal segments were less organized.

2.3.2.3 Miller's elastic fiber stain

Urethras were stained with Miller's elastic fiber stain. Sections were qualitatively assessed for orientation and condition of elastic fibers throughout the urethra. In general, elastic fibers were located throughout the medial and adventitial striated portion of the urethra and enveloped smooth muscle fibers (**Figure 2.13**), both circumferential and longitudinal.

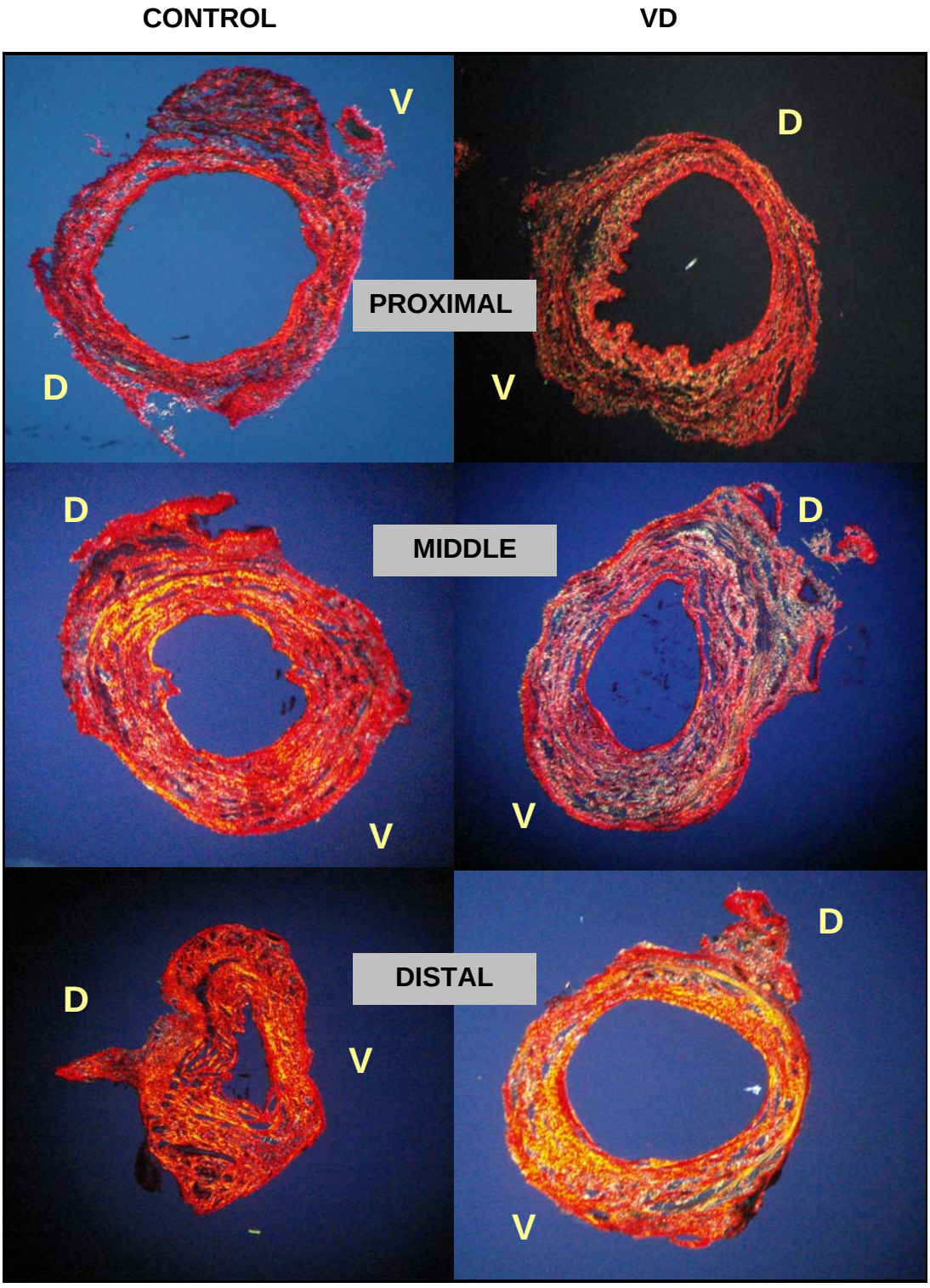

Figure 2.12 Urethral sections stained with picrosirius red and visualized with polarized microscopy for the proximal (top), middle (center) and distal (bottom) segments of control (left) and VD (right) specimens. Colors ranging from orange to red represent thick and highly oriented collagen fibers, and light yellow to green represent thin and loose collagen fibers. V is the ventral side of the urethra and D is the dorsal (or vaginal) side of the urethra.

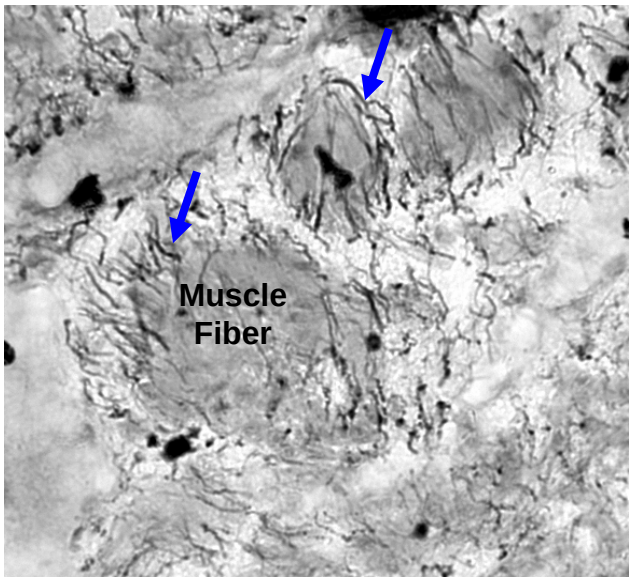

Figure 2.13 Smooth muscle fibers surrounded by elastic fibers (black) is a representation of a control section. Blue arrows exemplify elastic fibers. Acquired at 60x magnification.

Control proximal, middle, and distal segments showed differences in elastic fiber arrangement. Proximal urethras were dominated by thick fibers radially oriented throughout the urethral wall in the medial part of the wall (**Figure 2.14**, top). There were some stray fibers aligned circularly with the circumferential oriented smooth muscle fibers. In the dorsal quadrant of the urethral wall, the elastic fibers were much shorter than the fibers of the lateral and ventral quadrants.

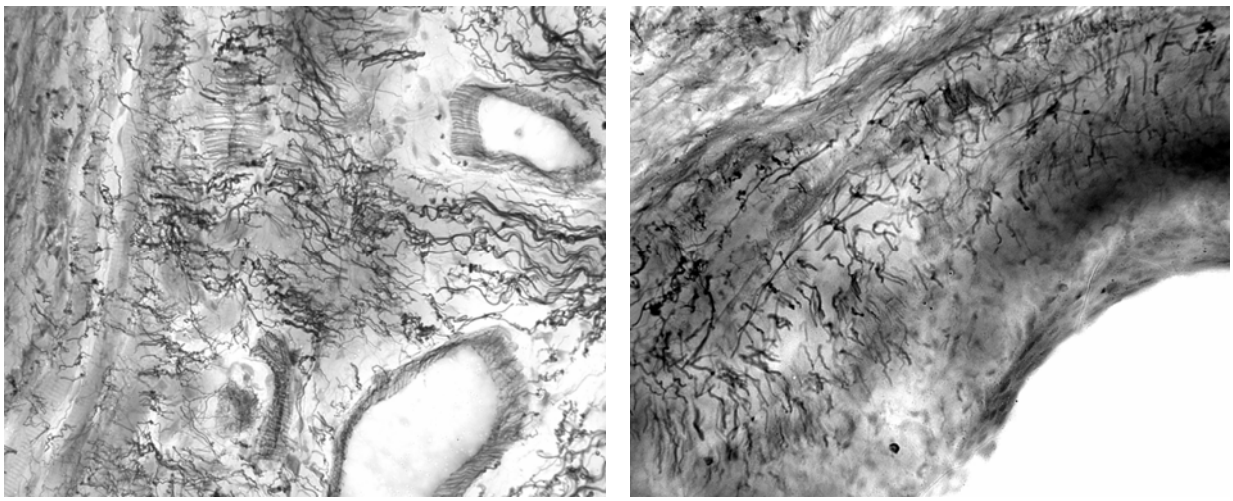

Figure 2.14 Radially oriented short elastic fibers in the control proximal urethra (right); thick wavy elastic fibers around a control middle urethra (left). Acquired at 40x magnification.

Elastic fibers in middle segments were sparser, but they were radially-oriented juxtaposed to each muscle fiber. Additionally, the fibers were much thinner and longer compared to that of proximal segments, and there was an increased prevalence of circular orientation of elastic fibers around circumferentially-oriented muscle fibers. The striated sphincter had a dense population of mature thick, wavy elastic fibers (**Figure 2.14**, bottom). Finally, distal controls had a dense population of randomly oriented elastic fibers located in the medial portion of the urethra; whereas, the fibers were shorter and oriented radially near the outer edge of the urethra.

VD urethras were also stained for elastic fibers and compared to control urethral segments (**Figure 2.15**). Proximally, the fibers were much more random in orientation after VD compared to the controls. Additionally, the fibers were shorter and less continuous. In the VD middle segment, elastic fibers were somewhat shorter; however, the fibers surrounding the smooth muscle remained thin and similar to controls. The thick wavy fibers in the striated sphincter were present, but interrupted. Finally, elastic fibers in the distal segment were not affected by VD, as were the proximal and distal segments. Still, occasionally VD tissue exhibited patches of unevenly distributed elastic fibers, which was not common in distal controls.

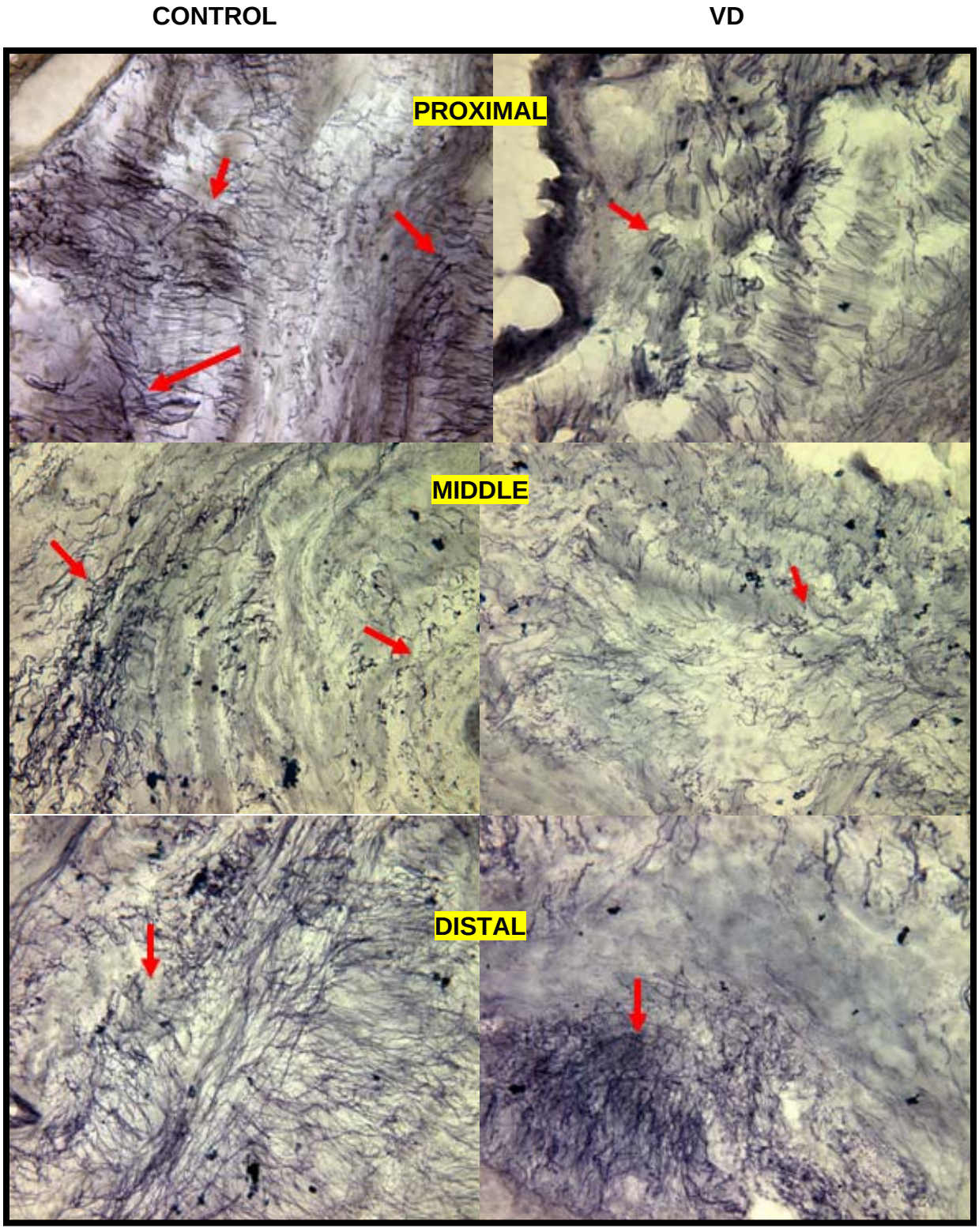

Figure 2.15 Representative sections of control (left) and VD (right) urethras stained with Miller's elastic stain for proximal (top), middle (center), and distal segments). Elastic fibers are black hair-like structures and are illustrated by the red arrows. Pictures acquired at 40x magnification.

2.3.3 Biochemical assays

2.3.3.1 Collagen assay

The collagen concentration of the proximal, middle, and distal segments of control (n=8) and VD (n=8) urethras was determined using a colorimetric binding assay. There were no differences between control and VD proximal (11 ± 3% vs. 8 ± 2%) and distal (10 ± 2% vs. 13 ± 4%) segments. However, for VD middle segments, the amount of collagen (16 ± 6%) was decreased compared to that in the middle portion of controls ((7 ± 1%; $p<0.05$; Figure 2.16).

2.3.3.2 Elastin assay

Whole urethras were assessed for changes in elastin concentration after VD. Results showed that control urethras had a small amount of elastin (1.22 ± 0.34%). VD (3.63 ± 0.76%) caused a significant increase in elastin concentration compared to that of controls ($p<0.05$; **Figure 2.17**).

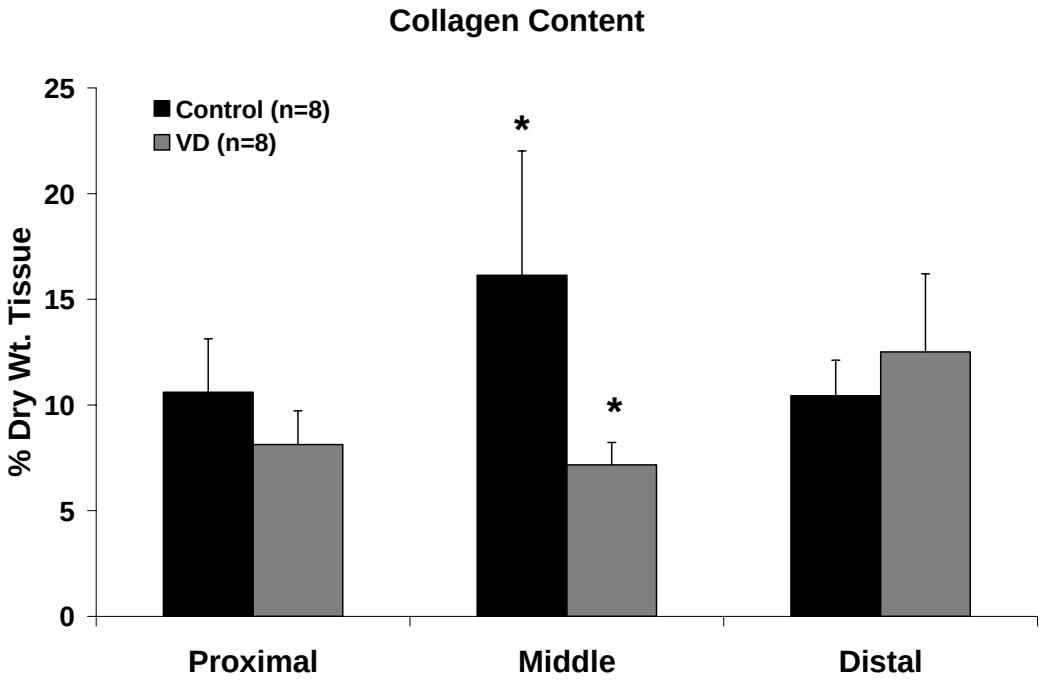

Figure 2.16 Collagen concentrations calculated as % dry weight for proximal, middle, and distal segments for control and VD urethras. * indicates a statistically significant difference ($p<0.05$).

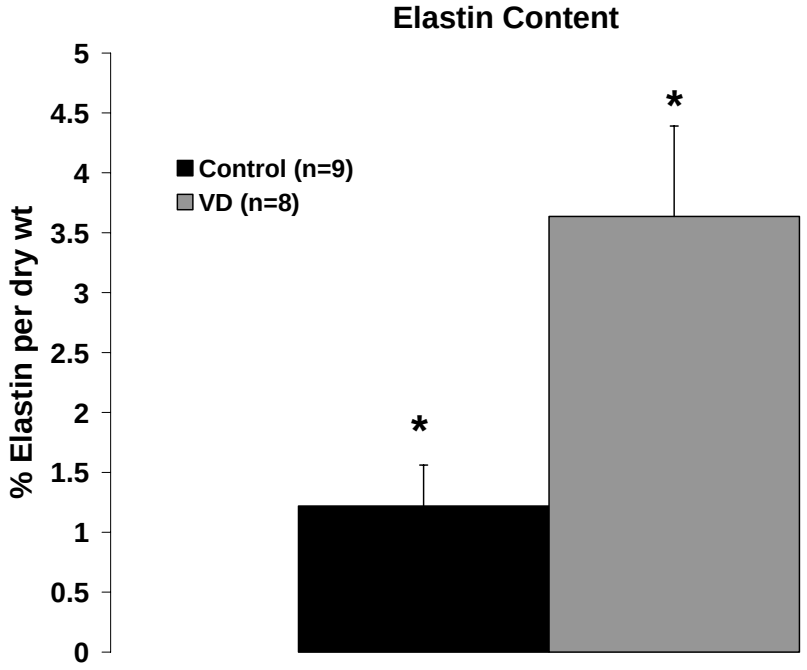

Figure 2.17 Elastin concentrations calculated as % dry weight for whole urethras for control and VD urethras. * indicates a statistically significant difference ($p<0.05$).

2.4 DISCUSSION

Our findings suggest that VD results in increased low pressure compliance in the proximal urethral segment and increased beta stiffness in the middle segment. In order to assess the influence of basal tone on the biomechanical properties of the urethra, we also compared both control and VD urethras under baseline and passive conditions. Our results indicate that basal tone influences the general biomechanical response of the urethra (**Figures 2.5 and 2.8**), and in particular, increases middle- and high-pressure compliance and decreases beta stiffness in all urethral segments (**Figures 2.6 and 2.7, Tables 2.1 and 2.2**). To further this concept, we have also proved that VD causes remodeling of the collagen, elastic, and muscle component of the urethra (**Figures 2.10-2.17**).

Biomechanics is a useful tool to understand structural changes in diseased tissue [76, 84]. Past research has shown that separate components of soft tissue (i.e., muscle, collagen, and elastin) contribute distinctly to separate components of the pressure-diameter or stress-strain curves [77, 85]. Compliance, a linear relationship between pressure and volume, is commonly used in urology for assessment of lower urinary tract dysfunction. In this study, the pressure-diameter curve was separated into linear portions to accommodate the linear characteristics of this measure, and also to reveal possible structural changes in the urethra. For example, compliance at low pressure was significantly higher in the proximal urethra after VD than that of control specimens. Since increased low pressure compliance was distinguished in both the baseline (not significant, $p=0.055$) and passive states ($p<0.05$), both a lack of muscular tone and an altered ECM are likely related to this change in compliance following VD. This difference occurred only at low pressures (0 to 6mmHg) in the passive state, suggesting further that VD

alters elastic fiber networks, which are known to be dominant at low pressure in biological soft tissues (**Figure 2.6**, top) [86].

Elastin (a.k.a., elastic fibers) was assessed in VD urethras and compared to controls. Histological results indicated that there were alterations in elastic fiber arrangement after VD (**Figure 2.15**), more specifically in the proximal portion. VD disrupted the orientation of the elastic fibers in the smooth muscle portion of the proximal urethral wall. The lack of orientation and the fact that most of the elastic fibers were located around each muscle bundle could largely contribute to the increase of compliance and lack of basal tone. Preliminary biomechanical studies were performed on the role of elastin in compliance by digestion of the elastin component (see Chapter 3). Elastin digestion caused the tissue to dramatically dilate and also increased compliance values. Thus, elastin may aid the muscle in maintaining urethral tone (**Figures 3.1-3.3**).

Additionally, elastin was assessed using a colorimetric assay. Results indicated a significant increase of elastin in the whole urethra compared to controls (**Figure 2.17**). This finding agreed with the histological studies of Rocha et al. [52], in which they found an increase in elastin after vaginal distension in rats. Additionally, histological studies performed on periurethral samples taken from hypotonic urethras of women with SUI indicated that elastin was very much fragmented [87]. The elastin concentration in our study, in **Figure 2.17**, is a combination of elastin and tropoelastin. Thus, since our histological analysis and elastase treated tissue indicated elastic fiber damage may be the culprit for the increased compliance and lack of tone after VD, the smooth muscle cells may be trying to produce tropoelastin, a protein that plays a large role in elastin remodeling, in order to repair the damaged elastic fibers.

Comparisons of compliance in baseline and passive states also indicated changes following VD. Most differences were found in the middle pressure ranges (6 to 12 mmHg). Middle and distal control urethral segments in the baseline state had significantly higher compliance values compared to that of passive state. This may be due to the presence of basal tone, providing a muscle contraction that creates a "reserve" of stretch; whereas, in the absence of the active tone, the passive tissue is stretched to the maximum with the increasing pressure. For VD specimens this was only true for the proximal segment, not the middle and distal urethral segments, indicating that the basal tone of the middle and distal urethras may largely be affected.

The concept of beta stiffness was developed in order to address the issue of a nonlinear pressure-diameter curve [78]. Like Young's incremental elastic modulus for linear materials (e.g., steel), this parameter provides one constant that represents stiffness for biological soft tissues over the entire pressure range providing an idea of general urethral resistance to pressure. VD middle segments had a significantly higher beta stiffness value than that of control middle segments and VD proximal segments in the baseline state; thus, providing evidence for a change in middle urethral stiffness after VD. This indicates that the urethra may have higher stiffness due to the lack of basal tone that provides reserved stretch over the entire pressure range. The increase in beta stiffness value may also be due to damaged collagen. In Chapter 3, urethral compliance was assessed after imposed collagen damage with sodium hydroxide treatment (**Figures 3.1-3.3**). Results indicated significant decreases in compliance, which is similar to our beta stiffness finding. Additionally, changes in collagen orientation were evident from polarized microscopy in the middle segment. Again, this verifies an altered collagen skeleton which may contribute to altered middle urethral biomechanics.

To further evaluate this correlation, tissue was assessed both histologically and biochemically for changes in collagen amount and orientation. Masson's trichrome stain indicated a significant increase in the percentage of collagen per urethral cross sectional area in the middle segment from VD. This finding agrees with that of Rocha et al. [52], and other studies have revealed an alteration in the amount of urethral collagen in women with genuine stress urinary incontinence [88]. However, one should be careful when interpreting these results since this increase in collagen could also be due to the fact that the amount of muscle has decreased from VD (**Figure 2.11**). For this reason, collagen concentration was assessed using a biochemical assay. It was determined that the amount of collagen in the middle portion decreased after VD (**Figure 2.16**). This finding was supported by the work of Goepel et al. [89]. This group assessed collagen with immunohistochemistry in periurethral tissues of women with incontinence. They also found weak staining of collagen in the urethral tissue of the incontinent group.

Comparing baseline and passive states, it is clear that the basal tone was defective after VD. Baseline control urethras had lower beta stiffness values compared to that of the passive state. There were no difference between baseline and passive states in the VD proximal, middle, and distal urethral segments.

Incremental elastic modulus provides a more rigorous measure for urethral stiffness or resistance at each step in pressure ranging from 0 to 20 mmHg. In contrast to low pressure compliance values, in the control proximal segment, this part of the urethra had the highest E_{inc} value at maximum pressure, 20mmHg, indicating at maximum pressures it is the stiffest of all three segments of the urethra. This may be indicative of the least amount of basal tone present in the proximal urethra compared to that of middle and distal baseline controls. Further studies

must be performed to evaluate the importance of orientation and amounts of muscle and extracellular matrix components to the biomechanical measurements.

The biomechanical changes observed in our model for acute SUI may stem from functional, structural, neural or vascular alterations that result from VD [47, 90-92]. Previous in-vivo investigations using a similar model showed that simulated birth trauma produces lower bladder leak point pressures compared to healthy controls [47]. VD has been found to cause neural degeneration, necrosis in both smooth and striated musculature, as well as irregularly shaped muscle fibers [45, 47]. In the present study, the amount of muscle (smooth and striated) present in urethral cross sections was evaluated, using Masson's trichrome stain. While we found a decrease in the amount of muscle in the all three segments, these differences were not statistically significant (**Figure 2.11**). On the other hand, Rocha et al. [52] reported a significant decrease in urethral muscle after birth trauma.

The observed biomechanical changes may also stem from damaged lower urinary tract vasculature. Using a rat model similar to the one used in the current work, Damaser et al. [91] studied blood flow to three major pelvic organs: bladder, vagina, and the urethra. The bladder and the urethra experienced periods of hypoxia during VD, which can greatly affect the urothelium and neuromuscular components of this tissue.

Defective nerve mediated urethral closure mechanisms have been considered an important factor in SUI induced by vaginal parity. Researchers have found that pudendal nerve blockade in healthy women decreases urethral resistance [56] and after transection of the pudendal nerve in rats, the middle urethra loses 80% of its activity [41]. Sievert et al. [46] also found that immunoreactivity in proximal and middle urethral segments for neuronal nitric oxide synthase and tyrosine hydroxylase (marker for sympathetic nerves) significantly declined after

inducing VD. Neurally-mediated urethral closure mechanisms (via somatic nerves) have been proposed by Kamo et al. [18, 93] to mediate increases in urethral pressure before sneeze transmission, followed by an increase in urethral resistance as sneeze-induced abdominal pressure exceeds increased bladder pressure. The involvement of neural mechanisms in urethral resistance is also supported by the fact that, with bilateral pudendal nerve block, there is a significant decrease in urethral closure pressure [94].

Our study was conducted in the absence of neural activity (neither electrical field stimulation nor neurotransmitters were present) and without any stress conditions other than intralumenal pressure application. However, the basal smooth muscle activity may act as a prime contributor to the continual maintenance of continence. The results of our studies have revealed a decrease in basal smooth muscle activity in a given pressure range and a reduction in urethral resistance after VD. Lack of basal tone may contribute to the deficiency of neural control found in the previously mentioned studies. Since the basal smooth muscle tone is commonly stretch-sensitive [74], it may help to provide an initial resistance to the increase in intravesical pressure during a stress episode. Urethral spontaneous myogenic tone may act as a pre-existing and constant tone preparing the contractile mechanisms to contract more if neurotransmitters are released to prevent leakage [95]. Such a basal tone may allow a rapid and efficient control of the urethra both as a tight seal and as a controlled conduit.

The VD-induced changes in the biomechanical properties of the proximal urethral segment may have significant implications, as this segment aids in maintaining urinary continence via sympathetic nerve excitatory control of the urethral smooth muscle [96]. This has been shown to be a major factor in promoting tonic contraction and maintaining urine storage [97]. The observed increase in proximal urethral low pressure compliance may be due to a

change in proximal urethral geometry (open bladder neck [98]), altered intrinsic basal urethral tone, or changes in ECM properties, more specifically, elastin, which is responsible for responding to low pressures. An increase in proximal urethral compliance may also contribute to the "funneling" of the proximal urethral neck seen in patients with SUI [92]. Indeed, our data supports the notion that VD-induced biomechanical changes are associated with changes in the basal smooth muscle tone activity. The sigmoidal shape of the proximal urethral pressure-diameter curve in the baseline state was not present after VD; i.e., it is more exponential in shape, similar to that for the urethra in the passive state (**Figure 2.5**).

The middle segment of the urethra also contributes to the urethral continence mechanism, though in a distinct manner from the proximal segment. The middle urethral segment contains the most abundant proportion of smooth and striated muscle (**Figure 2.10**), and is the site of pudendal nerve innervation, which mediates striated sphincter muscle-storage reflexes. Our results indicated a significant increase in beta stiffness of the middle segment of the urethra under baseline conditions following VD (**Table 2.1**). This may be due to structural or neural damage induced by VD, to alterations in basal tone or extracellular matrix components within this segment. It is possible that defects in both basal tone and matrix occurred since beta stiffness is a parameter represented over the entire pressure range. Reduced basal tone is consistent with our observation that there are significant differences in biomechanical properties of the healthy middle urethral segment between the passive and baseline states, but not for the VD group (**Figures 2.6, 2.7 and 2.9**). In addition, the middle segment of the VD urethra has a less pronounced sigmoidal shape in its pressure-diameter response under baseline conditions compared to the same segment of the control urethras (**Figure 2.5**). An initial, pressure-induced myogenic contraction in the control urethras may provide a reserve capacity of distensibility so

that the middle segment of the control urethra may be distended further in response to pressure than VD urethras.

The role of the distal urethra is unclear [9], though it is thought that its contribution to the continence mechanism increases when the proximal urethral region is damaged and weak [99]. As with the other segments, our results suggest VD-induced alterations in basal tone within the distal segment. However, we did not note any significant differences in the biomechanical properties of this segment between VD and control urethras, nor any changes in the ECM.

Very few studies, to our knowledge, have been previously performed to assess the influence of SUI on the biomechanical properties of the urethra. Thind and Lose [61] studied urethral viscoelasticity in both continent and incontinent women with symptoms of genuine SUI. They concluded that urethral stress relaxation was significantly greater in SUI than for healthy females, with the greatest differences occurring at the bladder neck or proximal urethral segment. The viscoelasticity of muscular tissues is related to the basal tone of the tissue [100, 101]. Therefore, our observation that VD leads to a decrease in basal tone in the urethra is consistent with the finding by Thind and Lose that urethral viscoelasticity is altered in SUI. Measurements of passive length-tension curves in urethral strips indicated a significant increase in urethral compliance in post-partum rabbits compared to urethras of virgins [97]. This is consistent with our current results (**Tables 2.1 -2.3**).

There are some important limitations to these studies that should be kept in mind. First, the urethra is an organ surrounded by supporting pelvic floor musculature, the pubo-urethral ligament, and the anterior vaginal wall. As a result, physiologic transmural urethral pressure is difficult to measure [102]. The pressure range chosen in this study was based on measured maximal voiding pressures for a female rat [69]. Secondly, the urethra consists of musculature

arranged in two directions: circumferential and longitudinal. The results of this study were limited to the circumferential biomechanical behavior of the urethra, and do not provide insights into the longitudinal biomechanical properties/behavior. The maximum urethral closure force is generally attributed to the circumferential musculature [9]; yet, the longitudinal properties of the urethra could affect its overall biomechanical, and functional behavior. Simultaneous analysis of both circumferential and longitudinal properties could lead to important new insights into urethral biomechanics and function. Finally, the design of the current study only assessed the contribution of the biomechanical properties of the urethral basal smooth muscle tone and ECM, and the external urethral striated sphincter remained passive. However, striated muscle does not have stretch sensitive qualities similar to that of smooth muscle that is responsible for generating basal tone.

In conclusion, we have shown that VD leads to biomechanical changes in the urethra that are potentially relevant to the mechanisms that underlie the development of SUI. While these changes have been supported by histological and biochemical evidence of damage in the extracellular matrix components, we provide evidence that VD leads to altered urethral basal smooth muscle tone.

3.0 THE ROLE OF COLLAGEN AND ELASTIN IN URETHRAL BIOMECHANICS

3.1 SIGNIFICANCE OF COLLAGEN AND ELASTIN IN THE URETHRA

Biomechanics has firmly established that collagen contributes to the stiffness of most biological materials and elastin contributes distensibility of biological soft tissues. An essential study performed by Roach and Burton [85] described the separate role of collagen and elastin by incorporation of formic acid and trypsin, respectively. After treatment, the collagen-digested curve indicated an increased compliance; whereas, the elastin-digested curve revealed an increased stiffness. This is only one of many attempts to characterize the biomechanical role of the extracellular matrix components in many biological tissues. Alternatively, this study has never been attempted on the urethra. There have been hypotheses drawn on the role of collagen and elastin based on histology [14, 15, 103], but no studies to our knowledge have actually assessed the biomechanical role of each component in the urethra. In order to assess the impact of any disease state on the urethra, it is important to identify the role of each component. Thus, a study similar to that of Roach and Burton was performed, but on the female rat urethra.

3.2 METHODS

Urethras were isolated as discussed in **Section 2.2.2.**, implanted in the ex vivo system described in **Sections 2.2.4** and assessed biomechanically in the passive state in the same manner as described in **Sections 2.2.5**. Tissue was assessed in one of two conditions: "elastin-digested" or "collagen-compromised".

For the elastin-digested urethra, the EDTA-media 199 solution was replaced in the testing protocol with fresh Media 199. This was important since elastase is calcium dependent [104]. Elastase solution (0.1 mg/ml; [104]) was injected into the lumen of the urethra, which was then clamped off to maintain 4-8 mmHg of static pressure. Exposure to elastase (n=4) was maintained for 1 hour at 37°C. Next, elastase solution was flushed from the lumen using media 199 and biomechanical testing was resumed.

For compromised collagen, the bath and luminal solution was replaced with as solution of 0.05 N [105] sodium hydroxide (NaOH; n=4). NaOH is known to dissolve the amino side chains of the collagen structure, impairing the collagen so that it is unable to provide stiffness to biological tissues [105]. After NaOH treatment, the solution was emptied and replaced with fresh Media 199. It should be noted that collagenase was not used due to the fact that collagen composes ~ 70% urethral cross sectional area (**Section 2.3.2.1**). If collagenase was used, the result would be a very weak tissue with a high likelihood of leaking and an inability to maintain static pressures.

Pressure-Diameter data was used to calculate compliance, as described in **Section 2.2.6**. Additionally, histological endpoints (Miller's elastic stain, **Section 2.3.2.3**, and polarized microscopy, **Section 2.3.3.3.**) were used to assess (qualitatively) the completeness of these treatments in the urethra.

3.3 RESULTS

Elastase treatment caused urethral tissue to dramatically dilate and turn a whitish color. On the other hand, NaOH treatment caused the urethra to shrink and turn a yellowish (**Figure 3.1**). Pressure-diameter data (**Figure 3.2**) showed major differences, as well. Elastase treatment caused the pressure diameter curves to shift to the right compared to the passive control urethras. NaOH treatment (compromised collagen) shifted the curve to the left compared to passive controls, most notably for the proximal segment.

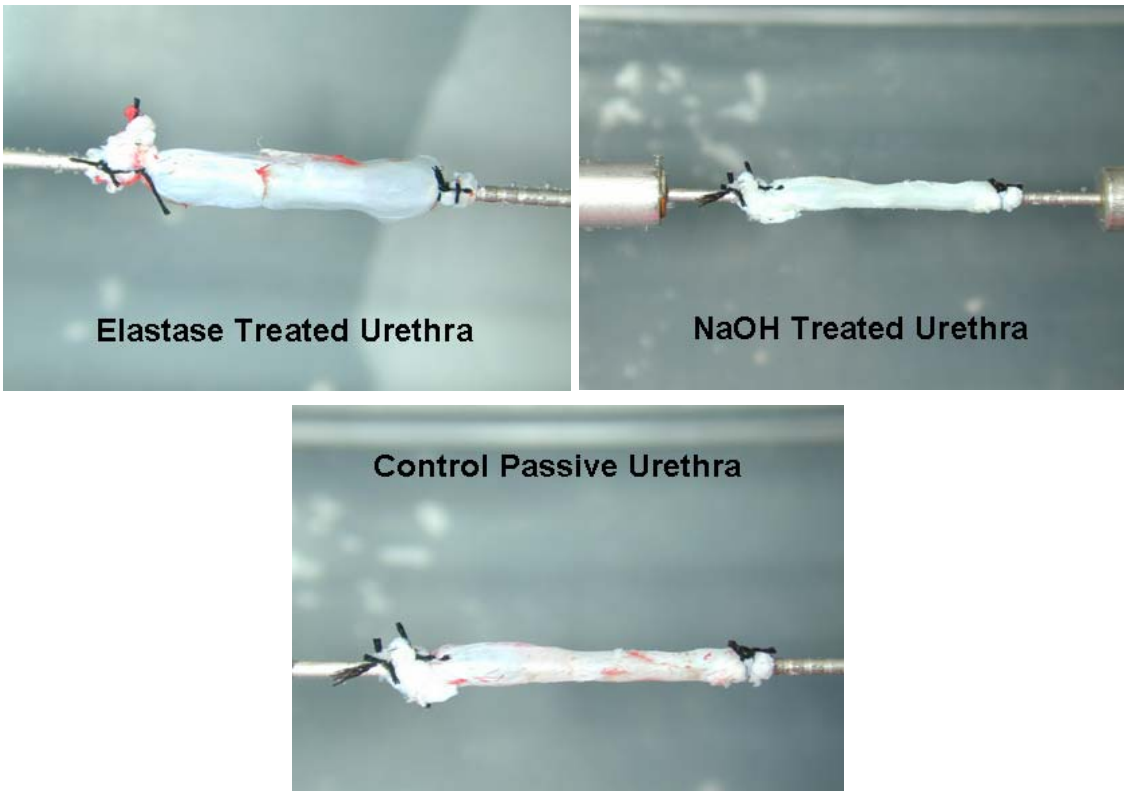

Figure 3.1 Urethras maintained at static pressures of 20 mmHg for elastase treatet, NaOH treated, and passive controls.

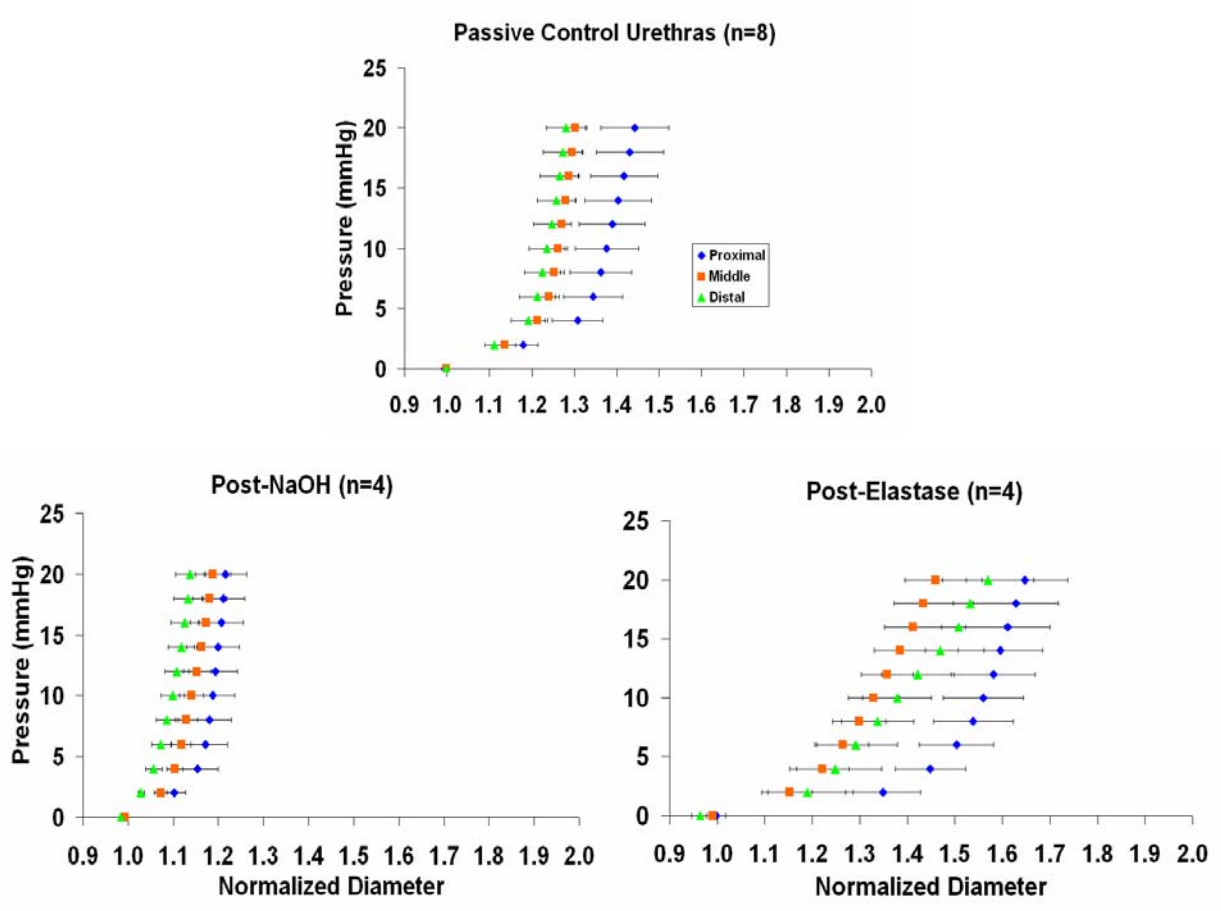

Figure 3.2 Pressure diameter data for control urethras in the passive state (left), compromised collagen (bottom, left), and elastsase treated (bottom, right).

Compliance values also indicated many changes (**Figure 3.3**). Overall, isolated collagen tissue had a significantly decreased compliance compared to isolated elastin tissue at all pressure ranges, with the exception of the proximal segment compliance at middle and high pressure ranges. For low pressure compliance, collagen compromised middle segments (0.020 ± 0.003 $mmHg^{-1}$) had a decreased compliance compared to that of controls (0.040 ± 0.004 $mmHg^{-1}$). This finding was true for distal segments, where compromised collagen decreased compliance compared to passive distal controls.

Middle and high pressure compliance values had similar results. Middle pressure ranges revealed that the elastin damaged treatment resulted in increased compliance values for middle (0.010 ± 0.004 $mmHg^{-1}$) and distal (0.020 ± 0.007 $mmHg^{-1}$) segments compared to that of controls (0.004 ± 0.001 $mmHg^{-1}$ and 0.005 ± 0.001 $mmHg^{-1}$, respectively).

Using Miller's elastic stain, it was clear that elastase treatment was successful in eliminataing elastic fibers (**Figure 3.4**). While the tissue was void of elastic fibers in luminal and medial portions of the urethral, a small amount of single, discontinuous strands remained on the outer wall of the urethra. Additionally, NaOH treatment did not affect the presence of elastic fibers in the urethra. All three segments clearly have elastic fibers well distributed throughout the urethral wall.

Polarized microscopy in combination with pircrosirius red staining indicated that NaOH treatment was successful to impair collagen function (**Figure 3.5**). This was indicated by the lack of red color and increased presence of light yellow in the proximal, middle, and distal segments of the NaOH treated group. Thus, proving that the NaOH treatment caused decreased organization of urethral collagen, as well as thinning of collagen bundles.

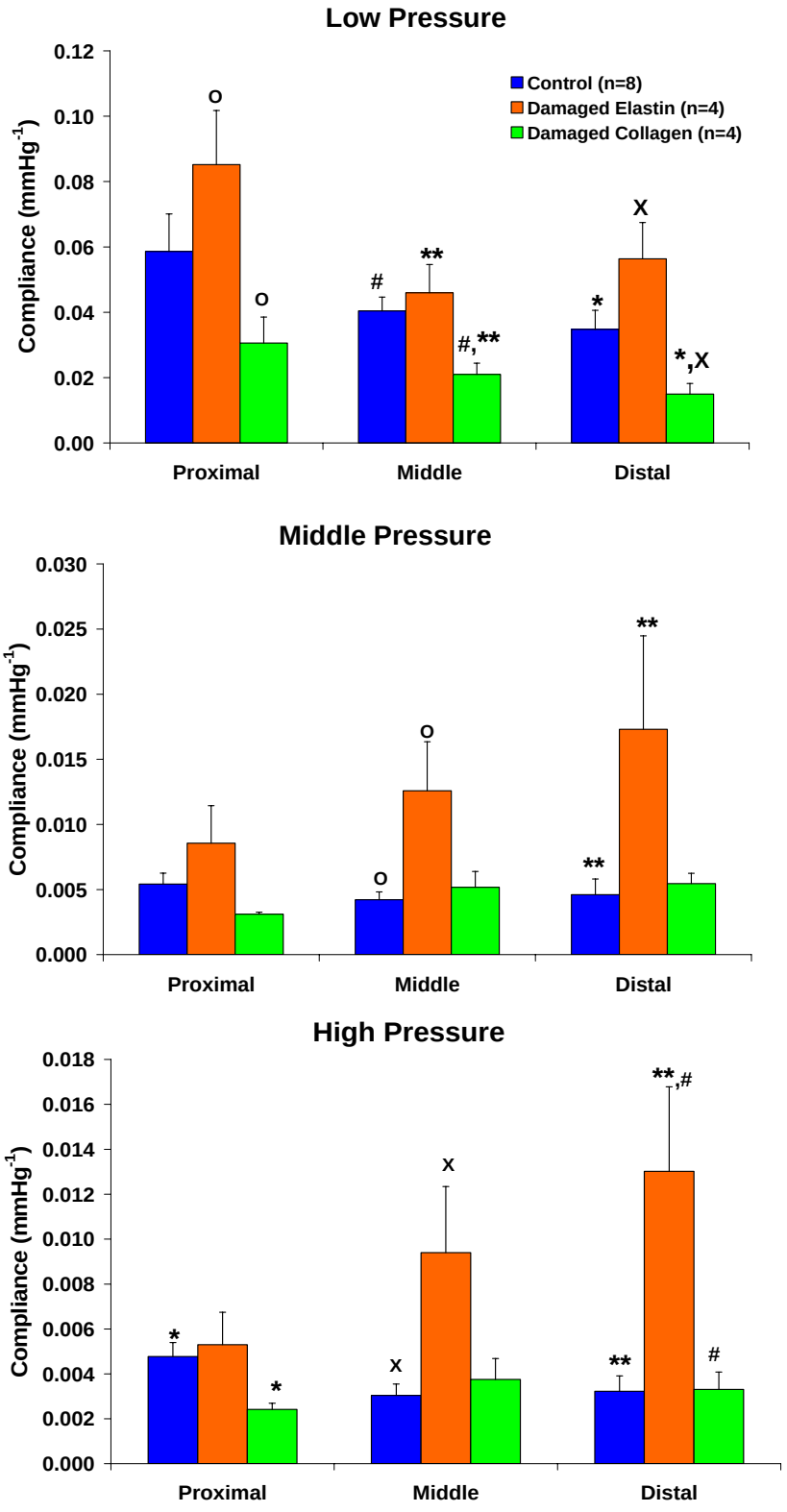

Figure 3.3 Low (top), middle (center), and high (bottom) pressure compliance values for control passive, damaged collagen (NaOH treated), and damaged elastin. Significance is represented by *,^{X},,#, ^{O} ($p<0.05$).**

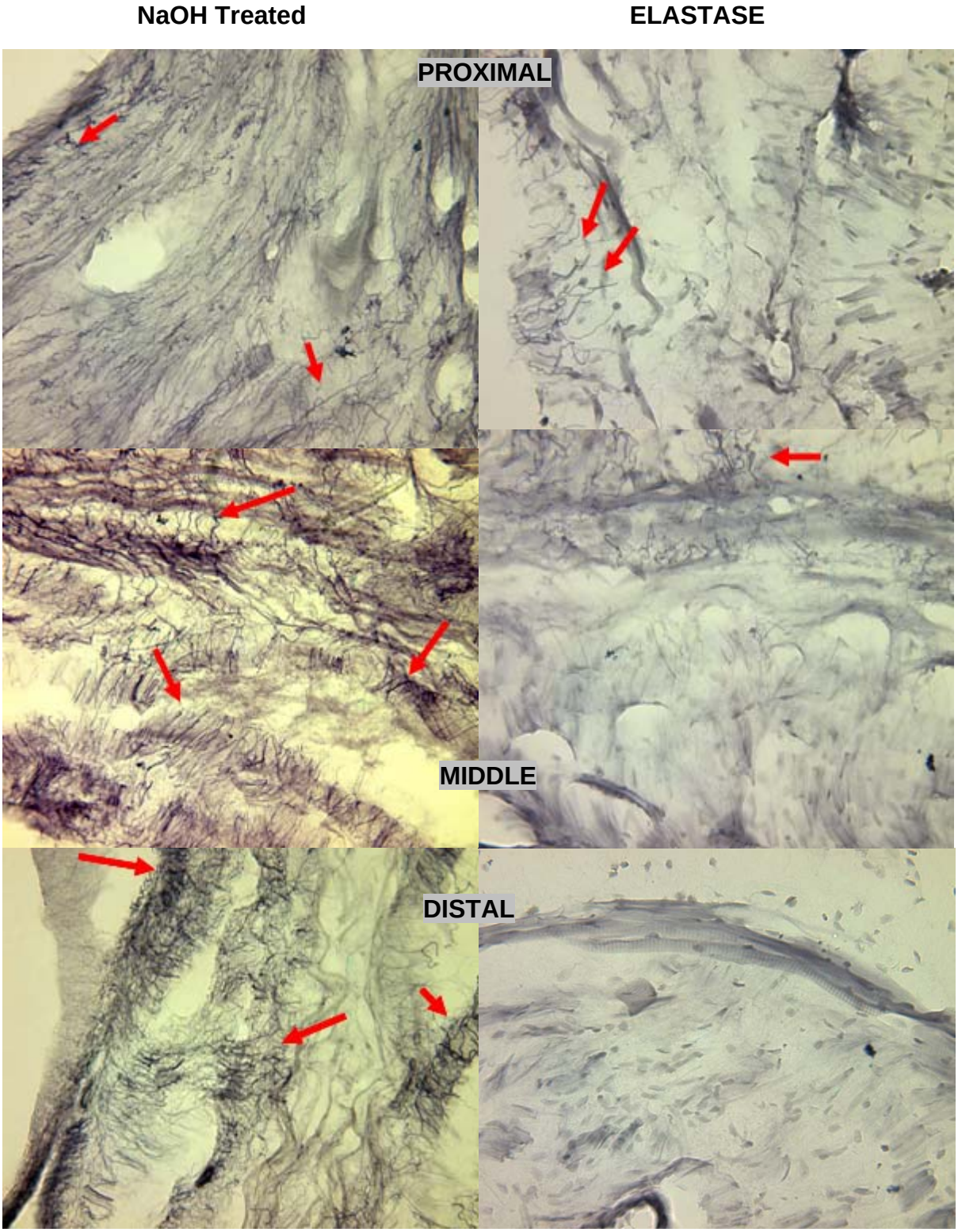

Figure 3.4 Miller's elastic stain for proximal (top), middle (center), and distal (bottom) segments of elastase treated (right) and NaOH treated (left) urethras. Red arrows exemplify bundles of elastic. Control and VD urethral sections can be seen in Figure 2.15.

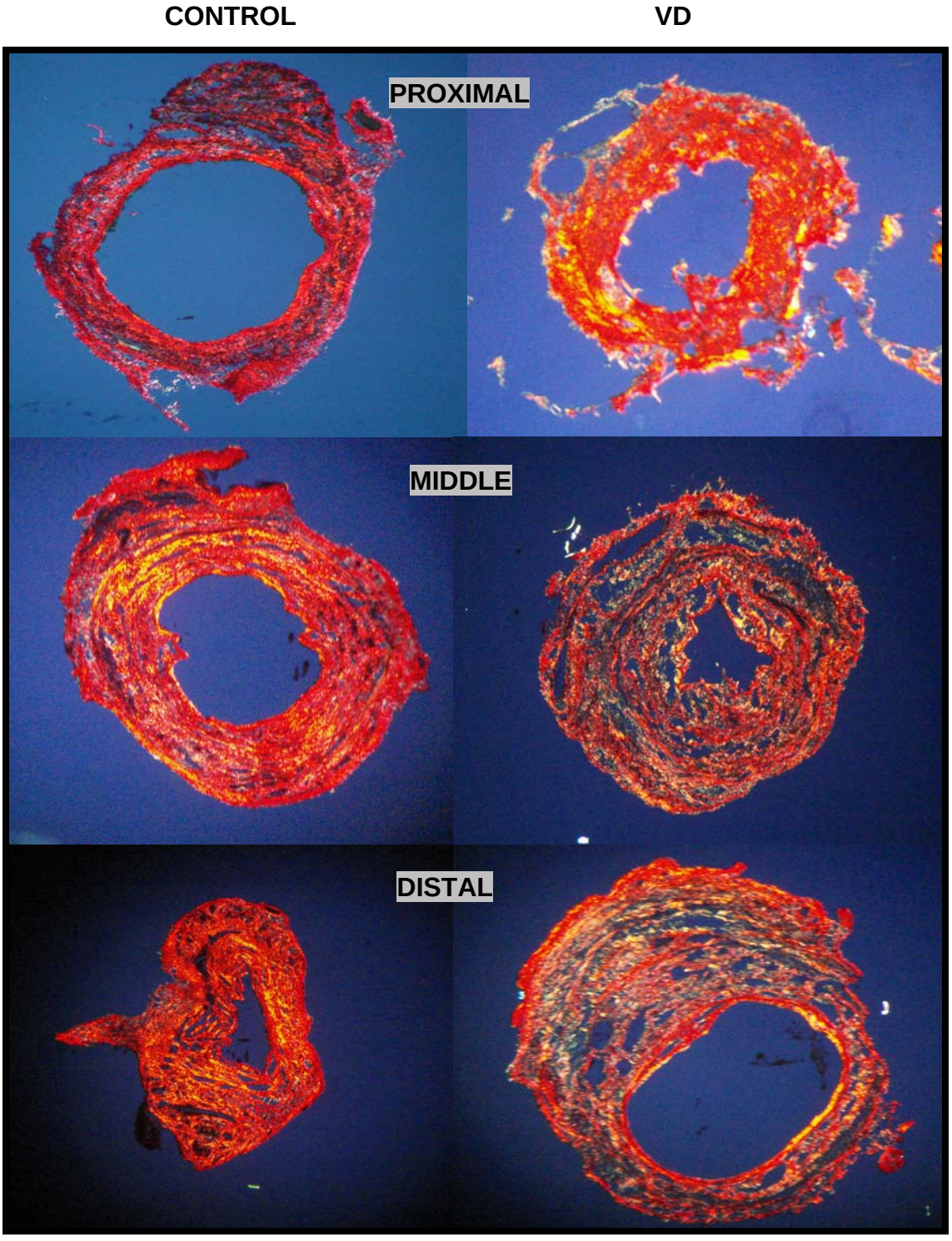

Figure 3.5 Picrosirius red stained urethral sections visualized with polarized microscopy for proximal (top), middle (center) and distal (bottom) segments of control (left) and collagen compromised (right) urethras. Images acquired at 4x. Control and VD urethras can be compared with Figure 2.12.

3.4 DISCUSSION

In summary, elastase treatment produced an increase in compliance, and compromised collagen (via NaOH treatment) caused a decrease in compliance (**Figure 3.3**). These results oppose that of similar studies performed on the vasculature. Of course, the results found for the urethra are credible, since the urethra has very different properties than that of a blood vessel, as well an extremely different function. Thus, it is important to pay attention to the structure and the correlate the results that have been established.

With elastase treatment, the urethra dramatically dilated (**Figure 3.1**). Assessment of control urethra histology (**Figures 2.13-2.15**) reveals that the elastic fiber bundles envelope the musculature as well as have a predominant radial alignment in the middle and distal submucosal region and have a predominat circular alignment in the proximal submucosal region and the outer striated and circular smooth muscle layers. All of this suggests that the elastic fibers role is to somehow "glue" the tissue together to maintain not only structure, but also urethral tone.

As for collagen compromisation with NaOH treatment, the urethra shrunk compared to that of passive controls (**Figure 3.1**). This indicated that collagen also helps maintain the stress on the tissue for urethral tone, although the finding was not as extreme compared to that of the elastase treated. Additionally, there was a significant decrease in compliance from damaged collagen (**Figure 3.3**). This may be due to the fact that the elastic fibers have no direction to transmit the stress of intralumenal pressure.

To illustrate the conclusions of these findings, Figure 3.6 offers a schematic of urethral wall components (smooth muscle, elastic fibers, and collagen) and their roles in a healthy urethra. Thus, it can be hypothesized from these findings that smooth muscles are embedded in elastic fiber bundles which are connected to a collagenous structural framework. Upon a sudden

increase in bladder pressure from a cough, sneeze or laugh, pressure is transmitted to the urethra wall where it receives a signal via innervation or mechanical distention. The urethral wall increases urethral pressure by contracting smooth musche and stretching the elastic fibers, which transmit their stress onto a collagen framework. This results in a urethral contraction and maintaining incontinence. Alternatively, if the elastic and collagen fibers are damaged, the smooth muscle would be unable to coordinate with the extracellular matrix and have the inability to maintain a high urethral pressure to avoid urine leakage.

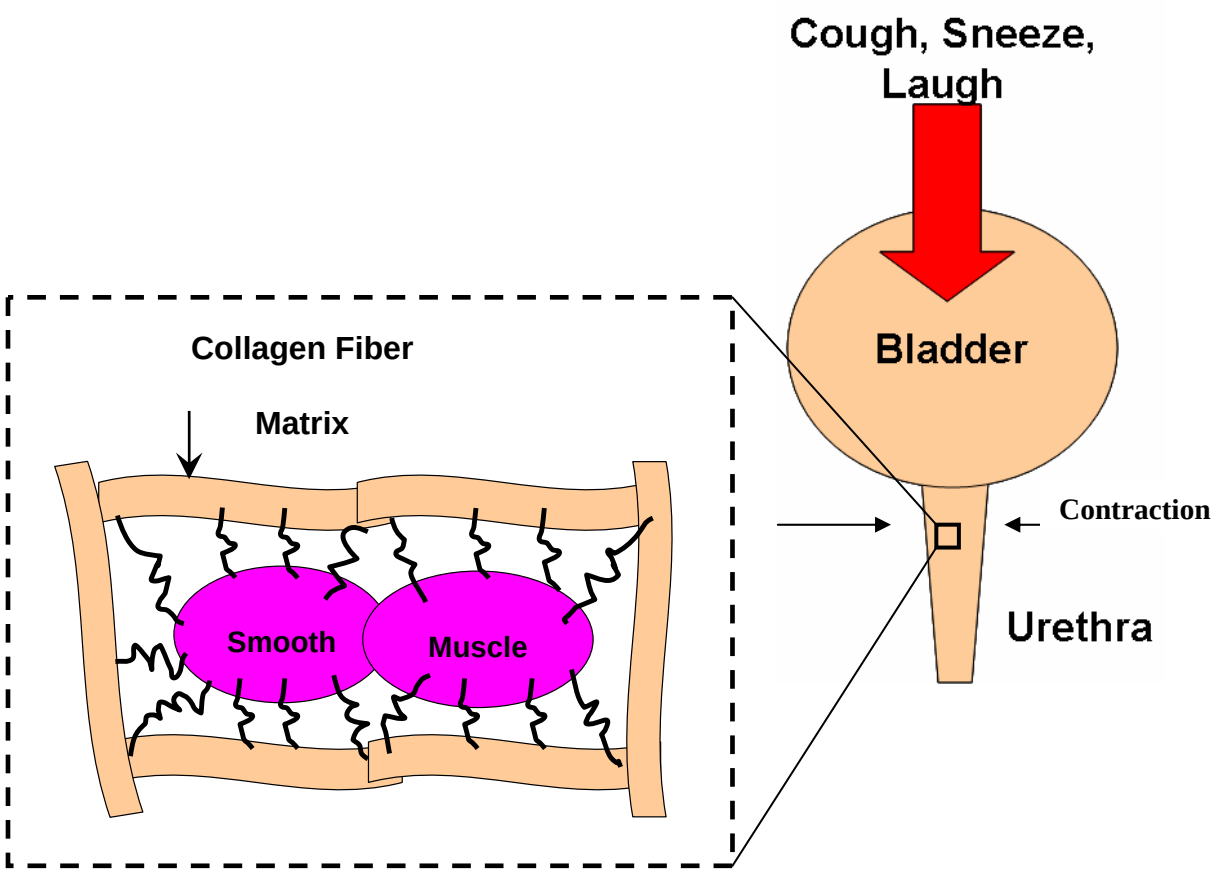

Figure 3.6 A schematic of the urethral components that are involved in urethral contraction in response to a sudden increase in bladder pressure. The smooth muscle fibers are connected via elastic fibers to a collagen matrix.

4.0 BIOMECHANICS OF THE FEMALE RAT URETHRA IN SUI IN THE PRESENCE OF AN ADRENERGIC AGONIST

4.1 SIGNIFICANCE OF THE ADRENERGIC RESPONSE OF URETHRAL SMOOTH MUSCLE IN SUI

In order to assess the contribution of urethral musculature to urethral function, it is important to assess the tissue in the active state. Active tone refers to a state where smooth and/or striated muscle is pre-contracted so that muscle activity may be evaluated biomechanically. As mentioned in Section 1.3.2, α_1-adrenergic agonists have been used as a pharmacotherapy for SUI, but the major side effects, including high blood pressure, outweigh the benefits.

Adrenergic receptors are thought to play a major role in the contraction of the circular urethral smooth muscle [106]. While there has been many attempts to characterize the urethra ex vivo in the presence of an adrenergic agonist, not many studies have concentrated on the effects of VD.

4.2 METHODS

4.2.1 Smooth muscle: adrenergic agonist assessment

Urethral smooth muscle was assessed with a sympathetic α_1 adrenergic agonist, phenylephrine (#P6126, Sigma Chemical Co., St. Louis, MO). Initially, the tissue was pressurized with 8 mmHg of intralumenal pressure. A nitric oxide inhibitor, Nω Nitro L-arginine (NOSi; 100 µM; #N5501, Sigma Chemical Co.), was added to the bath in order to inhibit the synthesis of nitric

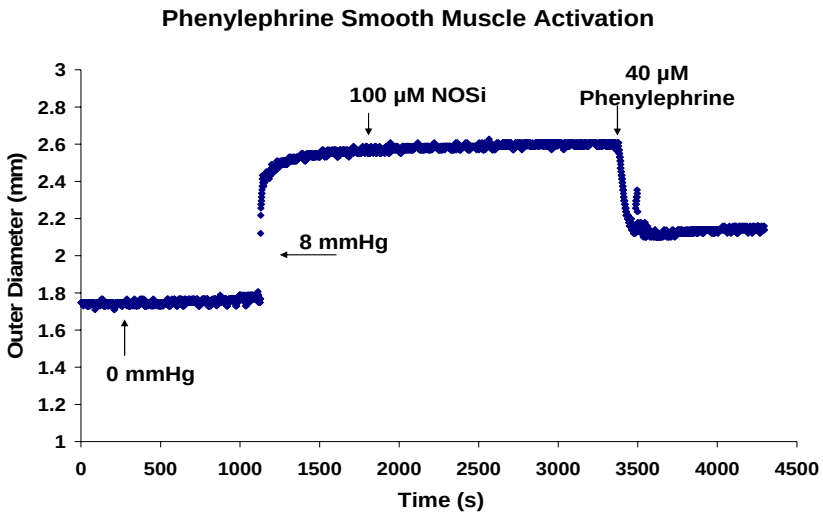

Figure 4.1 A depiction of the regimen for smooth muscle activation via phenylephrine (PE)

oxide and to ensure maximal smooth muscle contractility is achieved. A maximum concentration of phenylephrine (40 µM) was then added to the bath to induce a smooth muscle contraction (**Figure 4.1**). All maximum concentrations of agonists had to be verified with a concentration-response curve. *The details of these experiments are provided in Appendix E.*

4.2.2 Pharmacological assessment

Tissue responses were measured at proximal, middle, and distal portions of the urethra following addition of muscle agonists or antagonists for both normal and VD urethras. For these experiments, the urethra was exposed to a fixed intraluminal pressure of 8 mmHg, which caused the tissue to be dilated and allowed for a measurable amount of contraction to take place. Upon pressurizing the urethra at 8 mmHg, the specimen was permitted to reach a constant outer diameter (D_{8mmHg}). This measurement allowed the determination of the relative percentage change in outer diameter (%ΔD), following the addition of muscle-responsive agents. Most agents were added consecutively and in a similar manner to active biomechanical protocols: 100μM [107] Nω-Nitro-L-arginine (NOSi), a nitric oxide synthase (NOS) inhibitor, 40 μM phenylephrine, a nonselective α_1-adrenergic receptor agonist, and 3 mM [108] ethylenediamine tetraacetic acid (EDTA), a calcium chelator. Specifically, %ΔD was calculated as in equation 4.1:

$$\%\Delta D = \left(\frac{D_{drug} - D_{8mmHg}}{D_{8mmHg}} \right) \times 100 \qquad \textbf{(4.1)}$$

where D_{drug} represents the diameter response to each respective pharmacologic agent, and D_{8mmHg} is defined as the baseline diameter measured at an intralumenal pressure of 8 mmHg prior to addition of any pharmacological agents. At the time of pressure application or drug addition, the diameter was taken as an average of the last 100 data points of recorded diameter before the addition of pressure or drug. Calculations for %ΔD were performed for the maximal diameter response to 8 mmHg, NOSi, and EDTA. Comparisons were made between control and VD urethras. VD urethras were prepared using the animal model discussed in **Section 2.2.2**.

4.2.3 Biomechanical experiments

Urethras were isolated and implanted into the system as detailed in **Sections 2.2.3** and **2.2.4**, respectively. Once the tissue was fully contracted, the pressure was decreased from 8 mmHg to 0 mmHg of intralumenal pressure. The tissue was then subjected to stepwise increases in pressure ranging from 0 to 20 mmHg in 2 mmHg increments. Each step was held for 10 seconds to ensure that the testing occurred during the duration of muscle contraction. This process was repeated for proximal, middle, and distal portions in random order for smooth muscle assessment.

4.2.4 Parameters for active measurements

Circumferential stress and strain was calculated for a thick walled, homogeneous cylinder as detailed in **Section 2.2.5.3**. In order to compare the cirumferential stress between control and VD groups, the stresses in the same strain range needed to be known [109]. Thus, each calculated stress-strain curve was fit to a third order polynomial for active curves. Strain ranges were chosen for low, middle, and high strain values for control and VD urethras. Fits were performed with a statistical software package, SPSS (version 15.0, SPSS Inc., Chicago, Illinois). All fits had values of $R^2 \geq 0.987 \pm 0.013$. This procedure was performed for all active biomechanical procedures.

Fridez et al. [110] developed a method to assess the contribution of smooth muscle activity to the vascular wall properties. This method was adapted for the urethral wall so that muscular changes in the urethral wall could be detected post-VD. The functional contraction ratio (FCR) index is a non-dimensional index that depicts the relation of pressure to the contraction of the urethra and its passive response. Plotting the FCR versus static pressure

provides an idea of muscle behavior with increasing pressure (**Figure 4.2**). FCR is calculated using:

$$FCR = \frac{\Delta D_n}{D_p} \tag{4.2}$$

Here, ΔD_n represents the difference between active and passive outer diameter measurements at each respective pressure, and D_p is the corresponding passive outer diameter measurement at each pressure.

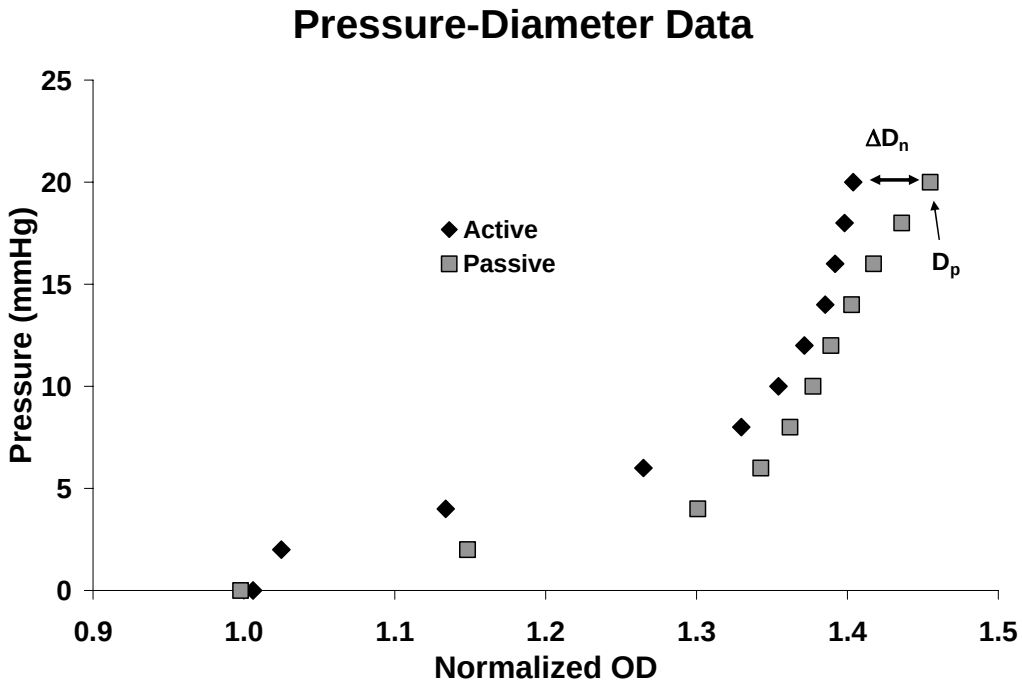

Figure 4.2 Graphical representation of FCR using active and passive pressure diameter data

4.2.5 Immunohistochemistry

For analyses of neural changes from VD, the urethra was analyzed with protein gene product 9.5 (PGP 9.5; Accurate Chemical Co., #YBG78630507, Newbury, NY) to assess general nerve damage and tyrosine hydroxylase (TH; Immunostar Inc., #22941, Hudson, WI) to assess sympathetic nerve fiber changes. Tissue sections had a thickness of 10 microns for immunohistochemical analyses.

PGP 9.5 is a rabbit polyclonal antibody, which is highly specific for an enolase commonly found in all nerve tissues. Sections were washed in PBS several times for 10 minutes each. The antibody was diluted to 1:1000 in a solution (a.k.a., PBDT) composed of phosphate buffered saline (PBS), 0.3% triton, and 2% donkey serum (Jackson Laboratories, #017-000-001, Bar Harbor, Maine). Sections were incubated with the diluted primary antibody overnight at 4°C. Next, sections were washed in PBS several times for 10 minutes each. Secondary antibodies (cy3, IgG fragment f(ab)2 donkey anti-rabbit, Jackson Laboratories, #711 165 152, Bar Harbor, Maine) were diluted to 1:800 in PBDT and incubated on tissue sections for 2 hours at room temperature. Slides were rinsed with PBS, dried and coverslipped with aqueous mountant.

TH is common to nerves that release catecholamines. It is the enzyme responsible for catalyzing the conversion of the amino acid, L tyrosine, to dihydroxyphenalanine (DOPA). DOPA is a precursor for dopamine, which is also a precursor for norepinephrine. Sections were rinsed with PBS several times for 10 minutes each followed by an incubation in PBDT for 45 minutes at room temperature. Sections were then incubated in a diluted primary antibody (1:1000; mouse TH) for 24 hours at 4°C. Sections were rinsed with PBS, and the secondary antibody (cy3, IgG fragment f(ab)2 donkey anti-mouse; Jackson Laboratories, #715 166 151, Bar Harbor, Maine) was diluted to 1:1000. Sections were incubated with the secondary antibody for

2 hours at room temperature. Finally, sections were rinsed with PBS several times and coverslipped with aqueous mountant.

4.2.6 Statistical analyses

Statistical comparisons were performed similarly to **Section 2.2.8**, and curve fits were performed with the software package, SPSS. For active biomechanical data, FCR was compared using two factor ANOVA with repeated measures where group (VD vs. control) was one factor and pressure level (0 to 20mmHg) was the second factor. Post-hoc testing was performed with a Student-Neuman Keuhl's test. For non parametric data, Friedman Repeated Measures Analysis of Variance on Ranks was performed with a Dunn's pair-wise comparison post-hoc test.

Pharmacological data and results from biological endpoints (i.e., immunohistochemistry, histology, and biochemical assays) for control and VD comparisons were evaluated using a Students t-test for parametric data and a Mann-Whitney rank sum test for nonparametric data.

4.3 RESULTS

4.3.1 Effects of VD on urethral smooth muscle response to an adrenergic agonist

4.3.1.1 Functional results

While the adrenergic smooth muscle response in the distal urethra was relatively unchanged, VD affected proximal and middle urethral smooth muscle (**Figure 4.3**). In the

proximal urethral segment, there was no significant difference between control (n=8; 43.4 ± 6.5%) and VD (n=9; 50.9 ± 4.6%) in outer diameter response to an abrupt increase in static pressure to 8 mmHg, although the VD group had a slightly higher increase in urethral dilatation. There was no change in proximal urethral response to NOSi when comparing control (0.2 ± 0.4%) and VD (0.2 ± 1.5%). VD proximal urethras (12.5 ± 2.4%; p=0.02) had an increased contractile response to phenylephrine (PE) when compared to control proximal segments (5.9 ± 1.2%). Finally, the EDTA-induced relaxation was not affected significantly (9.8 ± 1.9% vs. 6.2 ± 1.5%; p=0.07), but trends indicated that there was a decrease in relaxation (i.e. dilated outer diameter) from VD in the proximal segment (**Figure 4.3**, top).

For middle urethral segments, the response to an increase in pressure to 8 mmHg was significantly less for VD urethras (n=8; 15.9 ± 1.9%) compared to controls (n=9; 29.4 ± 3.4%; p=0.005). VD did not affect urethral response to NOSi; yet, PE induced contraction for VD middle segments (3.6 ± 1.0%) was less than that of controls (6.3 ± 1.0%), although this did not quite reach significant (p=0.08). EDTA-induced relaxation was significantly higher for the VD group (10.54 ± 2.12%) compared to the control response (4.7 ± 0.7%; p=0.02; **Figure 4.3**, center).

All responses for the distal urethral segments were unaffected by VD, as indicated by the lack of significance for each agent. The response to an increase of pressure was similar for both controls (n=7; 18.69 ± 2.74%) and VD (n=7; 20.77 ± 4.51%), as well the response to NOSi (1.65 ± 0.43% vs. 1.52 ± 0.67%, respectively). Additionally, the contractile responses to PE and relaxation responses to EDTA were similar in control (4.19 ± 2.29% and 14.08 ± 3.79%, respectively) and VD (5.47 ± 1.90% and 10.96 ± 2.68%, respectively) distal segments (**Figure 4.3**, bottom).

4.3.1.2 Biomechanical Results

Average pressure-diameter data indicated changes of urethral properties pre-contracted with PE post-VD. For the proximal urethral segment, the VD (n=8) pressure-diameter curve was shifted to the right of that of controls along the entire pressure range (n=8; **Figure 4.4**, top). Pressure-diameter data for the middle urethral segment shifted to the left in VD compared to the control pressure diameter curve, especially for pressures ranging from 2 to 16 mmHg (**Figure 4.4**, center). Finally, there were no noticeable differences between the VD and control groups for the distal pressure-diameter curves.

FCR values (**Figure 4.5**) were analyzed utilizing paired changes between active and passive pressure diameter curves for both controls and VD. This provided the amount of smooth muscle activity contributing to the resistance of static intra-urethral pressure. FCR values for control proximal segments indicated that the urethral smooth muscle contributed to the active pressure-diameter curve by a maximum of 8.8% at 4 mmHg and then maintained steady tone (approximately 5-7%) for up to 20 mmHg. Conversely, smooth muscle in proximal segments of VD urethras only contributed a maximum of 6% at 2 mmHg to the active curve, followed by fading of contractile

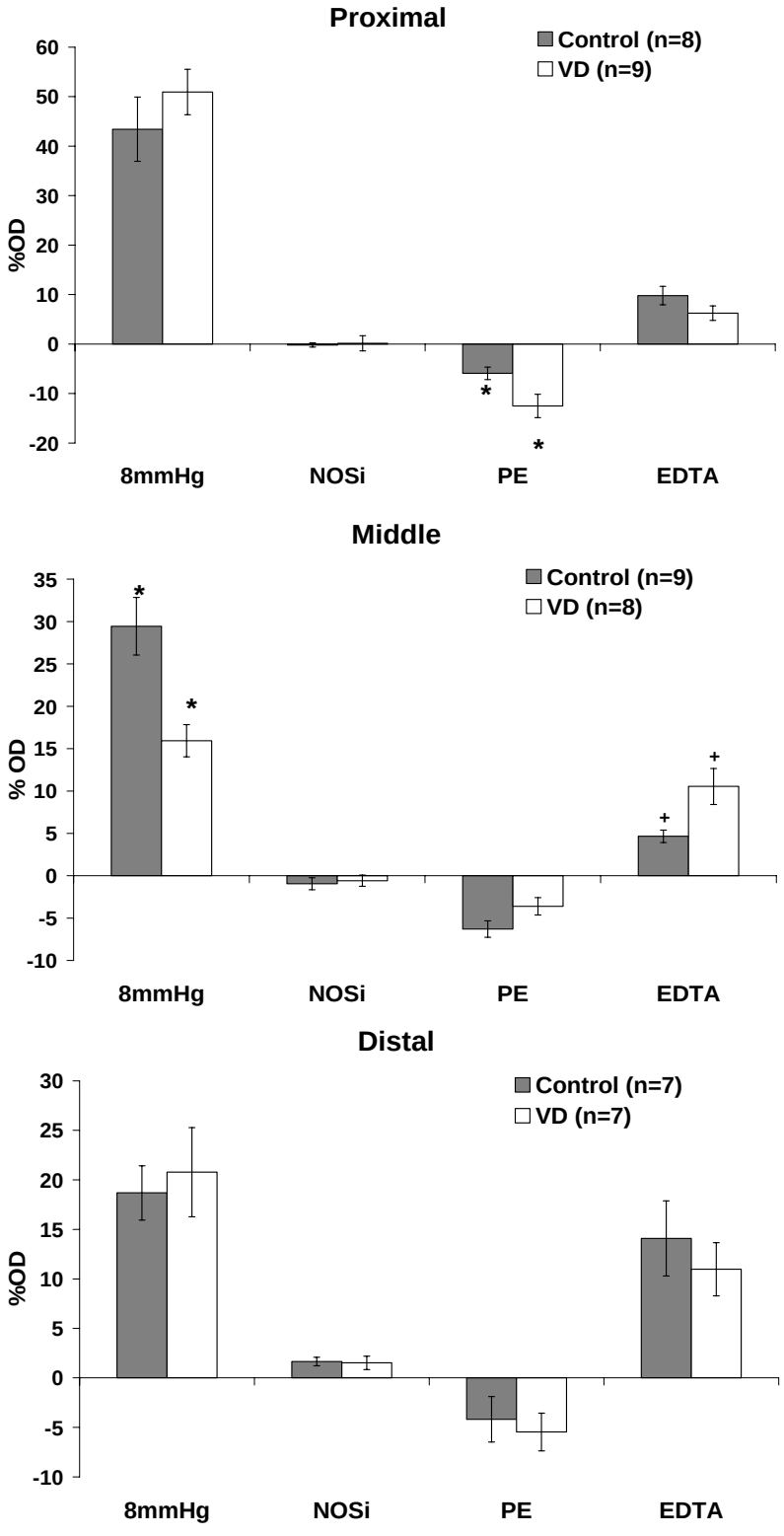

Figure 4.3 Urethral smooth muscle response to a pressure change of 8 mmHg, NOSi, PE, and EDTA for proximal (top), middle (center), and distal (bottom) in control and VD groups. Significant differences between groups are indicated by * and +.

smooth muscle tone with each increase in static pressure reaching negative FCR values by 6 mmHg (**Figure 4.5**, top). While the lack of smooth muscle contribution in the proximal segments of VD (-0.08 ± 0.07), urethras was dramatically less compared to controls (0.07 ± 0.02), the only significant decrease in FCR values was at 20 mmHg ($p<0.05$).

For middle urethral segments, FCR values indicated no changes after VD (**Figure 4.5**, center). However, trends indicated that control middle segments had higher FCR values (ranging from 0.08 ± 0.06 to 0.13 ± 0.05) than VD middle segments (ranging from 0.001 ± 0.02 to 0.08 ± 0.02) over the entire pressure range. Additionally, FCR values for segments indicated that VD did not alter smooth muscle response to adrenergic agonists under intralumenal pressure. Still, from pressure ranging from 6 to 20 mmHg, control distal segments (ranging from 0.07 ± 0.03 to 0.08 ± 0.04) maintained higher FCR values compared to that of VD (ranging from 0.06 ± 0.03 to -0.002 ± 0.02; **Figure 4.5**, bottom).

Similar to pressure-diameter curves, circumferential stress-strain (σ_θ-ε_θ; **Figure 4.6**) responses for proximal, middle and distal urethral segments were qualitatively evaluated for control and VD urethras in the presence of PE. For proximal segments, VD shifted the proximal σ_θ-ε_θ curve to the right of controls, indicating an increase in strain. VD also affected mid urethral segments. The shape of the control σ_θ-ε_θ curve for middle segments was exponential, but the curve for VD middle segments was sigmoidal. The σ_θ-ε_θ response curves for distal urethras appeared to be unaffected by VD.

Efforts were made to control for strain so that circumferential stress could be compared at low, middle, and high strain ranges. Data was pooled for each segment (i.e., proximal, middle, and distal) separately for control and VD active and passive data.

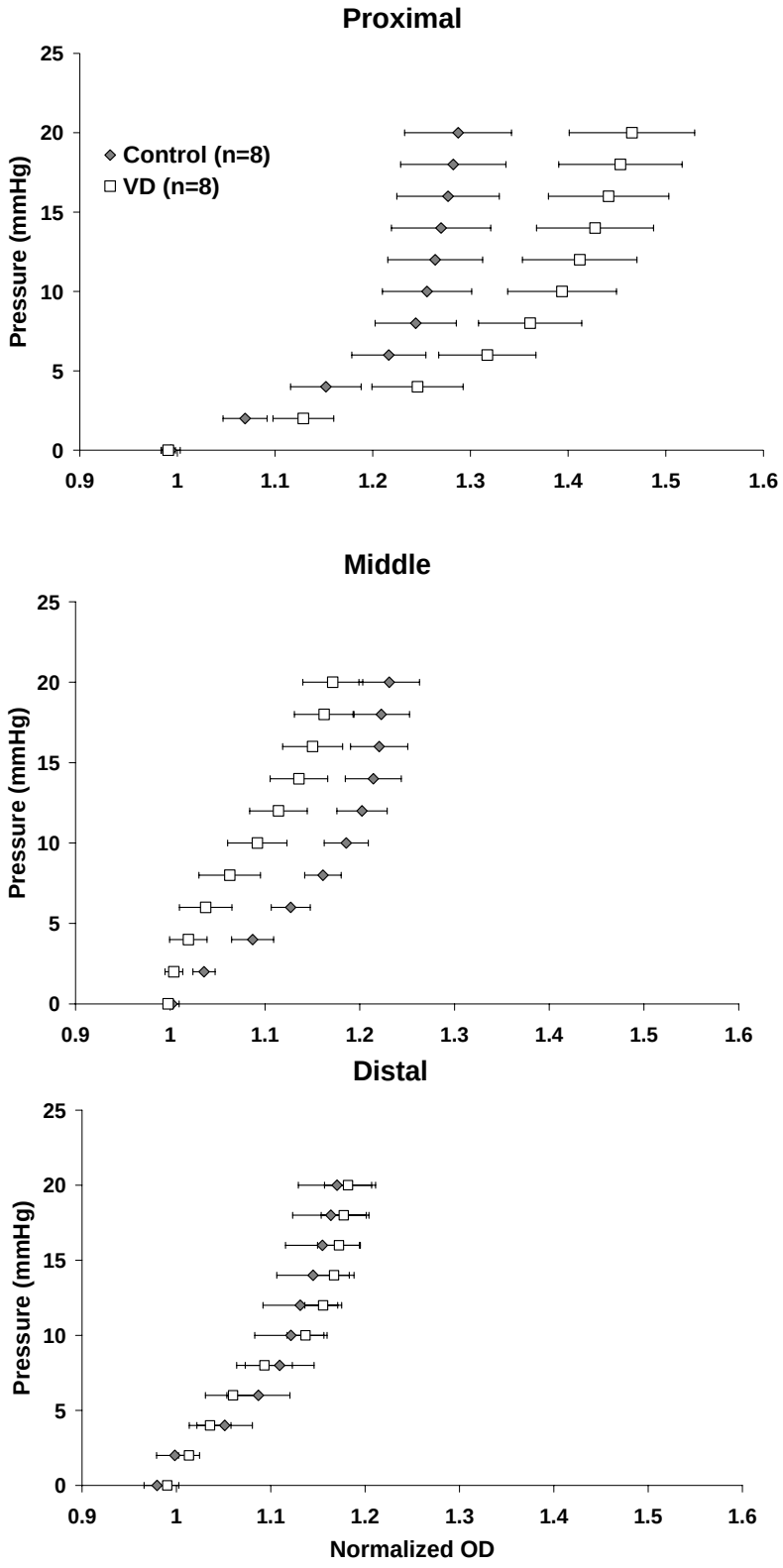

Figure 4.4 Pressure-diameter curves generated after pre-contraction with phenylephrine for the proximal (top), middle (center), and distal (bottom) segments.

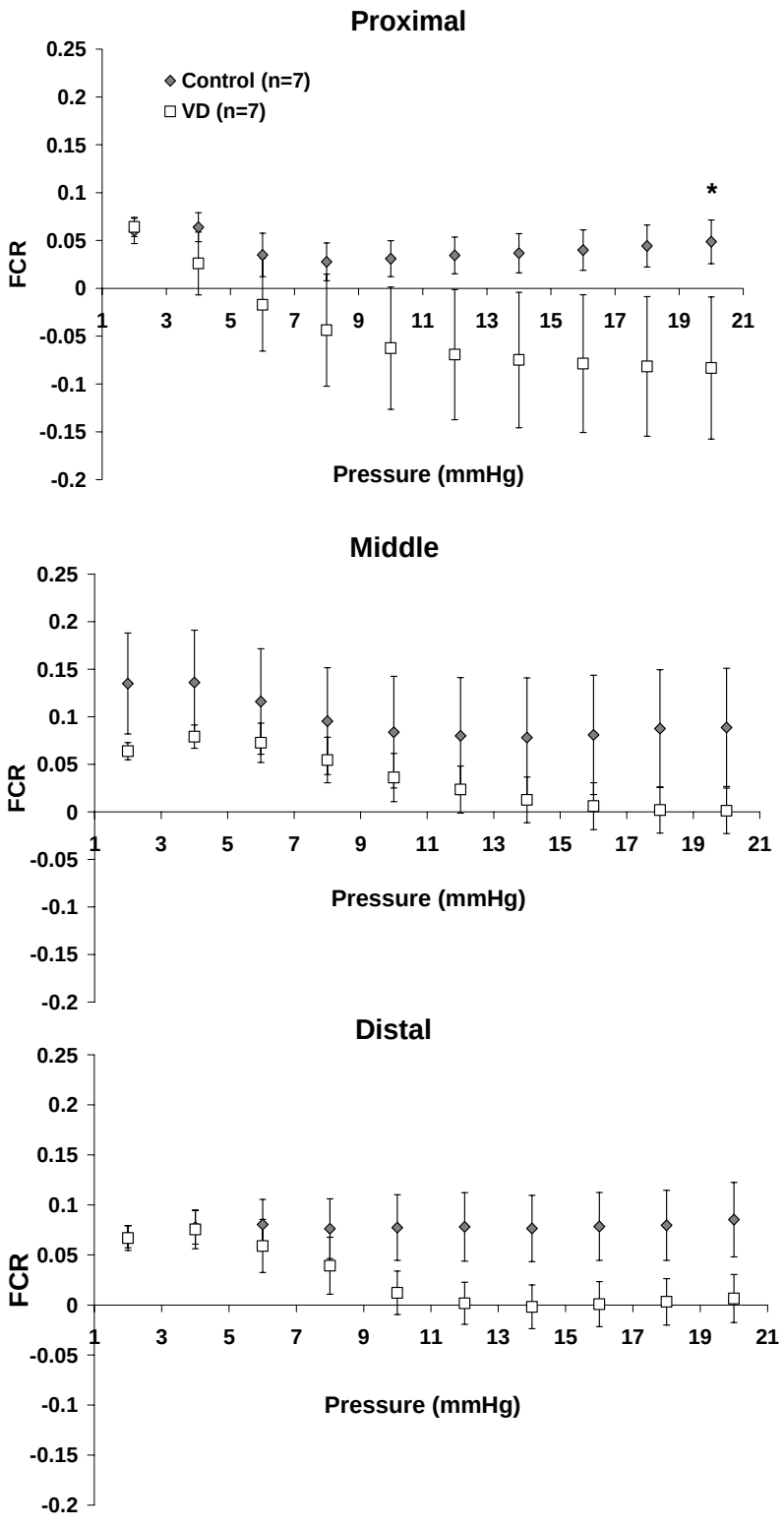

Figure 4.5 Functional contraction ration (FCR) value for proximal (top), middle (center), and distal (bottom) segments for both control and VD urethras. * indicates a significant difference between control and VD for the proximal FCR values at 20 mmHg ($p<0.05$).

Minimum and maximum strain ranges were determined. Proximal segments had low strain ranging from 0 to 0.3, middle strains from 0.4 to 0.9, and high strains ranging from 1 to 1.55. Low strains for middle segments ranged from 0 to 0.12, while middle and high strains ranged from 0.15 to 0.38 and 0.45 to 0.54, respectively. Finally, for distal segments, low strains ranged from 0 to 0.1, middle strains from 0.11 to 0.3, and high strains ranged from 0.31 to 0.55.

At low strain ranges, σ_θ values for VD proximal urethras (n=7) were significantly less than that of controls (n=7), more specifically for ε_θ ranging from 0.03 to 0.12 ($p<0.001$). The VD group maintained lower σ_θ values at mid strain rangines compared to that of controls, although this was not a significant comparison. Finally, there were no significant changes at high strain values, but at maximum strains, the VD group had a higher σ_θ value compared to that of controls (**Figure 4.7; Table 4.1**).

VD had the opposite effect of the adrenergically-induced mechanical activity of the middle urethral portion. For low ε_θ values, the middle urethra of the VD group (n=7) produced higher σ_θ values compared to that of controls (n=7; $p<0.001$) along the entire strain range from 0-0.12. At mid ε_θ values, the VD urethra maintained higher σ_θ values, but they were not significant. High ε_θ values indicated that the control group had higher σ_θ values although these values were not significant (**Figure 4.8; Table 4.1**).

The biomechanical response of the distal segment in the presence of an adrenergic agonist was not affected by VD. At all strain ranges there were not significant comparisons, and both the control (n=7) and VD (n=7) urethras had a similar σ_θ-ε_θ response (**Figure 4.9; Table 4.1**).

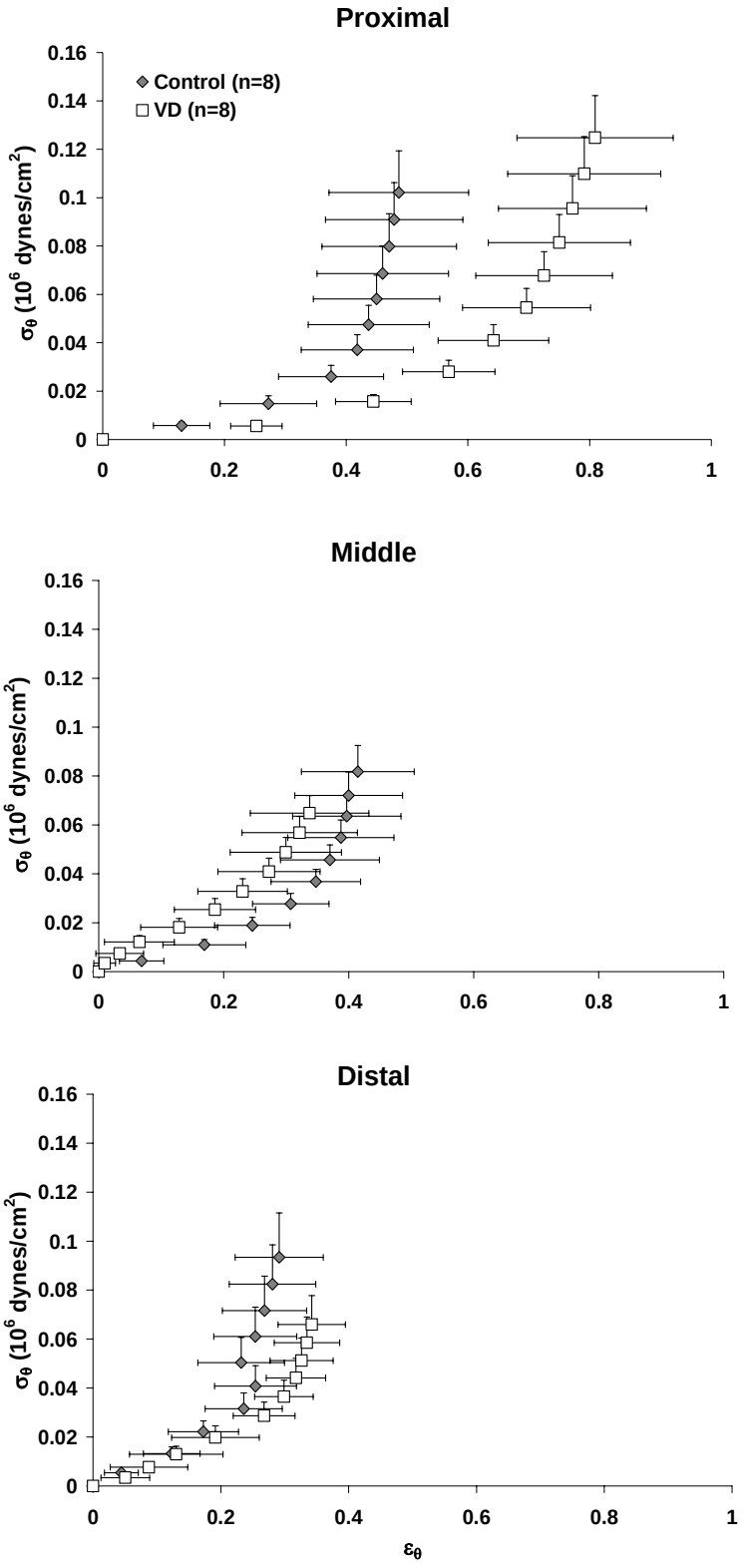

Figure 4.6 Circumferential stress-strain response for proximal (top), middle (center) and distal (bottom) for both control and VD groups in the presence of PE

Table 4.1 Peak stress values (x 10^6 dynes/cm^2) for peak ε_θ values within low, middle, and high strain ranges comparing control and VD urethras in the presence of an α_1 adrenergic agonist. * indicates a significant difference, where p<0.001

	CONTROL n=7			VD n=7		
	Proximal	**Middle**	**Distal**	**Proximal**	**Middle**	**Distal**
Low $\sigma_{\theta max}$	0.02 ± 0.01	0.01 ± 0.004*	0.02 ± 0.005	0.01 ± 0.003	0.03 ± 0.007*	0.02 ± 0.003
Mid $\sigma_{\theta max}$	1.54 ± 0.88	0.30 ± 0.18	0.20 ± 0.07	0.52 ± 0.21	0.38 ± 0.14	0.13 ± 0.10
High $\sigma_{\theta max}$	10.33 ± 6.00	10.06 ± 5.05	1.73 ± 0.57	13.24 ± 9.07	4.14 ± 1.50	1.12 ± 0.8

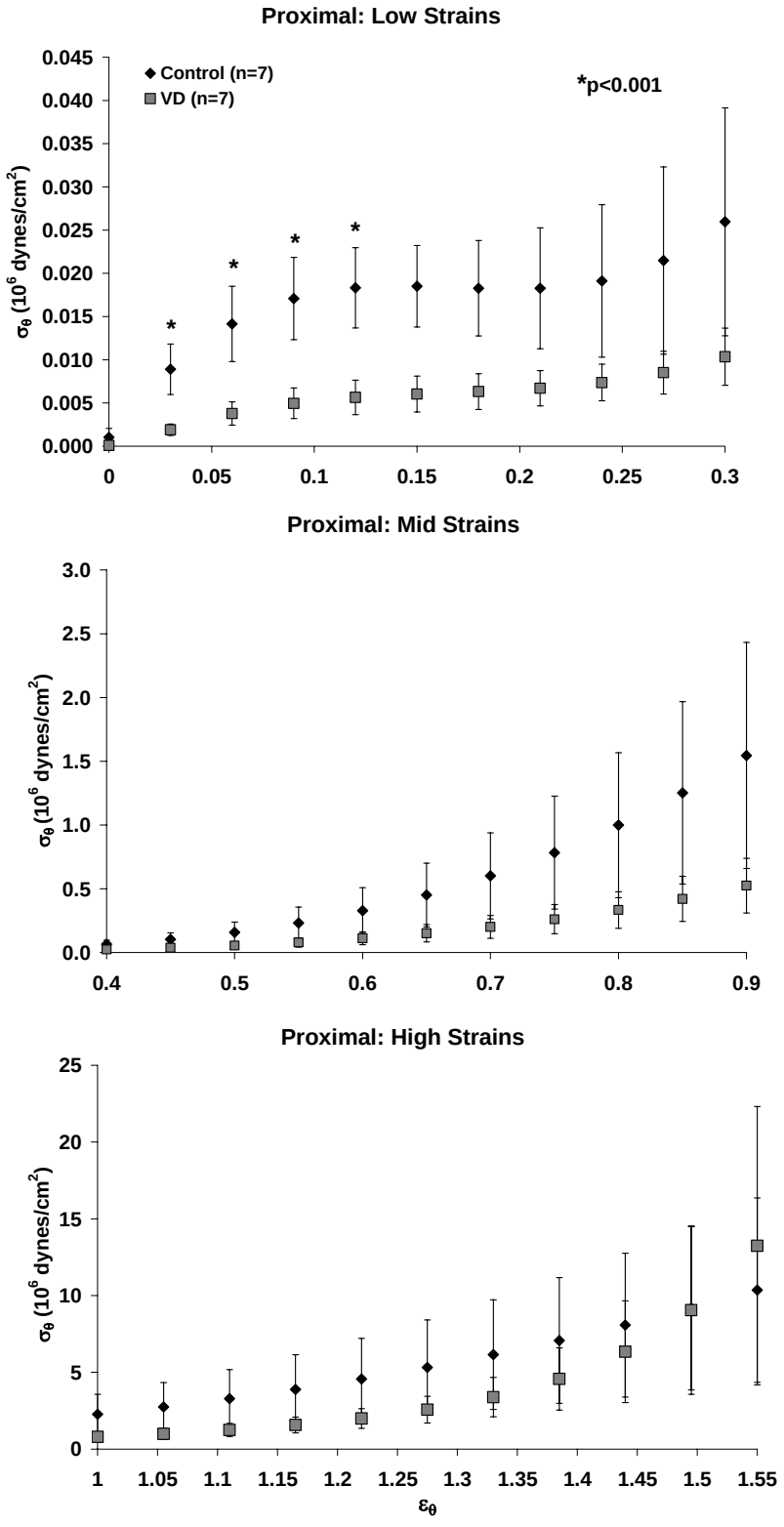

Figure 4.7 Proximal circumferential stress values for control and VD groups derived for low circumferential strains (0–0.3; top), middle circumferential strains (0.4–0.9; center), and high circumferential strains (1–1.55; bottom). Significance is indicated by * for comparisons between the control and VD groups at low strains ranging from 0.03 to 0.12 ($p<0.001$).

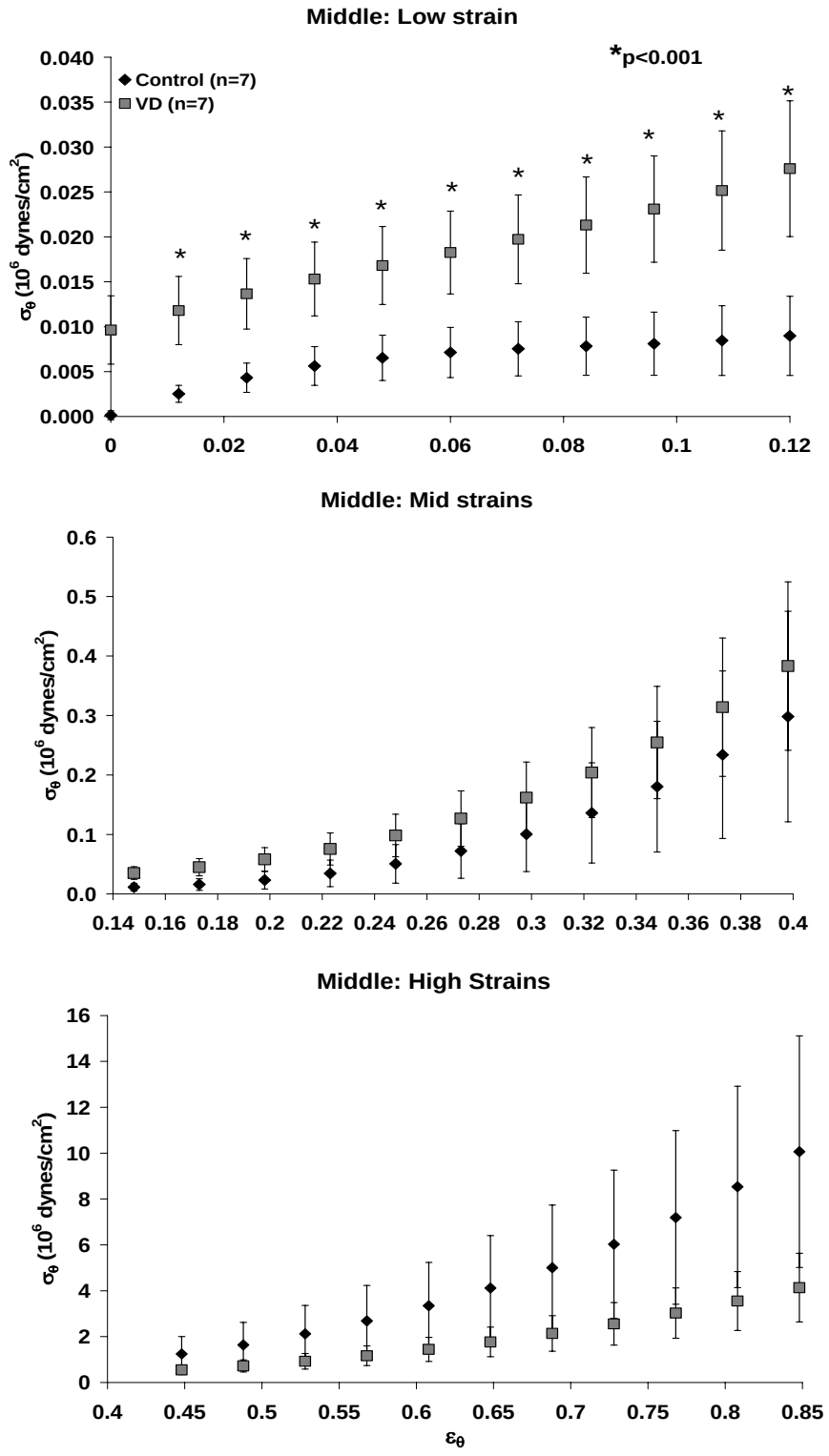

Figure 4.8 Middle circumferential stress values for low strains (0-0.12, top), mid strains (0.14-0.4, center), and high strains (0.45-0.85, bottom) for control and VD urethras. Significance is indicated by * where p<0.001 for low strain values, more specifically for values ranging from 0.012 to 0.12.

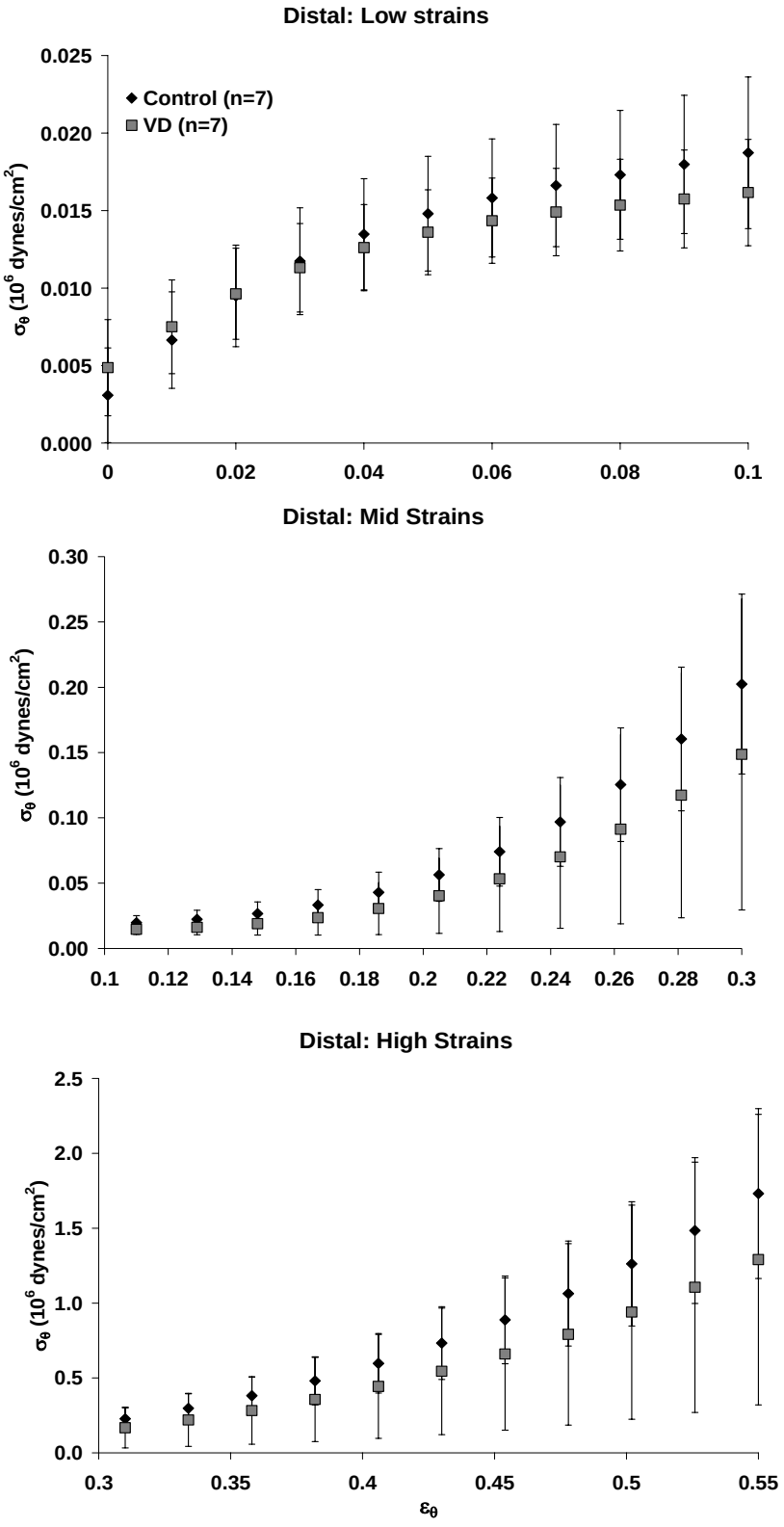

Figure 4.9 Distal circumferential stress values for low strains (0-0.1, top), mid strains (0.1-0.3, center), and high strains (0.3-0.55, bottom) for control and VD urethras.

4.3.1.3 Immunohistochemistry results: PGP 9.5 and tyrosine hydroxylase (TH)

PGP 9.5 was used in order to assess the density and distribution of nerve tissue for control (n=8) and VD (n=8) urethras. In control urethras, PGP 9.5 staining was localized in urethral smooth muscle, around the vasculature, throughout the striated muscle, and the urothelial layer. For VD urethras, much of the positive staining for the striated muscle, vasculature, as well as the smooth muscle layer, was lacking (**Figures 4.10-4.11**). The urothelial layer had thickened after VD, more specifically for the proximal and middle segments (**Figure 4.11**).

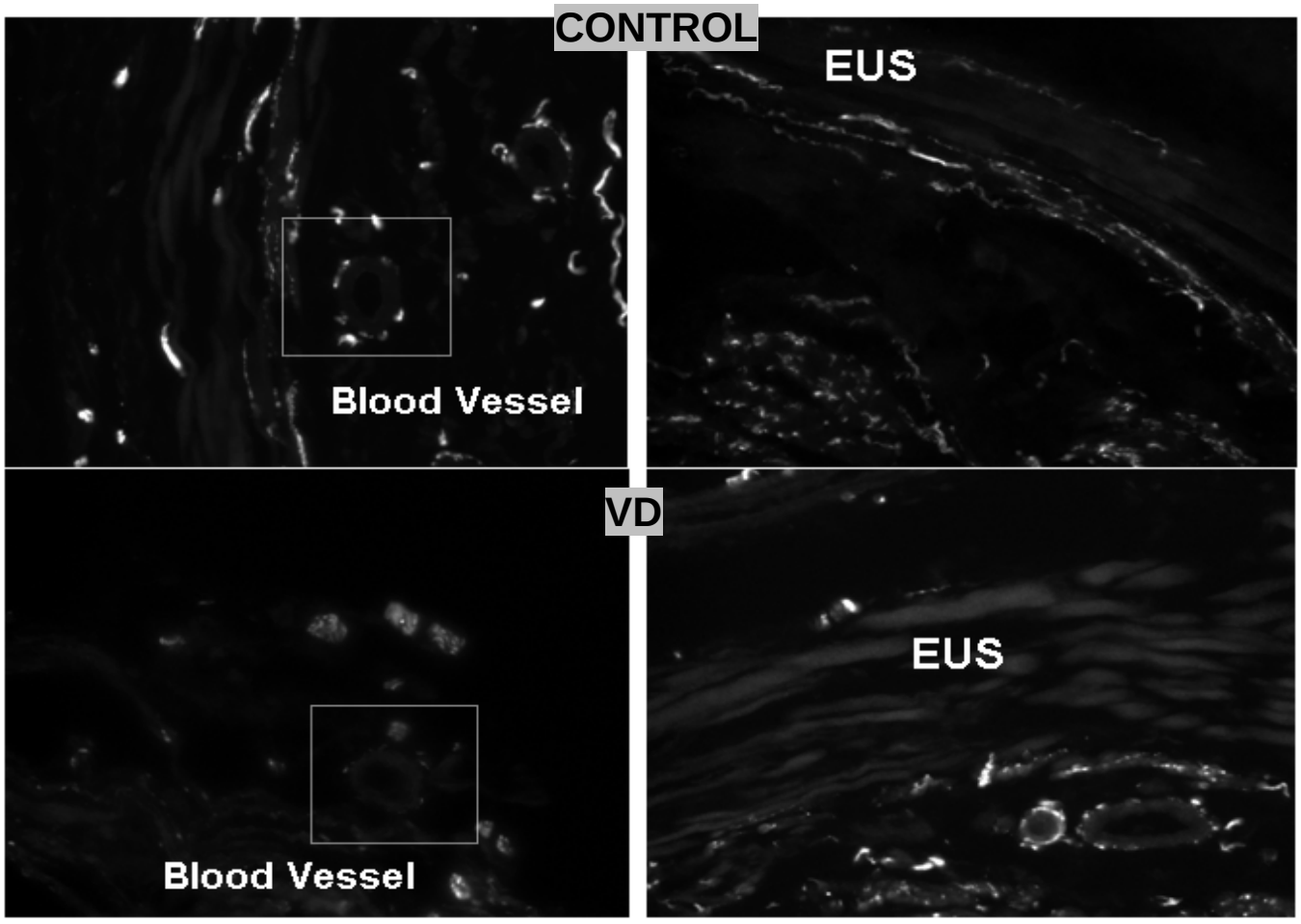

Figure 4.10 Positive PGP 9.5 staining surrounding blood vessels and throughout the external urethral sphincter (EUS; top) in representative sections of control and VD urethras lacked this positive staining (bottom); Images acquired at 40x magnification.

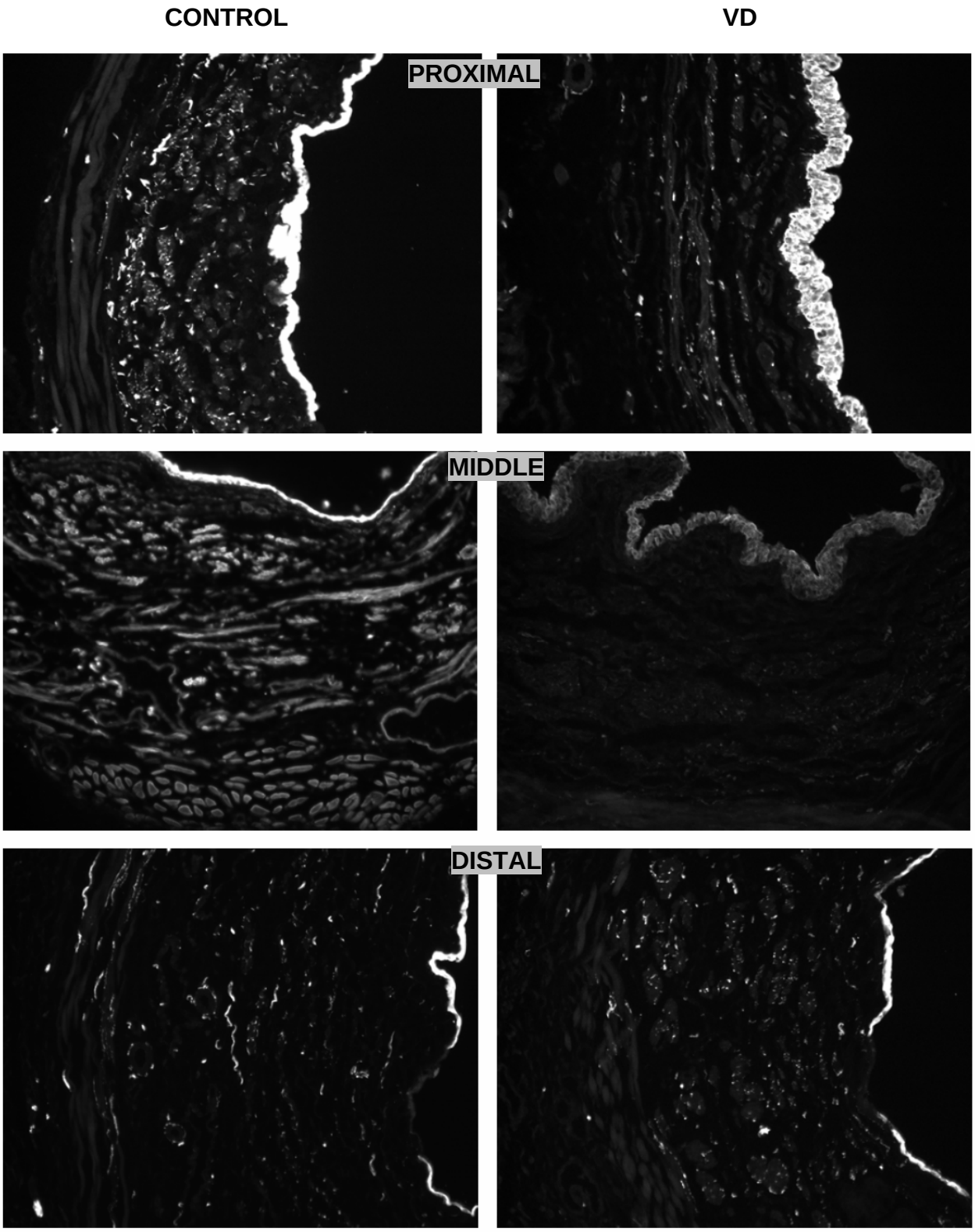

Figure 4.11 PGP 9.5 immunoflourescence acquired at 20x magnification for representative sections of control (left) and VD (right) proximal (top), middle (center), and distal (bottom) segments.

The urothelial layer was thicker in VD, area of staining was assessed not only as a whole, but also excluding the urothelium PGP 9.5 (**Figure 4.12**). In general, the control urethras had a higher percentage of positive staining than VD for proximal (12 ± 1% vs. 10 ± 0.8%), middle (10 ± 1% vs. 7 ± 1%), and distal (9 ± 1 % vs. 6 ± 1%) segments; although, this difference was not significant (**Figure 4.12**, top).

Alternatively, quantification of the medial and adventitial layer of the urethra (i.e., exclusion of the urothelium) revealed significant changes in the amount of PGP 9.5 staining (**Figure 4.12**, bottom). All three regions of the control urethra (6 ± 1%, 6 ± 1, and 5 ± 1% for proximal, middle, and distal segements, respectively) had a significantly higher amount of staining compared to that of VD (3 ± 1%, 3 ± 1, and 2 ± 0.4%, respectively; $p<0.05$) urethras.

TH was used to localize sympathetic nerve fibers. VD affected the presence of sympathetic nerves, as indicated by TH, but not significantly. Qualitatively (**Figure 4.13**), the urothelium did not stain positively as with the PGP 9.5. Most of this marker was found throughout the medial layer, where most smooth muscle is located, and in some small areas of the outer layer.

Quantifying the stained area for TH indicated significant changes for the proximal and middles segments. Proximal (2 ± 0.3%) and middle (4 ± 1%) controls had a higher percentage of TH compared to that of VD (1 ± 0.3% and 1 ± 0.3%, respectively; $p<0.05$). Unlike with PGP 9.5, there were no differences between control (3 ± 1%) and VD (2 ± 0.3%) urethras in the distal segment (**Figure 4.14**).

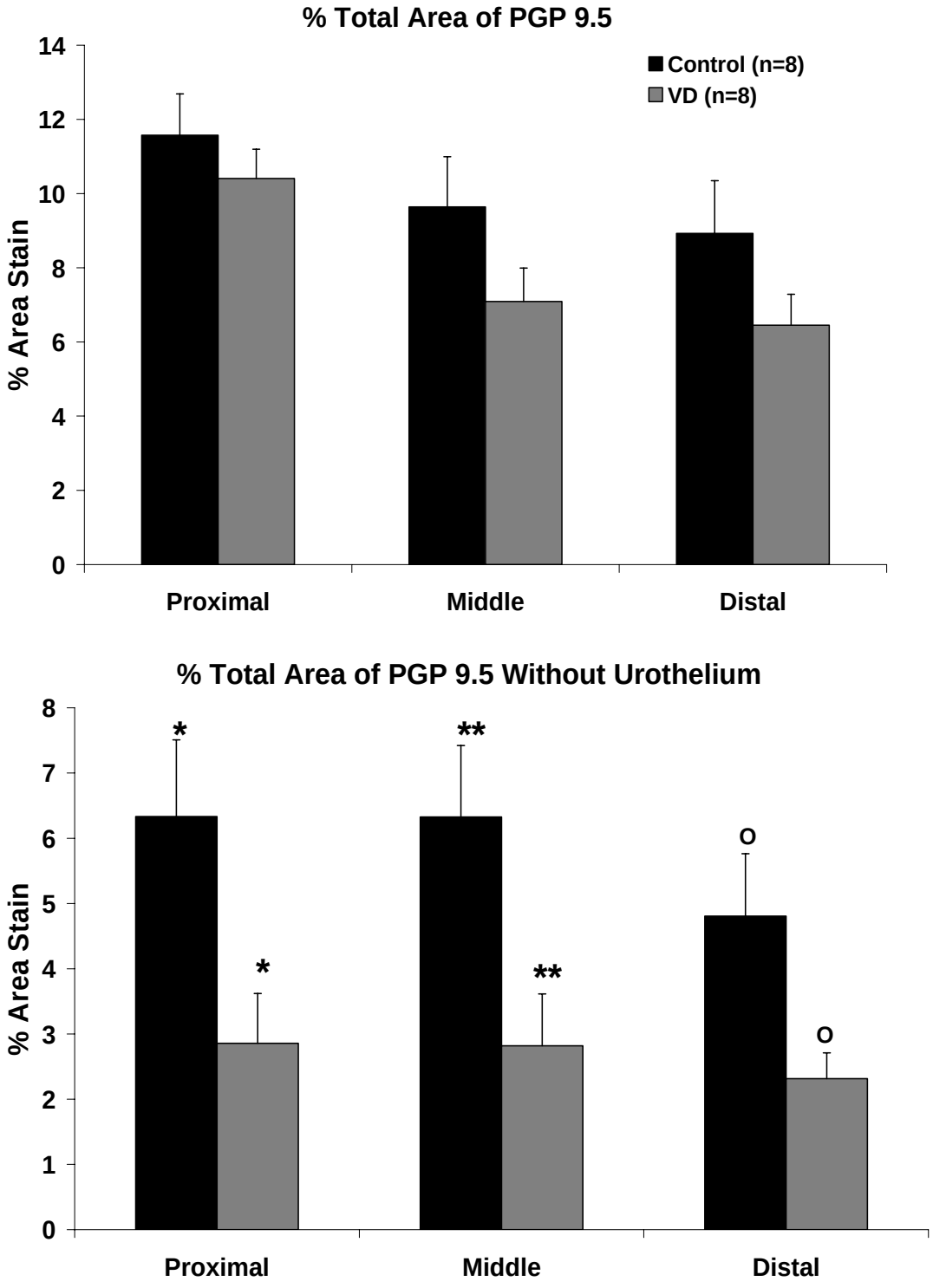

Figure 4.12 Area of positive PGP 9.5 staining for the entire urethral cross-section (top) and excluding the urothelium (bottom). Significant differences between groups are indicated by *,,O ($p<0.05$).**

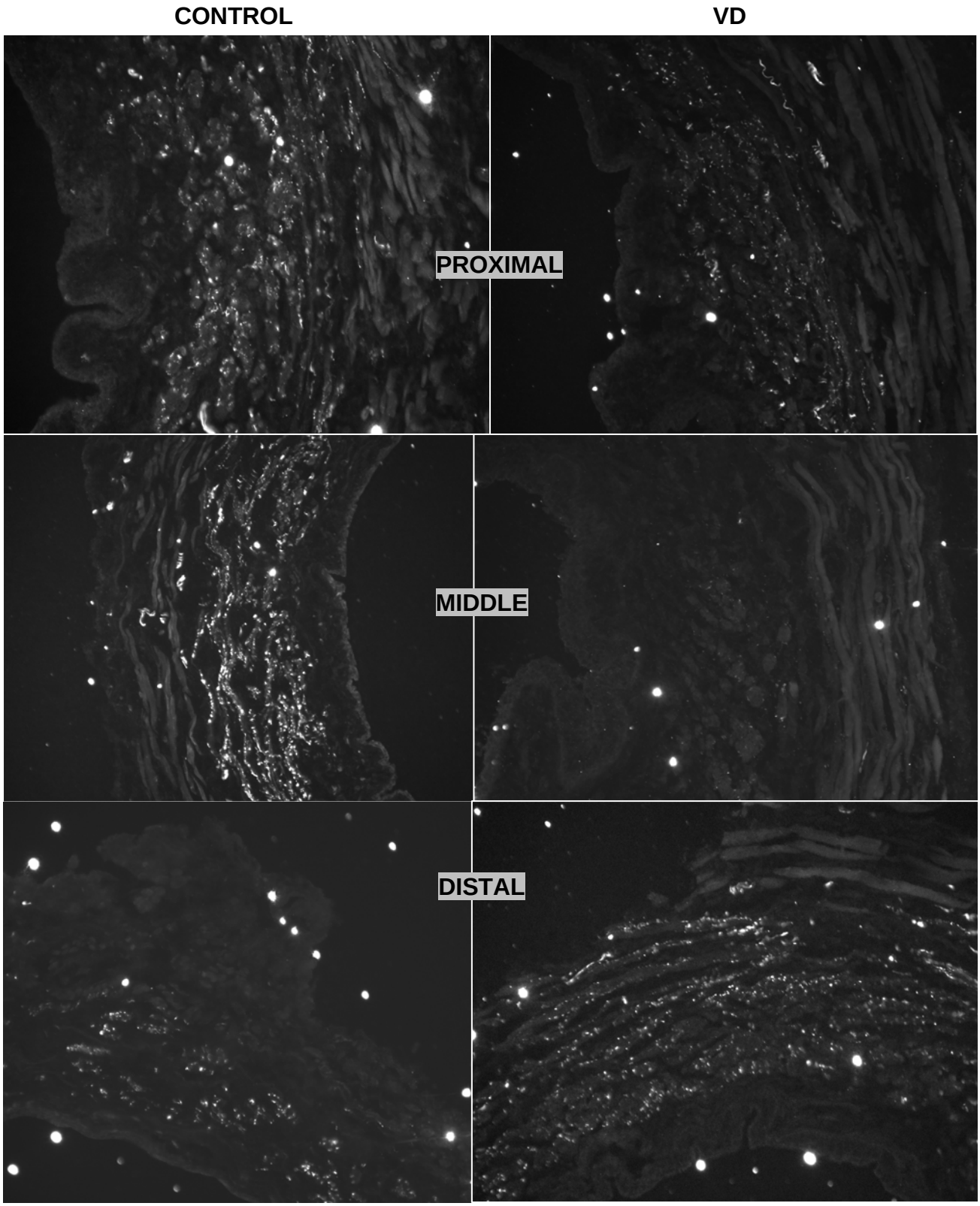

Figure 4.13 Tyrosine hydroxylase immunoflourescence acquired at 20x magnification; representative sections of control (left) and VD (right) urethras, for proximal (top), middle (center), and distal (bottom) segments.

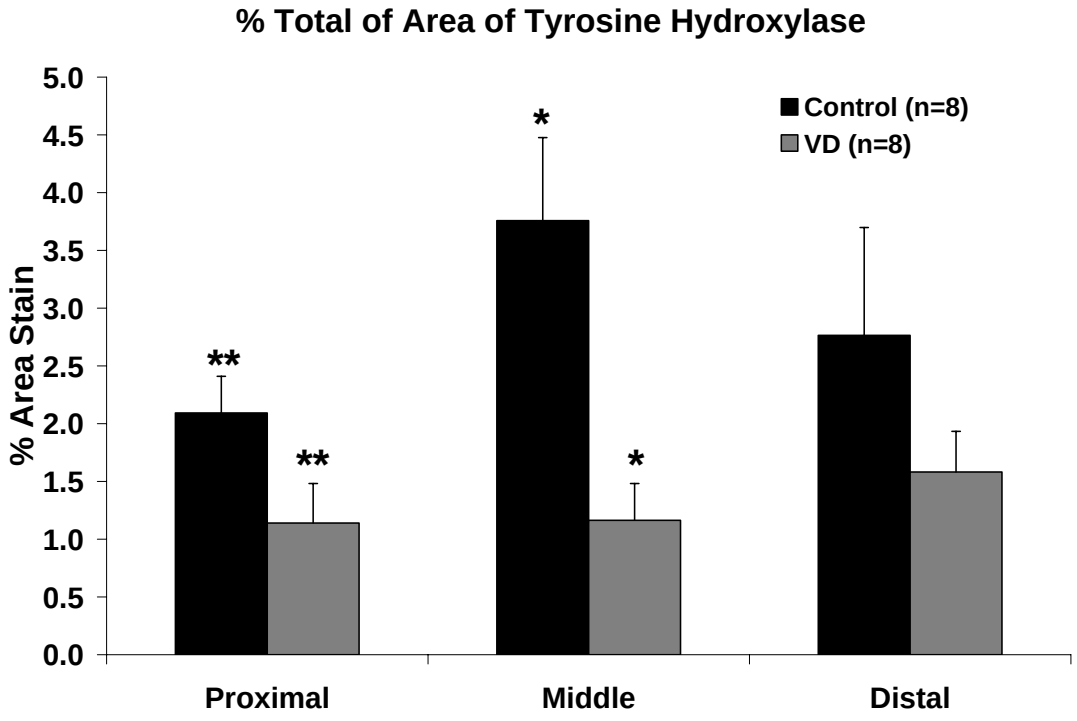

Figure 4.14 Percentage of positive staining for tyrosine hydroxylase in control and VD urethras for proximal, middle, and distal segments. *, represent significance, where $p<0.05$.**

4.4 DISCUSSION

The sympathetic storage reflex is one of the major mechanisms to maintain continence. Urethras have α_1 adrenergic receptors, and upon an increase in bladder pressure, the hypogastric nerve delivers norepinephrine, which acts on these receptors to reinforce the urethral contraction and maintain continence [11]. The biomechanical and functional studies performed in this section indicate damage to this storage mechanism from VD.

Functional studies were performed using a maximum concentration of 40 μM PE. Results indicated that VD increased the proximal urethral response to this adrenergic agonist

(**Figure 4.3**, top). These results disagree with those of Kuo [111], where urethral contractility was significantly decreased in response to norepinephrine. The main reason for this discrepancy is probably due to the fact that norepinephrine (a non-selective agent) was used instead of PE, a selective α_1 adrenergic agent), and the β adrenergic response to norepinephrine is increased in the urethra after simulated birth trauma.

The middle urethra was also assessed with PE, and while the response was less than that of controls (**Figure 4.3**, center), this finding was not significant. Still, this segment matched the findings of the previously mentioned study by Kuo [111]. The outer diameter response to the sharp increase in pressure to 8 mmHg was significantly decreased in VD compared to that of controls. This may be due to an increase in basal muscle tone in the middle segment after VD. This was further supported by an increase in EDTA-induced relaxation from VD, as well. The large amount of basal tone may also be a side effect of ischemic conditions [112, 113].

A reason for the increase in proximal urethral contraction in response to PE could be due to post-synaptic supersensitivity, where nerves are damaged/disconnected and the urethral smooth muscle increases its membrane potential so that its response is enhanced to lower doses of an agonist [114]. In VD urethras, general nerves in the proximal urethra were damaged as indicated by a decrease in PGP 9.5 staining, which a pan-neuronal stain, and sympathetic adrenergic nerves are damaged, which is revealed by a decrease in TH staining. The percentage area of stain for both PGP 9.5 and TH in the smooth muscle had significantly decreased (**Figures 4.11-4.14**). Sievert et al. found similar decreases in PGP 9.5 staining in the bladder neck/proximal urethra area after simulated birth trauma [46].

Evaluation of the biomechanical properties of the urethral proximal segment was also performed. The decreased FCR values (**Figure 4.5**) and the increased compliance (indicated by

the shift to the right of the control proximal pressure-diameter curve; **Figure 4.3**) from VD indicates that there is some damage in the phenylephrine-induced muscle tone, as well as maintenance with increases in static pressure. There are possible theories for this result. First, damaged sympathetic nerves (**Figures 4.13-4.14**) could cause an altered smooth muscle response. Furthermore, at low strain ranges, the VD proximal urethra was unable to maintain circumferential stress levels compared to that of controls (**Figures 4.14-4.15, Table 4.1**). Either the smooth muscle becomes desensitized or fatigued much easier after VD compared to controls. Additionally, it has been proven that blood flow to the vagina, bladder, and urethra was significantly decreased during vaginal distension [91]. This reduction in flow may produce ischemic conditions that may not only contribute to the nerve damage and connective tissue damage that may weaken the smooth muscle contractility. It is has been proven in the left ventricular muscle of the heart that ischemia induces tissue remodeling that increases collagen to replace necrotic myocytes, yielding scar formation [115]. Urethral smooth muscle cells may be coupled to the matrix via integrins and similar type of remodeling may occur after VD.

Biomechanical induced changes for the middle segment from VD were evident. The pressure-diameter curves exhibited an increased stiffness after VD (curve shifted to the left of the control curve). There were no differences in FCR values (**Figure 4.5**, center) for the middle urethra, but with increasing static pressures, the VD middle segment exhibited significantly increased circumferential stress compared to controls, specifically at low strain levels (**Figures 4.6-4.8**). This finding may be a result of the increased basal smooth muscle tone that was apparent in the functional studies and may contribute to the urethral hypermobility commonly found in SUI.

The obvious changes in the middle urethral segment may, in part, be due to peripheral nerve damage, because PGP 9.5 indicated a remarkable loss of nerve staining in the middle segment after VD. Additionally, there was a lack of positive TH staining indicating adrenergic nerve damage (**Figures 4.11-4.14**), as noted in one previous study [46].

No changes were found for distal segments in functional and biomechanical measures. Immunohistochemical changes were only found for PGP 9.5. The fact that there were no significant changes in the distal percentage of TH indicates that the distal urethra may not play a major role in the sympathetic continence mechanics.

Finally, an increased urothelial thickness after VD in all three segments of the urethra was observed. Similarly, spinal cord injury (lack of neural input) causes a significant increase in the bladder urothelium thickness [116]. The urothelium also stained positive for PGP 9.5; however, we are not convinced that this staining is real. There is supporting data to prove that the urothelium plays in an important part in neuronal nitric oxide mechanisms of the urethra [117]. If this is the case, the urothelial thickening could reflect an inflammatory response induced by the mechanical damage caused by birth trauma.

Limitations of theses studies are similar to that described in Section 2.4. An additional limitation of this study was that one could not assess the outer diameter at 3 different positions. In the current study, it was necessary to run the drug regimens, as well as biomechanical tests, 3 times separately (for proximal, middle, and distal segments) with several washes of Kreb's solution in between each run. Not only would having the ability to simultaneously measure each segment save time, but it would also reduce error.

In summary, VD causes the following: (1) increased proximal adrenergic contraction; (2) increased basal tone in the mid-urethral segment; (3) decreased functional contraction ratio and

circumferential stress in the proximal segment; (4) increased circumferential stress in the middle segment; and (5) lack of nerve tissue in all three segments and a lack of sympathetic nerves in the proximal and distal urethral segments, as well as an increased urothelial thickening. All of these findings point to a damaged sympathetic storage mechanism after birth trauma. However, more histochemical and mechanistic studies must be performed in order to pinpoint the problem area in the sympathetic peripheral control in the urethra.

5.0 URETHRAL BIOMECHANICS IN THE PRESENCE OF A CHOLINERGIC MUSCARINIC AGONIST OF THE FEMALE RAT URETHRA IN SUI

5.1 SIGNIFICANCE OF THE CHOLINERGIC MUSCARINIC RESPONSE OF URETHRAL SMOOTH MUSCLE IN SUI

Past studies have assessed the muscaranic smooth muscle activity in both male and female urethras [118, 119]. Using a greyhound model, it was established that the male membranous urethra has a large amount of cholinergic innervation and contractility, but the muscarinic response to contractile agents in female urethras is not as strong as that in the male [66]. Additionally, Bridgewater and colleagues [120] determined from muscle strip studies that the female pig urethra had no variation of cholinergic nerve density between proximal, middle, and distal segments, and the only segment responsive to carbachol was the proximal urethral segment. Separating the longitudinal and circumferential smooth muscle layers, Mattiasson et al. established that adrenergic responses dominated the circumferential layer and contributed significantly to the longitudinal layer; whereas, the cholinergic component was largely responsible for the longitudinal contraction [19]. Most smooth muscle contractile activity, induced by muscaranic agonists, originates from the longitudinal smooth muscle [121]. Taki et al. [122] investigated the entire length of female human urethra and established that acetylcholine activated the strongest contraction in the proximal segment.

From the past literature summarized above, it has been well established that the cholinergic muscarinic component plays some role in urethral function. Still, the role of muscarinic activity in urethral smooth muscle remains a mystery. While these studies assessed a healthy urethra, the following studies, described in this chapter, attempt to answer these issues utilizing pharmacologically-induced cholinergic muscarinic contractions of the smooth muscle, as well as biomechanical testing and cholinergic nerve assessment.

5.2 METHODS

Evaluation of muscarinic cholinergic activity for control and VD urethras was achieved using the rat model described in **Section 2.2.2**. The isolation procedure and urethral testing system described in **Sections 2.2.3 and 2.2.4** were also utilized for these experiments.

5.2.1 Smooth muscle: muscarinic agonist assessment

For parasympathetic smooth muscle activation, a selective smooth muscle muscarinic agonist, carbamyl-β-methylcholine (a.k.a, bethanechol; #C5259, Sigma Chemical Co., St. Louis, MO), was employed. Similar to the protocol used for PE activation, described in **Section 4.2.2**, the urethra was subjected to steady intralumenal pressure of 8 mmHg. NOSi (100 μM) was added to the bath to inhibit the secondary nitric oxide release that occurs in response to parasympathetic activation. Finally, a maximum dose of bethanechol (300 μM; See **Appendix E**.) was added to the bath to ensure maximum contraction of urethral smooth muscle (**Figure 5.1**).

Pharmacological assessment is detailed **Section 4.2.2**. The only difference is that bethanechol is added instead of phenylephrine.

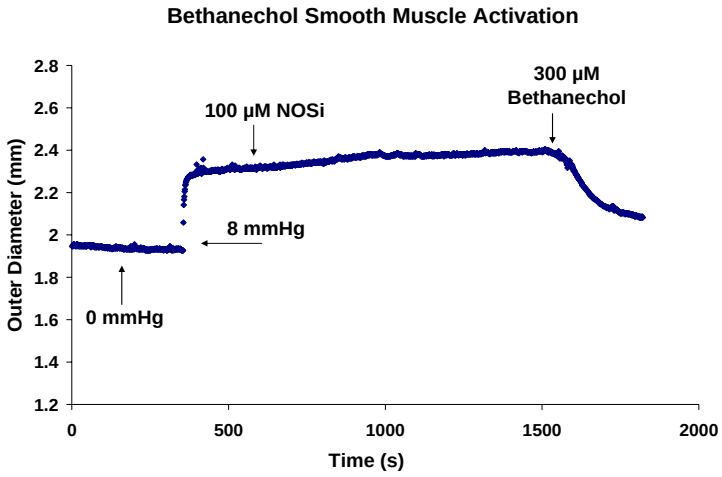

Figure 5.1 Regimen of drugs for induction of a muscarinic cholinergic urethral smooth muscle contraction

5.2.2 Active biomechanical assessment and parameters

Active biomechanical testing was performed as described previously in **Section 4.2.3**. Additionally, parameters for FCR and σ_θ-ε_θ relationships were calculated, as detailed in **Section 4.2.4.**

5.2.3 Immunohistochemistry

Specimens were prepared for immunohistochemistry in the same manner as described in **Section 4.2.5.** Section thickness was cut to 10-12 microns in the cryostat.

Cholinergic nerves are characterized by vesicular acetylcholine transporter (VACht; Chemicon, polyclonal anti-goat, Temecula, CA). VACht is a neurotransmitter transporter that is responsible for transporting acetylcholine into synaptic vesicles. Sections were washed in 0.1 M PBS for 30 minutes (3 times with 10 minute duration each wash), and incubated with 5% donkey serum (Jackson Laboratories, Bar Harbor, ME) for 1 hour at room temperature. Tissue sections were incubated with the primary antibody (1:1000) for 2 days at 4°C. Sections were rinsed with PBS (3 times, 20 minute duration each wash). Sections were incubated with a secondary biotinylated antibody (1:800; Cy3 donkey anti-goat fragment F(ab)2; Jackson Laboratories, #705165147, Bar Harbor, ME) for 2.5 hours at room temperature. Sections were then rinsed for 30 minutes with PBS and coverslipped.

Quantification was performed using the same methods described in **Section 2.2.6** and equation 2.9.

5.2.4 Statistical Analyses

The same methods and statistical tests were used for biomechanical, functional, and immunohistochemical data as with the tests involving adrenergic agonists. This was detailed in **Section 4.2.6**.

5.3 RESULTS

5.3.1 Results for the pharmacological assessment

In the proximal segment, control urethras did not have a different response to NOSi (1.2 ± 6.6% vs. 0.6 ± 0.9%) or EDTA-induced relaxation (8.3 ± 2.5% vs. 0.6 ± 0.9%). The contraction in response to BE was significantly increased in VD (13.7 ± 1.1%) urethras compared to that of controls (5.2 ± 1.7%; $p<0.01$).

On the other hand, middle segments (**Figure 5.2**, center) had no differences for the contractile response to BE when comparing between control (5.9 ± 1.8%) and VD (6.6 ± 2.4%) urethras. The response to NOSi was also similar for control (0.5 ± 1.4%) and VD (1 ± 1.5%) urethras. The dilatative response to a sharp increase of pressure was significantly less in VD (22.0 ± 3.5%) urethras compared to controls (12.8 ± 2.4%; $p<0.05$). This difference was similar to that found in the middle segment of the adrenergic agonist experiments (Section 3.3.1). Additionally, the EDTA-induced relaxation was higher in VD (11.6 ± 2.6%) compared to controls (18.2 ± 2.2%), but this was not significant ($p=0.07$).

Finally, distal segments (**Figure 5.2**, bottom) showed no changes for any pharmacological agent or addition of pressure. Still, the control VD (6.0 ± 2.7%) distal segment had a decreased contractile response to BE compared to controls (2.9 ± 1.2%). Again, this observation was not significant.

5.3.2 Results for the biomechanical assessment

Pressure-diameter curves generated in the presence of BE indicated some changes for VD urethras compared to controls (**Figure 5.3**). The proximal segments for both VD (n=7) and control (n=7) urethras had a nonlinear sigmoidal pressure-diameter response (**Figure 5.3**, top). However, the VD proximal segment had greater distensibility from 12 to 20 mmHg, where the outer diameter was approximately 25% greater than that of controls at 20 mmHg of pressure.

Active muscarinic pressure-diameter curves for middle and distal segments appeared to be unaffected by VD (**Figure 5.3**, center and bottom, respectively). These curves were almost linear in shape, with exception of the control pressure-diameter curve for the distal segment, which was more sigmoidal.

5.3.2.1 FCR

FCR values varied between proximal, middle, and distal segments (**Figure 5.4**) of both control (n=6) and VD (n=7) urethras. For the proximal segment, there were no significant changes from VD compared to controls, but it was observed that negative FCR values were more prominent in the VD proximal urethras compared to controls, specifically from 10 to 20 mmHg.

For middle urethral segments, control FCR values were higher than that of VD, but the only significant difference was at a pressure of 2 mmHg (0.14 ± 0.02 vs 0.09 ± 0.01; $p<0.05$). Additionally, the middle segments of both groups behaved similarly to the proximal segment, where the maximum FCR value was at 4 mmHg and declined thereafter.

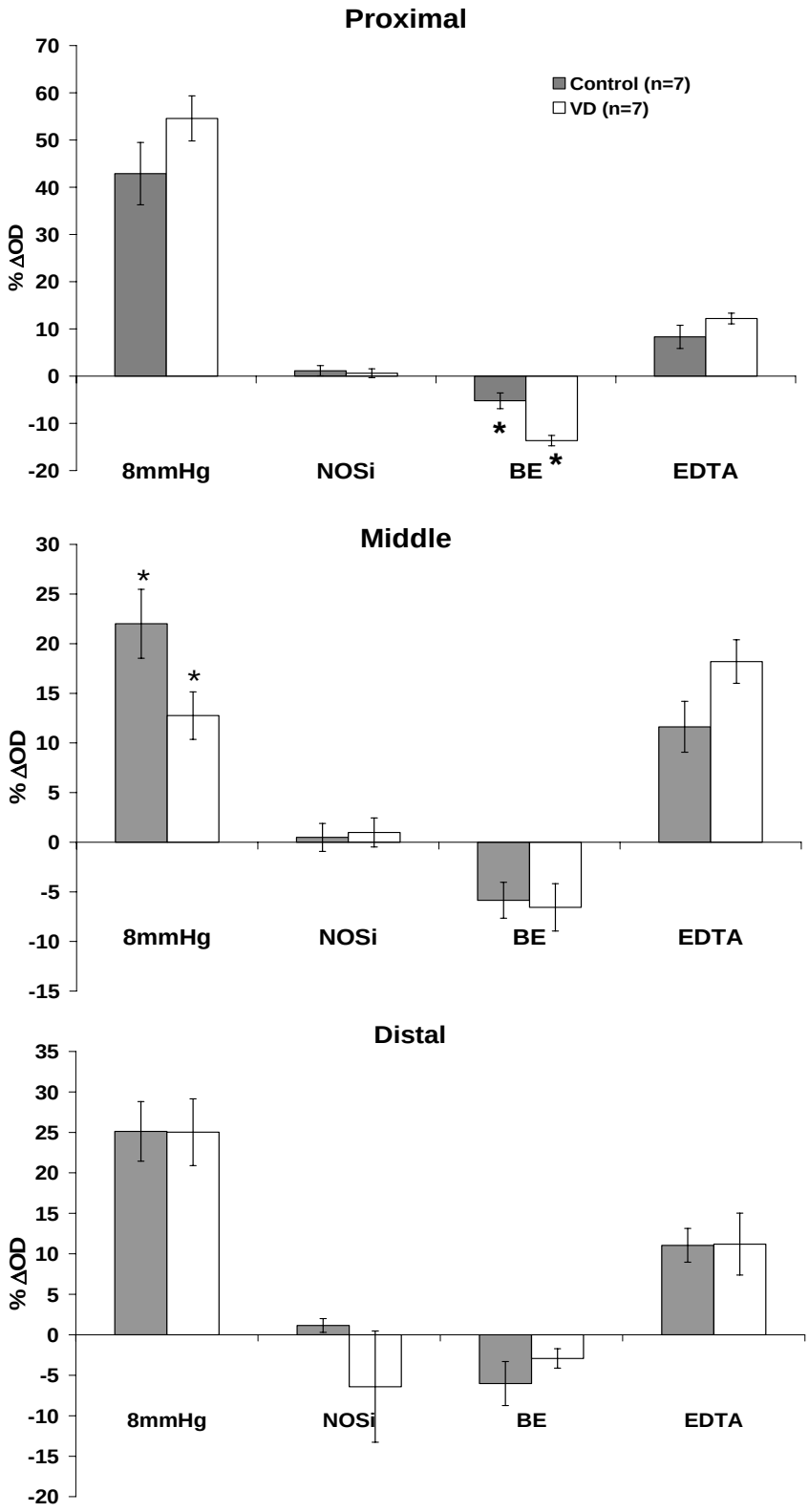

Figure 5.2 Urethral smooth muscle response to bethanechol (BE) for proximal (top), middle (center) and distal (bottom) for control and VD urethras. Significant differences are indicated by *, where p<0.05.

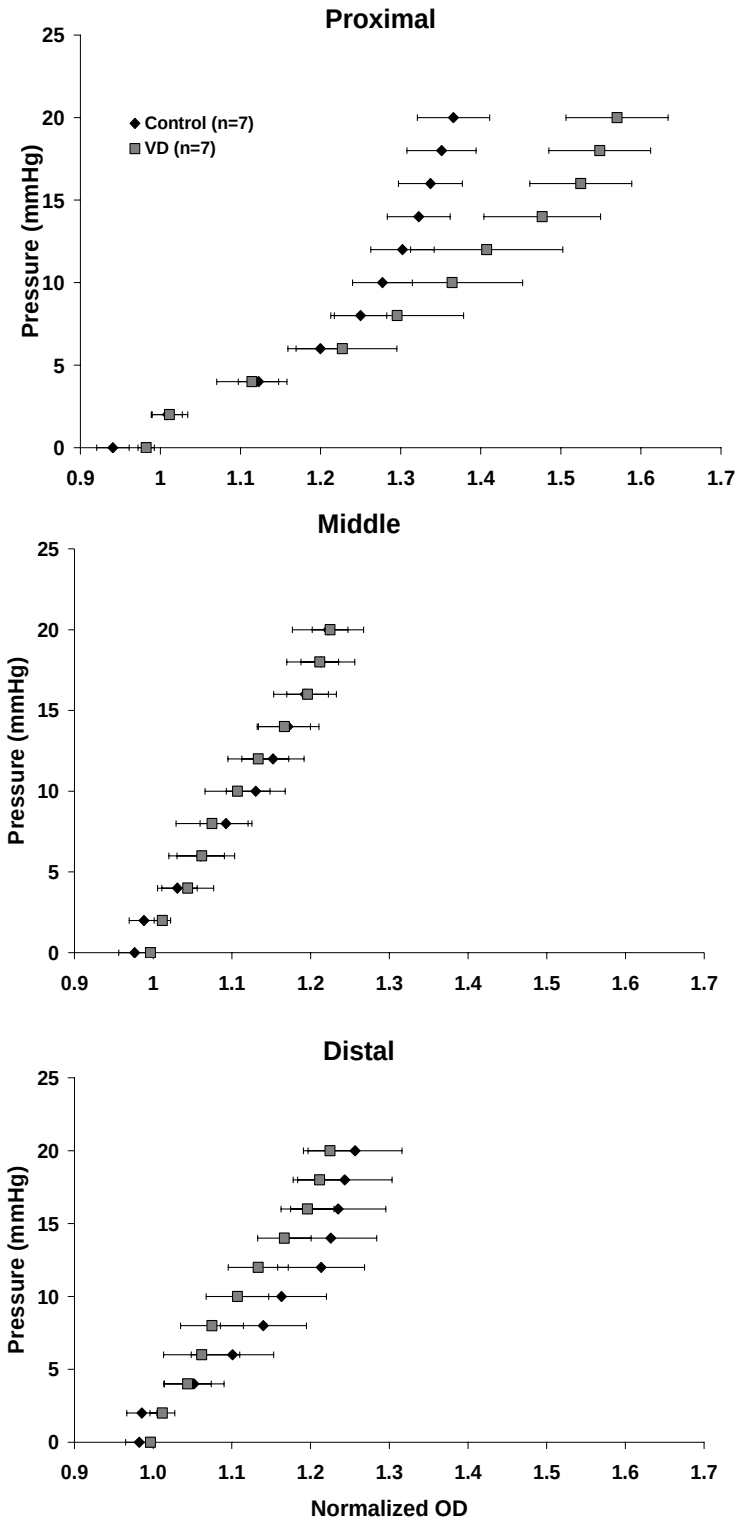

Figure 5.3 Pressure-diameter curves generated after pre-contraction with bethanechol (BE) for the proximal (top), middle (center), and distal (bottom) segments.

Finally, the FCR at distal urethral segments were also not affected by VD. However, a trend was observed, where the FCR values of controls were maintained throughout the entire pressure range, whereas, the VD distal FCR values reached a maximum value at 4 mmHg and gradually decreased with increasing static pressures.

5.3.2.2 Circumferential stress-strain response

The most difference in the general behavior of the σ_θ-ε_θ responses of the urethra in the presence of BE were found in the proximal segment. VD (n=7) caused this curve to shift to the right of the control (n=7) curve, most noteably for strains ranging from 0.7 to 0.9 (**Figure 5.5**, top). Middle and distal segments had similar σ_θ-ε_θ curves for both groups. All curves were non-linear in shape.

Similar to the data analyzed in Section 3.3.1.2, the σ_θ-ε_θ data was relcalculated at constant values of ε_θ so that σ_θ could be statistically compared. All fits had an average value of R^2 =0.98 ±0.02. VD most affected the proximal segment (**Figure 5.6, Table 5.1**). No differences were found at low strain ranges, but there were many alterations due to VD in the mid and high strain ranges. Once urethral tissue reached a strain value of 0.5, the control urethra had significantly higher σ_θ values compared to that of VD in the proximal segment.

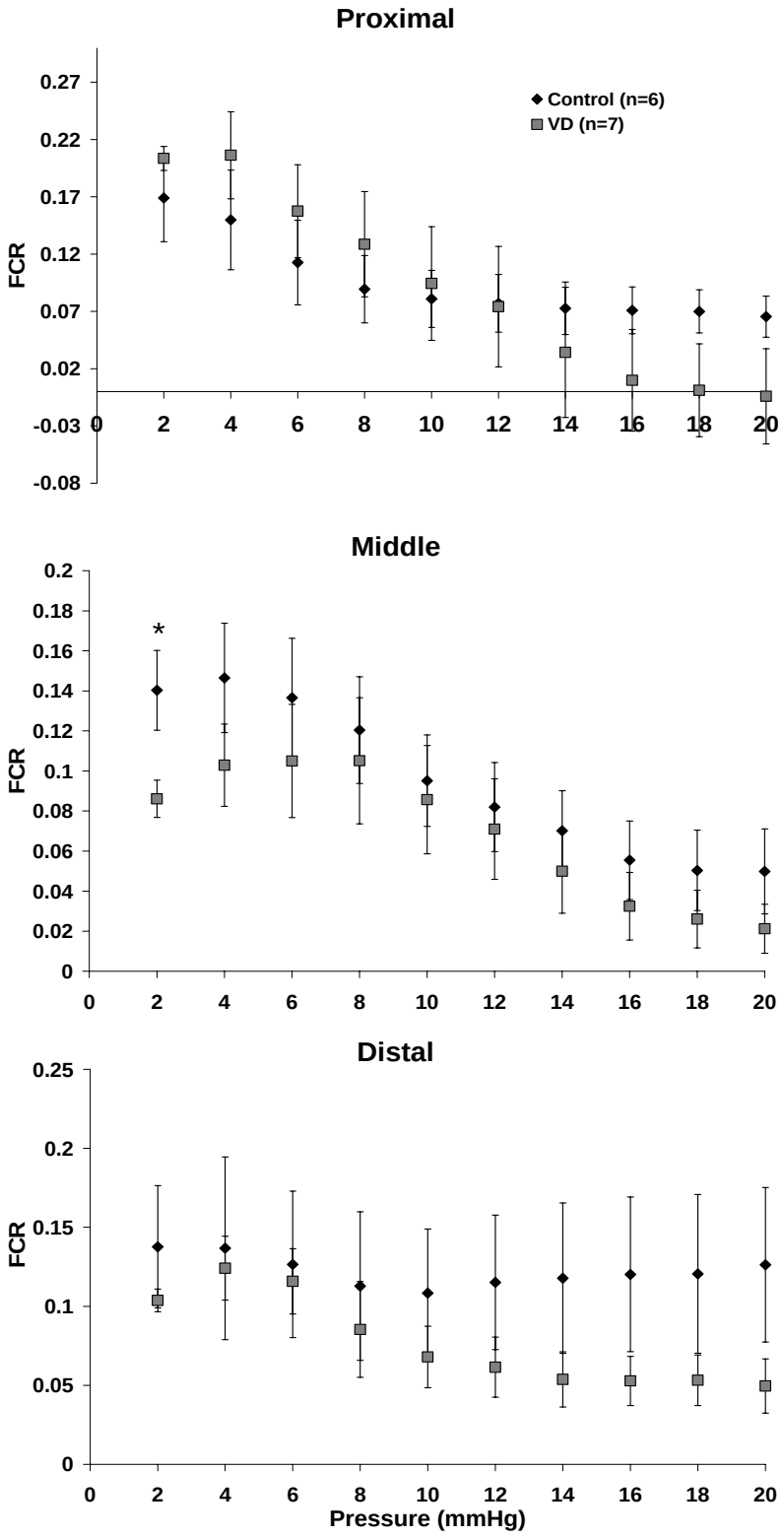

Figure 5.4 Functional contraction ratio (FCR) value for proximal (top), middle (center), and distal (bottom) segments for both control and VD urethras. * indicates a significant difference between control and VD for middle FCR values at 2 mmHg ($p<0.05$).

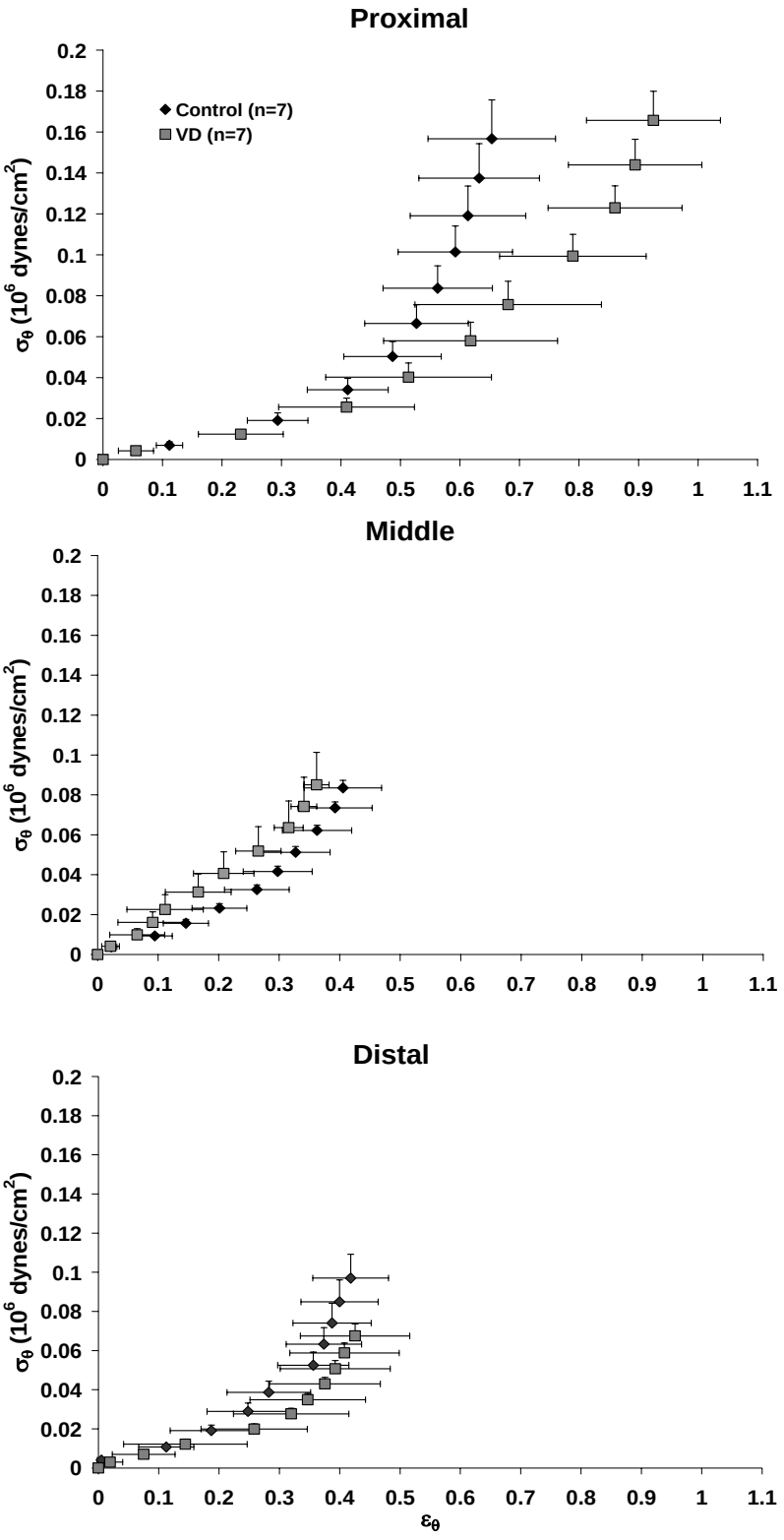

Figure 5.5 Circumferential stress-strain response for proximal (top), middle (center) and distal (bottom) for both control (n=7) and VD (n=7) groups in the presence of BE

Middle segments only had significant alterations from VD at low strains. VD had higher σ_θ values than controls, specifically at ε_θ range of 0-0.12. Although not significant, control σ_θ values were higher than VD at mid level strains. When urethras of both groups reached high strain ranges, the σ_θ-ε_θ behavior was very similar for the middle segment (**Figure 5.7 and Table 5.1**).

VD did not significantly affect the σ_θ-ε_θ behavior of distal segments (**Figure 5.8**) in the presence of BE. While VD distal segments had higher σ_θ values for all strain levels, these values were not significant from control.

Table 5.1 Peak stress values (x 10^6 dynes/cm^2) for peak ε_θ values within low, middle, and high strain ranges comparing control and VD urethras in the presence of a cholinergic muscarinic agonist. *,^{x} indicates a significant difference between control and VD, where p<0.001

	CONTROL n=7			VD n=7		
	Proximal	**Middle**	**Distal**	**Proximal**	**Middle**	**Distal**
Low $\sigma_{\theta max}$	0.03 ± 0.007	0.02 ± 0.004	0.02 ± 0.003	0.03 ± 0.001	0.02 ± 0.002	0.04 ± 0.003
Mid $\sigma_{\theta max}$	2.02 ± 0.90*	0.27 ± 0.17	0.03 ± 0.01	0.29 ± 0.17*	0.10 ± 0.14	0.9 ± 0.05
High $\sigma_{\theta max}$	14.50 ± 5.57^x	1.46 ± 0.57	0.52 ± 0.40	1.34 ± 0.40 ^{x}	1.33 ± 0.40	1.54 ± 1.23

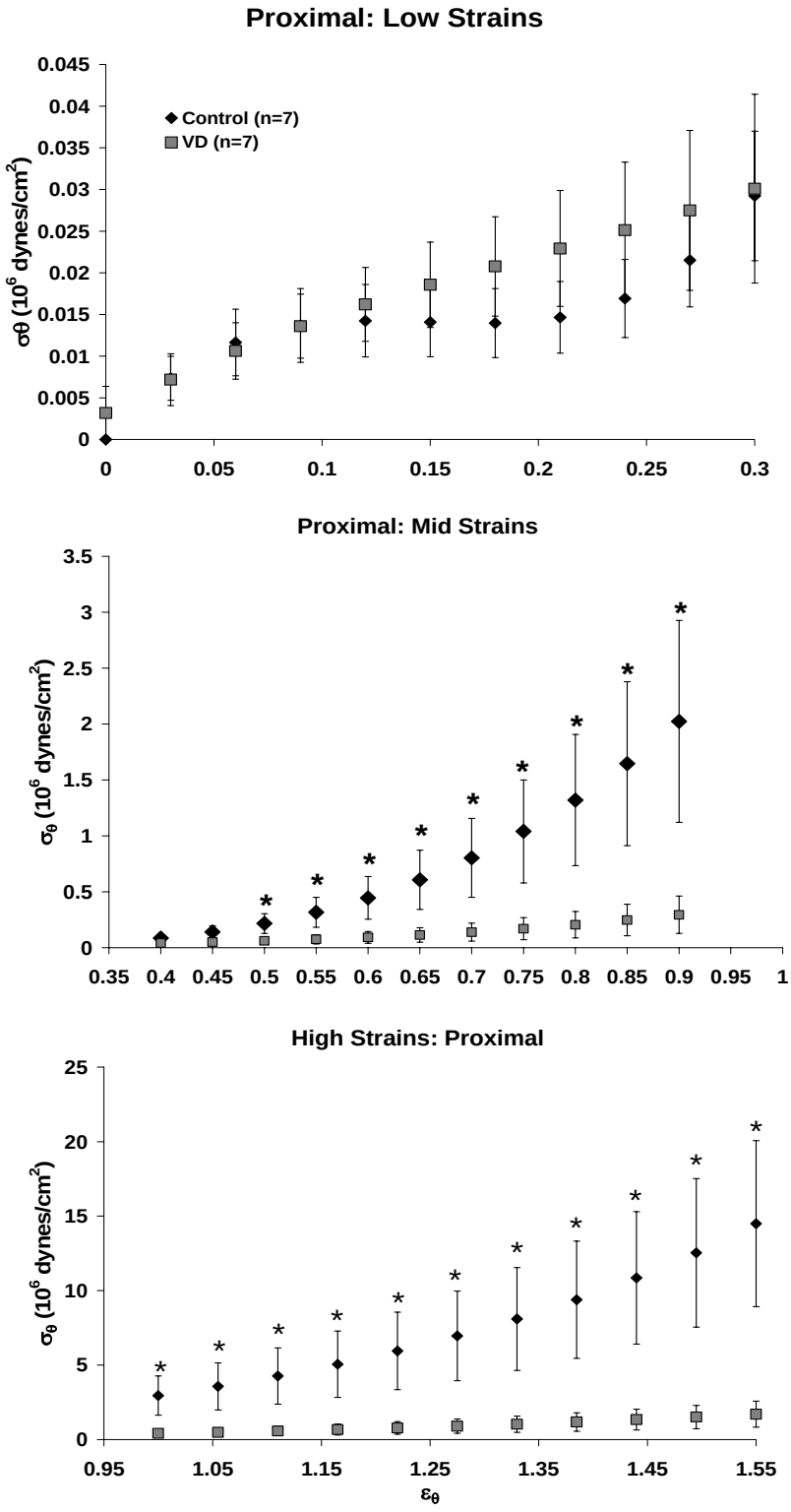

Figure 5.6 Proximal circumferential stress values for control and VD groups proximal segments derived for low circumferential strains (0–0.3; top), middle circumferential strains (0.4–0.9; center), and high circumferential strains (1–1.55; bottom). Significance is indicated by * for comparisons between the control and VD groups at each respective strain level ($p<0.001$).

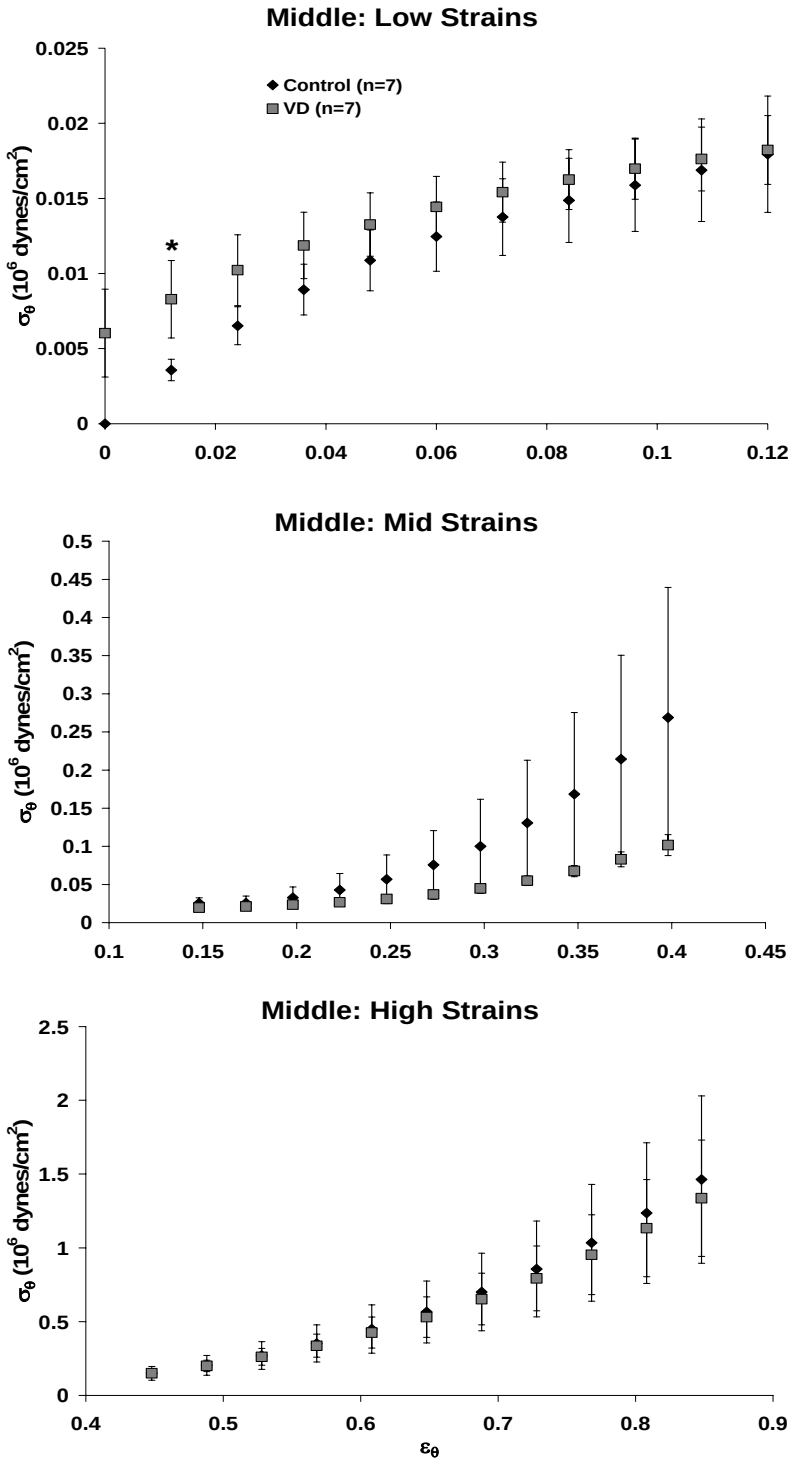

Figure 5.7 Middle circumferential stress values for control and VD middle segments derived for low circumferential strains (0–0.12; top), middle circumferential strains (0.15–0.4; center), and high circumferential strains (0.45–0.85; bottom). Significance is indicated by * for comparisons between the control and VD groups at each respective strain level ($p<0.001$).

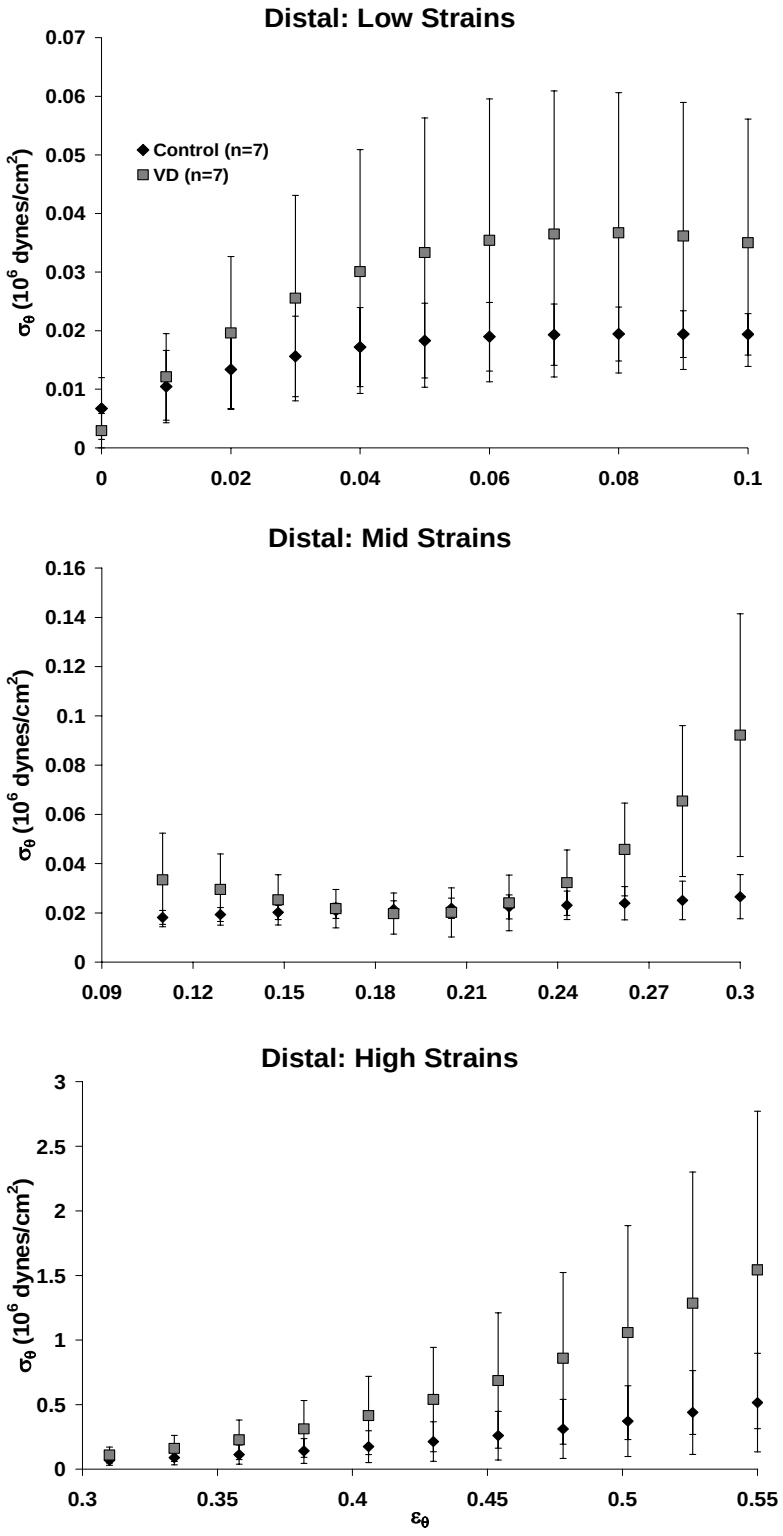

Figure 5.8 Distal circumferential stress values for control and VD middle segments derived for low circumferential strains (0–0.1; top), middle circumferential strains (0.11–0.3; center), and high circumferential strains (0.31–0.55; bottom).

5.3.3 Immunohistochemistry: VACht

The presence of cholinergic innervation was assessed both qualitatively and quantitatively. VACht was used to localize these nerves. VACht was found abundantly through out all segments of control urethras (**Figure 5.10**). Positive staining was also present in the VD urethras, but the stain was not as intense as for controls. In fact, VD mid urethral segments were almost absent of any positive staining.

Area of positive staining was quantified and showed significant changes in the amount of positive staining for VACht between control and VD urethras (**Figure 5.9**). VD urethras had significantly less staining than that of controls in the proximal (6.3 ± 0.4% vs. 4.1± 0.5%) and middle (6.3 ± 0.7% vs. 3.3 ± 0.6%) segments. There was no significant difference detected in the distal urethral segment (p=0.053), but trends show that again VD (3.5 ± 0.4%) segments had less VACht than controls (5.2 ± 0.7%).

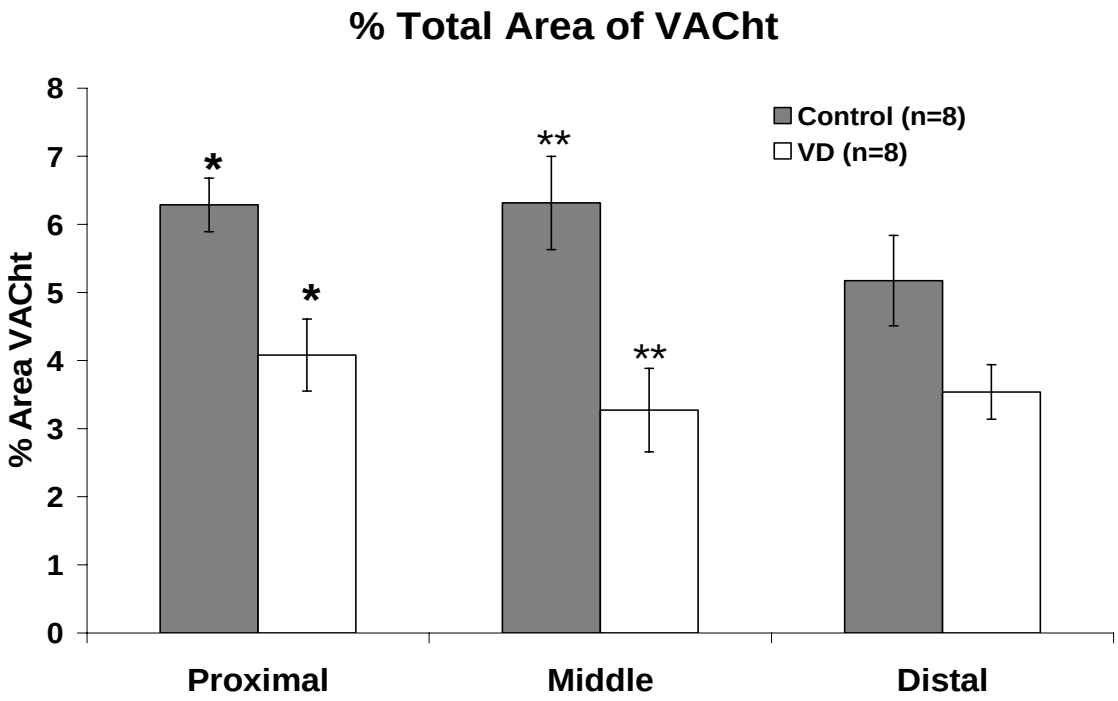

Figure 5.9 Quantified area of positive VACht present in the proximal, middle, and distal segments of control and VD urethras.*, indicate significant differences between control and VD urethras ($p<0.01$).**

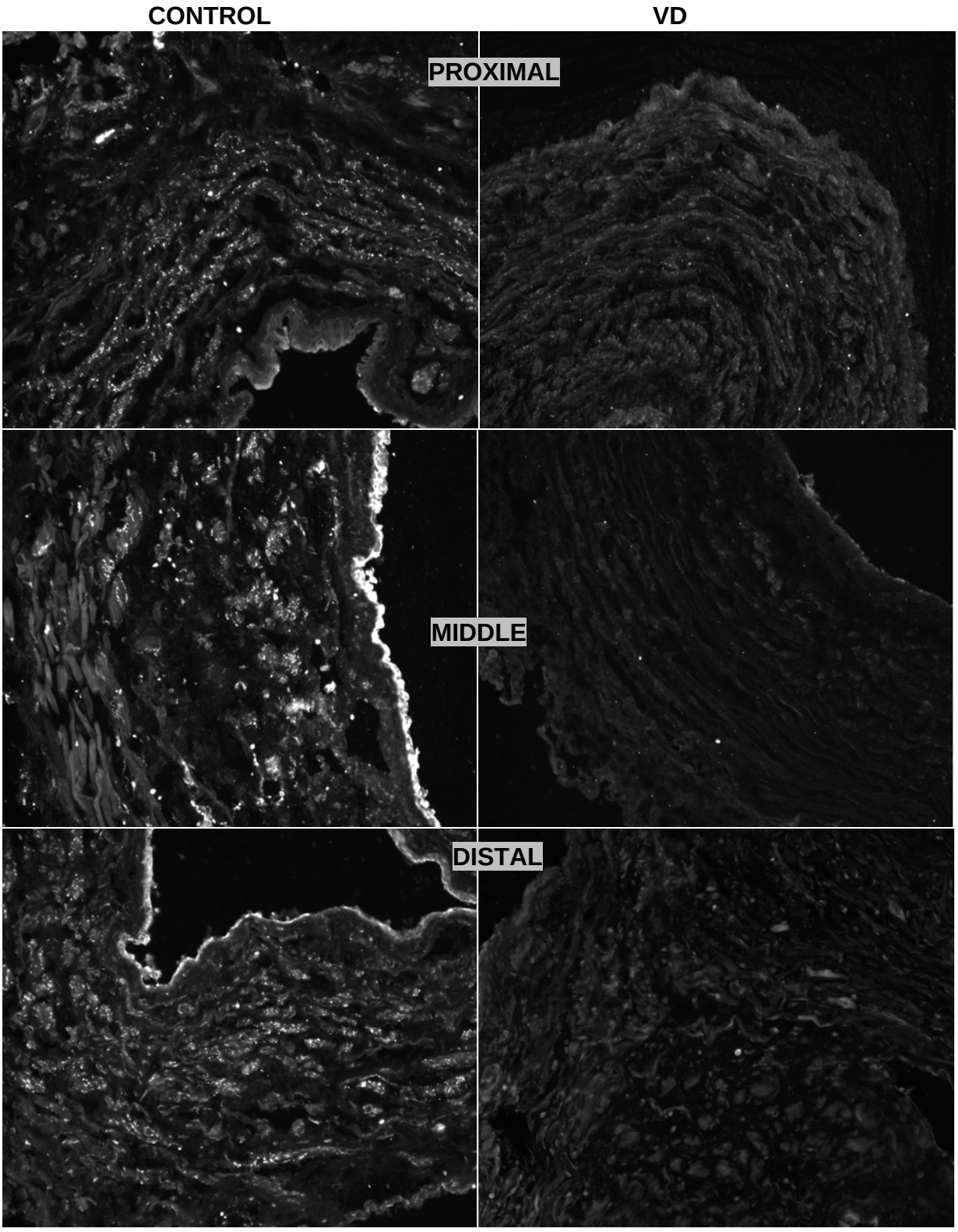

Figure 5.10 VACht immunostaining for proximal (top), middle (center), and distal (bottom) segments of control (left) and VD (right) urethras. Pictures acquired at 20x magnification.

5.4 DISCUSSION

Urethral smooth muscle receives rich cholinergic innervation, the role of which is largely unknown [123, 124]. In our ex vivo studies, we found that all segments of the urethra had robust, but slow, smooth muscle contractions in response to BE. However, there were some changes due to VD.

Functional studies show that the proximal urethra was affected after VD (**Figure 5.2**); namely, there was a significant increase in smooth muscle contraction in response to BE. There were no changes for the middle and distal segments. While not many studies are available to compare these results, it has been established that parasympathetic innervation contributes to proximal urethral function, but does not seem to play a large role in middle and distal segments [118]. If this is true, then it could be possible that VD has damaged one of the mechanisms for bladder to urethra coordination.

Basal smooth muscle tone was increased after VD in the middle urethra segment. This was further supported by the trend of increased EDTA-induced relaxation (**Figure 5.2**). While this somewhat agrees with our beta stiffness values for the middle urethral segment in the baseline state [83], this disagrees with in vivo studies where they found a decrease in baseline urethral pressure from VD [18]. Since damaged nerves or denervation are commonly associated with birth trauma, this could be one reason for the increase in mid-urethral basal tone. This phenomenon has been verified with peripheral arteries, such as that of the middle ear [125]. This study established that peripheral denervation increased spontaneous myogenic tone of arteries in the middle ear.

Biomechanical analyses uncovered possible damage to the proximal urethral segment in the VD groups. Circumferential stress values were significantly less in the VD proximal urethras

compared to that of controls (**Table 5.1, Figure 5.6**), particularly for mid to high strain ranges. This indicates that while the proximal urethra has no trouble responding to BE (**Figure 5.2**) it is unable to maintain urethral resistance via muscarinic receptor stimulation. Thus, this could be due to ECM is damaged as well. To our knowledge these findings are novel with respect to urethral biomechanics and the affects of birth trauma. With respect to the matrix, pilot studies focusing on the role of elastin and collagen in urethral biomechanics (**Chapter 3**) indicated that elastin is responsible for maintaining urethral tone. Thus, it is a strong probability that damaged elastin contributes to this decrease in stress.

VD caused small biomechanical changes in the middle urethral segment in the presence of BE. FCR analysis (**Figure 5.4**) indicated a lack of smooth muscle muscarinic-induced contractile activity in the lower pressure ranges for the middle portion. This is likely due to weakened muscle fiber bundles [47] or a slowed activation of muscarinic induced contraction from VD. Still, no other differences were noted between control and VD urethras (**Figures 5.3, 5.5, and 5.7, Table 5.1**). The increase in stretch-dependent basal smooth muscle tone activity may compensate for the impaired smooth muscle response to BE, or, at the same time, increased spontaneous basal tone may be masking any changes of the middle VD urethra activity.

Finally, the distal segment was not affected by VD (**Figure 5.2-5.4, 5.8, Table 5.1**). Muscarinic cholinergic receptors do not have a proven importance in the distal urethral portion, as do the α adrenergic receptors [118].

One previous finding that may relate to both biomechanical and functional changes is post synaptic supersensitivity, where the muscle is denervated and the tissue becomes hypersensitive to contractile agents [114, 126]. Localization of cholinergic nerves with VACht proved that there was a significant lack of cholinergic nerves present in the proximal and middle

segments of the urethra from VD (**Figures 5.9-5.10**). The lack of proximal cholinergic nerves may explain the significant increased BE contraction in the VD group, as this is evidence of nerve damage. There were little changes to the muscarinic contraction of the middle urethra (**Figure 5.2),** as well as the biomechanical properties, which does not match the significant lack of VACht present after VD (**Figures 5.9-5.10**). This may be due to the fact that the cholinergic nerves that primarily innervate the middle urethra are that of somatic origin from the pudendal nerve innervating striated muscles [127]. This means that if we were to assess the middle striated sphincter or use electrical field stimulation, we may likely find a deficit of activity. Other studies have found a loss of nerve fibers after birth trauma, but other methods were used. Immunohistochemistry with S100 (a general nerve fiber marker) was lacking in the mid urethra after VD [128]. Also, vasointestinal peptide (VIP; found in post-ganglionic cholinergic nerves), nNOS (nitergic nerves) and cGRP were significantly decreased after birth trauma in the proximal and middle urethra [46].

Additionally, many of these alterations could be due to hypoxic conditions brought on by simulated birth trauma. It has been verified that blood flow to the lower urinary tract is significantly reduced during vaginal distension [91]. Not only would this damage the lower urinary tract organs, but the innervation as well. Hypoxic conditions are known to have a damaging effect on the urethral response to many agonists [129].

Limitations to these studies are similar to those described in **Sections 2.4 and 4.4**. One of the limitations to this study deal with the fact that the main urethral smooth muscle responses during reflex bladder contractions is nitric oxide-mediated relaxation in the female rats, but atropine-sensitive contractions in the male rats [130]. It has also been proposed that cholinergic nerves in the urethra cause relaxation of the outflow region at the start of micturition by releasing

nitric oxide and other relaxant neurotransmitters [123]. Though it is true that the cholinergic system still is unclear in urethral function, it seems that too little is known in order to understand exactly what these findings mean. Further studies are needed.

From these studies, it is clear that muscarinic cholinergic properties of the urethra contribute to urinary tract function, especially in the proximal urethra. Results indicate that the urethral response to a muscarinic agonist is altered after simulated birth trauma, as well as the active muscarinic biomechanical properties. Further understanding of this mechanism in the urethra may provide better therapies in SUI.

6.0 DEVELOPMENT OF A LONGITUDINAL TESTING DEVICE FOR BIAXIAL ASSESSMENT OF A WHOLE MOUNT RAT URETHRA

6.1 SIGNIFICANCE OF URETHRAL LONGITUDINAL ACTIVITY

As described in **Section 1.1.2**, longitudinal muscle is a component of the urethra that lies beneath the inner urothelial layer of the urethra and runs the entire urethral length. While the circular muscle contributes to the closure force of the urethra [7, 9], the role of longitudinal muscle has been less clear.

Previous researchers have utilized strip studies to characterize differences between urethral longitudinal and circumferential smooth muscle [7, 19, 106, 131]. It has been established in female rabbit urethral strips that there is a significant adrenergic component in the circumferential smooth muscle; yet, the parasympathetic component contributes largely to the longitudinal smooth muscle, as well as circumferential smooth muscle [19]. Another study using the same animal model proved that the circular muscle had tonic contractions, whereas, longitudinal strips had phasic activity with shortening velocity higher than that of circumferential muscle [20].

Longitudinal muscle has also proven to have smaller contractile responses compared to circumferential muscle [10]. Additionally, it was established that longitudinal muscle had a much larger relaxation response to calcitonin gene related peptide (cGRP) and capsacin, and a

larger contraction to 5-hydroxytryptamine (5-HT) compared to circumferential smooth muscle. Another study revealed that noradrenaline and acetylcholine increased longitudinal tension of both cat and guinea pig urethras without affecting urethral resistance to flow [131].

It is clear that further studies must be performed on the simultaneous activity of longitudinal and circular smooth muscle in the urethra in order to more clearly elucidate their differential roles. The following chapter will describe a device that aims to address this issue.

6.2 SYSTEM DESIGN AND METHODS

The urethral testing system described previously [64] and detailed in **Section 2.2.4** was modified so that both longitudinal and circumferential smooth muscle may be assessed. The following sections detail the system and methods for the biomechanical assessment of urethral tissue in the baseline, active and passive states.

6.2.1 System design and modification for longitudinal assessment

A differential variable reluctance transducer (DVRT; Microstrain, Inc., Williston, VT) is an electromechanical device that provides an electrical output proportional to the displacement of a separate moveable core and has been useful in the assessment of micromotion and small changes of displacement [132, 133]. This device has many advantages, including: measurement is frictionless, an infinite mechanical life, infinite resolution, and insensitivity to off-axis loading.

How a DVRT measures displacement on a small scale is depicted in **Figure 6.1**. A primary coil (e.g. the first coil) is energized with an AC power source. Voltages in the secondary coils are generated and are polar opposites. The net output of the DVRT is the difference between the secondary coil voltages. If the core moves left towards the negative coil, the voltage becomes increasingly negative, and, at the same time the positive coil becomes less positive. This voltage can be sent to a computer where it is continuously recorded.

For urethral tissue, there were several things to consider when choosing a DVRT. First, the stroke length of the core needed to be within the range of tissue motion. Post-passivation of the tissue, urethral relaxation indicates longitudinal smooth muscle activity by forming a curve from relaxation (**Figure 6.2**). Based on the approximation of the circumference of an ellipse (C_E; calculating parameters, a and b) and known in vivo length (IVL), the stroke length (SL) was determined to be 3 mm ($SL=C_E/2 - IVL$) for the urethra.

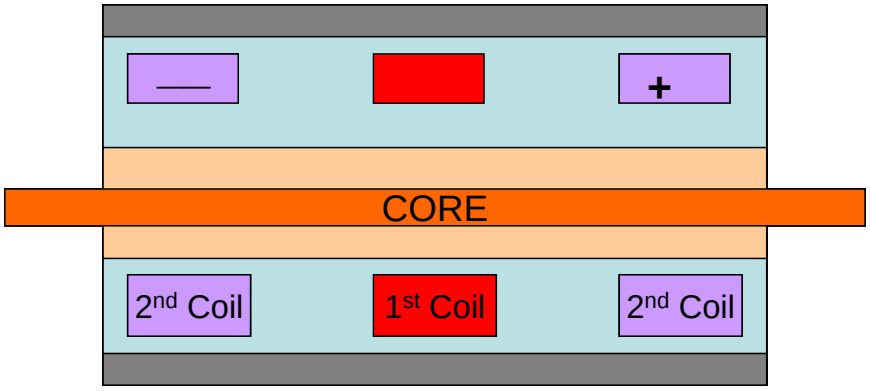

Figure 6.1 A schematic of the inner machinery of the DVRT

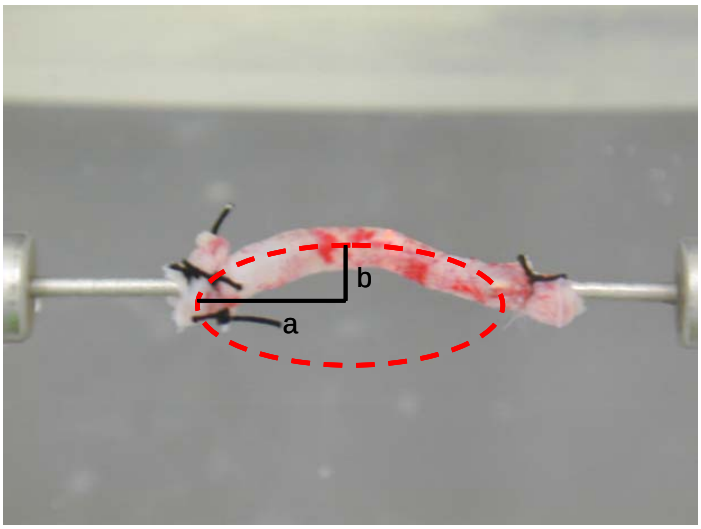

Figure 6.2 Example of a urethra fixed at both ends and completely relaxed with EDTA

Secondly, the core (a.k.a., plunger) must be extremely light weight, so that the urethra would only have horizontal translation without any concern of off-axis loading in the vertical direction from the weight of the core. Finally, the DVRT must have small, opposing resistance so that the tissue could be stretched to in vivo length during testing. To achieve this requirement, a tensile spring was attached to the core. Additionally, past research [16] indicates that the force generated by urethral longitudinal contraction is low; therefore, the spring chosen for this application had a low spring constant, 0.11 N/mm.

From a design standpoint, the body of the DVRT was secured in line with the stationary perfusion tee (**Figure 6.3**). Since the DVRT had a threaded body, an adapter plug was made with a threaded inlet for the DVRT to be fixed directly across from the stationary tee. The tissue is tied onto the proximal perfusion tee (stationary tee), and the distal end is tied onto the plunger of the DVRT.

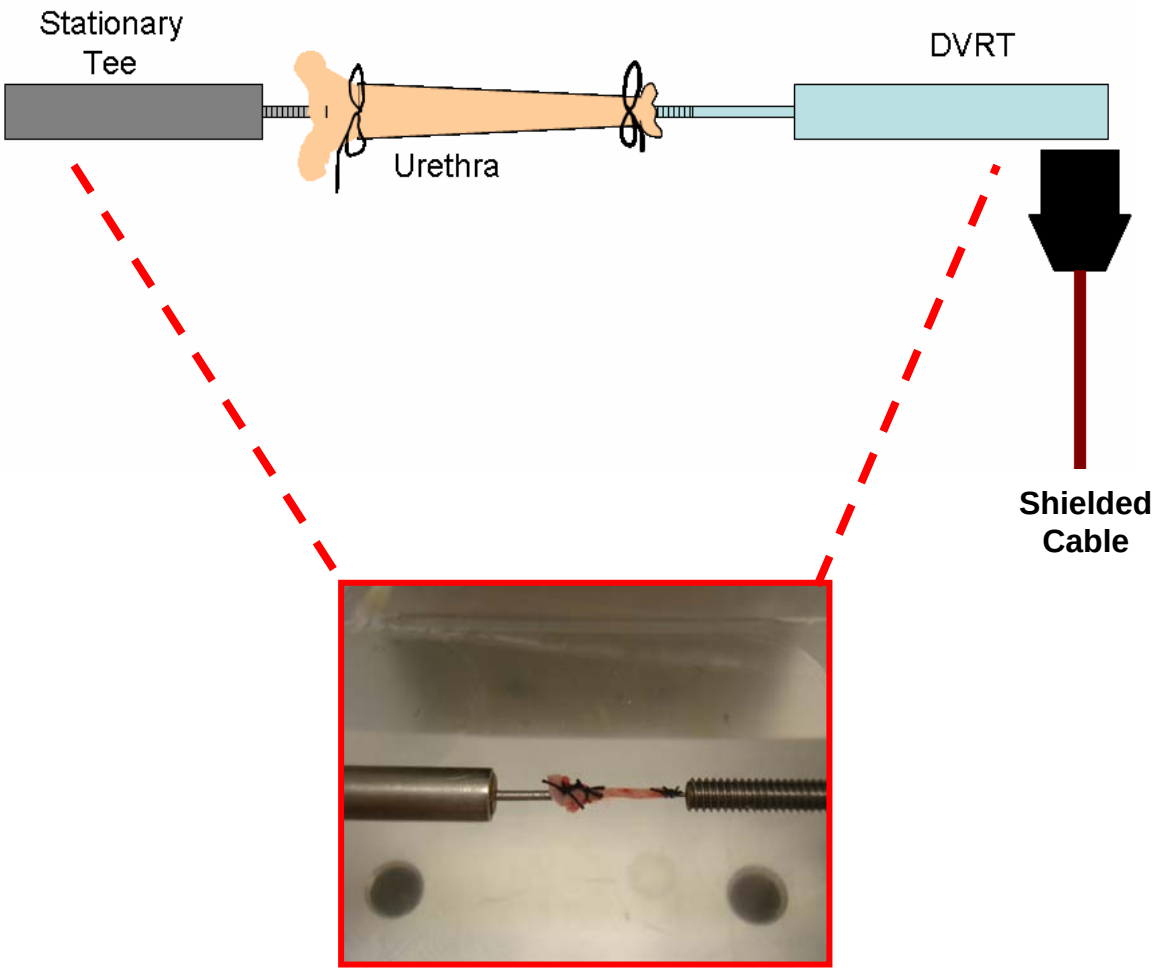

Figure 6.3 A schematic of longitudinal measurement using a DVRT

6.2.2 Biomechanical testing

All active, baseline, and passive biomechanical tests were performed in the same manner as described in **Sections 2.2.5.1 and 4.2.3**. The only change dealt with the modification for longitudinal measurement. The urethra was pre-stretched to an extra 5% of in vivo length and allowed to equilibrate to a somewhat constant length (due to stress relaxation) for 45 minutes.

Next it was inflated with the static intralumenal pressures ranging from 0 to 20 mmHg with increments of 2 mmHg. With increasing static pressures, the DVRT measured the motion in the longitudinal changes and the outer diameter was measured with a laser micrometer. Pressure, outer diameter, and longitudinal changes were simultaneously recorded via computer.

6.2.3 Biomechanical parameters

Biomechanical parameters were used to quantify both longitudinal and circumferential activity, as described previously [110, 134-136]. Circumferential stress (σ_θ) and circumferential strain (ε_θ) were calculated in the same manner as described in **Section 2.2.5.2**. (equations 2.5-2.6). Again, the incompressibility assumption was maintained and histology was used (**Section 2.2.5.3**) to evaluate unloaded inner and outer diameters, but in this application the change in length at each loaded condition was accounted for via:

$$r_{iPx} = \sqrt{r_{oPx}^2 - A/\pi\lambda} \qquad \textbf{(6.1)}$$

Here, r_{iPx} is the inner radius to be calculated for each pressure step, r_{oPx} is the outer radius measured for each step of pressure, A is the cross sectional area of the urethra in the unloaded state (measured from histology, **Section 2.2.5.3**) and λ is the stretch ratio ($\lambda=L/L_o$) calculated for length (L) measured for each step of pressure divided by the initial length (L_o) measured.

Several aspects of the testing set up had to be considered. Smooth muscle is stretch sensitive, and in order to ensure that the smooth muscle was active, similar to circular smooth muscle, the tissue needed to be stretched beyond in vivo length. In order to determine how much stretch was required, a preliminary study was performed where urethral tissue was tied onto the

system as described in **Section 6.2.1**. Tissue was either stretched to 0%, 3%, 5%, or 8% of in vivo length. Biomechanical tests were performed, similar to those in Section 2.2.5.1. in the smooth muscle active (BE and PE were added in random order) and passive states. To assess the magnitude of muscle activity, FCR was calculated (**See Section 4.2.4, Equation 4.2**). Results indicated that 5% strain beyond in vivo length was optimal to activate longitudinal smooth muscle for biomechanical testing (**Figure 6.4**). This was made obvious by the higher FCR values at 5% stretch, which means that the muscle activity was higher at this stretch. The other attempts, provided minimal amount of muscular activity.

To calculate longitudinal stress, two factors were considered: the stress placed on the urethra in the longitudinal direction and the stress imposed on the urethra in the longitudinal direction by the intralumenal distension [134-136].

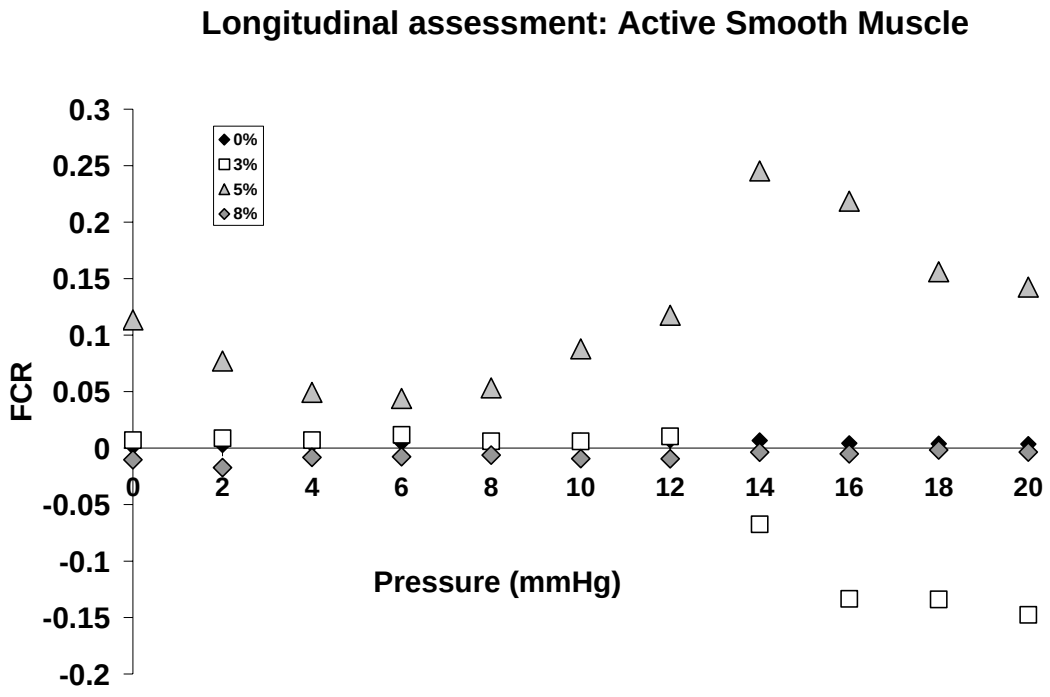

Figure 6.4 FCR values for longitudinal smooth muscle tested under 0%, 3%, 5%, and 8% strain beyond in vivo urethral length. Results indicated that 5% was optimal pre-stretch for biomechanical testing.

From a simple force balance consideration, the longitudinal force (σ_L) is given by:

$$\sigma_L = \frac{F_L + \pi R_i^2 P}{\pi\left(R_o^2 - R_i^2\right)} \quad \textbf{(6.2)}$$

where F_L is the longitudinal force imposed on the tissue, R_o and R_i are the outer and inner radius, respectively, at intralumenal static pressure, P. Additionally, FCR was calculated for both outer diameter (OD) and longitudinal changes using equation 4.2.

6.2.4 Pharmacological assessment

Each urethra was first biomechancially tested in the baseline state at the mid urethral portion (**Section 2.2.5**). Following this, the tissue was allowed to equilibrate for 45 minutes to 1 hour, and then it was assessed with PE and BE (added in random order) in a similar manner as described in **Sections 4.2.1-4.2.2**. However, no static pressure was applied during this testing; all functional assessments were performed at 0 mmHg. This was in order to assess longitudinal activity only. Both outer diameter and length changes were continuously measured during testing. Circumferential smooth muscle changes were quantified by percent changes in outer diameter (i.e., with Equation 3.1). While, longitudinal muscle changes were quantified in an analogous manner using measured length changes with Equation 6.3.

$$\%\Delta L = \frac{\left(L_{Drug} - L_{Previous}\right)}{L_{0mmHg}} \times 100 \quad \textbf{(6.3)}$$

where, L_{Drug} is the maximum length change after addition of the drug (e.g., NOSi, BE, or PE). $L_{Previous}$ represents the length measurement prior to the drug addition, and L_{0mmHg} is the length measured at 0 mmHg. It should also be noted that PE and BE were added in random order so that it could be assumed that sequential effects were not an issue.

6.3 RESULTS

6.3.1 Biomechanical Results

Bidirectional assessments of active and baseline pressure-diameter curves for middle segments were no longer sigmoidal in shape compared to tests performed in **Section 2.3.1** (**Figure 6.5**). and indicated that the circular smooth muscle was able to maintain stiffness before dilation at 8 mmHg of static pressure for baseline urethras (n=6) and 12 mmHg for active urethras (n=6; **Figure 6.6**, bottom). The passive pressure-diameter curve was almost linear.

Stretch ratios for longitudinal changes (ΔL) varied between the different conditions, as well. Baseline and passive ΔL values were similar until 14 mmHg, where passive stretch ratios increased beyond that of baseline. The least stretch was evident in the active smooth muscle state where there was very little change (**Figure 6.6**., top).

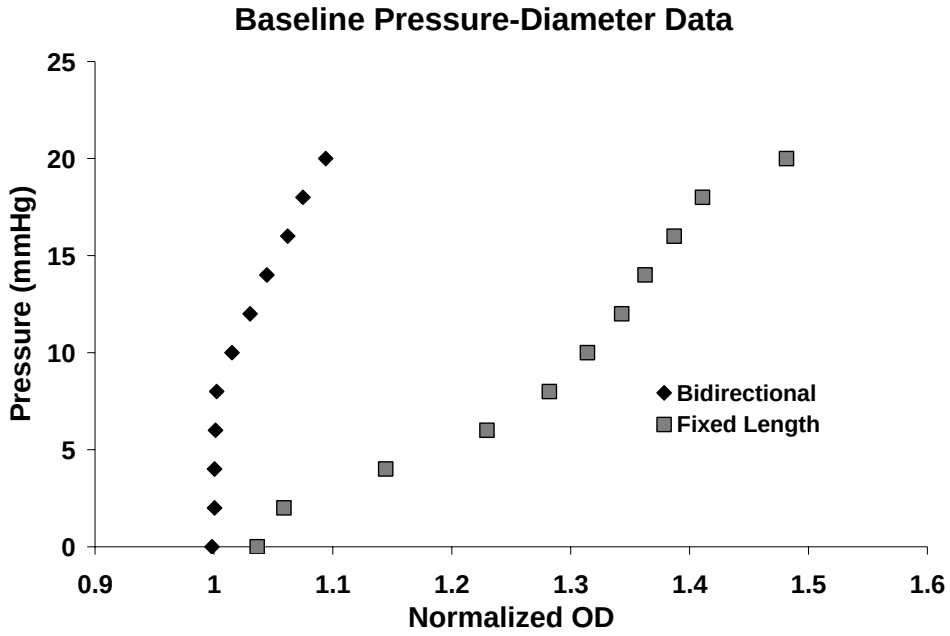

Figure 6.5 Baseline pressure-diameter data generated from bidirectional (inflation and longitudinal pre-stretch) and static pressure inflation tests for the control mid urethral segment.

Figure 6.7 depicts the simultaneous circumferential stress-strain response (top) and longitudinal stress (bottom) behavior. There was more variation in the circumferential direction compared to longitudinal in all three states. For longitudinal stress, the active (at 14 mmHg, $p<0.05$) state had higher values compared to both baseline and passive, which had similar longitudinal stress values. For circumferential stress-strain, the responses were less exponential than described in previous chapters where both ends of the tissue were fixed. Actually, passive tissue had a linear stress-strain response. As expected, active stress-strain behavior was stiffer compared to baseline and passive response; yet, passive responses had the highest stress values.

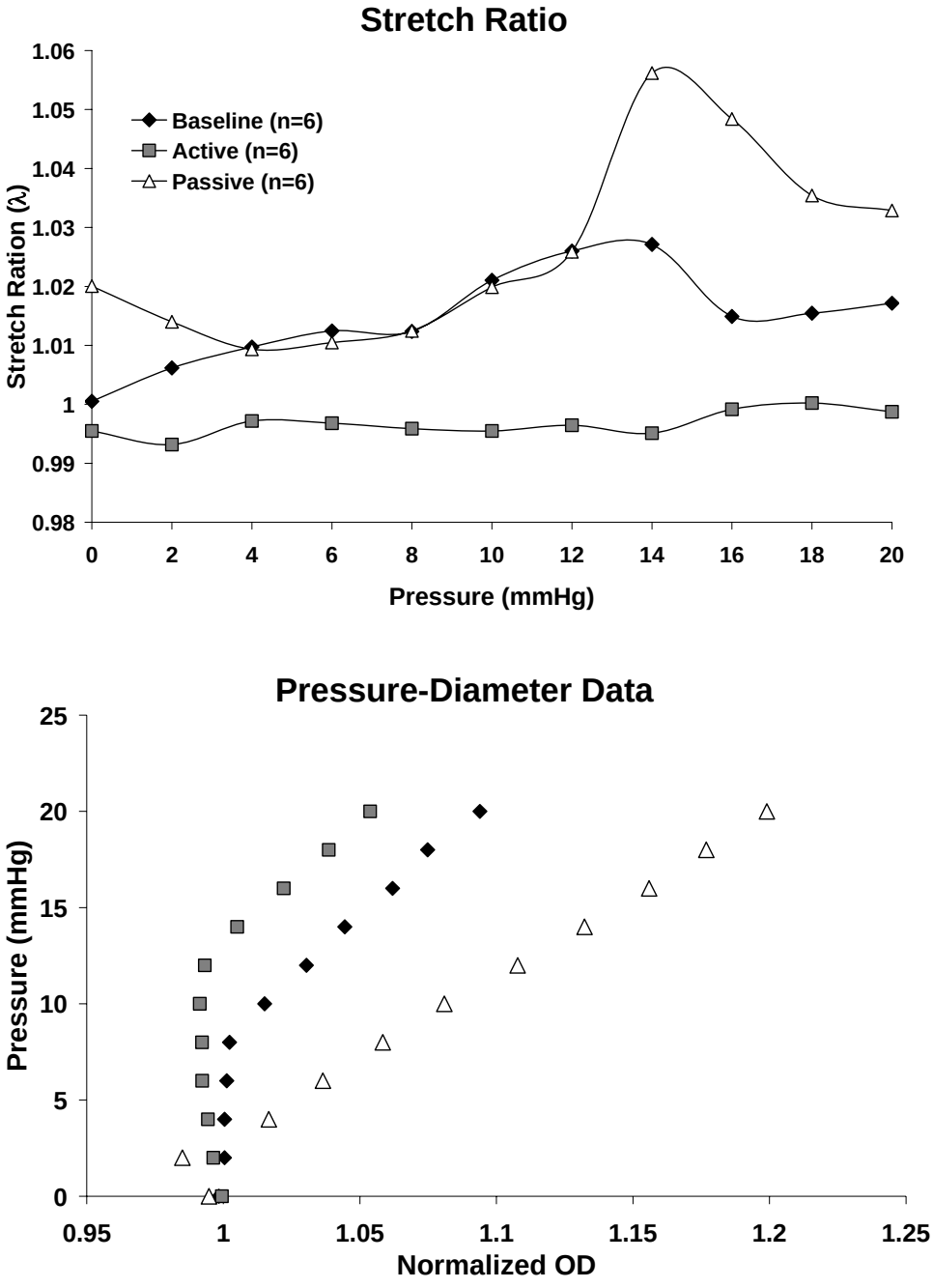

Figure 6.6 Variations of stretch ratio and outer diameter for biaxial testing of control tissue for baseline, active, and passive conditions. All experiments were performed on the middle segment.

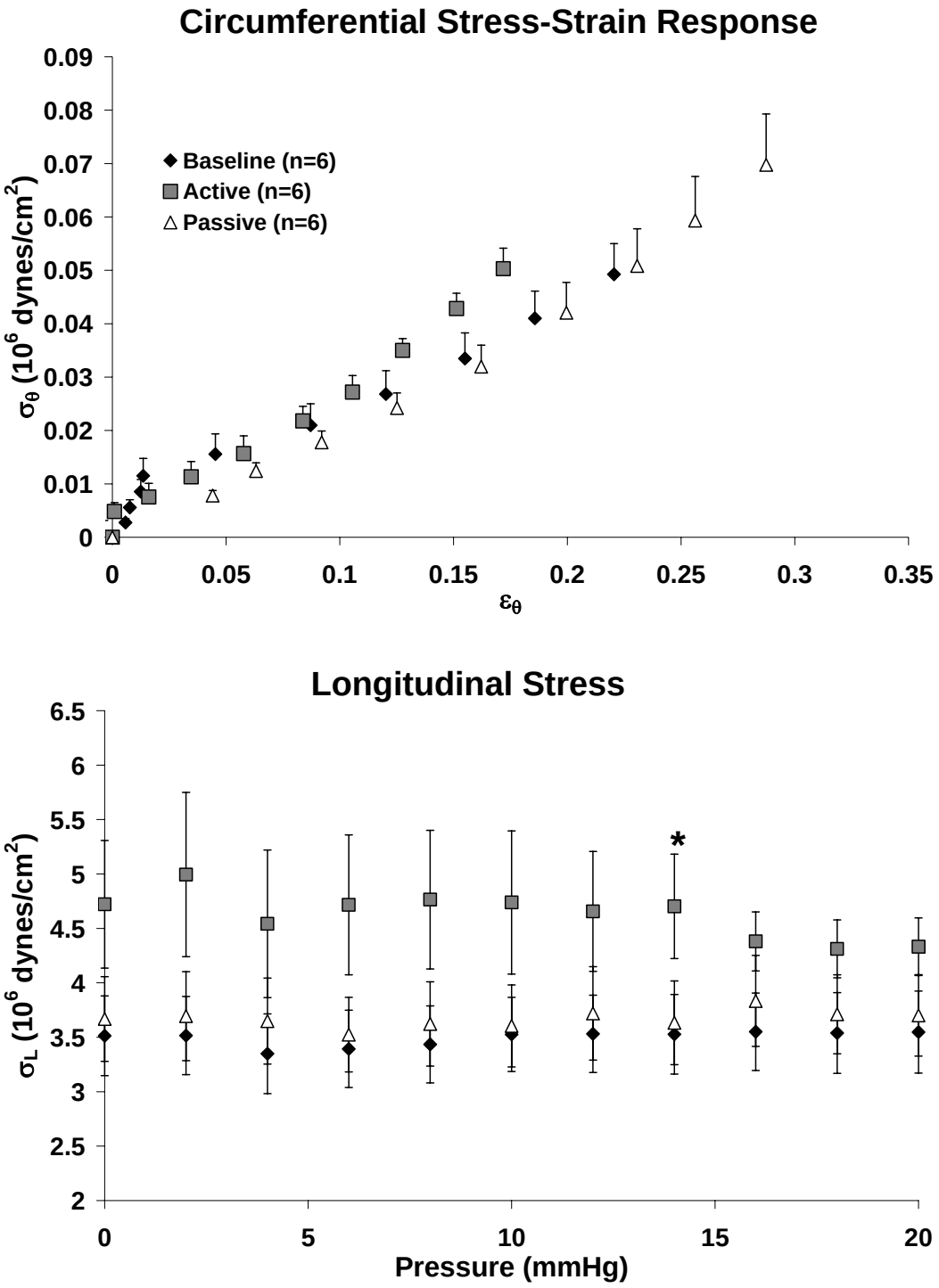

Figure 6.7 Circumferential stress-strain response (top) for the middle segment of the urethra and longitudinal stress values (bottom). * represents a significantly higher longitudinal stress value compared to that of baseline and passive at 14 mmHg.

FCR values were assessed in order to study muscular activity in the longitudinal direction in all three states. Circumferential smooth muscle had a much larger amount of muscular activity than longitudinal muscle in both baseline and active conditions. Active conditions have increased FCR values compared to baseline. For outer diameter, baseline and active FCR are similar until 8 mmHg of pressure, and then average FCR values sharply increase in the active state. Longitudinal FCR values behaved differently. Active conditions had higher FCR values than that of baseline over the entire pressure range (**Figure 6.8**). No significant differences were found between baseline and active states.

6.3.2 Pharmacological Results

NOSi induced a gradual decrease in outer diameter (-2.0 ± 0.5%), while the longitudinal muscle increased in length (3.5 ± 0.9%). PE caused a strong circumferential contraction (-1.4 ± 0.6%), but for longitudinal measurement there was little change (0.2 ± 0.2%). BE yielded a contraction in both orientations, but circumferential smooth muscle contraction was more robost (-2.7 ± 1.0% vs. -0.5 ± 0.2%). Finally, EDTA induced relaxation was larger for circumferential than longitudinally- oriented smooth muscles (9.2 ± 4.1% vs. 2.2 ± 0.3%, respectively; **Figure 6.9**).

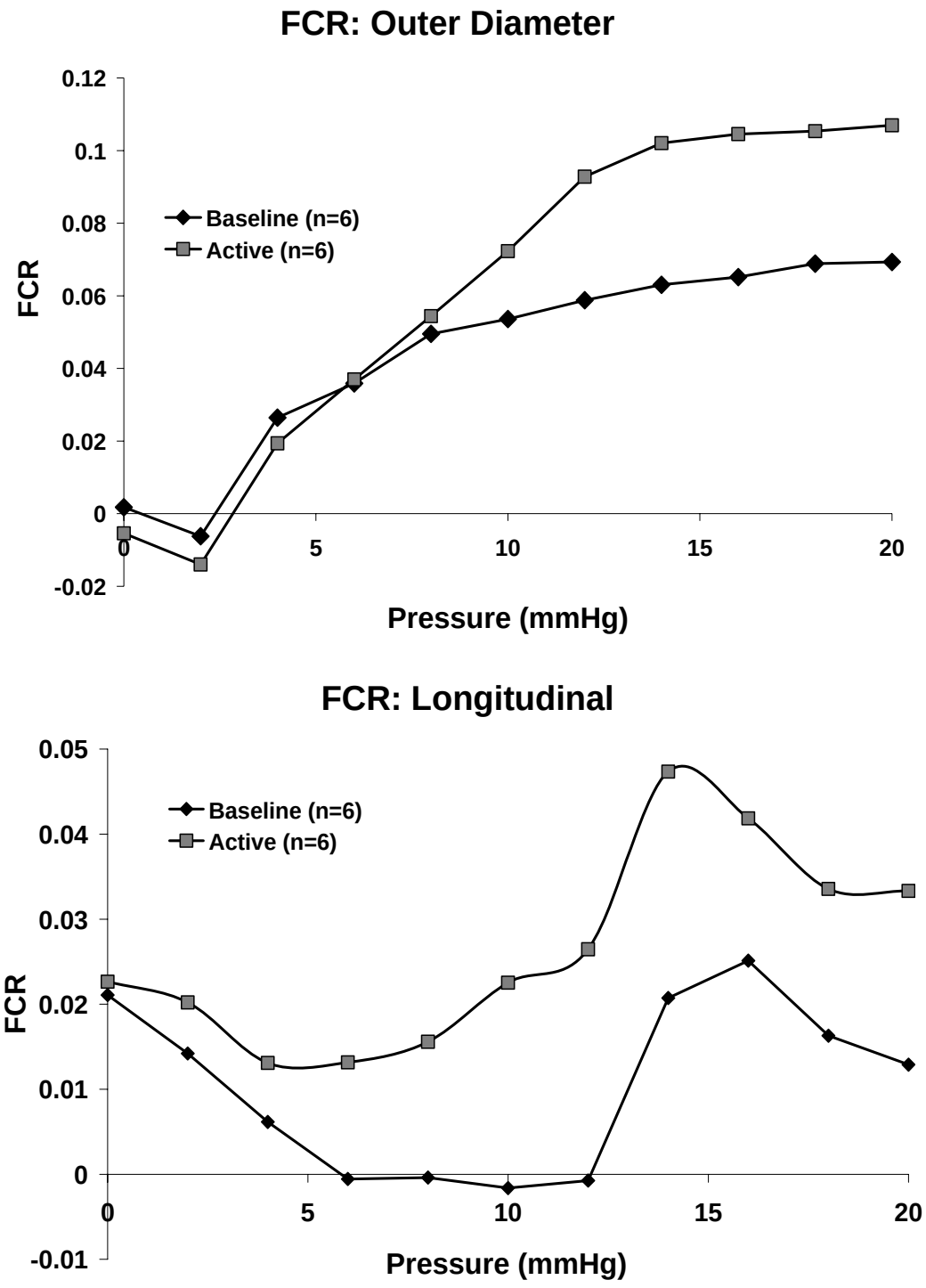

Figure 6.8 FCR for mid urethral outer diameter (top) and longitudinal (bottom) changes in the baseline and active states.

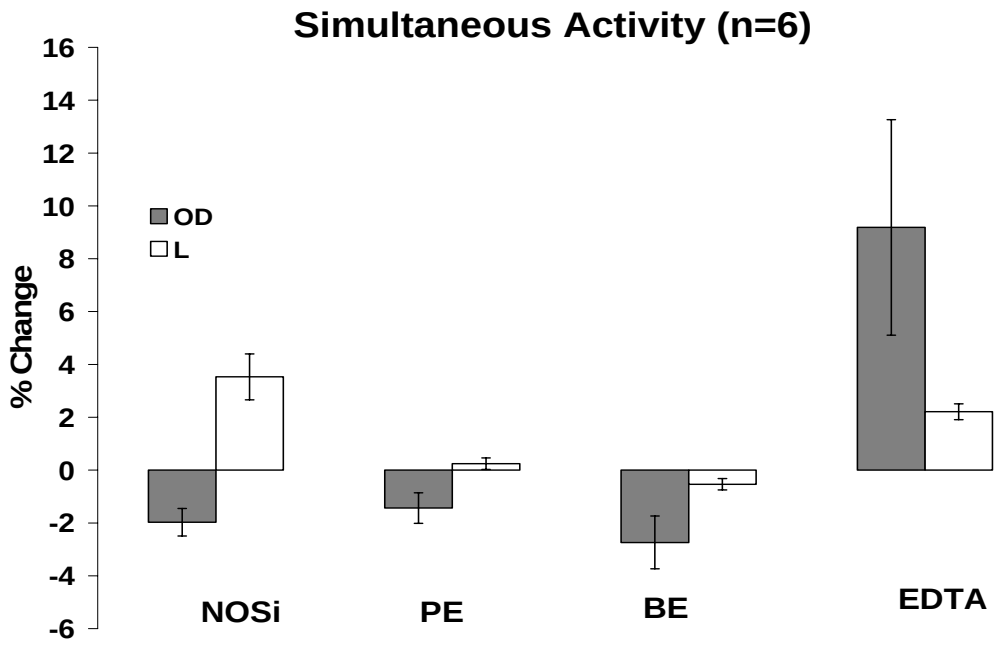

Figure 6.9 Quantified simultaneous changes of mid urethral outer diameter and length in response to NOSi, PE, BE, and EDTA. Error bars represent standard error.

6.4 DISCUSSION

While the striated sphincter is given much of the credit for maintaining continence, the circumferential smooth muscle is thought to be the next line of defense for providing the bulk of urethral closure force. Still, there is one component to the urethra, the longitudinal smooth muscle, that has not only been ignored, but its role remains speculative. The most popular hypothesis for the longitudinal role is that the longitudinal urethral smooth muscle relaxes, allowing the circular muscle (both striated and smooth) to maximally contract on the inner-mucosal lining, providing a water-tight seal [7]. In this study, a device was designed to evaluate

this hypothesis. Simultaneous assessment of circumferential and longitudinal smooth muscle both biomechanically and circumferentially could make this hypothesis fact or fiction.

Utilizing the DVRT, 5% pre-stretch was determined to be the optimum stretch to activate the longitudinal smooth muscle (**Figure 6.4**). Outer diameter of the middle urethral segment was assessed since it is the location of the bulk of muscle and highest urethral pressure. As expected, active smooth muscle had the highest stiffness, followed by the baseline state, and the most compliant (least stiff) was the passive curve. This was true for both longitudinal and circumferential data (**Figures 6.5-6.6**). Additionally, muscular activity was highest in active muscle than for both baseline and passive (**Figure 6.7**). An important and consistent observation was that longitudinal changes were minimal compared to circumferential. This observation was similar to that of past research [10, 16]. It is proposed that different cross-bridge turnover rates contribute to this difference and that longitudinal muscle has different actin-myosin interactions [20].

Pharmacological studies had interesting results (**Figure 6.8**) on the two muscles. NOSi produced opposite results, where circumferential muscle gradually decreased outer diameter and longitudinal muscle gradually relaxed, and PE caused a contraction in circular muscle and little or no response to the longitudinal muscle. This is not surprising since it has been well established that circumferential contractions have a large adrenergic component [106]. For muscarinic response, the circumferential and longitudinal muscle both resulted in a contraction, where the circumferential response was stronger. This could be due to the fact that the longitudinal muscle has a population of muscarinic receptors [19, 123] .

The longitudinal contraction was minimal. Therefore, it is difficult to establish a role for this urethral component from these studies. Still, smooth muscle activity is increased for the

longitudinal muscle after activation with PE and BE, as indicated by FCR (**Figure 6.7**). FCR also indicated a sharp increase of spontaneous myogenic tone in the urethra from at 14 mmHg. This may suggest that the urethral basal tone of the longitudinal muscle may play a larger role at higher intravesical pressures during the storage phase. It has been suggested that this spontaneous tone may help the urethra smooth muscle adjust to bladder filling [25]. However, comparing circumferential stress-strain data for biaxial tested versus the fixed length indicates that the longitudinal smooth muscle does play some role in urethral function. This is indicated by the change in the shape of the stress-strain curve for the biaxial tested (Figure 5.9). Although experiments are performed in presence of 5% pre-stretch, longitudinal smooth muscle involvement induced a sigmoidal stress-strain response in the baseline state of the middle urethra compared to the exponential shape of the baseline state at a fixed length (no pre-stretch).

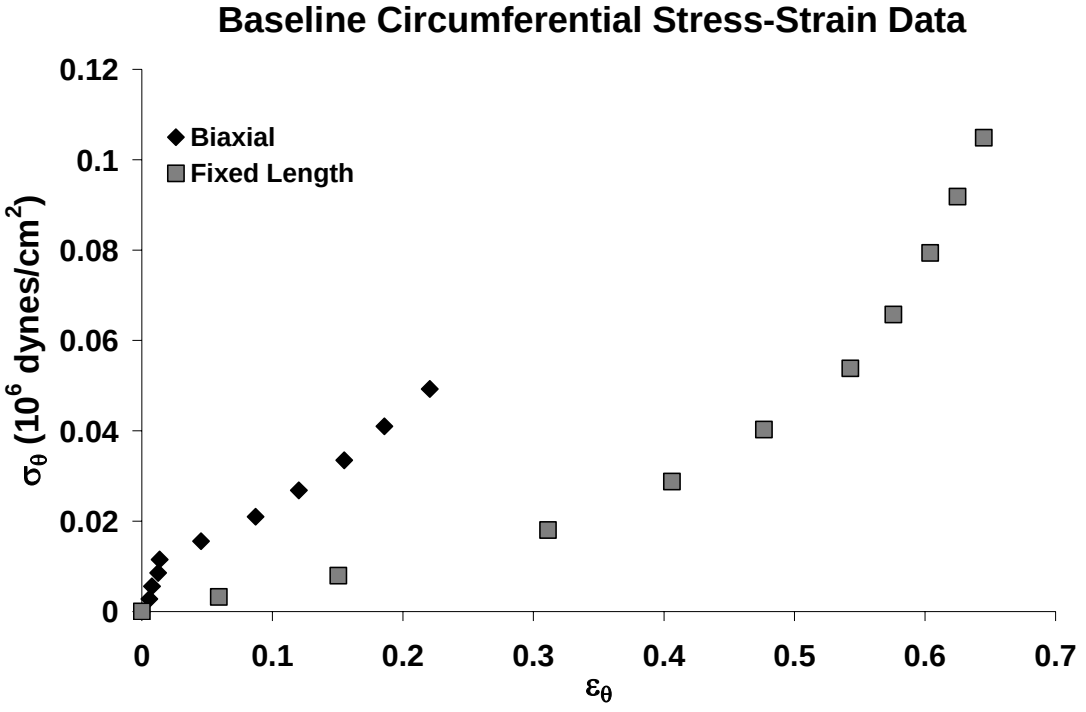

Figure 6.10 Comparison of biaxial testing and testing at a fixed length for the mid urethral response in the baseline state.

The modified device has proven its ability to assess simultaneous circumferential and longitudinal smooth muscle responses. While the longitudinal muscle had a small amount of activity in the presence smooth muscle activating agents, it appeared to changes the response in the circumferential direction compared to testing performed at fixed lengths. Still, more studies must be performed to further clarify the role of longitudinal smooth muscle.

7.0 SUMMARIZED DISCUSSION AND CONCLUSIONS

The components of the urethra can be categorized into three parts: nerves, muscle, and extracellular matrix (ECM). These three components coordinate with each other to aid the bladder in providing a successful storage mechanism, as well as a mode of urine to exit the body. This dissertation has provided supporting evidence that birth trauma induced by vaginal distension harms these three factors in the urethra, contributing to the complications of urethral hypermobility and ISD (both discussed in **Section 1.3.1**) in SUI.

7.1 DISCUSSION

The following discussion will be separated into three sections that focus on the data based on the three segments of the urethra examined here (i.e., proximal, middle, and distal) and will focus on the damage brought on by VD.

7.1.1 Proximal urethra in SUI

In women with SUI, the proximal urethra/bladder neck is often open and contributes to urethral hypermobility [92]. Indeed, the proximal urethra is particularly vulnerable to damage during

birth trauma, since this segment is the least supported in vivo. Our studies provided evidence that the muscle, innervation, and ECM of the proximal urethra were damaged from simulated birth trauma in a rat.

Basal smooth muscle tone was defective after VD. This was evident from changes in the baseline biomechanical properties, such as compliance (at low pressures; **Figure 2.6**), beta stiffness (**Figure 2.7**), and incremental elastic moduli values (Figure **2.9**). More specifically, the baseline data was not significantly different from passive data in the VD groups; whereas for controls, both curves were different in all three segments. This may be due to the decrease in muscle mass in the proximal urethral segment supported this concept and agreed with other studies [45, 47, 52]. In these experiments, Masson's trichrome analysis (**Figures 2.10-2.11**) of tissue sections revealed approximately a 20% decrease in muscle tissue.

Changes in proximal smooth muscle function were also evident in the active biomechanical studies. In the presence of PE (an α_1-adrenergic agonist), proximal urethral circumferential stress was significantly less at low strains in the VD group (**Figure 4.6**). Furthermore, FCR was less for the VD group compared to that of control, indicating that smooth muscle activity was absent with increasing pressure (**Figure 4.4**). The adrenergically-induced smooth muscle activity could not maintain urethral resistance with increasing static pressures for the proximal urethra after birth trauma. This could be due to hypoxic conditions that transpire during vaginal distension [91]. It has been confirmed that hypoxic conditions to urethral smooth muscle impair the adrenergic response, [129] which could damage the smooth muscle and its innervation. PGP 9.5 and TH staining further supported the idea since there was a lack of sympathetic nerve fibers in the proximal urethra (**Figure 4.10**). A damaged proximal urethral response to PE implicates an injured sympathetic storage reflex as a contributor to SUI.

The proximal urethra also had altered active biomechanical properties in the presence of BE. While the role of parasympathetic innervation is not well established in the urethra, this finding implicates the muscarinic cholinergic properties of proximal urethral smooth muscle in the maintenance of continence. Results indicated that the proximal urethral smooth muscle in the presence of BE had decreased circumferential stress and mid and high strain ranges (**Figure 5.6**). Lack of muscular resistance in the presence of BE after VD may be due to two reasons. Parasympathetic activity has been pinpointed to the longitudinal smooth muscle by past studies of urethral strips [19]. The longitudinal muscle is also closest to the lamina propria area where most of the vasculature is located [137]. Thus, it is quite possible that the longitudinal muscle may be the most affected by hypoxic conditions. Still, the longitudinal muscle was not assessed in VD and the longitudinal smooth muscle response to PE was very small (**Figure 6.9**).

PGP 9.5 staining indicated a significant urothelial thickening in the proximal urethral segment after VD (Figure 3.10). Although we are uncertain of the pathology of this finding, one possible reason could be that this thickened lining may be an inflammatory response, which may have a significant effect on the longitudinal muscle since it is closest to the inner lining and inflammatory cells are known to carry cholinergic properties [138].

Damage to proximal urethral innervation was made evident by the lack of PGP 9.5, TH (sympathetic), and VACht (cholinergic) staining (**Figures 4.10-4.13 and 5.9-5.10**). These histological results reinforce the idea that the increased PE and BE contractility in the proximal urethra post-VD was caused by post synaptic supersensitivity (Figures 3.2 and 4.2). Denervation has been well associated with post-synaptic supersensitivity in other muscular organs [114, 139].

The most likely reason for proximal urethral insufficiency is the ECM damage or alteration in VD. This is supported by the increase in proximal urethral compliance in the passive

state (**Figure 2.6**). The conventional biomechanical theories applied here, which had been previously derived for blood vessels, may lead one to think that this is mainly due to lack of collagen to provide stiffness. However, urethral structure is quite different from that of the blood vessel. Studies described in **Chapter 3** specify that damaged elastin may be the primary ECM damage that occurs as a result of VD, where there is increased proximal urethral compliance at low pressures. However, according to the findings in blood vessels, this does not intuitively fit with the observation. Miller's elastic stain on VD urethras indicated a lack of radial orientation of elastic fibers in the proximal portion (**Figures 2.13-2.15**). Elastic fibers envelope muscle fibers, and urethras dramatically dilate with elastase treatment (**Figure 3.3**). It is probable that elastic fibers act as the strut that transmits the stress of a muscle contraction to the collagen matrix; thus, holding the tissue together. Damaged elastin in the urethra is supported by other studies of periurethral tissue in women with SUI [87]. However, elastin concentrations for the entire urethra increased for VD urethras (**Figure 2.17**). Since the assay measures different forms of elastin, including tropoelastin, this may be due to the urethral cells attempting to repair the elastic fiber matrix. Changes in collagen could also contribute to this concept. While there was no increased collagen concentration for the proximal urethral segment post-VD, there is a change of collagen orientation as indicated by the polarized microscopy performed (**Figure 2.12**).

7.1.2 Middle urethra in SUI

The middle urethra is considered the most important portion for maintaining continence [94]. It has been established as the high pressure zone due to its high urethral pressures after an increase from sneezing [17, 94]. Although the external urethral striated sphincter was not studied in the

present experiment, there were many changes found in the smooth muscle behavior, nerve tissue, and ECM in the middle segment.

Basal smooth muscle tone had increased activity in the middle segment of VD urethras. This was suggested by the increase in beta stiffness value for the baseline state in the VD middle segment (**Figures 2.7, 2.9**), and by the significant decrease of urethral dilation after application of 8 mmHg during the functional tests (**Figures 4.2, 5.2**). This could be due to damage of the peripheral nerves, as noted in denervated arteries of the middle ear [125], but this increase in baseline pressure does not agree with in vivo studies, where the baseline urethral pressure was less in VD [18]. Increased basal smooth muscle tone in the middle urethral segment for VD urethras possibly contributed to the lack of any changes found with BE or PE contractility and might also have contributed to the significant increase in circumferential stress derived for low strain ranges in the middle VD urethra (**Figure 4.7**). The basal smooth muscle tone may be trying to compensate where these mechanisms are defective. Little or no changes were found in the muscarinic active biomechanical properties of the VD urethral middle segment. This may be due to the observation that muscarinic receptors do not play as large a role in maintaining continence as do the nicotinic receptors at the neuromuscular junction of the striated muscle sphincter [140].

Innervation was severly damaged as indicated by immunohistochemical staining that showed a marked decrease of PGP 9.5, TH, and VACht staining (**Figures 4.10-4.13**). This finding was similar to that of other studies for innervation in a rat model of birth trauma [46, 128]. VACht indicated damaged cholinergic innervation to the middle urethra even though we did not find any changes to the response of BE or its biomechanical changes. This may be due to

the fact that the pudendal nerve is the primary innervation at this site, and there is much evidence that it is damaged during birth trauma [41, 141].

ECM may also be a large contributor to damaged mid urethral continence mechanism. Not only did we find that collagen concentration was significantly decreased after VD in the middle segment (**Figure 2.16**), but an alteration in collagen orientation was evident using polarized microscopy indicating that collagen may have been severely weakened (**Figure 2.12**). Other studies not only found changes in the amount of collagen in birth trauma and SUI [52, 89], but they also found an increased amount of collagen III, which may point toward scar formation [88]. Eroding collagen may also contribute to the significant increase in basal tone found in the middle segment of VD urethras. Biomechanical studies for compromised collagen in the urethra (**Chapter 3**) indicate that this causes decreased compliance for the middle and distal urethras (**Figure 3.3**).

7.1.3 Distal urethra in SUI

Not many changes were found in the distal segment of the urethra with the exception of biomechanical studies in the baseline and passive states. Here, VD appeared to cause alterations in the basal tone of distal portion (**Figure 2.9**, bottom). Since the distal portion is required to be strong if the proximal urethra is weak [99], any damage to the distal segment could contribute to SUI induced by birth trauma.

PGP 9.5 and VACht staining indicated that the both sympathetic and cholinergic innervation of the distal urethra post-VD is reduced compared to distal controls, though not siginificant ($p=0.055$,$p=0.053$, respectively). However, sympathetic innervation was unaffected as indicated by TH staining. The location of the distal urethra makes it vulnerable to severe

stretch during birth trauma. Most of this damage is probably due to direct mechanical damage by stretch during labor.

ECM changes were present but not as obvious as seen in proximal and middle segments. No changes were distinguished for collagen concentration, but a small change in collagen orientation was seen via polarized microscopy. The distal urethra is not credited as a contributor to urine storage; however, any damage to this segment may still contribute to SUI.

7.2 CLINICAL RELEVANCE

These studies have proven that numerous factors contribute to SUI induced by simulated birth trauma. Biomechanical and functional studies verified damage in the muscular and ECM components, and histology supported a lack of cholinergic and sympathetic innervation.

While studies have proven the lack of urethral activity in women with SUI [142, 143], there has not been a clear-cut correlation to a lack of basal tone in the urethra (i.e., baseline urethral pressure). We have established from our biomechanical data an alteration of smooth muscle basal activity in the urethra after simulated birth trauma (**Section 2.3**). The basal smooth muscle tone may be responsible for providing the initial urethral tone, and innervation may simply enhance this tone during times of sudden or high increases in bladder pressure. Thus, the lack of this 'preliminary' tone could contribute to the lack of urethral activity described in women with SUI. Impaired basal activity may be an important observation, but there are few studies of basal activity in the urethra (described in **Section 1.2.3**). Further clinical investigation and establishment of the existence of basal smooth muscle tone in women may aid in better pharmacological therapies for women with SUI.

Another main finding involved an increased contractile response to PE, an α_1 adrenergic agonist (**Figure 4.3**). It was proposed that this was due to post-synaptic supersensitivity, which was supported by the lack of TH innervation as indicated by histology (**Figures 4.13-4.14**). Adrenergic agonists have been used clinically and have successfully restored continence to only 14% of patients [144]. Other than lack of specificity of adrenergic agonists used clinically (e.g., increased cardiovascular side effects, headaches, anxiety), this smooth muscle contractile mechanism has been altered in response to damaged sympathetic nerves from birth trauma. Unless steps could be taken clinically to protect peripheral innervation (that is, if this is the only reason for smooth muscle changes) of the lower urinary tract, adrenergic stimulation via pharmacotherapy may not be very efficient.

Finally, not much credit has been given to the ECM in maintenance of urethral pressures, with the exception of studies performed by Awad and Downie [67]. Furthermore, many histological studies have deemed the urethral elastic fiber networks useless in the continence mechanism [14, 103] due to the fact that there is a small amount of elastic fibers compared to muscle and collagen in the urethral volume. Our findings in **Chapter 3** drastically oppose these conclusions. Urethras exposed to elastase treatment suggested increased compliance compared to passive controls, indicating that elastic fibers may help to control muscular tone in the urethra (**Figures 3.5-3.6**). On the other hand, compromised collagen has been found to decrease compliance, indicating that collagen probably plays more of a structural role than a functional one.

Clinically, there has not been much focus on the ECM. Some studies have attempted to quantify collagen and elastin damage to periurethral and urethral tissues in women with SUI [50, 87, 89, 145]. While all of these studies have established that collagen and elastic fibers are

altered or damaged in women with SUI, none of them try to understand how this damage correlates to SUI. Additionally, if the ECM is damaged, the effects on urethral smooth muscle and striated muscle are relatively unknown. This, in itself, could aid in a better understanding of the pathology of SUI in the clinic.

7.3 LIMITATIONS, CONCLUSIONS, AND FUTURE DIRECTION

7.3.1 Limitations

One of the most important possible sources of uncertainty and possible error was in maintaining the urethral in vivo length. For example, the urethra was measured at the time of dissection, but the sutures, which ligated the urethra at in vivo length, were untied in order to tie the urethra onto the tees of the ex vivo system. With hindsight, it would have been more prudent to develop an adjustable apparatus that could be used at the time of dissection, and versatile in a way that the proposed apparatus may fit into the perfusion system. Another limitation to the experimental set up was that the proximal, middle, and distal portions could not be measured at the same time. The laser could only be positioned at one point during testing. Thus, mechanical testing needed to be performed at one position at a time and in random order each time in order to avoid any variations in the results due to the strain history effects of biological viscoelastic tissue. A similar problem occurred during pharmacological testing. However, this was addressed by washing with Kreb's solution (not as costly as media 199) three times between each test and lengthening wash time to ~ 45 minutes.

For future experiments, one might also consider altering the system so that the urethra is exposed to continuou, yet minimal flow (approximately 1.5 ml/min). The system used in this work was set up so that the distal end was clamped off to allow application of intraluminal pressure. With this approach, the media contained within the urethra was not being circulated as was the adventitial bathing media. As a result, the tissue may not have received sufficient gas balance or nutrients. This may have contributed largely to any inconsistencies seen in the functional data. Tissue viability is a limitation to ex vivo systems, also. This obstacle may contribute to possible variations for the biomechanical and functional results. Kwon et al. [129] found that urethral strips exposed to anoxic conditions exhibited an immediate decrease in the contractile response to phenylephrine. Steps should be taken to understand affects on healthy urethral tissue from factors, such as mechanical isolation of the tissue, duration of time after excision, time in the perfusion system, and distension of the tissue. This was attempted with the use of a live/dead stain to assess necrosis, but the tissue was not permeable enough in order to gain a trustworthy assessment. Perhaps the lactate dehydrogenase assay, which indicates the amount of cell death by the release of lactate dehydrogenase from the cytosol of the damaged cell, should be incorporated.

Other limitations relate to the ex vivo nature of the experiments. The urethra is a highly innervated structure involving both somatic (external striated sphincter via pudendal nerve) and autonomic (sympathetic and parasympathetic) nervous systems. By excising the urethra and testing it ex vivo, all neural input to the urethra is eliminated, except for possible spontaneous release of transmitter from intramural nerve terminals. Future work might examine the effects of electrical stimulation to provide a model of the urethra that is closer to its in vivo environment and to maintain the integrity of the nerve tissue.

Finally, another limitation to this study involved the application of pressure. As described in **Section 2.2.4.1**, a reservoir filled with media 199 attached to a graduated ringstand was manually displaced to apply intralumenal pressure. While much care was taken to calibrate each graduation to increments of 2 mmHg using a water manometer, there still was more likely error of achieving exact increments of 2 mmHg. Also, by using manual displacement, the preconditioning regimen could only be performed at an approximate maximal rate of 0.5 Hz. Much faster strain rates are typically employed for mechanical testing of soft biological tissues [146]. An automated system involving a computer controlled stepper motor could possibly solve this problem, and could also allow the application of the pressure in smaller increments (1 mmHg) or even less, more accurately.

While the vaginal distension in a rat provides a model to separate mechanically-damaging effects from hormonal factors associated with birth, there are nonetheless many limitations. Also, typical stresses on the bladder are not similar to a human, since the rat walks on four legs, instead of two. Also, we chose four days after vaginal distension as the hallmark time point to perform our studies in the model of SUI. This was based on studies performed previously [47], but preliminary studies were never performed to show to verify that 4 days with our animal model was the optimal time for demonstrating urethral damage.

The longitudinal testing device also has its limitations. Compared to findings of similar studies [10, 16], the modification was successful in terms of enabling bidirectional assessment (i.e., of urethral function and mechanics of circular and longitudinal smooth muscle). It is recommended that a way to purge the tissue is developed for successful recirculation of the intralumenal flow.

There also are limitations with mathematical models and assumptions used to assess circumferential stress and strain, compliance, and incremental elastic moduli. The assumptions involve assuming that the tissue is a thick-walled cylinder, elastic, incompressible and orthotropic [83]. Unfortunately, the urethra is tapered, which we address by assessment of 3 different regions. As discussed, it is not homogeneous in structure. Still, while the orthotropic assumption is more appropriate than an isotropic one, this too has its limitations. Although there is much room for improvement with our assumptions, our compliance, stress, and moduli calculations were similar to the ranges of other tissues studied in various laboratories (**Table 7.1**).

Table 7.1 Beta stiffness (β), compliance (C), incremental elastic modulus (E_{inc}), and circumferential stress (σ_θ) values for the human saphenous vein [147], porcine carotid artery [148], rat middle cerebral artery [149], and the proximal urethra in the baseline state. C, E_{inc}, and σ_θ are reported for designated pressure values or ranges, P.

SPECIMEN	β	C ($mmHg^{-1}$)	E_{INC} ($10^6 dynes/cm^2$)	σ_θ ($10^6 dynes/cm^2$)
Human Saphenous Vein	23.55	0.007 (P=20 mmHg)	NA	0.18 (P=10 mmHg)
Porcine Carotid Artery	NA	0.2 (P=70 mmHg)	0.67 (P=150 mmHg)	1.07 (P=150 mmHg)
Rat Cerebral Artery	8.5	NA	5.0 (P=50-75 mmHg)	2.25 (P=200 mmHg)
Proximal Urethra	7.31	0.69 (P=12-20 mmHg)	3.20 (P=20 mmHg)	0.25 (P=20 mmHg)

7.3.2 Conclusions and future directions

Birth trauma is a crucial etiological factor in the genesis of SUI [3, 32, 150]. Unfortunately, the pathological factors involved in this process are not fully understood. In this dissertation, the studies have helped to further our knowledge and will help to pinpoint a solution or therapy for this lower urinary tract disorder.

Biomechanical properties of the baseline and passive states were altered in VD urethras for all segments. This gives importance to basal smooth muscle tone involvement in urethral function. It is proposed that urethral basal smooth muscle tone provides a pre-existing tone to allow for effective prevention of leakage (**Chapter 2, Section 2.4**). But what is the source of this basal tone? Is this the main contributor to the lack of circumferential stress for active adrenergic and muscarinic cholinergic smooth muscle responses found in proximal urethras post-VD? If it lacks in the proximal urethra, why does the sensitivity of basal tone appear to be heightened in the mid urethral segment from VD (**Figures 4.2, 5.2**, center)? There are many suggestions that basal smooth muscle tone is largely affected by ion channel activity or interstitial cells [25]. Also, does this stem from hypoxia, which has been mentioned previously? Hypoxyprobe staining should be performed to answer this question. All of these aspects are avenues to explore in order to comprehend the role of spontaneous, stretch-sensitive myogenic urethral tone in health and disease, such as SUI.

After VD, the proximal urethral response to BE and PE and histological studies of innervation, involving TH and VACht, were severely affected by post-synaptic super-sensitivity of the hypogastric (sympathetic) and pelvic (parasympathetic) nerves (**Figures 4.2, 5.2**, top). Thus, it was clear that the lack of innervation may have caused this increased in contractility. On the other hand, how does VD affect the ability of urethral smooth muscle to respond to

neurotransmitters such as norepinephrine and acetylcholine? The next step should be to assess the actual adrenergic and muscarinic receptors throughout the smooth muscle via immunohistochemistry or western blots. This too could be a reason for the damaged response.

Impaired ECM is the likely contributor to the altered active, baseline, and passive biomechanical properties. Studies indicated VD-induced changes in orientation and amount of collagen (**Figures 2.10-2.11, 2.16**) especially for the mid urethral segment) and damaged and increased elastin (**Figures 2.13-2.15, 2.17**). Additional data pointed to elastin damage as the main cause of the increase in compliance and damaged collagen as the cause of decreased beta stiffness (**Chapter 3**). Further studies should focus on the effects of collagen and elastin damage on urethral smooth muscle activity.

It would also be important to correlate these biomechanical and functional findings with what happens in vivo during vaginal distension. For example, during balloon inflation of the rat vagina it would be important to find that one of the highest points of stress would be on the proximal urethra/bladder neck region since this is where most of the urethral changes occurred ex vivo. Some studies have developed computer models to assess pudendal nerve and pelvic floor damage during birth [141, 151], but none have actually assessed damage of the lower urinary tract during child birth or simulated birth trauma.

Finally, the system was modified to assess longitudinal and circumferential smooth muscle simultaneously. Preliminary results indicated that circumferential muscle had much larger biomechanical and smooth muscle contractile responses than longitudinal muscle. Still, longitudinal smooth muscle must play some role in urethral function to alter the biomechanical response when comparing biaxial testing to that of testing at fixed length (**Figure 6.9**). Yet, this needs to be further examined. Still, these studies support the fact that in continence the

circumferential muscle provides the closure force during storage while the longitudinal muscle may relax or shorten during voiding [7, 10, 19, 20, 123]. Another thought may also be that the longitudinal muscle to act as a drawstring on the inner mucosal lining, cinching it for a water-tight seal. Either way, it would be important to repeat the studies using this device.

APPENDIX A

RESULTS FOR INDIVIDUAL SPECIMENS

BASELINE STUDIES

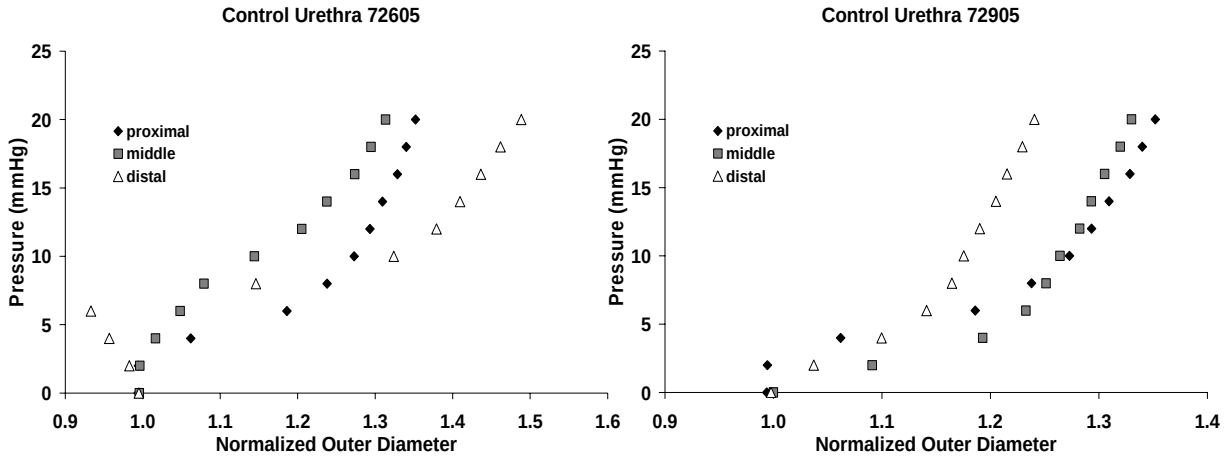

Figure A. 1 Baseline pressure-diameter data for control specimens.

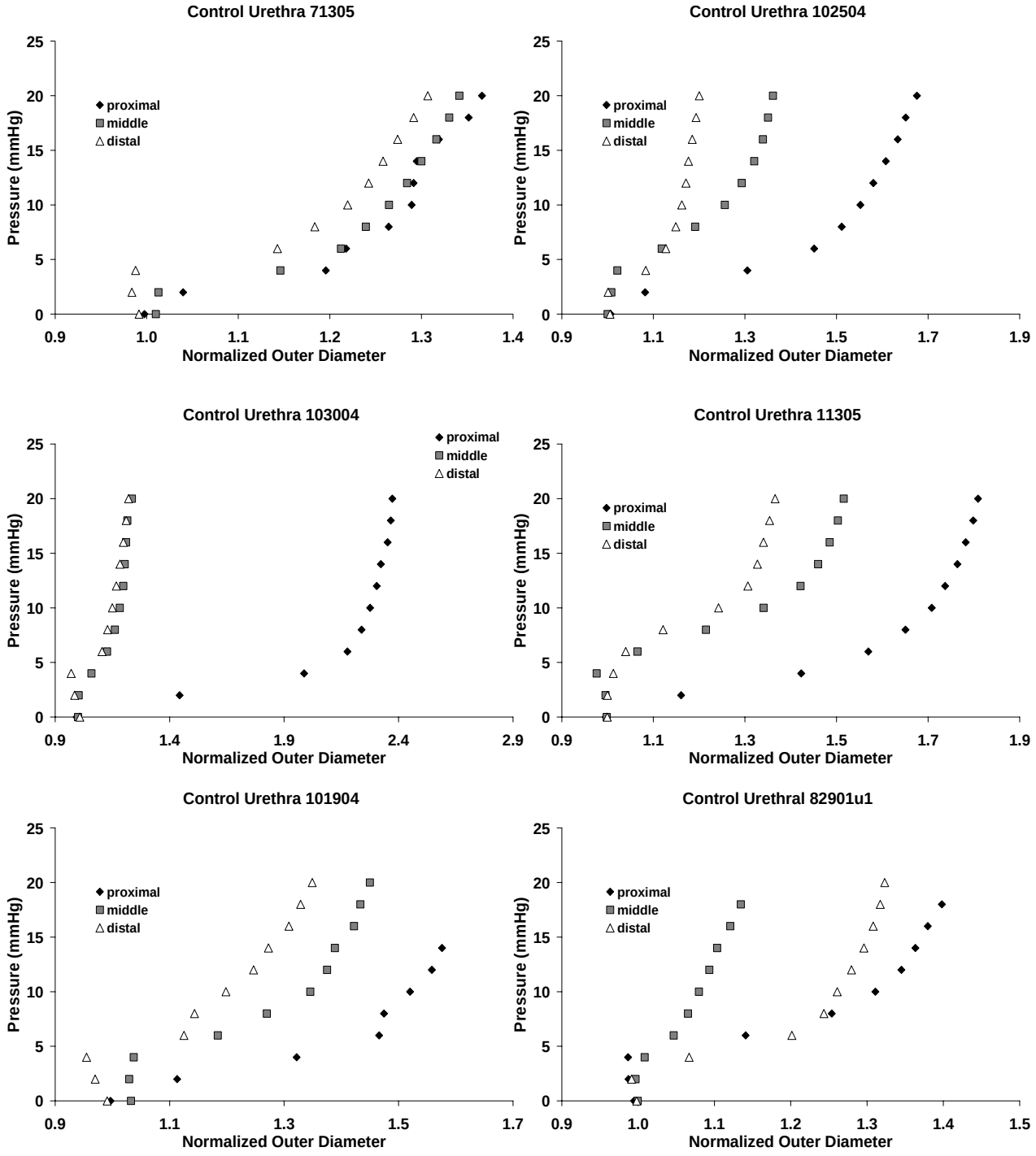

Figure A. 2 Baseline pressure-diameter data for control specimens.

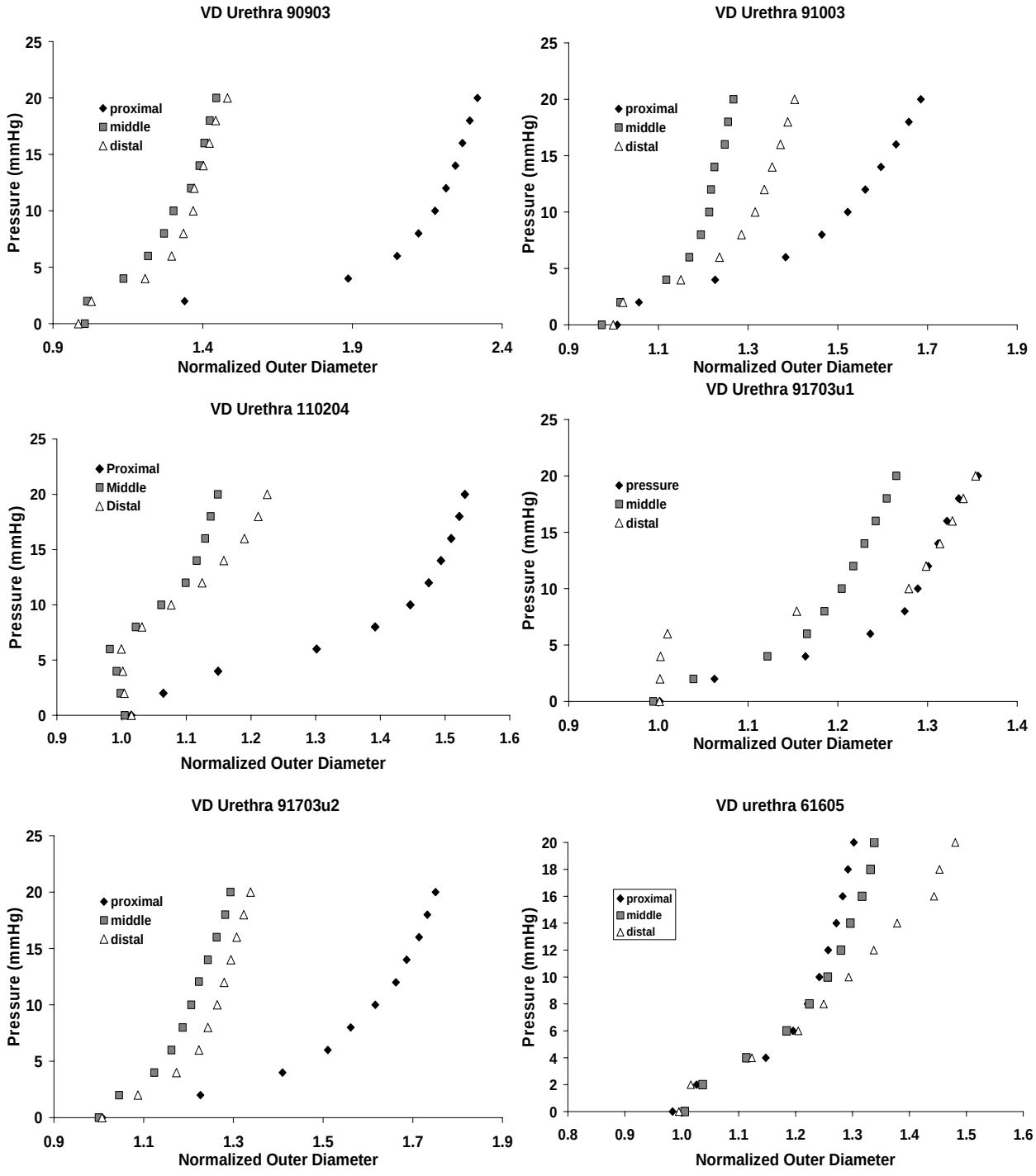

Figure A. 3 VD urethral specimens tested in the baseline state.

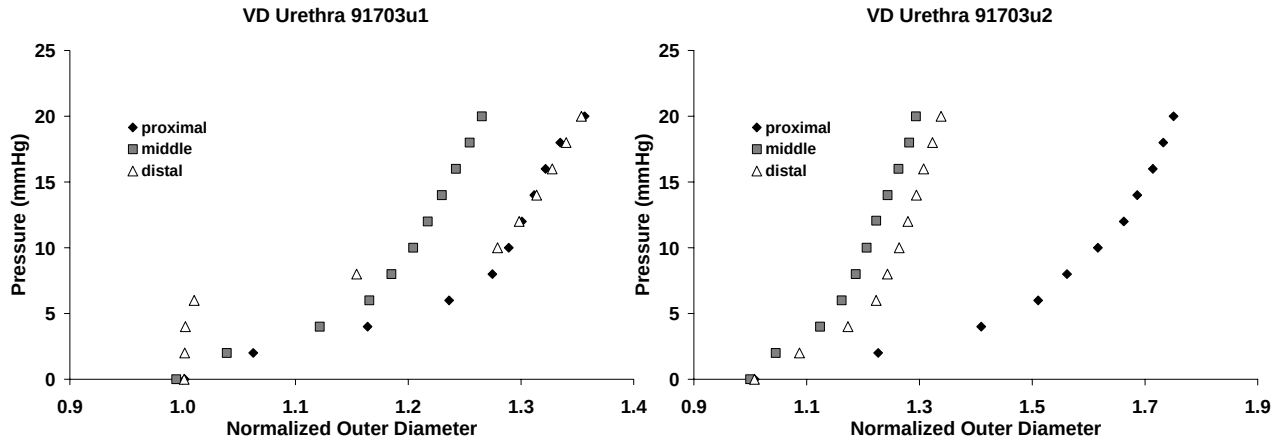

Figure A. 4 VD urethral specimens tested in the baseline state.

PASSIVE STUDIES

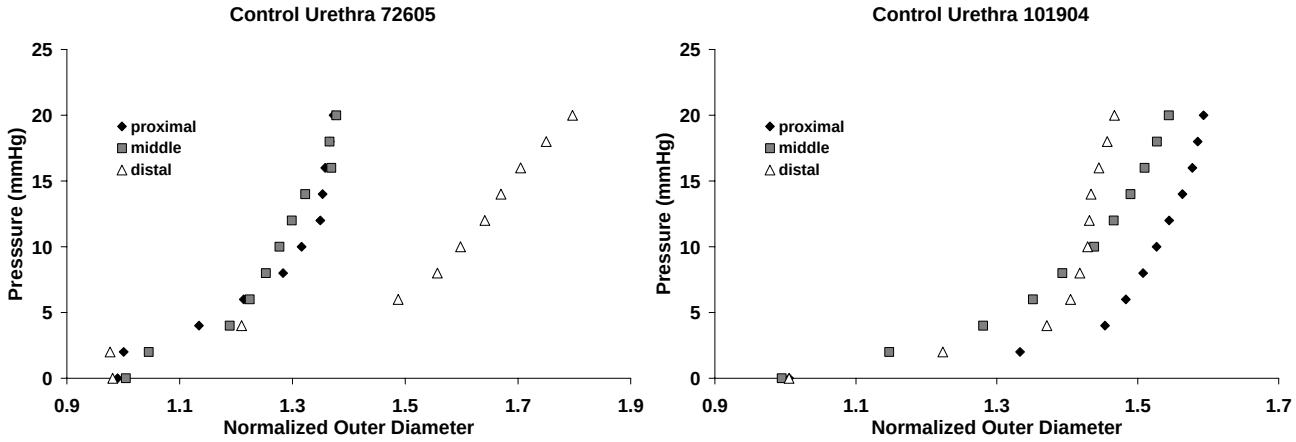

Figure A. 5 Passive pressure-diameter curves for control specimens.

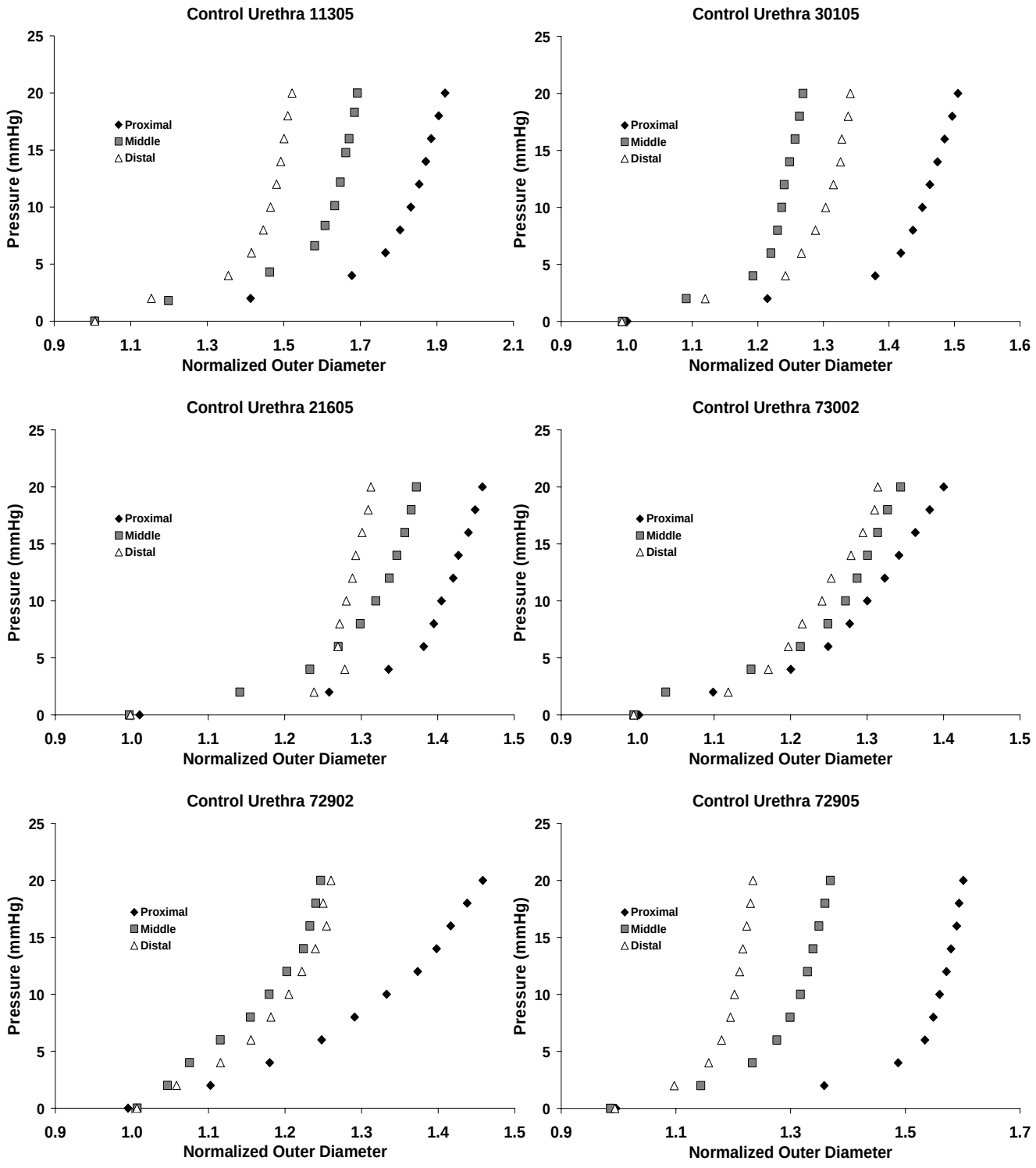

Figure A. 6 Passive pressure-diameter curves for control specimens.

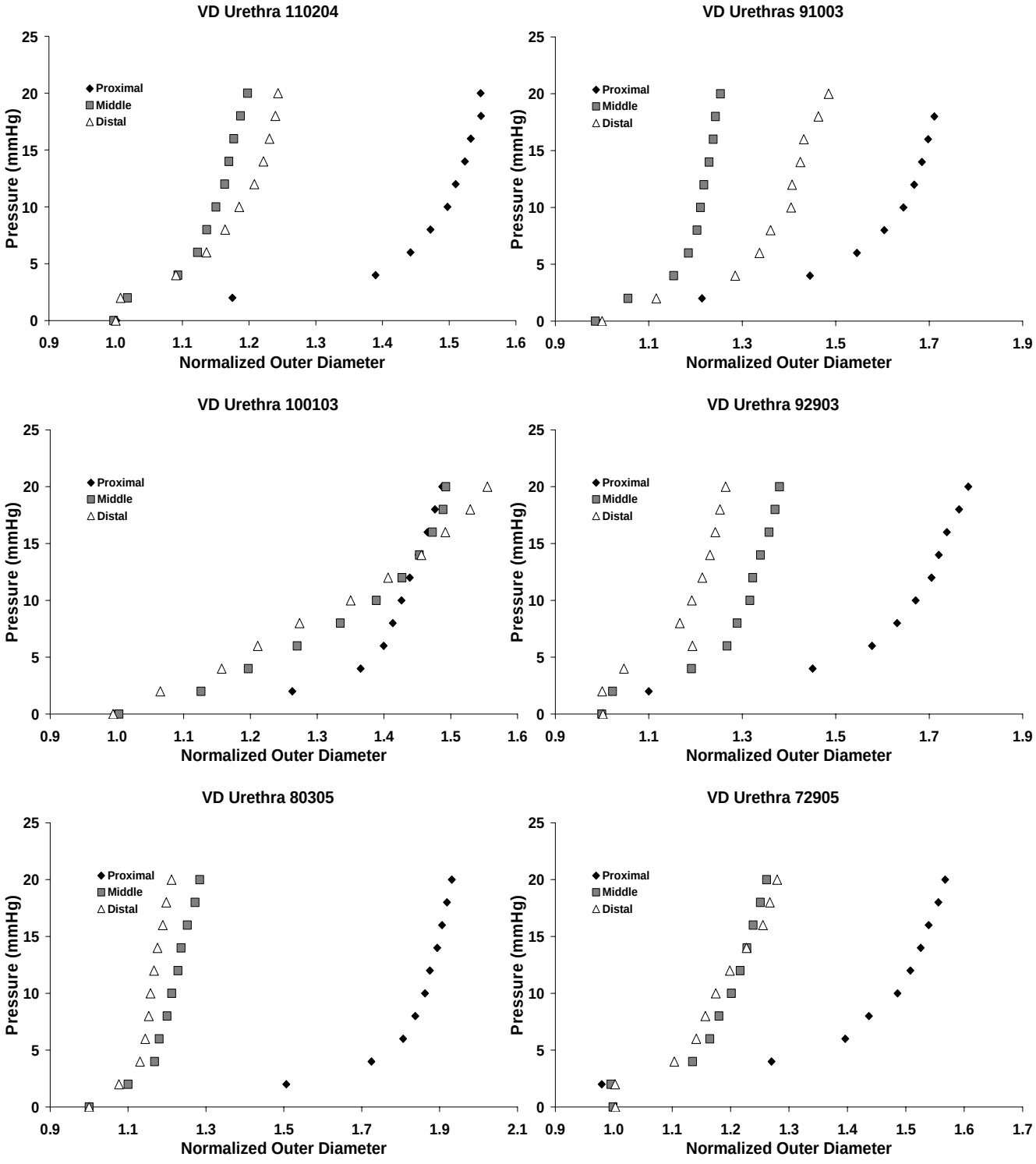

Figure A. 7 Passive pressure-diameter curves for VD specimens.

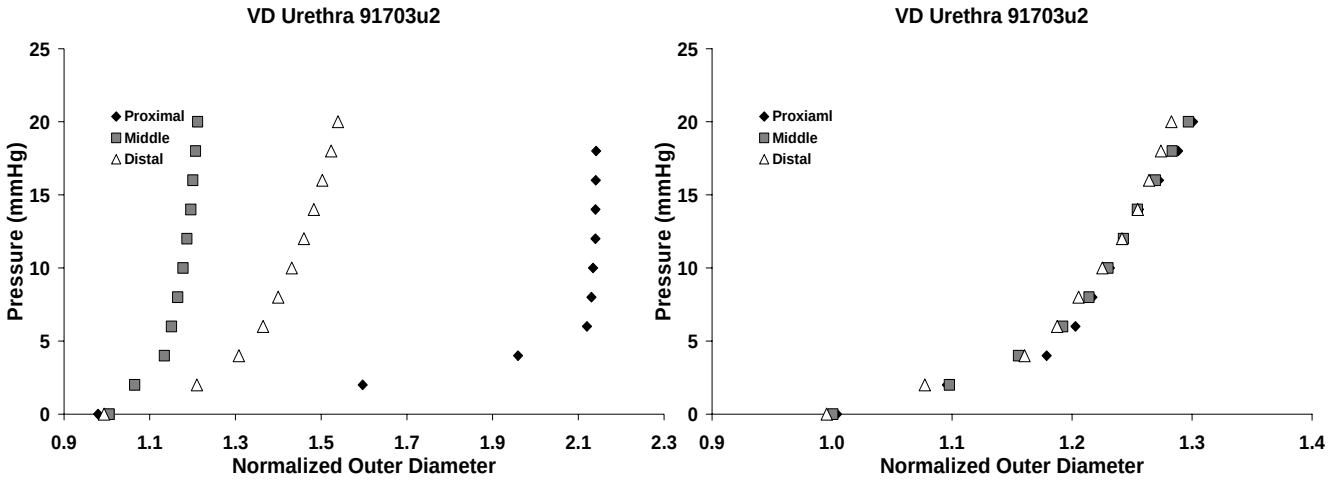

Figure A. 8 Passive pressure-diameter curves for VD specimens

FUNCTIONAL STUDIES: PHENYLEPHRINE

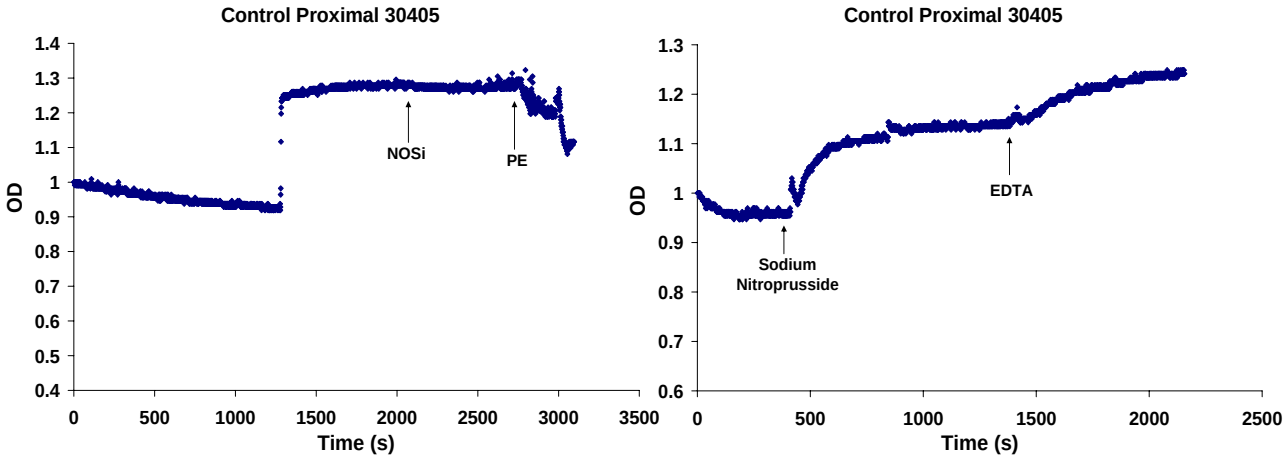

Figure A. 9 Contraction and relaxation of control proximal specimens.

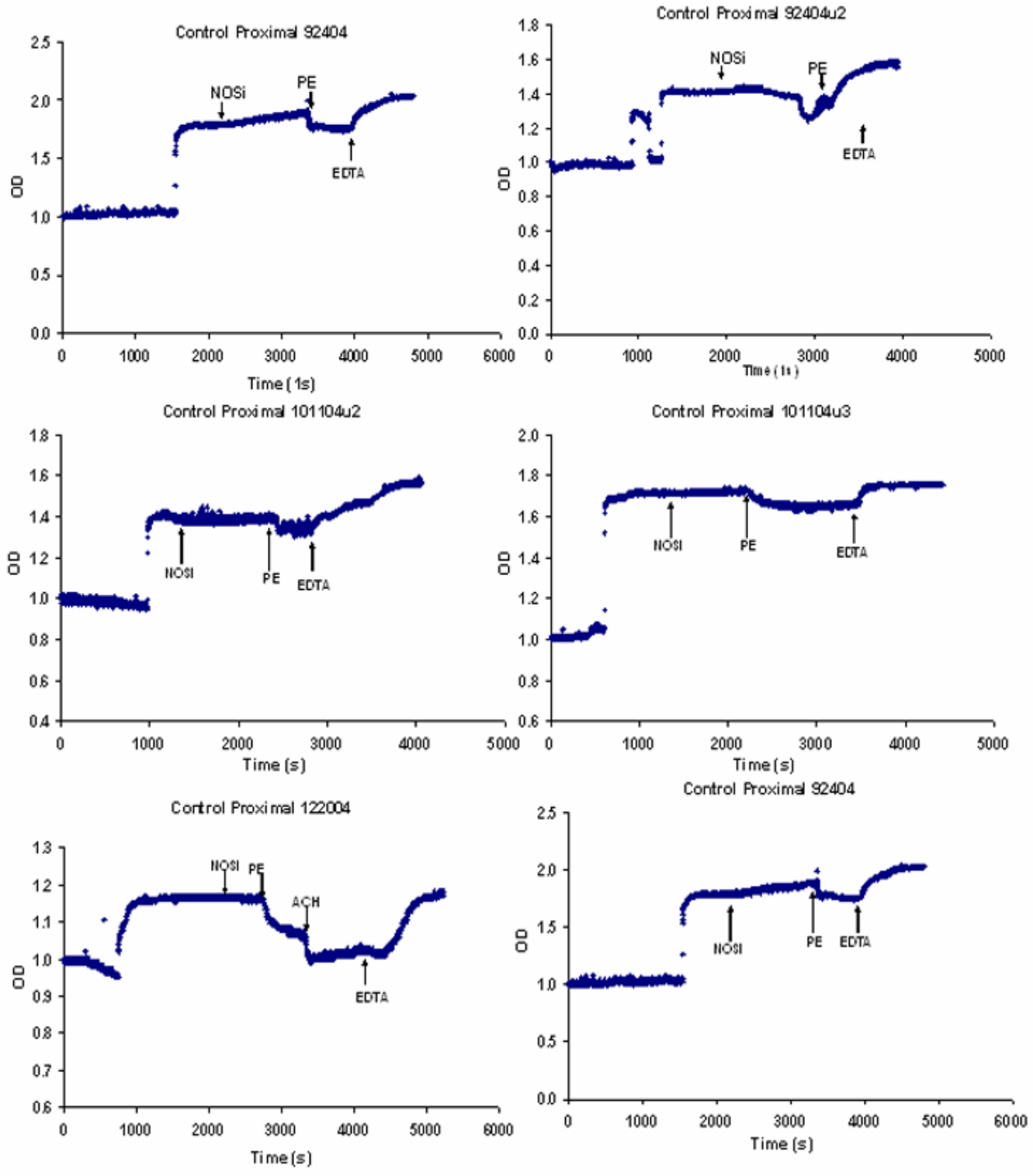

Figure A. 10 Contraction and relaxation of control proximal specimens.

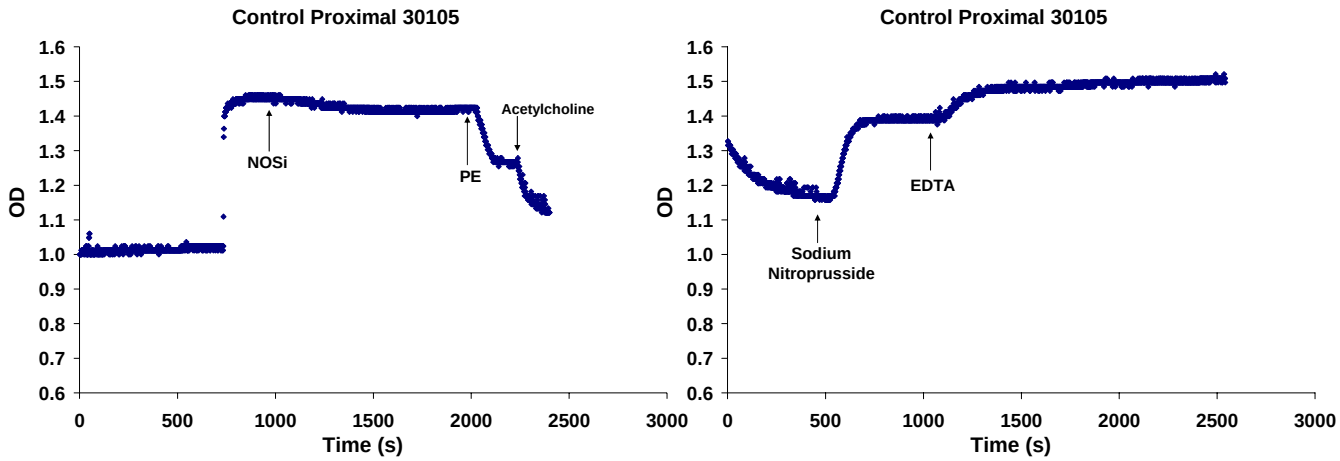

Figure A. 11 Contraction and relaxation of control proximal specimens.

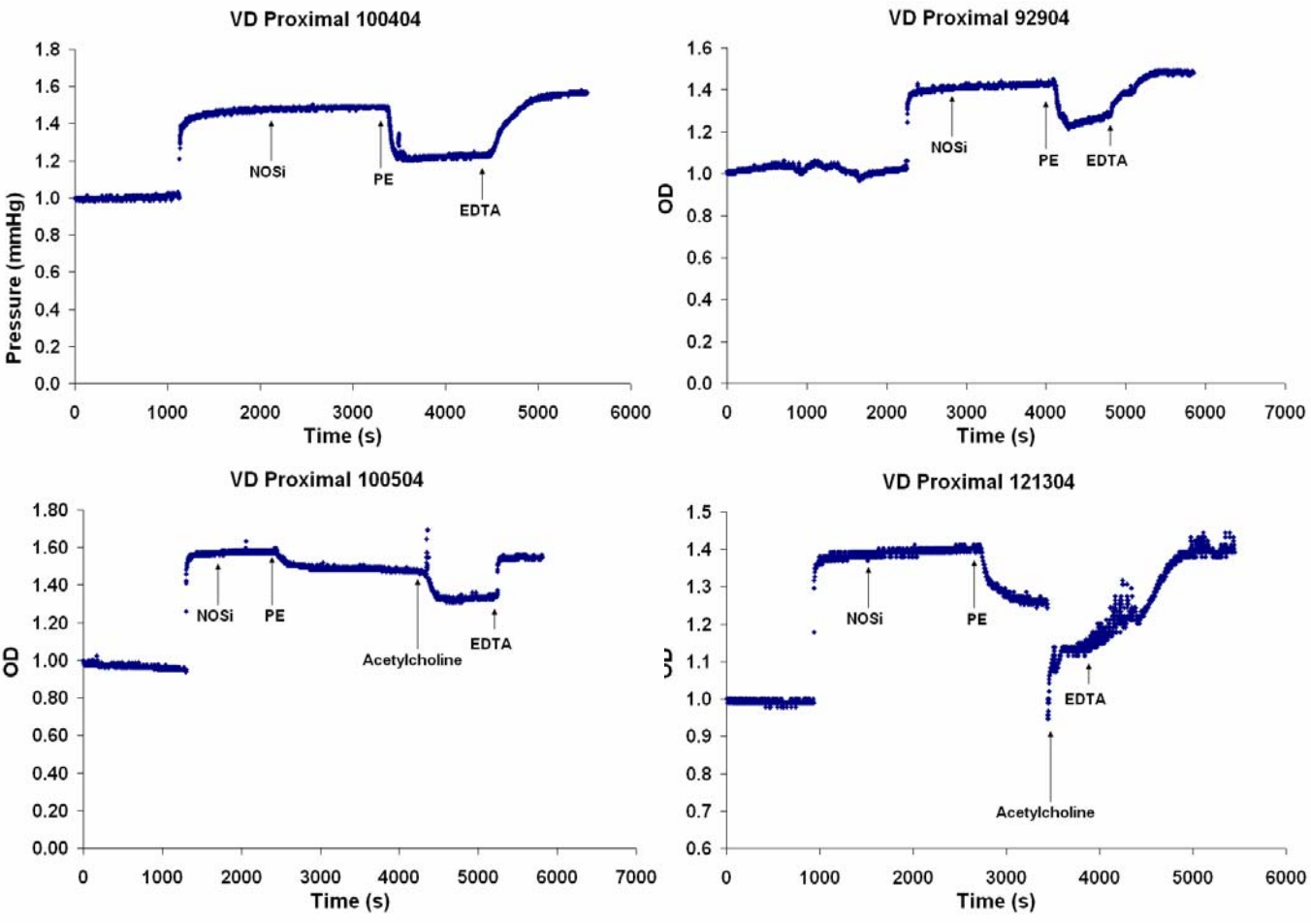

Figure A. 12 Contraction and relaxation of VD proximal specimens.

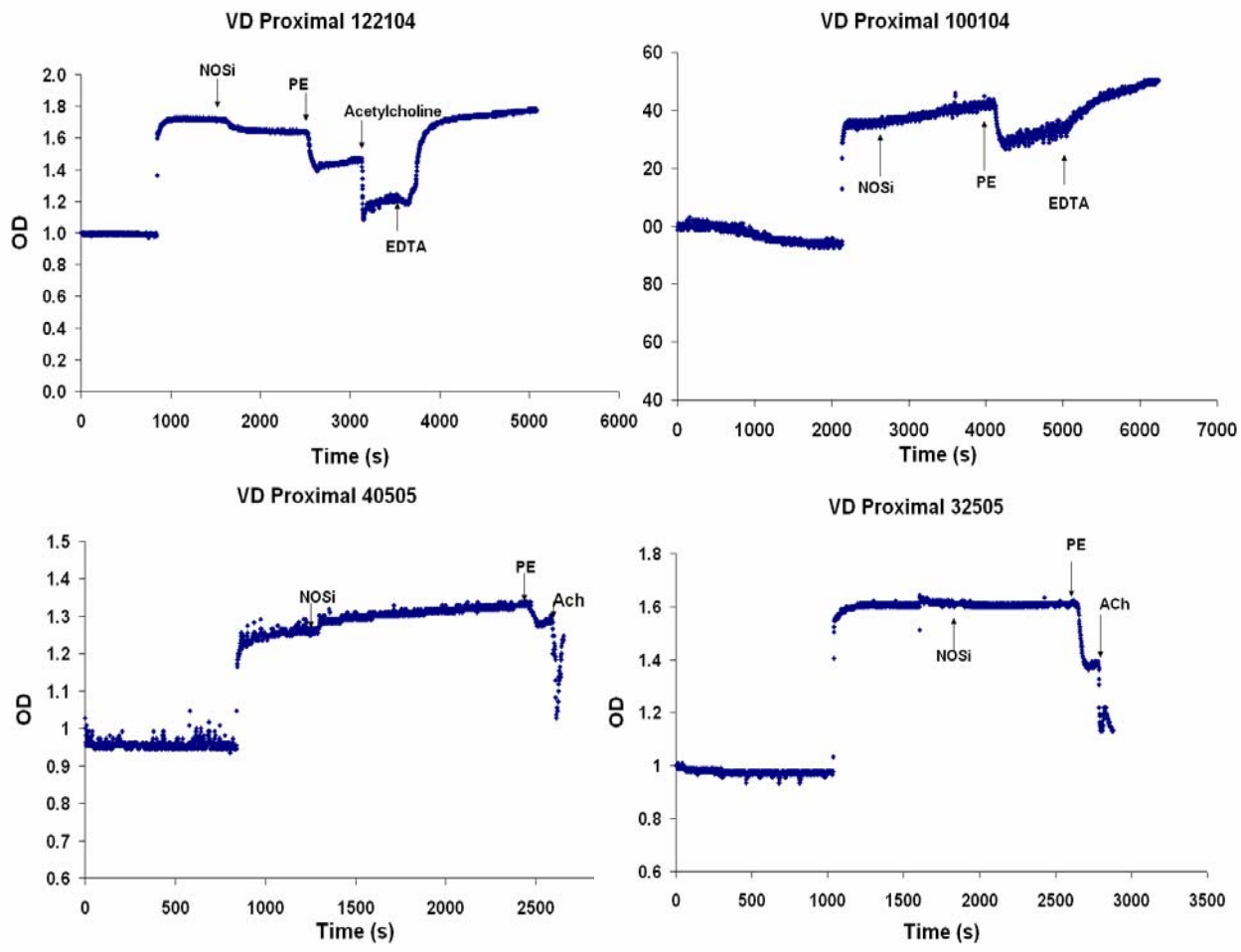

Figure A. 13 Contraction and relaxation of VD proximal specimens.

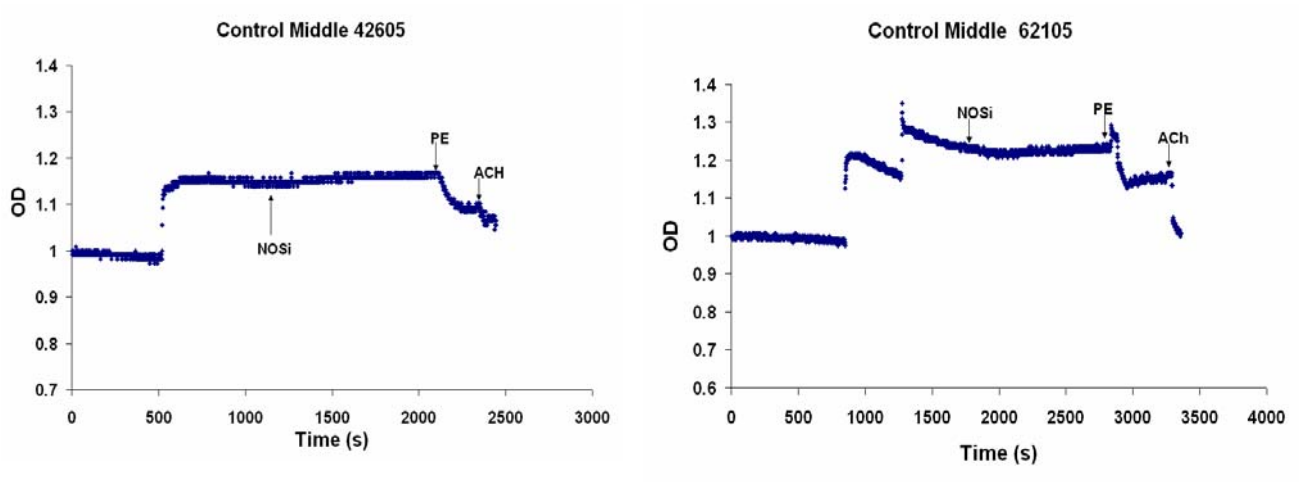

Figure A. 14 Contraction and relaxation of control middle specimens.

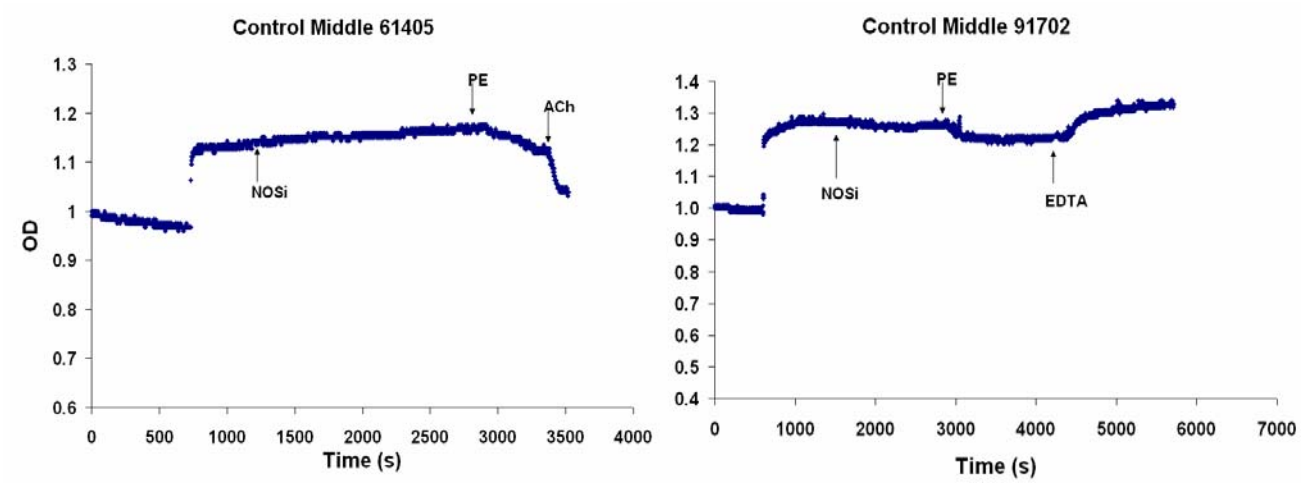

Figure A. 15 Contraction and relaxation of control middle specimens.

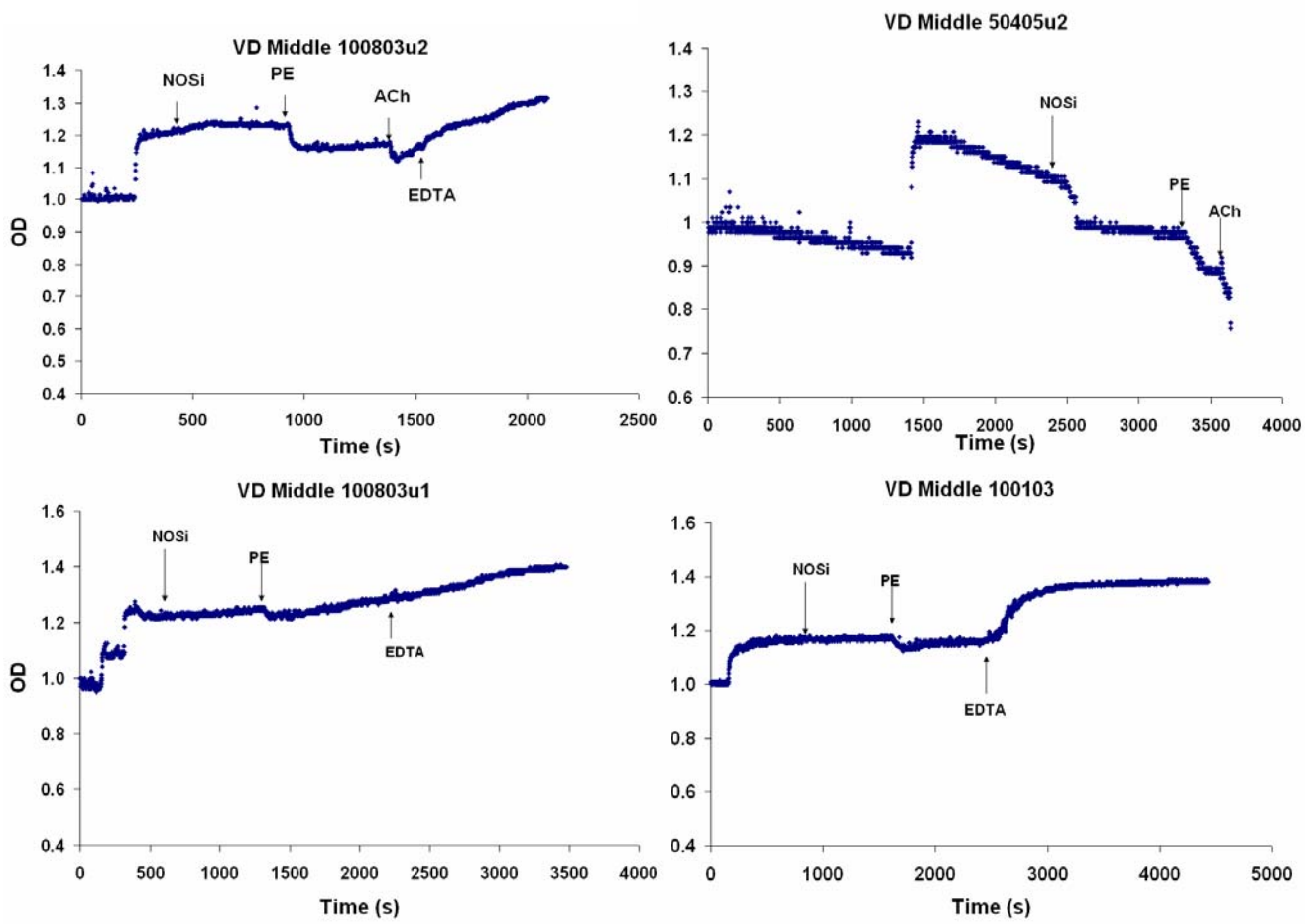

Figure A. 16 Contraction and relaxation of VD middle specimens.

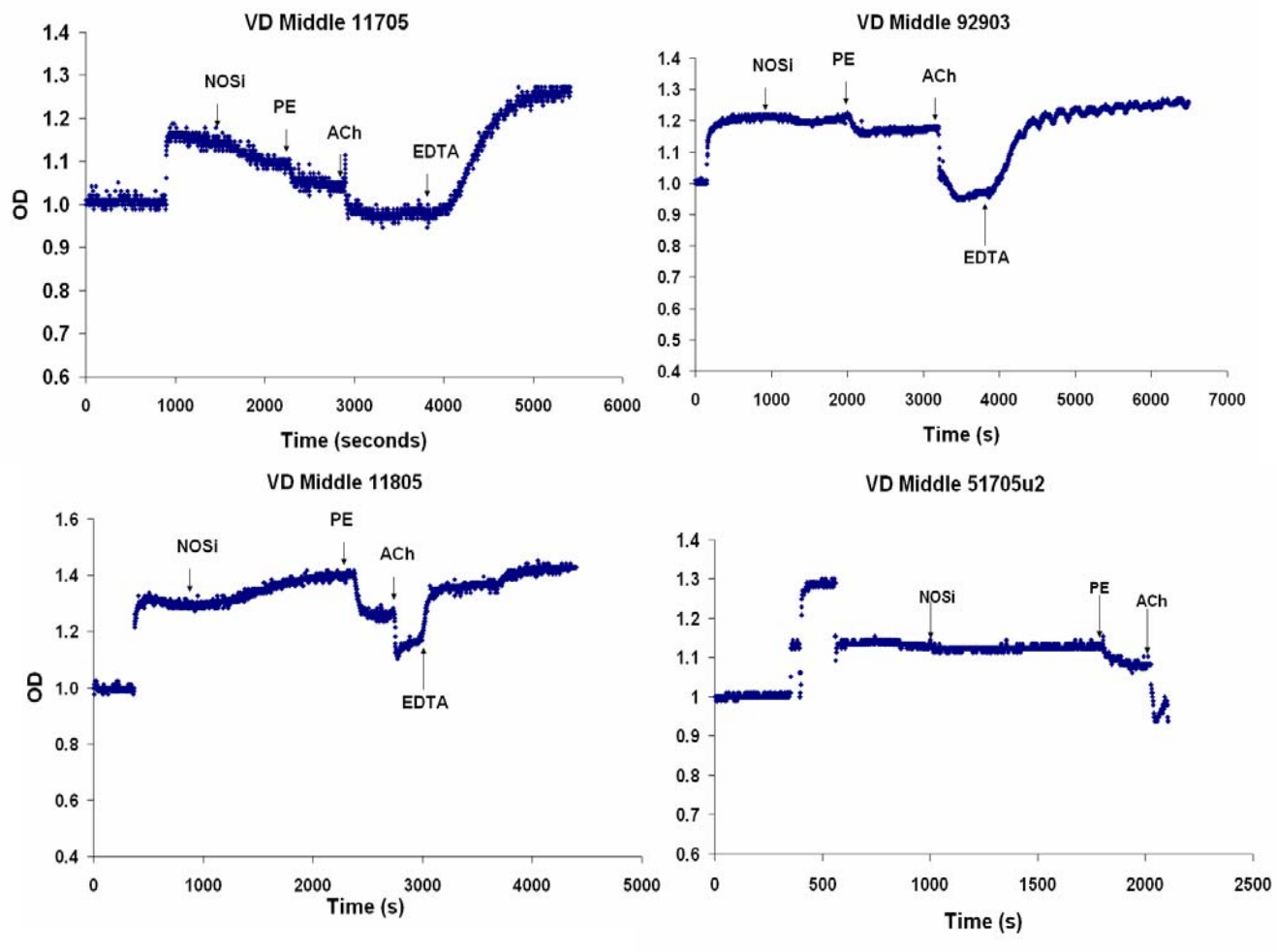

Figure A. 17 Contraction and relaxation of VD middle specimens.

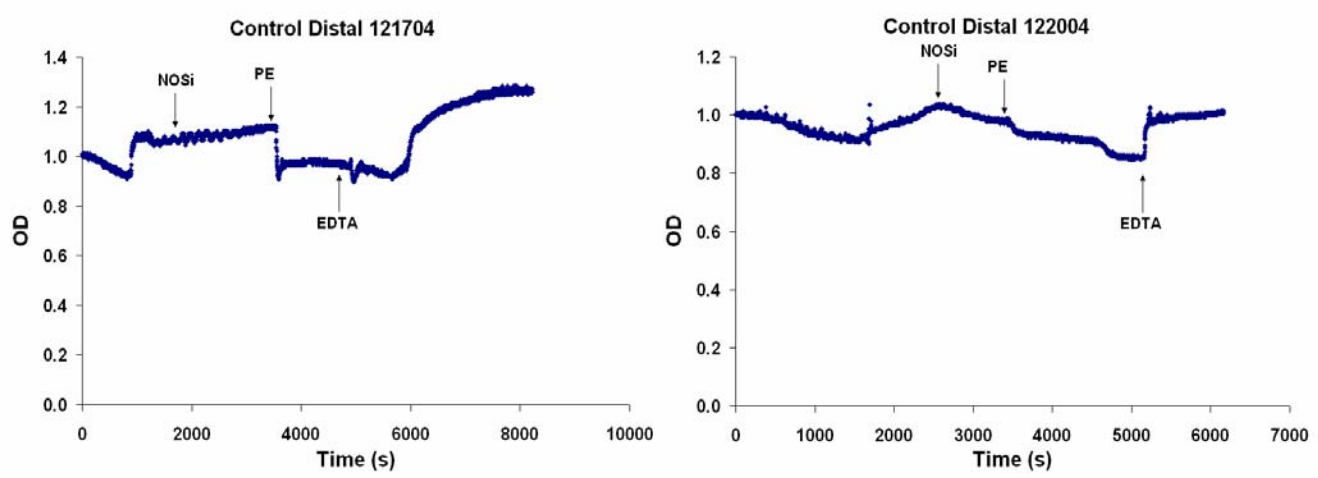

Figure A. 18 Contraction and relaxation of control distal specimens.

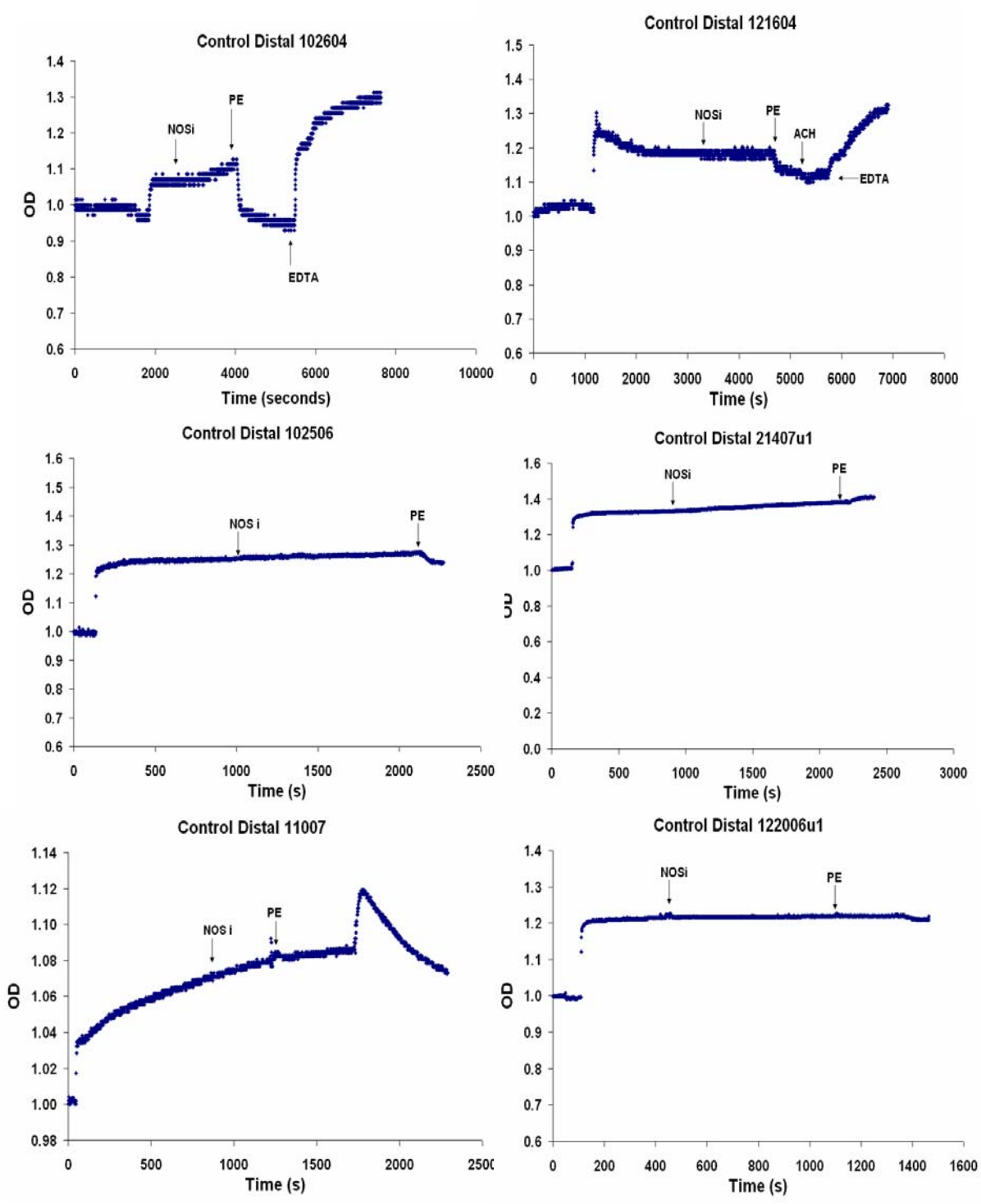

Figure A. 19 Contraction and relaxation of control distal specimens.

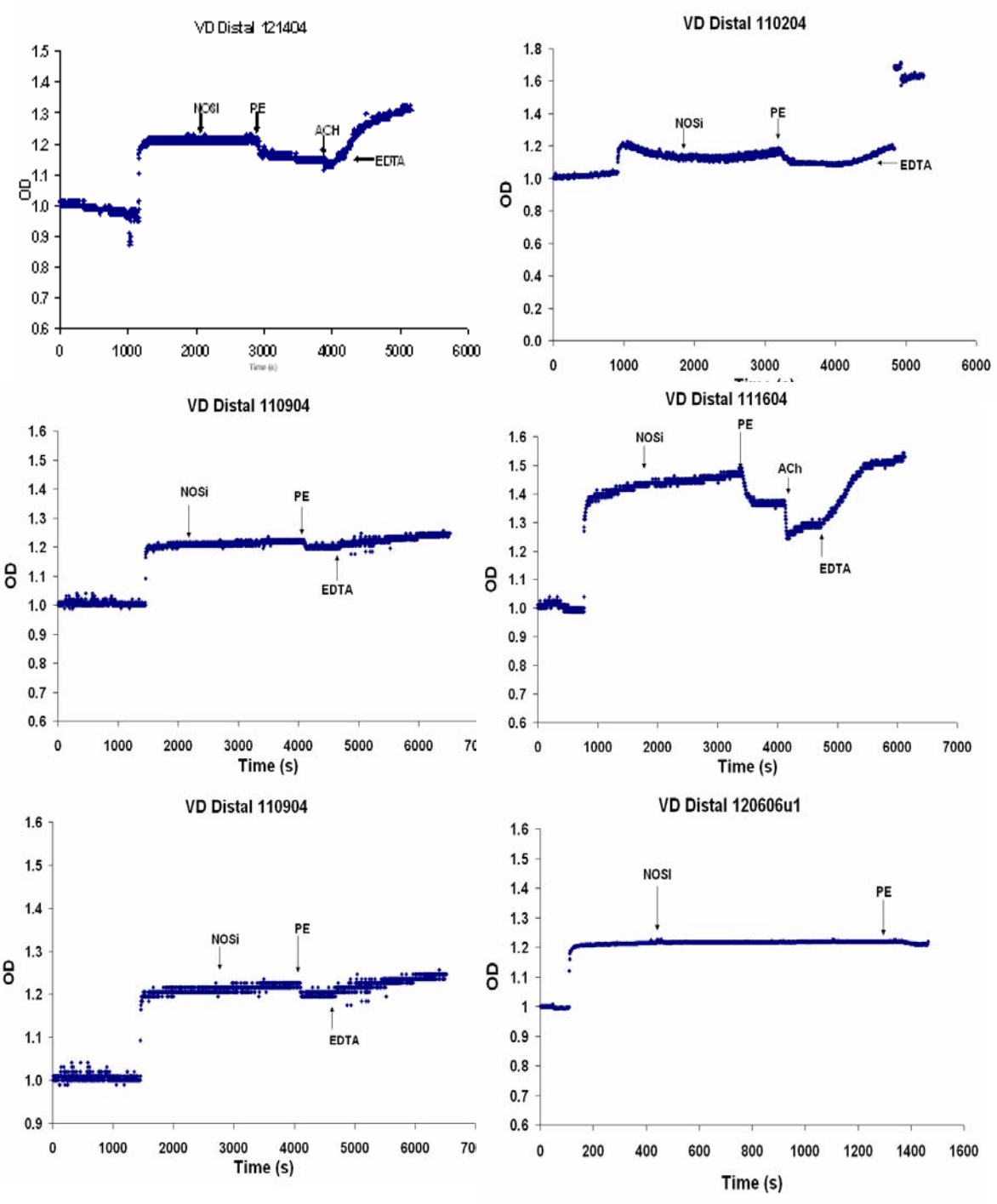

Figure A. 20 Contraction and relaxation of control distal specimens.

ACTIVE PRESSURE-DIAMETER DATA: PHENYLEPHRINE

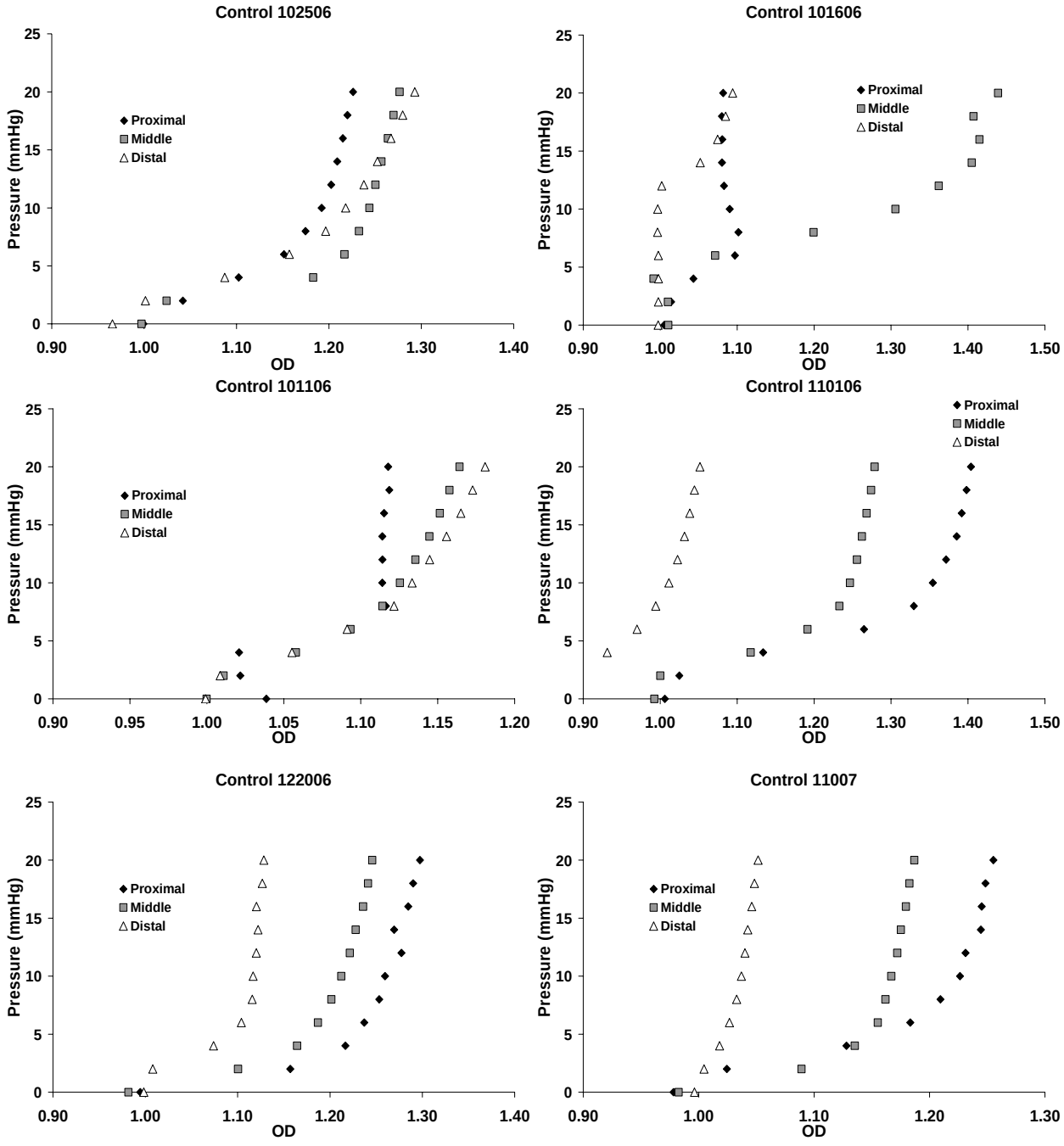

Figure A. 21 Active biomechanics in the presence of phenylephrine for control proximal, middle, and distal segments.

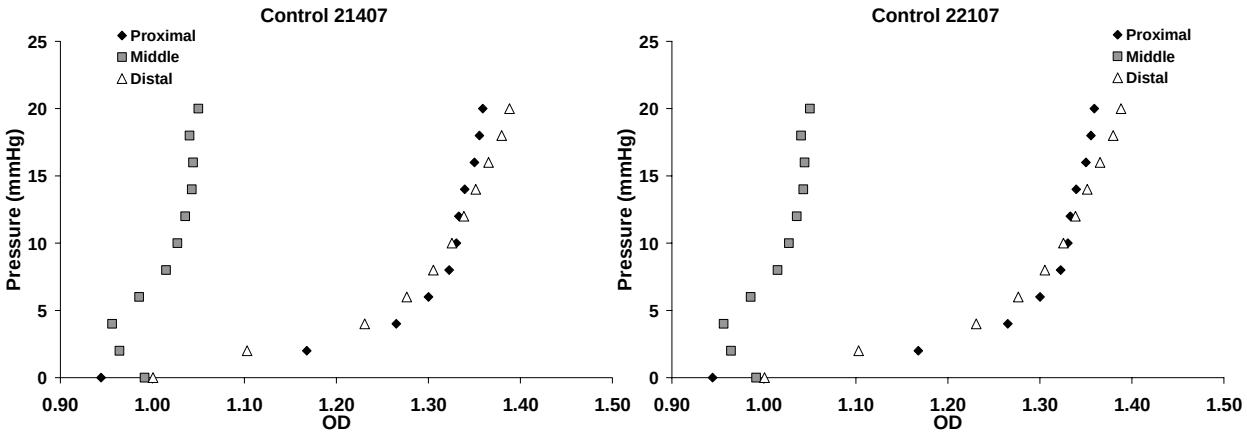

Figure A. 22 Active biomechanics in the presence of phenylephrine for control proximal, middle, and distal segments.

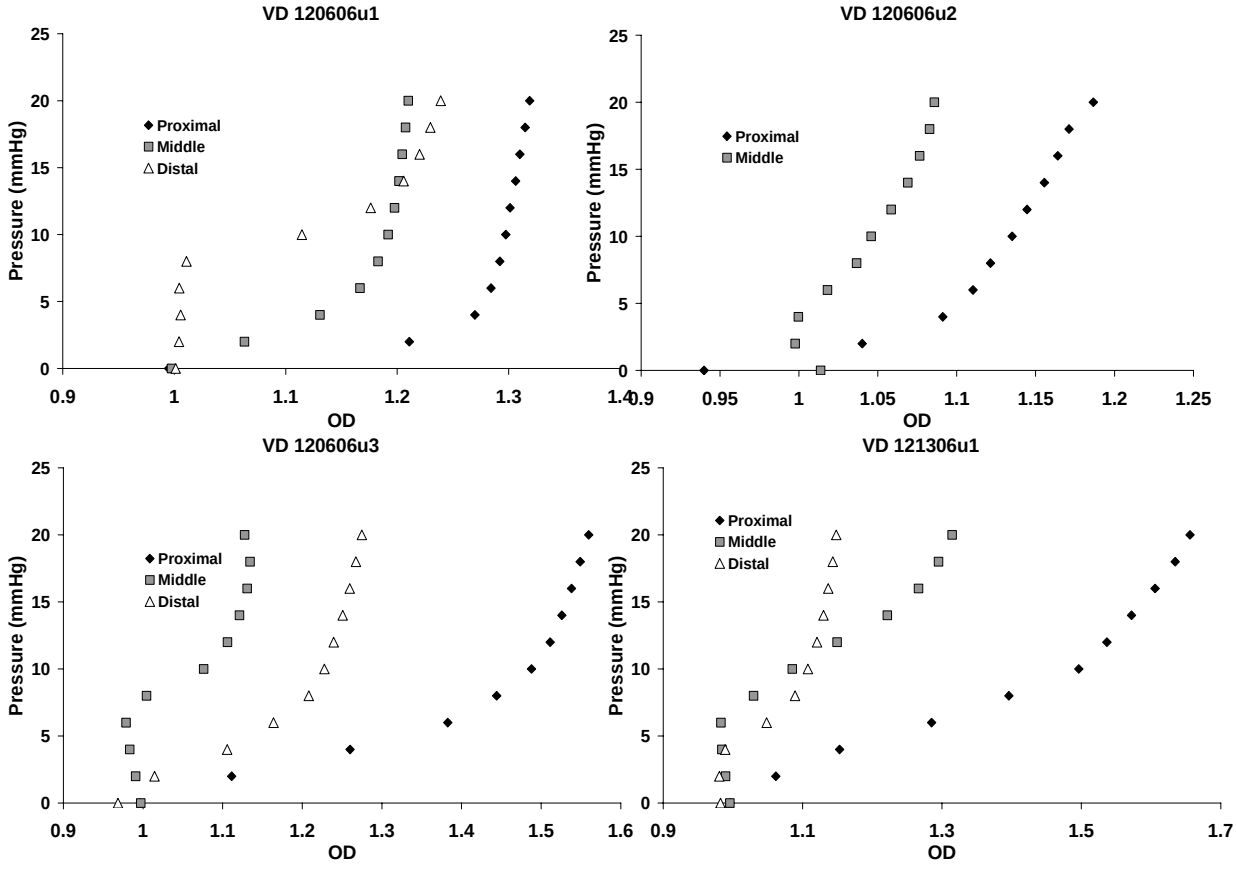

Figure A. 23 Active biomechanics in the presence of phenylephrine for VD proximal, middle, and distal segments.

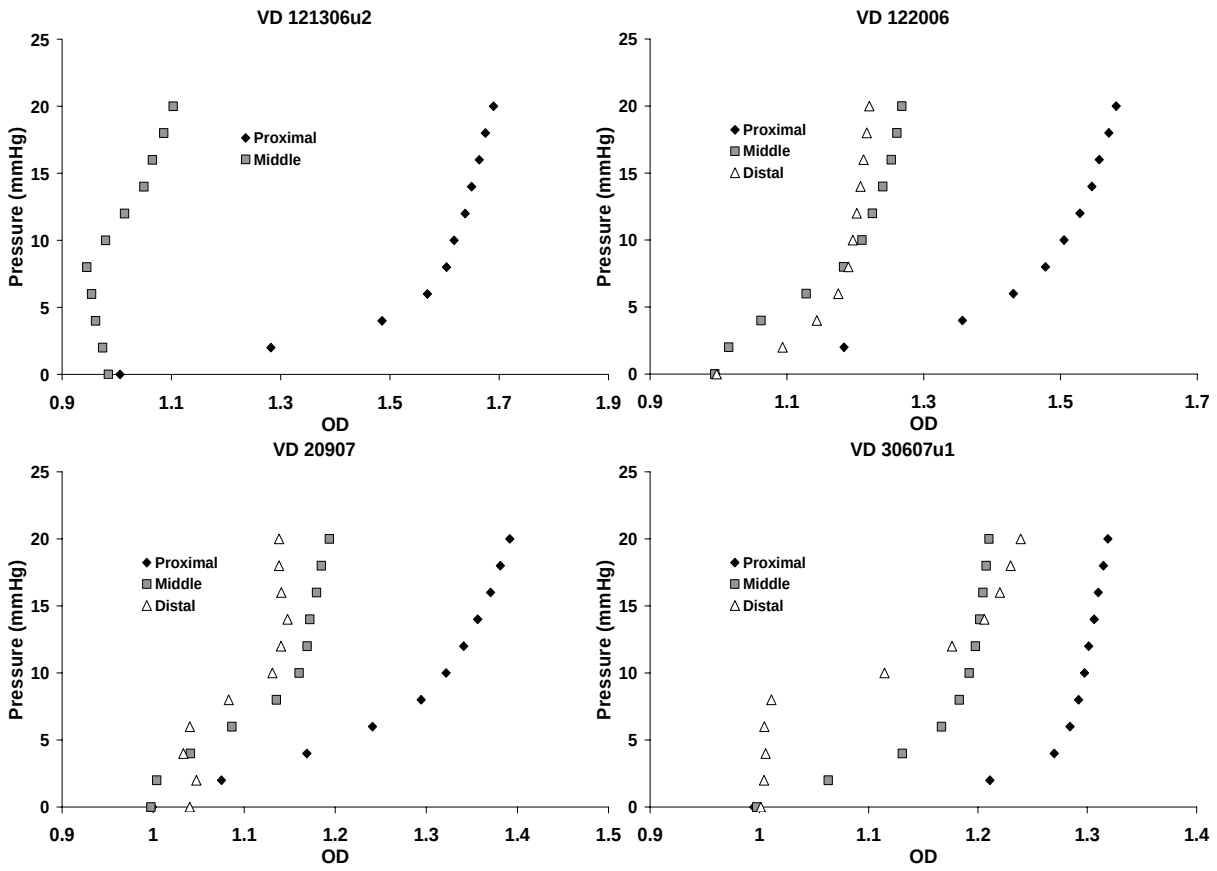

Figure A. 24 Active biomechanics in the presence of phenylephrine for VD proximal, middle, and distal segments.

FUNCTIONAL STUDIES: BETHANECHOL

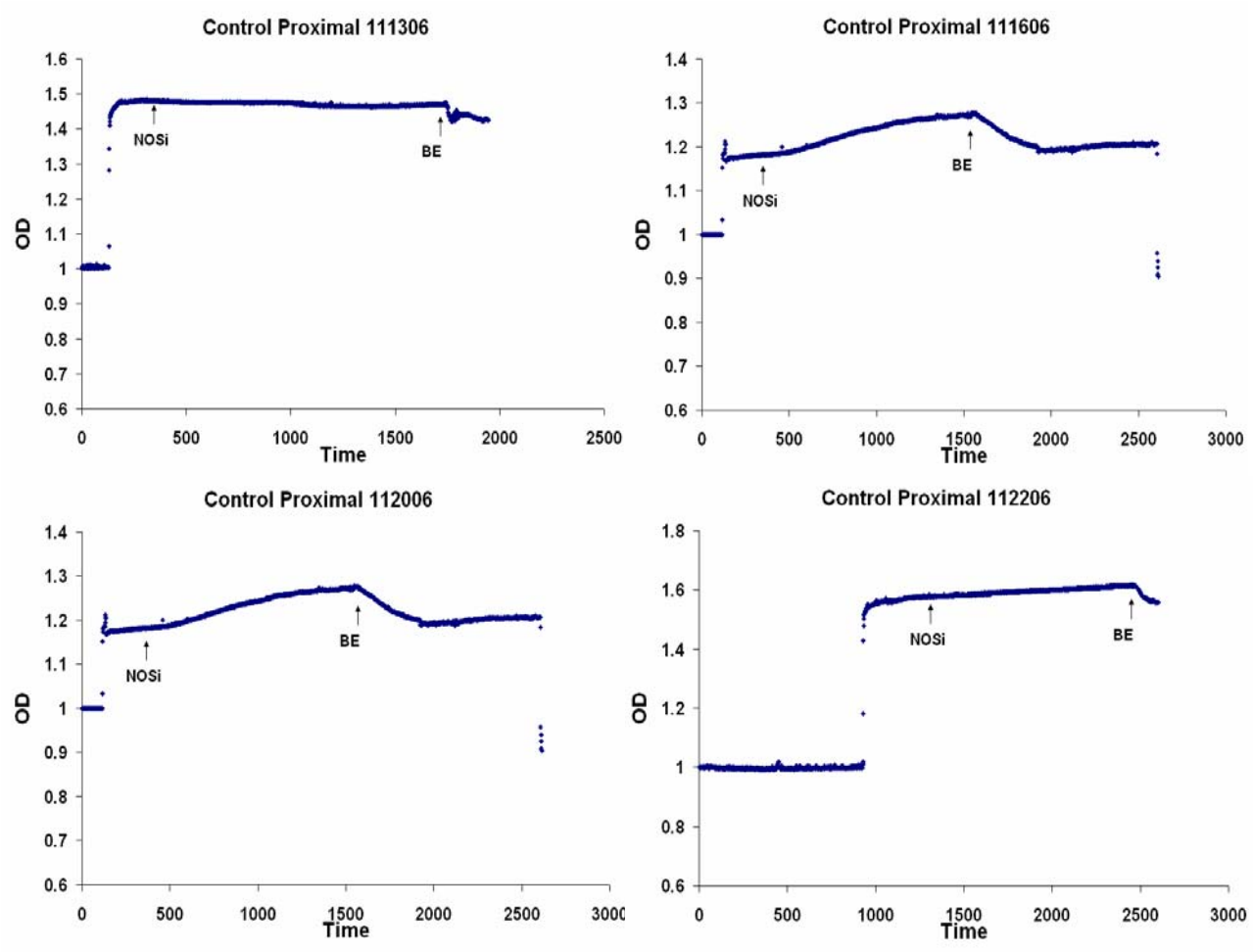

Figure A. 25 Proximal responses to bethanechol in control urethral specimens.

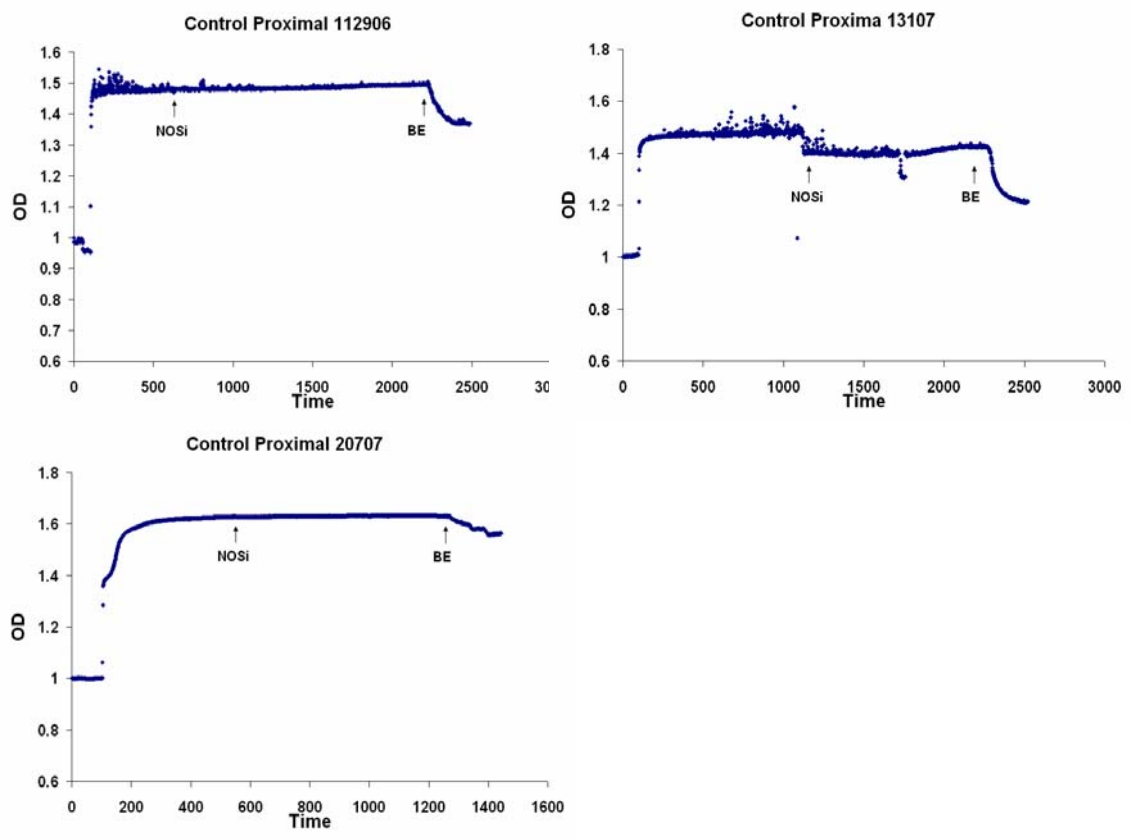

Figure A. 26 Proximal responses to bethanechol in control urethral specimens.

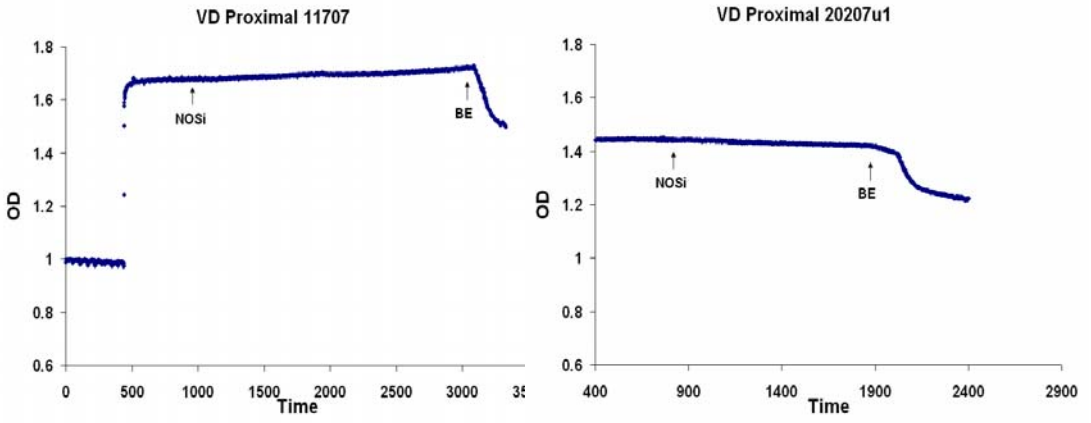

Figure A. 27 Proximal responses to bethanechol in VD urethral specimens.

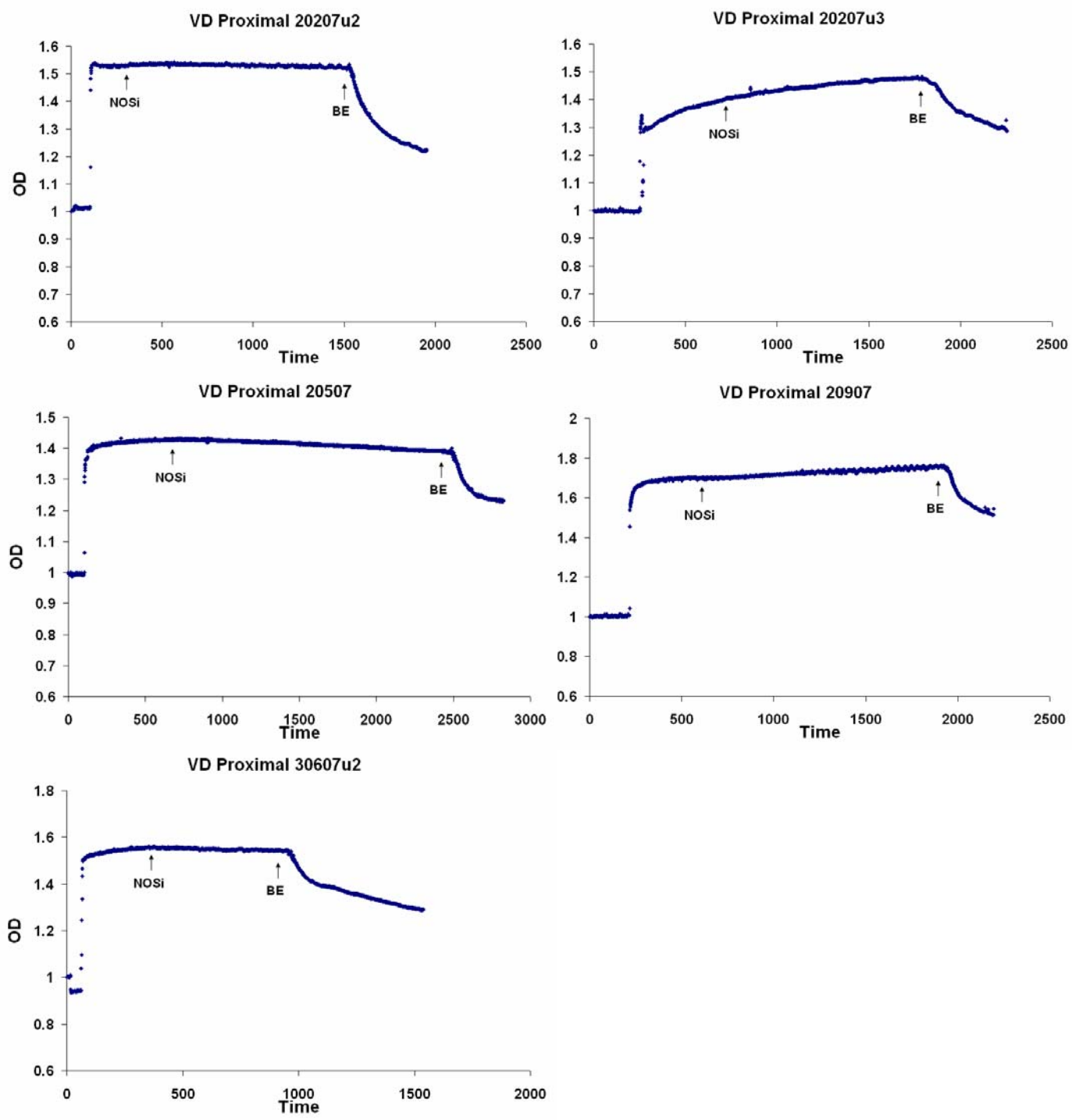

Figure A. 28 Proximal responses to bethanechol in VD urethral specimens.

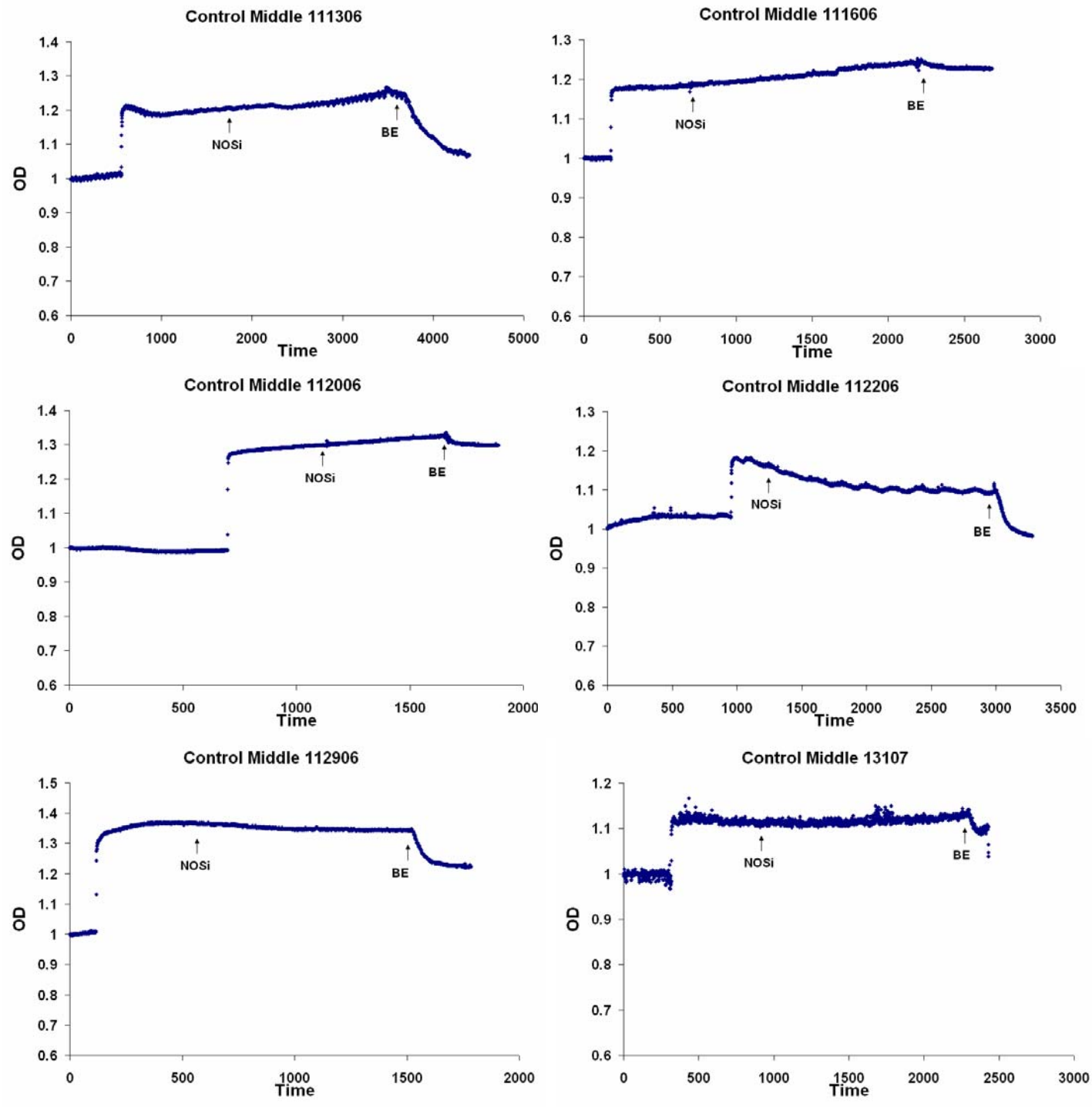

Figure A. 29 Middle responses to bethanechol in control urethral specimens.

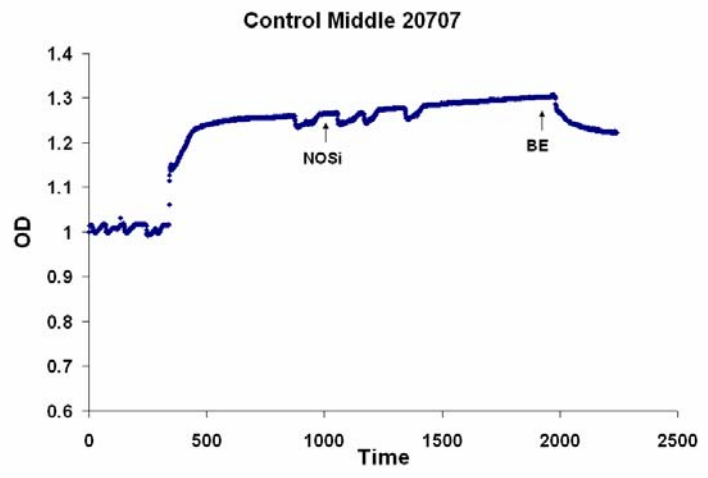

Figure A. 30 Middle responses to bethanechol in control urethral specimens.

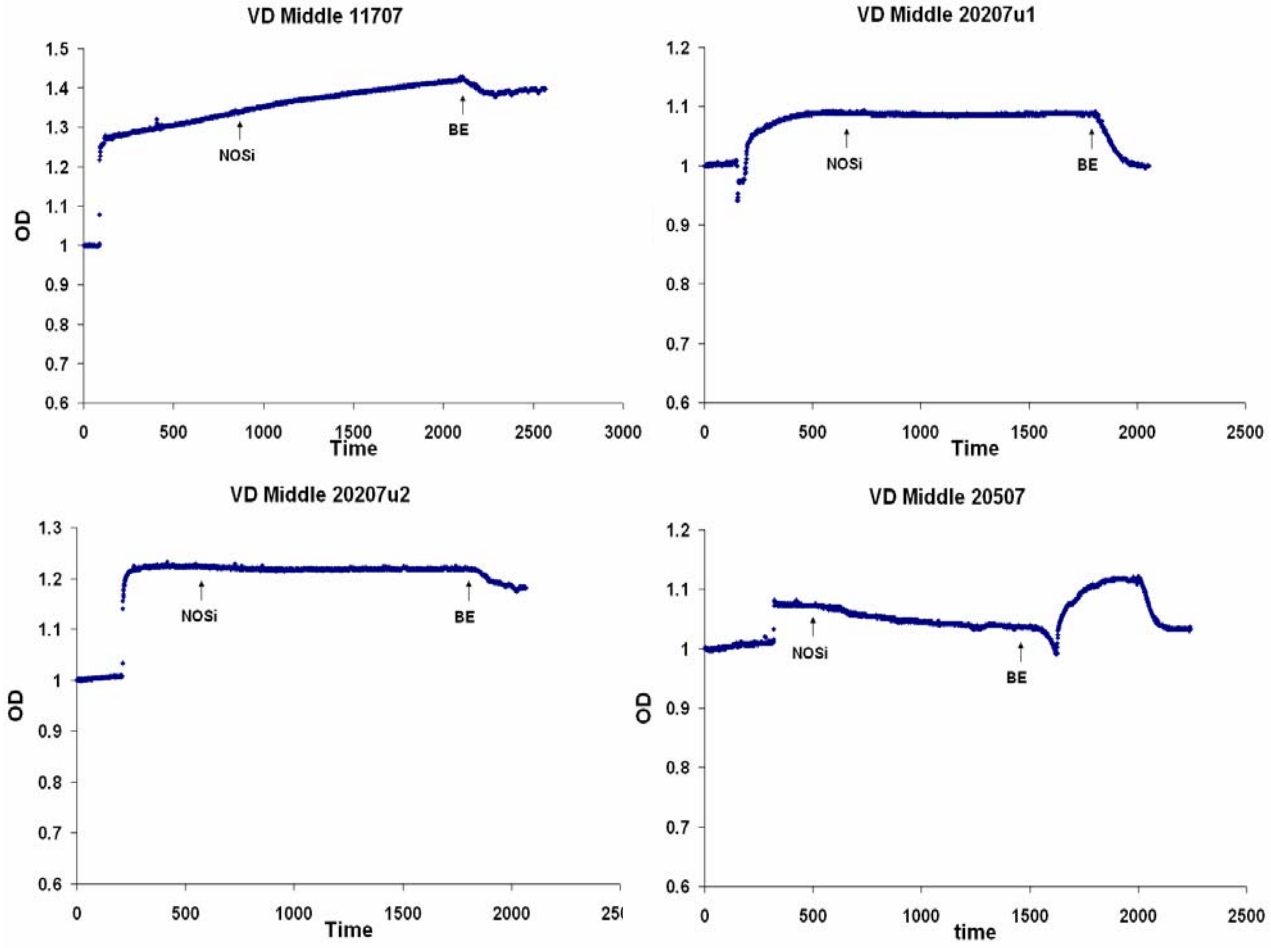

Figure A. 31 Middle responses to bethanechol in VD urethral specimens.

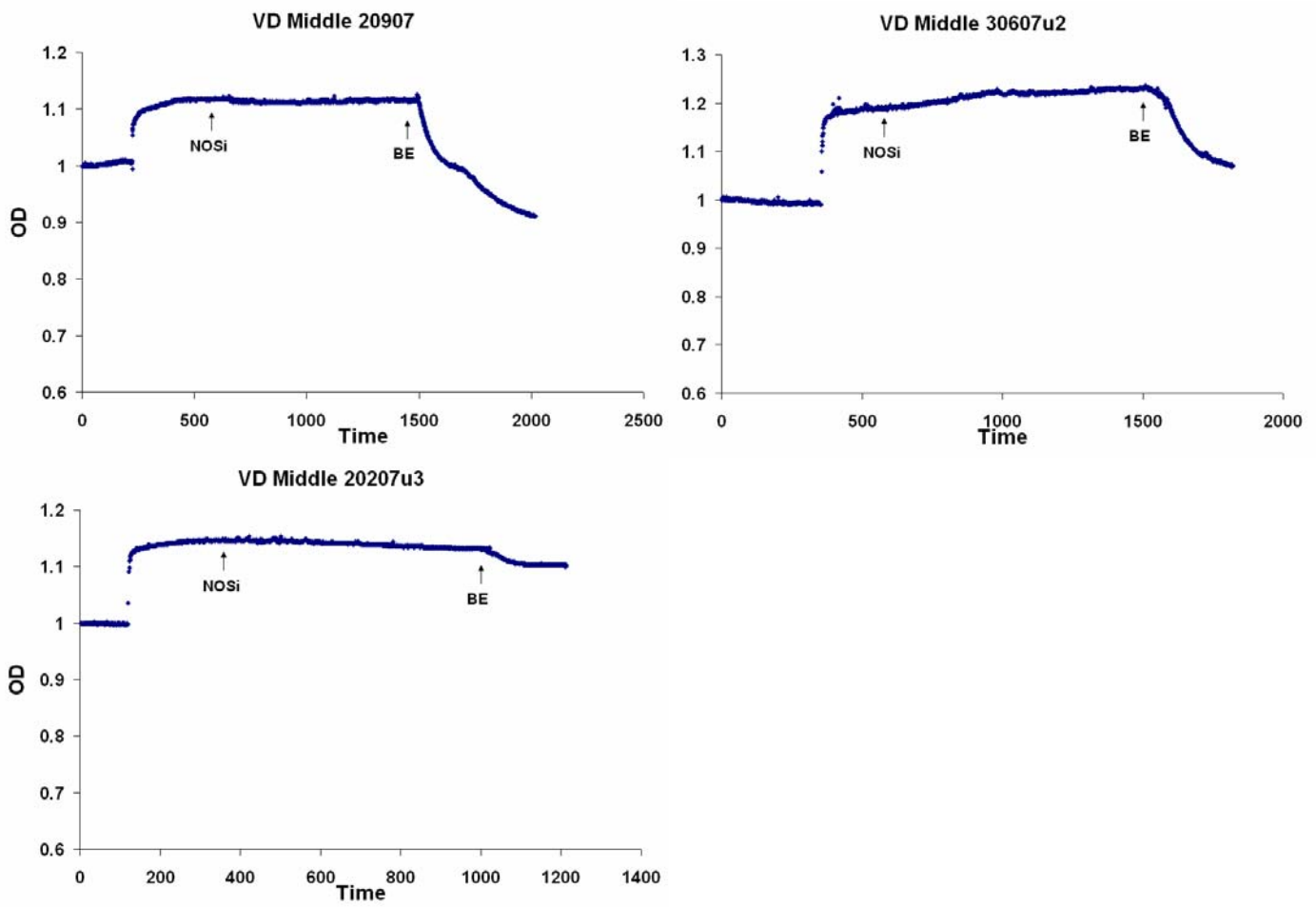

Figure A. 32 Middle responses to bethanechol in VD urethral specimens

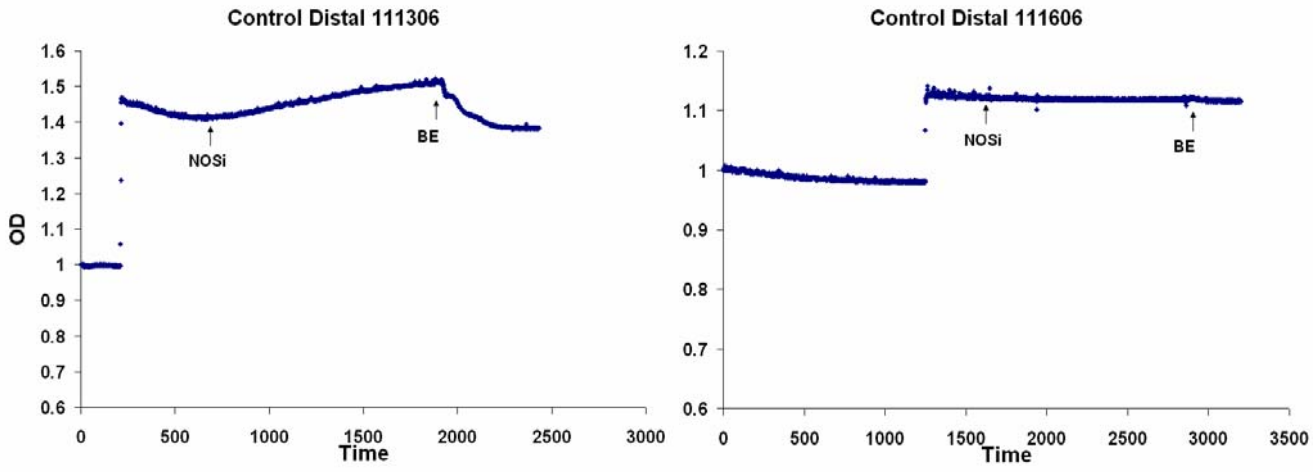

Figure A. 33 Distal responses to bethanechol in control urethral specimens.

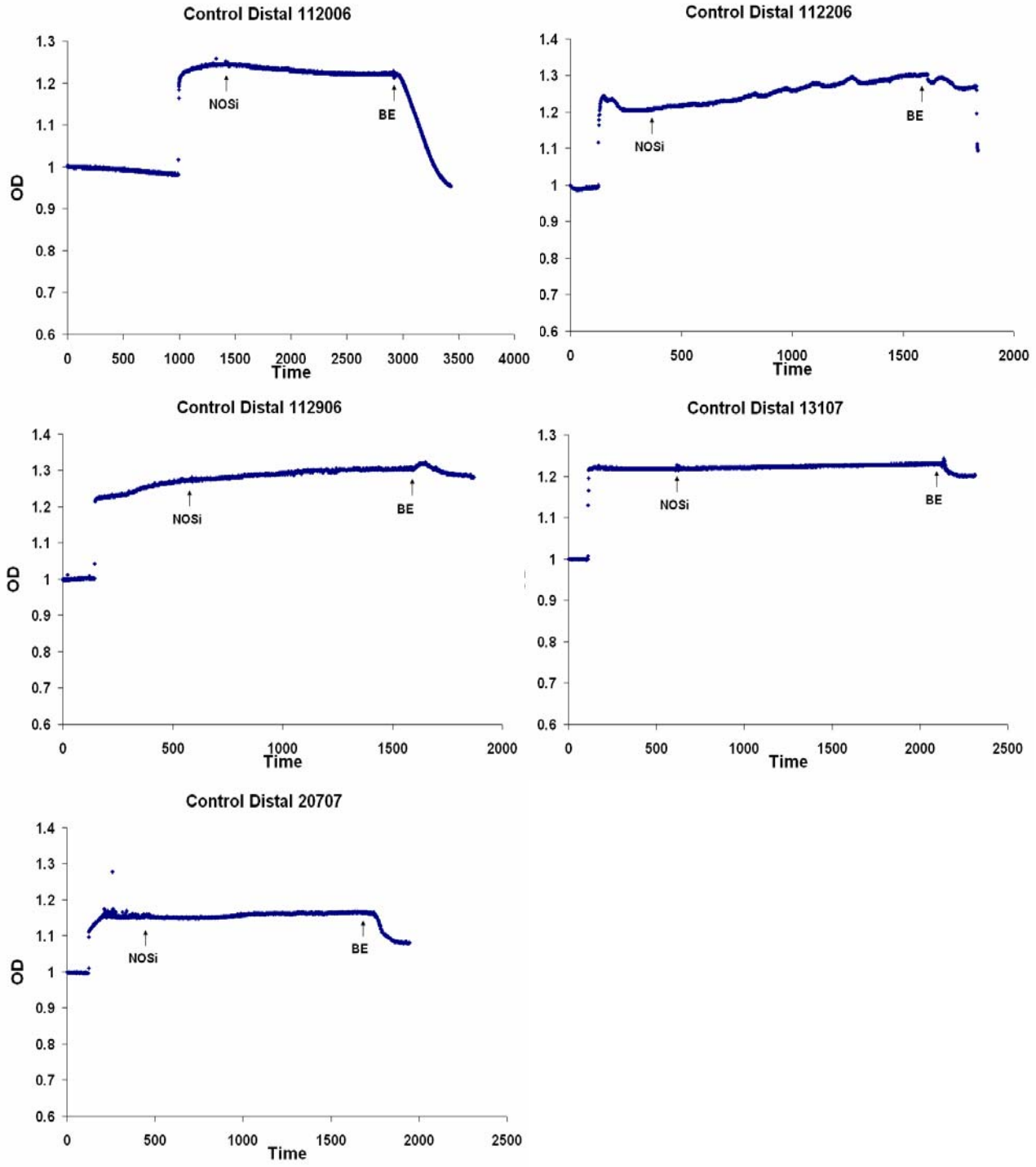

Figure A. 34 Distal responses to bethanechol in control urethral specimens.

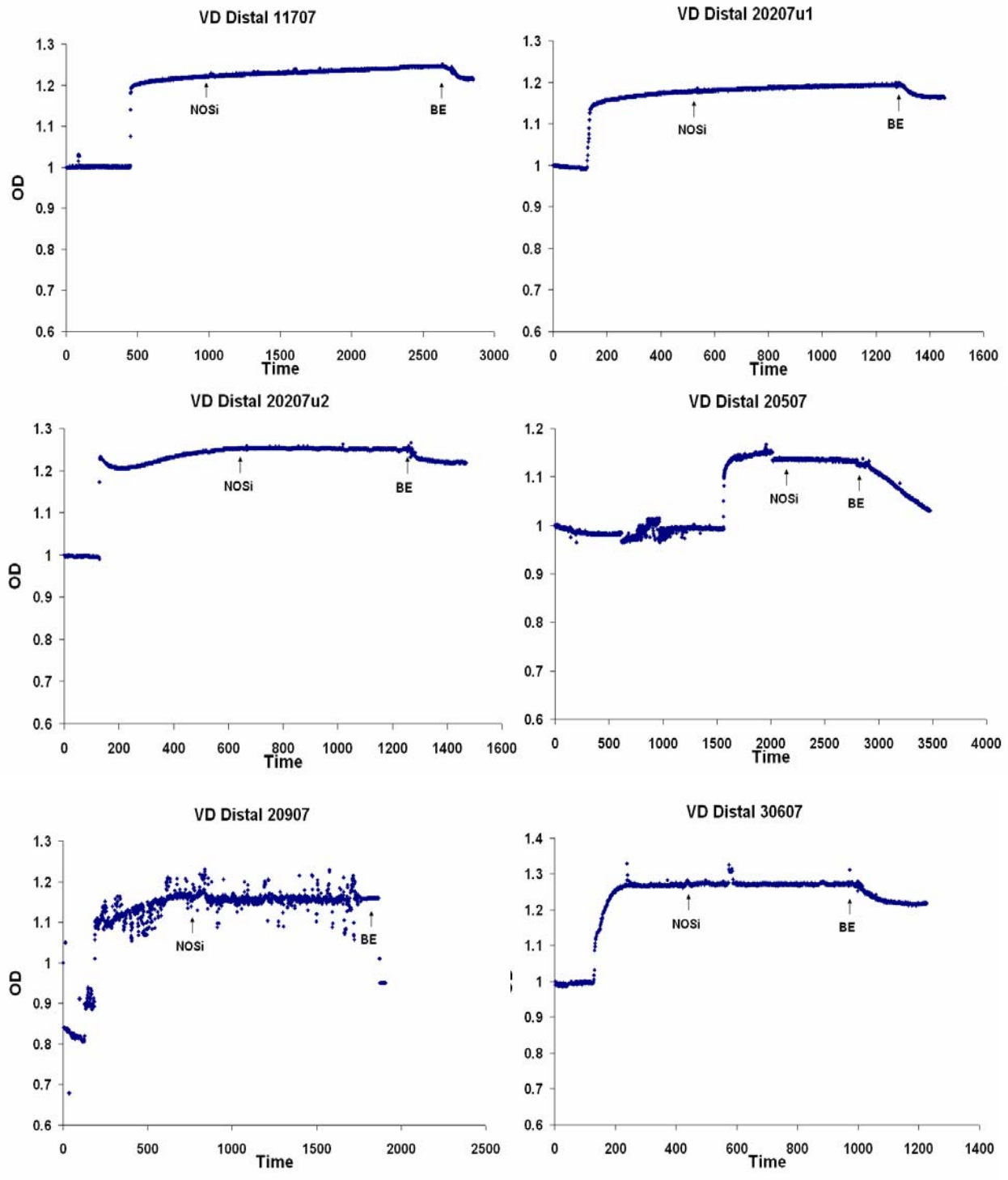

Figure A. 35 Distal responses to bethanechol in VD urethral specimens.

ACTIVE PRESSURE-DIAMETER DATA: BETHANECHOL

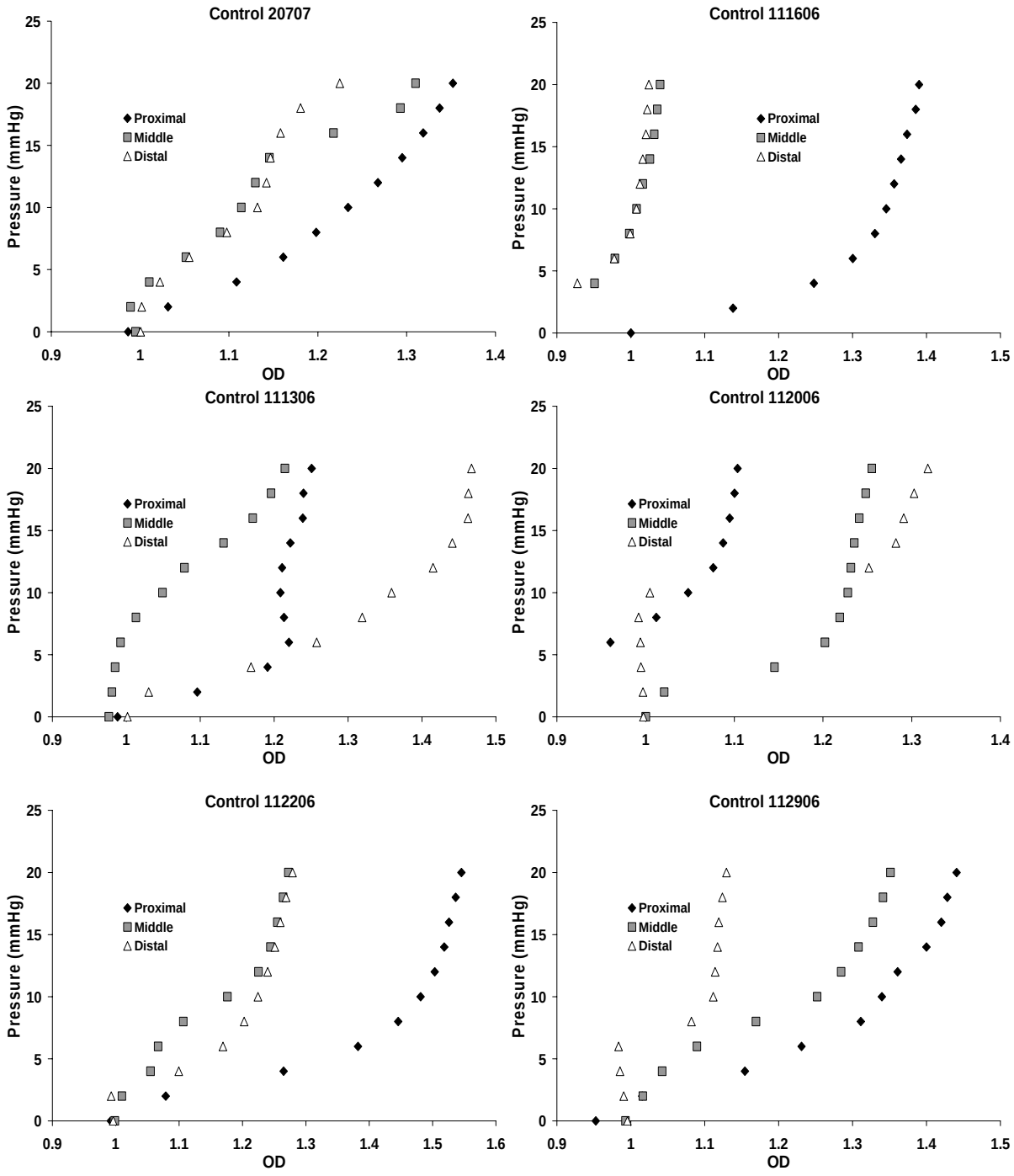

Figure A. 36 Active biomechanics in the presence of bethanechol for control proximal, middle, and distal segments.

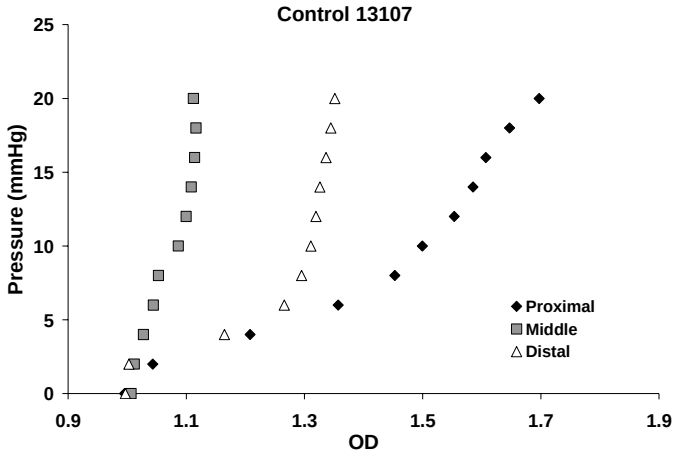

Figure A. 37 Active biomechanics in the presence of bethanechol for control proximal, middle, and distal segments.

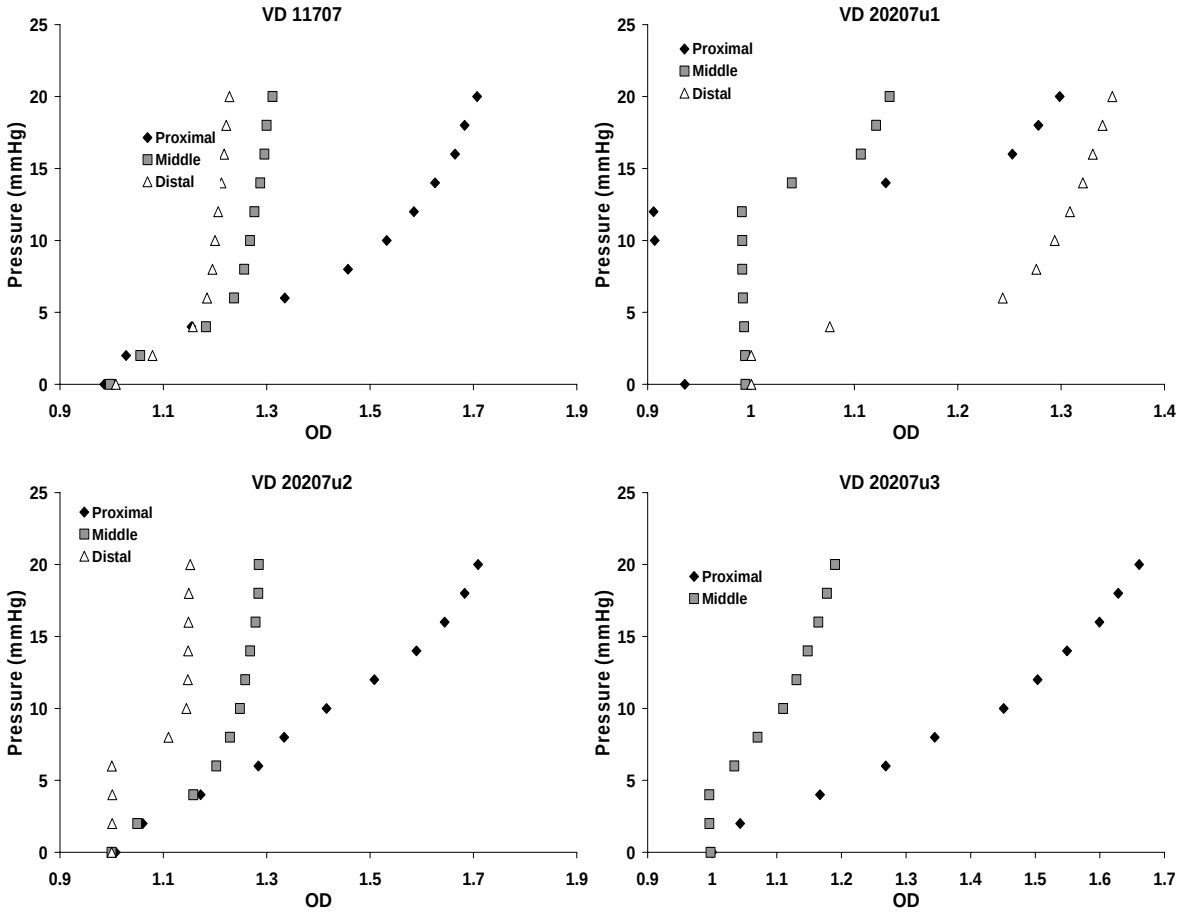

Figure A. 38 Active biomechanics in the presence of bethanechol for VD proximal, middle, and distal segments.

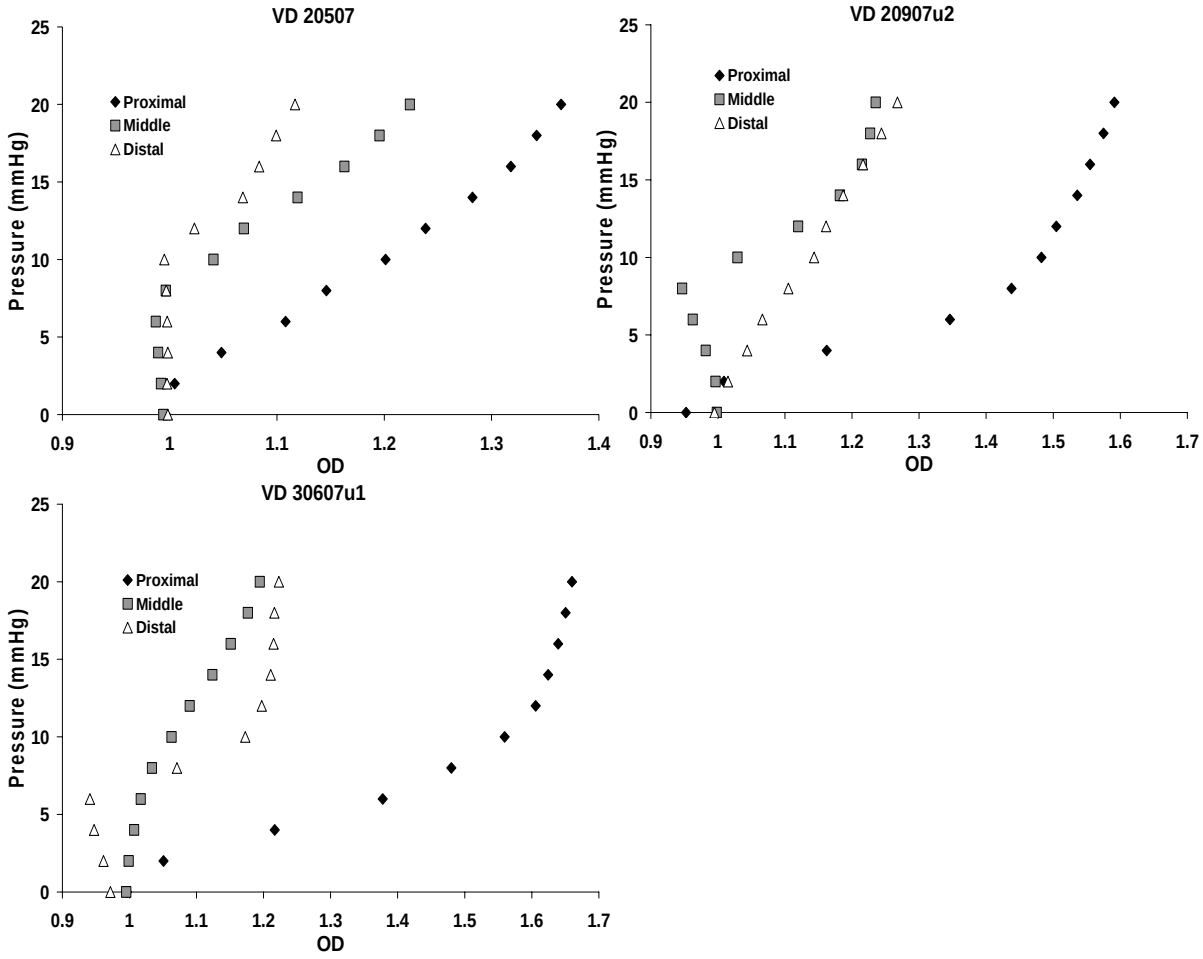

Figure A. 39 Active biomechanics in the presence of bethanechol for VD proximal, middle, and distal segments

APPENDIX B

PROPOGATION OF ERROR ASSOCIATED WITH PRESSURE AND OUTER DIAMETER MEASUREMENTS

The following error analysis was established from that of previous studies [152, 153]. Before assessing the propogation of error in calculated quantities, the uncertainty in the directly measured parameters used in the calculations must first be determined or estimated.

The system was set up with a piece of rubber tubing (Penrose^{TM} drain tube, Bard Medical, #0912010) tied onto the tees of the ex vivo system. A water manometer (cm H_2O) was used to measure each maximum and minimum pressure and outer diameter value for each pressure range used to calculate low (0-6mmHg), middle (6-12 mmHg), high (12-20 mmHg) pressure compliance values. This was repeated 5 times.

While increasing static pressure, the laser micrometer measured the outer diameter of the rubber tubing during inflation. This was repeated 5 times. Values for both pressure and outer diameter were averaged and standard deviations were computed. The uncertainty was taken as two standard deviations for 95% confidence limits and given by [152]:

Equation B.1: $$\sigma = 2 * 1.96 * \sigma_{measured}$$

where σ is the uncertainty value and $\sigma_{measured}$ is the standard deviation of the measured component (i.e., pressure or outer diameter). The resulting uncertainty values are provided in Table B.1.

Table B. 1 Uncertainty values for the different measurements used to calculate compliance and beta stiffness values

	PRESSURE (mmHg)					DIAMETER (mm)				
	0	**6**	**8**	**12**	**20**	**D_0**	**D_6**	**D_8**	**D_{12}**	**D_{20}**
σ	0.178	0.131	0.106	0.084	0.103	0.003	0.004	0.006	0.004	0.004

With these uncertainty values, the propogation of error could be calculated for both compliance and beta stiffness. Such a calculation could be broken down in the following manner (equations B.2 to B.6):

Equation B.2: $$\sigma_{\Delta P} = \sqrt{\sigma_{P\,max} + \sigma_{P\,min}}$$

Equation B.3: $$\sigma_{\Delta D} = \sqrt{\sigma_{D\,max} + \sigma_{D\,min}}$$

Equation B.4: $$\%\sigma_C = \sqrt{\left(\%\sigma_{\Delta D}\right)^2 + \left(\%\sigma_{\Delta P}\right)^2 + \left(\%\sigma_{D\,min}\right)^2}$$

Equation B.5: $$\%\sigma_{Ps,D} = \sqrt{\left(\%\sigma_P\right)^2 + \left(\%\sigma_D\right)^2 + \left(\%\sigma_{Ps}\right)^2 + \left(\%\sigma_{Ds}\right)^2}$$

Equation B.6:

$$\%\sigma_\beta = \sqrt{\left(\%\sigma_{P,D_{6mmHg}}\right)^2 + \left(\%\sigma_{P,D_{8mmHg}}\right)^2 + \left(\%\sigma_{P,D_{12mmHg}}\right)^2 + \left(\%\sigma_{P,D_{20mmHg}}\right)^2}$$

Here, uncertainties were calculated for pressure and outer diameter differences ($\sigma_{\Delta P}$,$\sigma_{\Delta D}$, respectively) using equations B.2 and B.3. This calculation was performed for compliance values calculated for low (0 to 6 mmHg), middle (6 to 12 mmHg), and high (12 to 20 mmHg) pressure ranges, where σ_{Pmax} and σ_{Pmin} are the uncertainty values for the maximum and minimum pressures and σ_{Dmax} and σ_{Dmin} are the respective maximum and minimum outer diameter values in each range. The percentage of error was calculated for each parameter by dividing the uncertainty value by the actual measured difference or measured value (i.e., $\%\sigma_{\Delta P} = \sigma_{\Delta P}/\Delta P$, $\%\sigma_{\Delta D}=\sigma_{\Delta D}/\Delta D$). Resulting values for the propagation of error analyses are in table B.2.

Table B. 2 Percentage of propogated error derived from uncertainty values and calculated using equations A.2 to A.6 for low, middle, and high pressure compliance (C) and beta stiffness values (β)

Propogation of Error			
$\sigma_{low\ C}$	$\sigma_{middle\ C}$	$\sigma_{high\ C}$	σ_{β}
5.09%	8.11%	10.10%	0.33%

APPENDIX C

MIXING PROPERTIES WITHIN HOUSING CHAMBERS USED FOR URETHRAL TESTING

In efforts to build an optimized urethral testing system and ensure equilibration of pharmacological agents in a timely manner, both boxes (DVT, 800ml volume, and the newer urethral chamber, 400 ml volume) were assessed for their mixing properties.

Both boxes were set up exactly as they would be experimentally (i.e. tubing was connected to a bath and circulated through a water bath; see **Section 2.2.4.3**). Boxes were filled with saline and allowed to equilibrate to a temperature of approximately 37°C. A dye consisting of bromophenol blue and tris-buffered saline was used and an 8 ml volume was injected into the mock loop. Syringe samples were taken in the proximity of the specimen at varying time ranges (i.e., 0 to 30 minutes). The comparison for optimal equilibration was an 8 ml volume of dye mixed (for 30 min) with either 400 ml or 800 ml volume of saline. All samples were read using a UV spectrophotometer. Absorbance and wavelength values were compared.

Results showed that for the 800 ml box equilibrium was not reached by 30 minutes (**Figure C.1.**). On the other hand, equilibrium of the injected dye was reached by 10 minutes in the 400 ml box (**Figure C.2.**). It should be noted that the differences in wavelength-absorbance curves for the two boxes are mostly due to the size and concentration of the dye. That is, since

the 8 ml injection was more concentrated for a smaller volume of saline (i.e., the 400 ml box), the curve represents this characteristic.

The smaller sized box not only had the advantage of a smaller volume, but also the placement of the inlet and outlet ports were different from that of the 800 ml box. The 800 ml box had inlet and outlet ports located on the same side and right across from each other; thus, observationally speaking, the dye simply hovered at the bottom and slowly rose to the site of the specimen. However, the 400 ml box had inlet and outlet ports located diagonally on each side of the box; therefore, the injected dye blended in all directions. It should also be mentioned that application of a magnetic stir bar shortened this equilibration period to 5 minutes in the 400 ml box. However, a stir bar was ultimately eliminated for the design since the magnetic properties might interfere with the operation of the DVRT (the longitudinal measuring device; see Chapter 6) and/or the laser micrometer measurements.

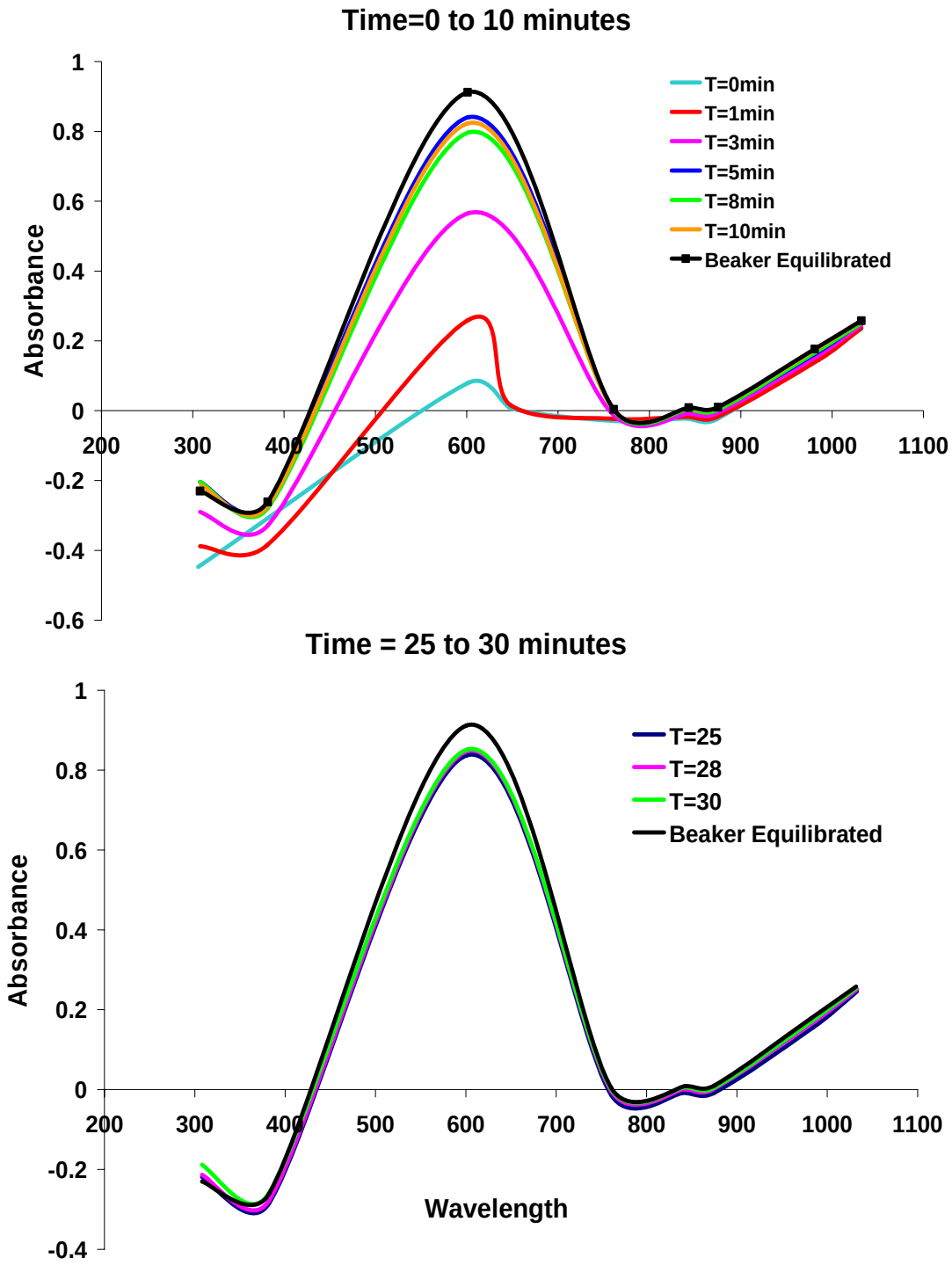

Figure C. 1 Absorbance readings for bromophenol blue circulated in an 800 ml volume box of saline at 37°C. Graphs represent sample readings from 0 to 10 minutes (top) and readins from 25 to 30 minutes (bottom).

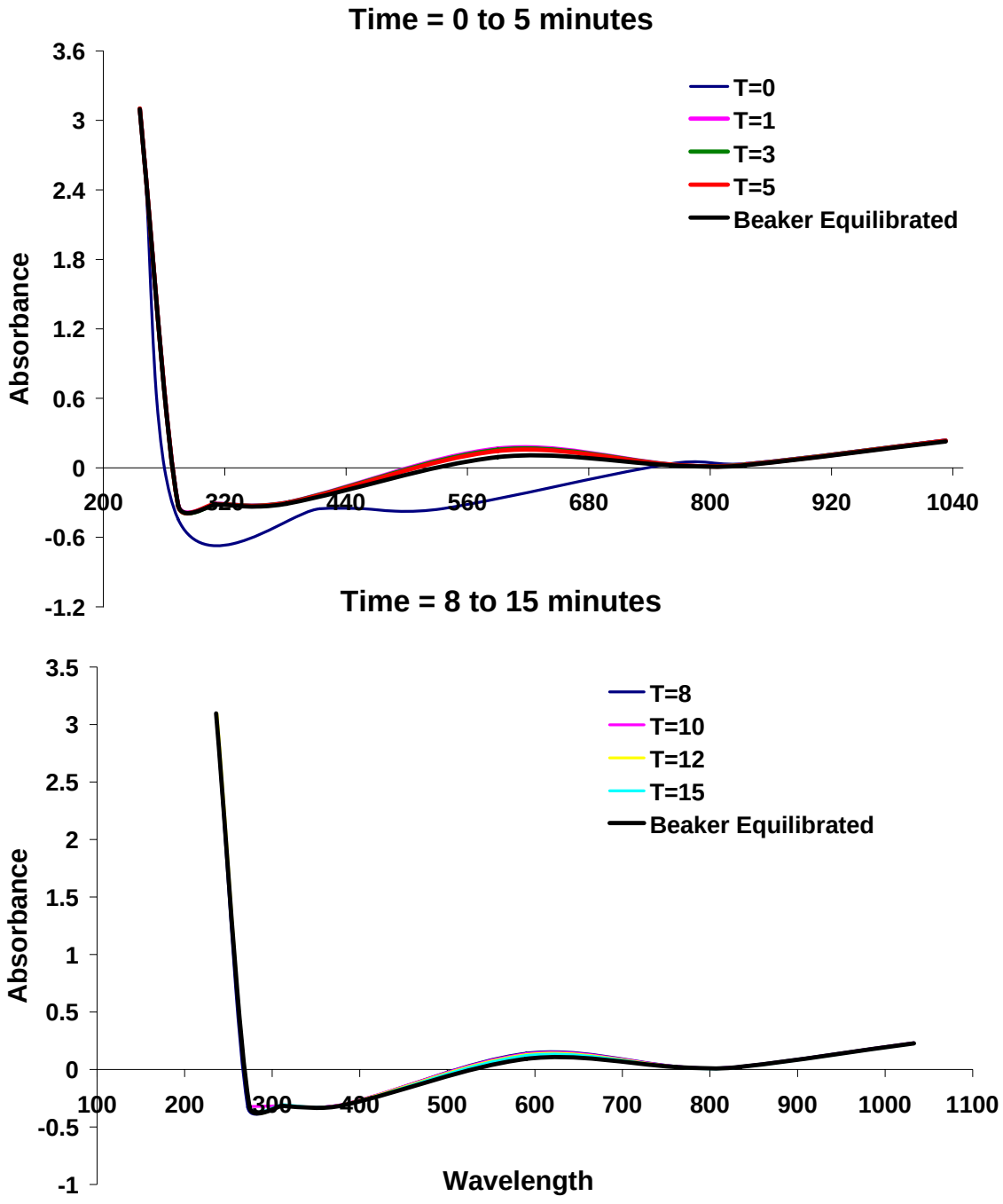

Figure C. 2 Absorbance readings for bromophenol blue circulated in an 400 ml volume box of saline at 37°C. Graphs represent sample readings from 0 to 5 minutes (top) and readins from 8 to 15 minutes (bottom).

APPENDIX D

TUNEL ANALYSIS FOR CELLULAR APOPTOSIS IN CONTROL AND VD URETHRAS

TUNEL staining was performed on control (n=4) and VD (n=5) urethras in order to assess whether the mechanically damaging effects of VD produced apoptosis in the urethral tissue. In the late stages of cellular apoptosis, extensive degradation occurs. Cleavage of DNA in this process may yield double stranded or single stranded. TUNEL identifies these strands via an enzymatic label, such as DNA polymerase or terminal deoxynucleotidal transferase, of the 3' OH termini with modified nucleotides (e.g., flourescein).

Urethras were prepared similarly to preparation of immunohistochemistry, discussed in **Section 4.2.5**. For the staining process, sections were cut 7 microns thick. Tissue sections were made permeable with tris-buffer for 10 minutes in an incubator. The in situ cell detection kit with flourescein (Roche Biosciences, Inc.) was used in order to complete the TUNEL analysis on the urethral tissue.

Results showed an increased presence of cellular apoptosis for the proximal urethral portion in VD compared to controls, specifically around the vasculature and dispersed throughout the smooth muscle portion of the urethra. The proximal portion had a significant increase in VD urethras compared to controls. Middle and distal portions had an increase in

positive TUNEL staining from VD, but this was not significant. However, one may conclude from that many of the functional and biomechanical changes found in the urethra from VD were not due to apoptosis. The reason for this is the small percentage of positive TUNEL staining (i.e., maximum amoung <1.00% in proximal VD urethras). Still, this was only at 4 days post VD.

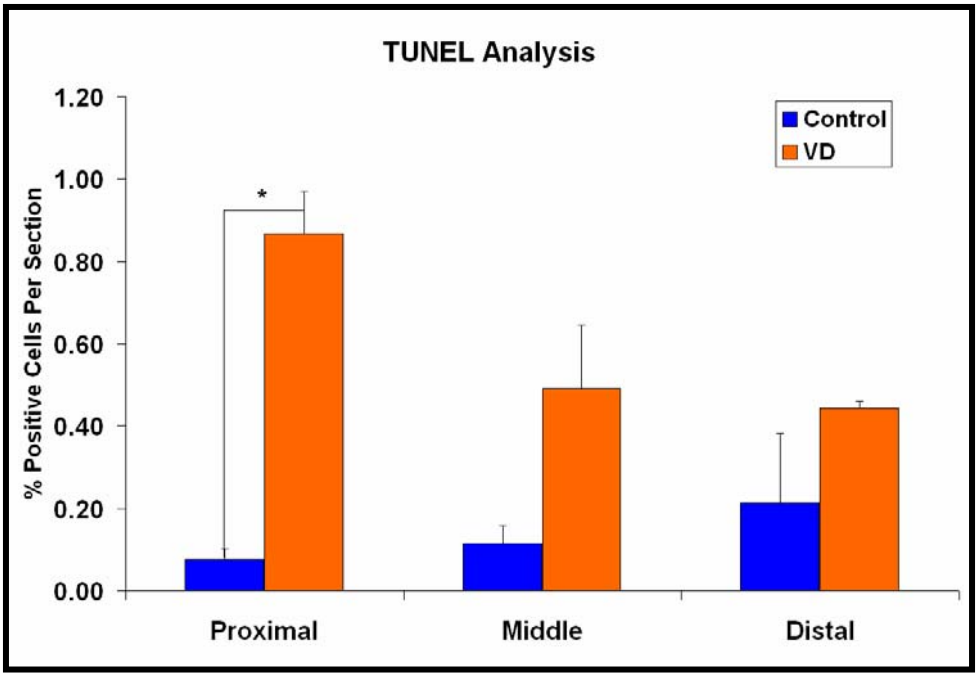

Figure D. 1 Results for the TUNEL assay performed to assess cellular apoptosis in the proximal, middle, and distal segments in control (n=4) and VD (n=5) urethras. * indicates significance.

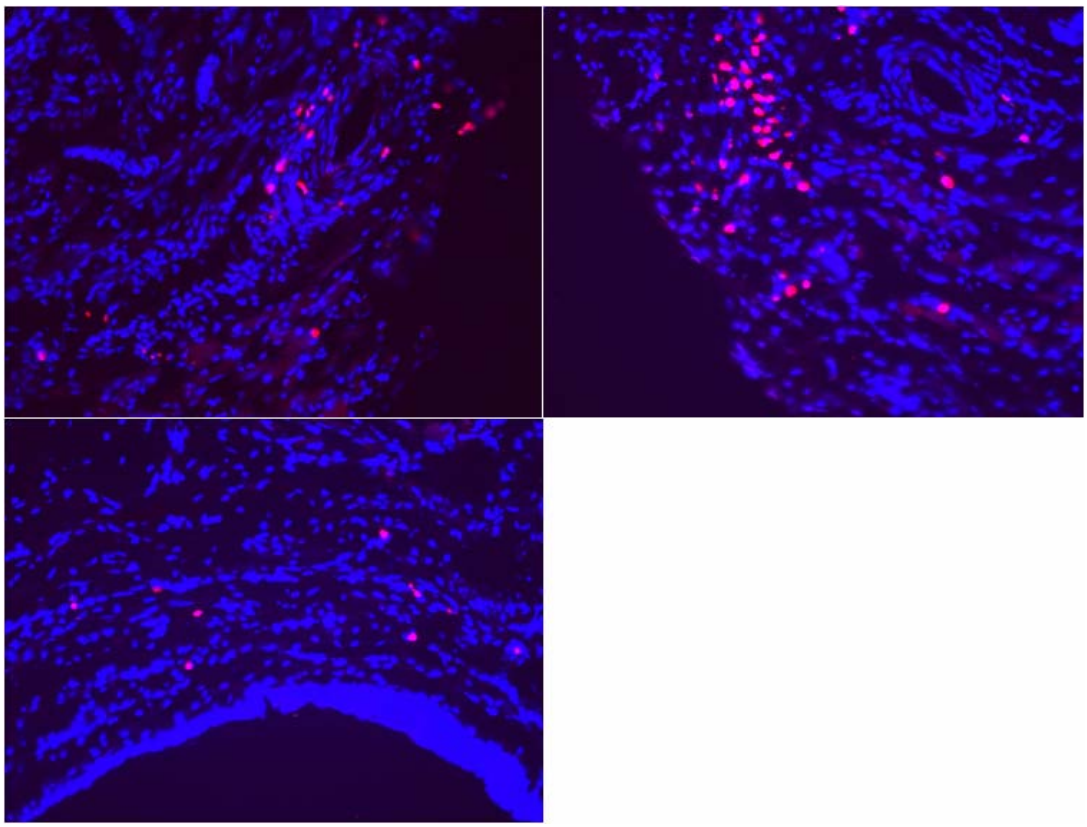

Figure D. 2 Positive TUNEL staining (pink) is found around the vasculature and dispersed throughout the media. Cells are stained with Hoesct (blue).

APPENDIX E

CONCENTRATION RESPONSE CURVES FOR PHENYLEPHRINE AND BETHANECHOL

In order to ensure that the concentrations used to induce a contraction, concentration response curves were performed on the middle segment of the urethra for PE (**Figure E.1**) and BE (**Figure E.2**), separately. Results indicated that concentrations to induce a maximum contraction for PE was 40 µM and for BE was 300 µM.

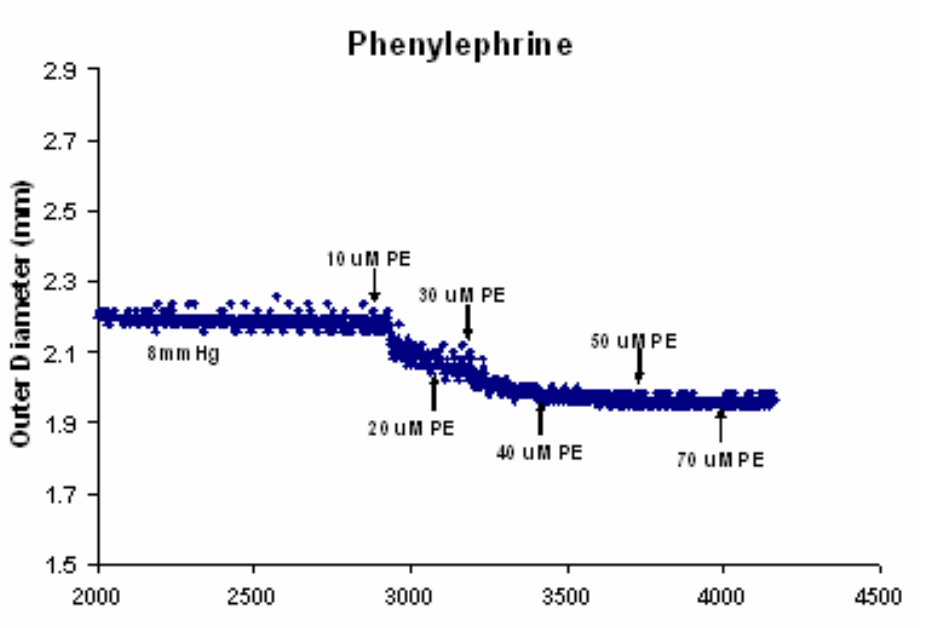

Figure E. 1 Concentration response curve for a control mid urethral segment. Maximum concentration for an adrenergic receptor contraction via phenylephrine (PE) was 40 µM. Maximum concentrations were assessed under 8 mmHg of static pressure and NOSi (100 µM).

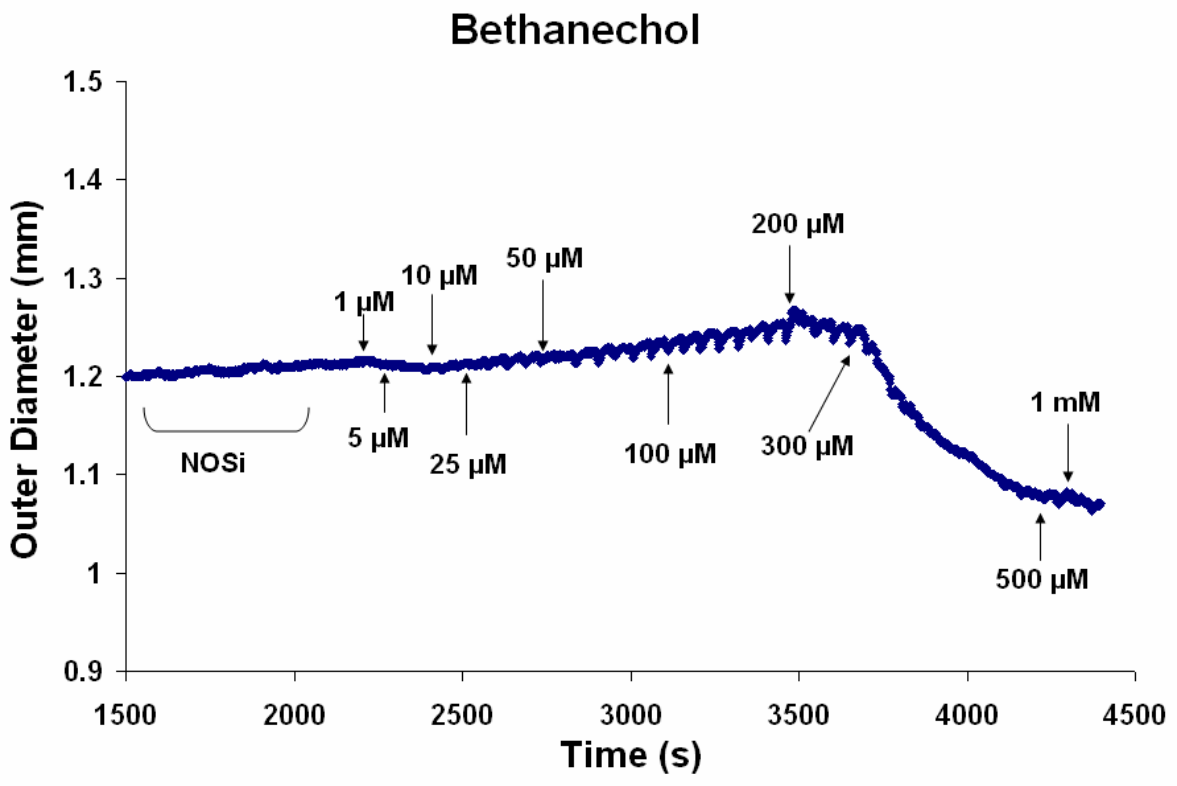

Figure E. 2 Concentration response curve for a control mid urethral segment. Maximum concentration for a cholinergic muscarinic receptor contraction via bethanechol (BE) was 300 µM. Maximum concentrations were assessed under 8 mmHg of static pressure and NOSi (100 µM).

APPENDIX F

ELECTRICAL FIELD STIMULATION AND STRIATED MUSCLE

In order to fully assess the urethra in health and disease, the striated muscle activity must be evaluated, as well as the smooth muscle. Unfortunately, this is a complicated task. Striated muscle contractions are activated by nicotinic receptors at the neuromuscular junction (**Figure F.1**). These nicotinic receptors desensitize quickly and make it difficult to make the muscle contraction last long enough for functional assessment. Additonally, large concentrations of acetylcholine are needed to activate striated muscle maximally (~1 mM).

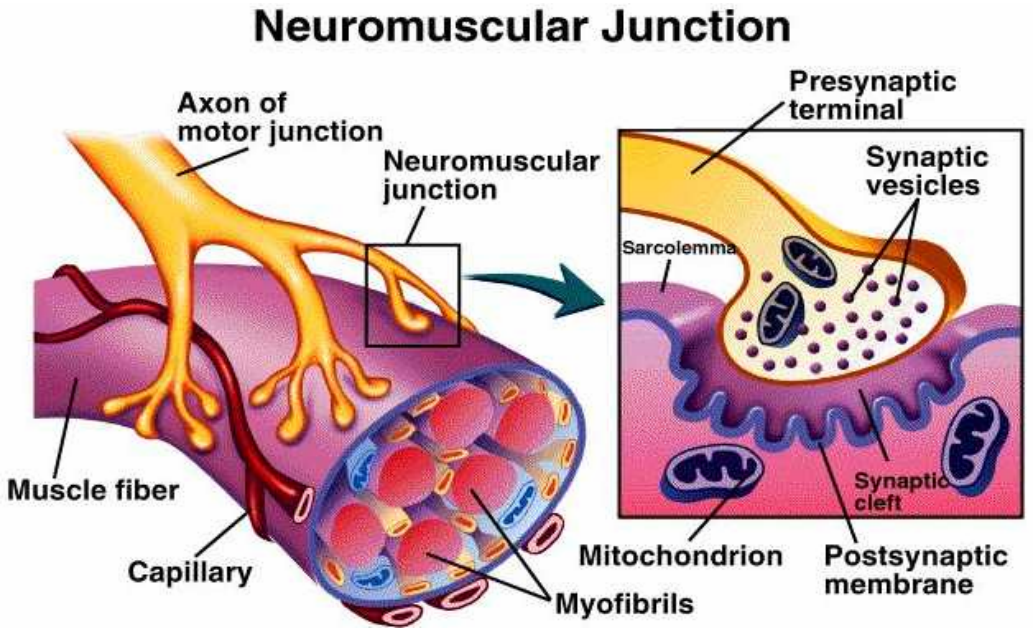

Figure F. 1 A schematic of the neuromuscular junction and the different components that make for successful motor control of a striated muscle fiber. [154]

Since acetylcholine is a non-selective cholinergic agonist, it is difficult to isolate activation of striated urethral muscle from that of a smooth muscle one via muscarinic receptors. It was attempted to contract striated muscle with acetylcholine and with the addition of atropine, a muscarinic antagonist, which would block the smooth muscle muscarinic receptors (**Figure F.2**). Still, the problem with atropine is the fact that high doses of atropine cause the agent to act as a neuromuscular blocking agent [155]. Therefore, concentrations of atropine greater than 5 μM could not be used. So, one must find a balance.

Eserine, a cholinesterase inhibitor, was used to maintain high concentrations of acetylcholine at the nicotinic receptor to maintain striated muscle contractions. Unfortunately, this did not work since nicotinic receptors desensitize so easily. To add to this, the eserine probably helped to overcome the atropine with high local concentrations of acetylcholine on muscarinic receptors and providing the long contraction that you see in **Figure F.2**. Also, notice the rhythmic waves within the contraction. This looks very similar to the bethanechol contraction in **Figure E.2**, in Appendix E.

Finally, succinylcholine, a depolarizing neuromuscular blocking agent, was added to assess the existence of the striated muscle contraction. While we should have seen a relaxation muscle, the contraction only strengthened; again, proving that the contraction was not striated, but smooth. Other drugs added, were hexamethonium, a ganglionic blocking agent, and EDTA to assess the amount of muscle tone left after blocking the contraction with succinylcholine.

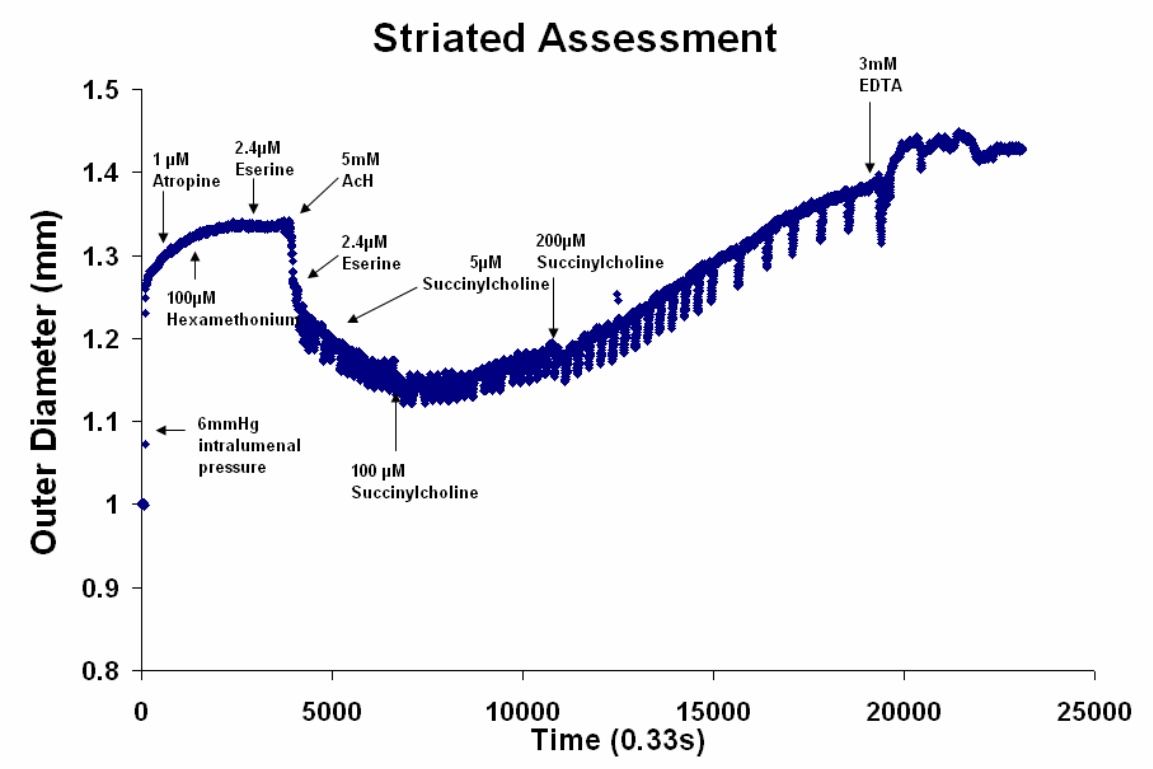

Figure F. 2 Striated assessment of the mid urethra with atropine, hexamethonium, eserine, acetylcholine (Ach), succinylcholine, and EDTA.

With all of these problems, it is clear why many investigators turn to in vivo studies of the external urethral striated sphincter. However, some ex vivo studies have been successful [16, 156]. Electrical field stimulation (EFS) has aided the progress made on ex vivo striated sphincter studies. Thus, it was our goal to utilize EFS for striated muscle assessment.

In a pilot study, urethras were tied onto the tees of the ex vivo system described in **Section 2.2.4**. Platinum electrodes (Fisher Scientific), extending from copper wire (Radio Shack), were placed in the bath across from each other with the tissue in the middle. Theses wires connected to a Grass stimulator (Astromed, Inc., S48 H series, West Warwick, RI). The

grass stimulator provided square wave electrical pulses to the tissue with voltages ranging from 0 to 150 volts.

To understand the effects of changing pulse duration on urethral response, static pressure (6 mmHg) was applied intralumenally, the voltage was set to 50 V. Single pulses were delivered and outer diameter was recorded for a tissue response (**Figure F.3**). Results indicated that at 50 V, pulses increased urethral outer diameter, causing relaxation. This was followed by a quick and very short contraction and then, a bigger relaxation. Next, the diameter returned to somewhat of a baseline diameter. This relaxation appeared to be prolonged by an increase in pulse duration (e.g., 5 ms).

The voltage was increased to 100V and also tested with varied pulse durations (0.1-10ms). The results were similar to that of 50V, except the relaxation magnitudes appeared to be larger and longer, with the short intermediate contractions decreasing with increasing pulse duration (**Figure F.3**).

While these results did not provide the fast twitch contractions typical of striated muscle contractions, it did respond in a repeatable fashion. The reason for the relaxation response could be that the voltage is too high. Thus, the next step would be to perform this experiment at voltage amplitudes less than 50 V. Additionally, these were single pulse experiments in an attempt to seek the optimal parameters for striated stimulation. Most studies use a train of pulses to achieve striated muscle contraction [16, 66, 156]. Therefore, the pulse duration, voltage, pulse frequency, train rate, and train duration must be optimized. Following this, the tissue should then be tested in the presence of a cocktail of antagonists to ensure that the contraction is one of the striated sphincter.

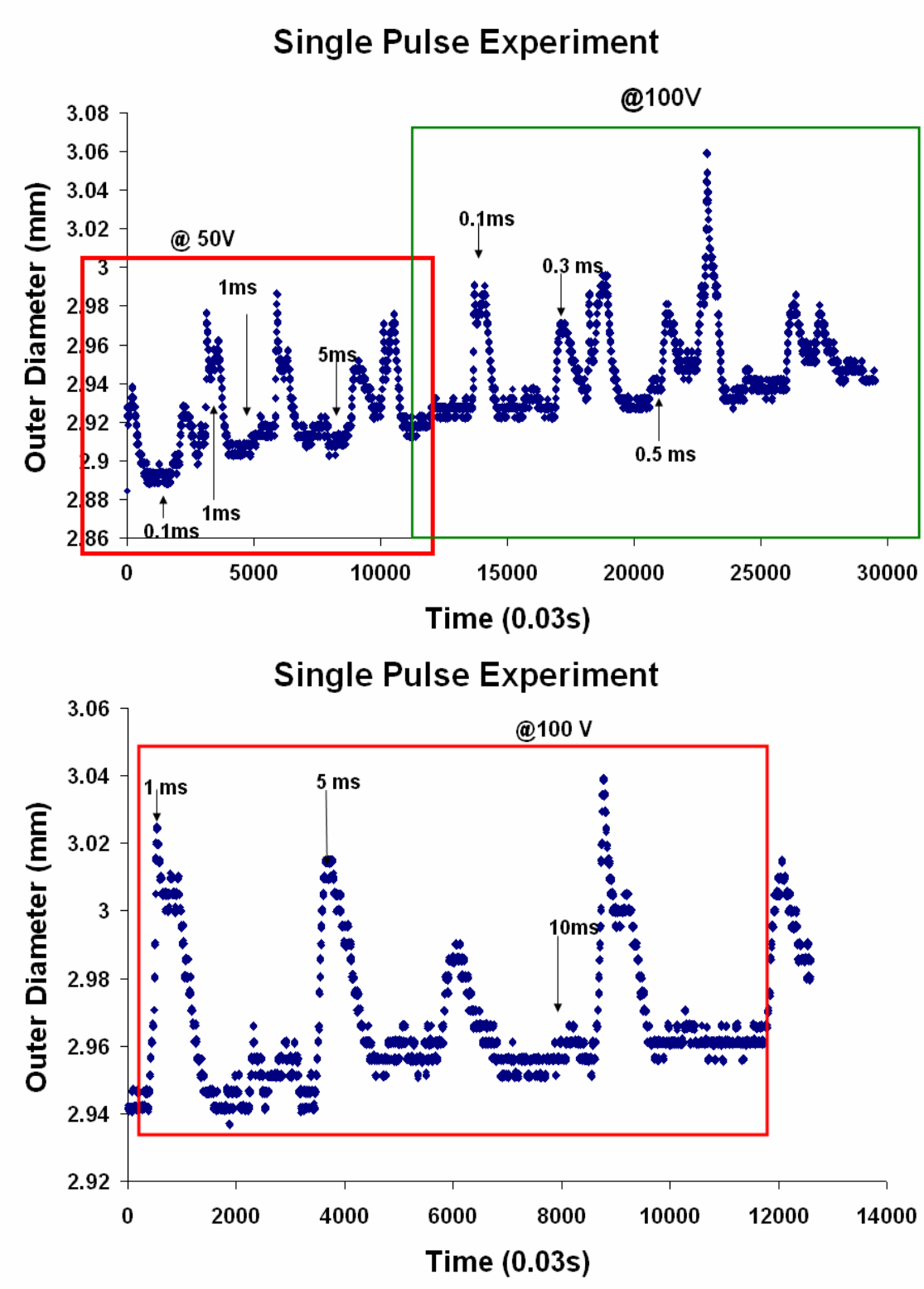

Figure F. 3 Results from the EFS experiments delivering a single pulse of varied pulse durations at two different voltages: 50 and 100 V.

APPENDIX G

A NOVEL METHOD TO MEASURE REGIONAL BIOMECHANICAL PROPERTIES OF THE MOUSE COLON: THE ROLE OF ICC CELLS IN DISTAL COLON

The combined assessment of physiologic function and ICC morphology provides a means to evaluate the potential role of ICC in distal colonic function. The following biomechanical data was generated in from distal colons of wildtype control and *c-kit* immunoreactivity in W/W^{v} mutant (CKD) mice.

Methods

After a midline abdominal incision under 4% isoflurane anesthesia, whole mount segments of distal colon, 2-3 cm in length (in-vivo), were harvested and immediately placed in cold, oxygenated medium 199 (Sigma Chemical Co, St. Louis, MO, #M3769) while maintaining their proximal-distal orientations. As previously described in **Section 2.2**, the colon was then secured to stainless steel tubing and restored to in vivo length inside the experimental apparatus. Pressure was applied intralumenally in 3mmHg increments with pressures ranging from 0-27mmHg, and pressure-diameter data was recorded for proximal, middle, and distal segments of the colon.

Pressure-diameter data was used to calculate compliance (**Equation 2.2**) and peristaltic amplitude (PA), as described in equation G.1.

$$PA = \left(\frac{OD_{max} - OD_{min}}{OD_{mean}} \right) \quad \textbf{(G.1)}$$

where, the minimum outer diameter (OD_{min}) was subtracted from the maximum outer diameter (OD_{max}) and divided by the mean outer diameter (OD_{mean}) for each step of pressure.

For statistical analyses, compliance and PA values between the control and CKD groups at each region were performed using a One-way ANOVA with Student-Newman-Keul's post hoc pairwise comparisons, or an equivalent nonparametric test (ANOVA on ranks with Dunn's post hoc analysis), was also used for multiple comparisons between all regions and tissue states for each calculated compliance.

Results

Pressure-diameter plots for averaged raw data showed segmental differences along the length of the colo-rectum (**Figure G.1**). The distal average pressure-diameter plot indicated that the distal colo-rectal portion was the most affected by the absence of c-kit receptors. Along the entire pressure range the CKD group shifted to the right of pressure-diameter curve of the control group. The middle segment was mostly affected by the absence of c-kit receptors in the lower pressure ranges (3-9 mmHg). It appeared that the proximal portion was not affected.

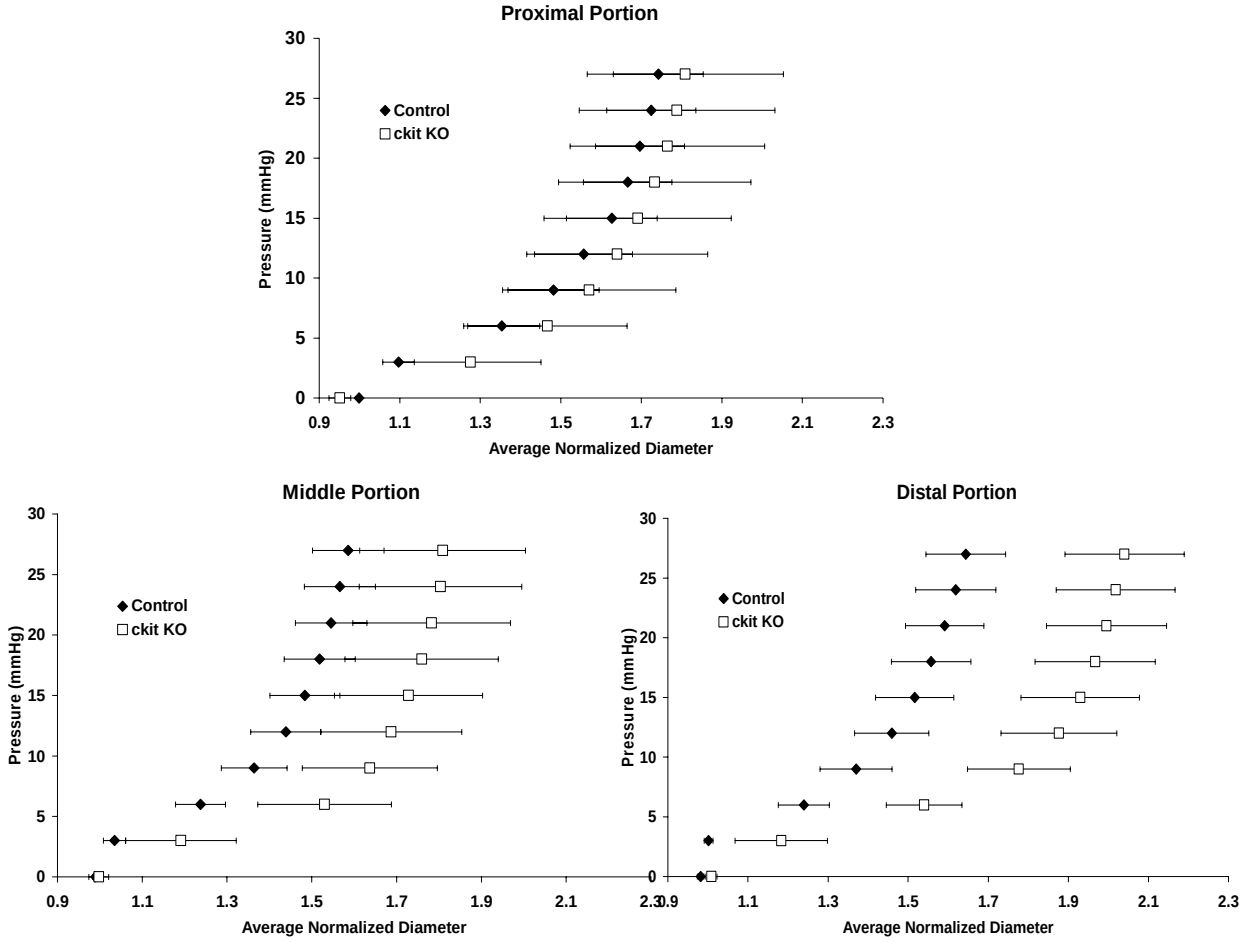

Figure G. 1 Pressure-diameter data for the proximal (top), middle (middle) and distal (bottom) portions of the mouse colo-rectum for control and ckit knock out (KO) mice

Quantification of compliance indicated significant differences for the distal portion, as well. Overall, the compliance values at low pressure ranges (0-9mmHg) were higher for the CKD groups compared to that of controls (**Figure G.2**). More specifically, distal compliance for the CKD ($0.085\pm0.01 mmHg^{-1}$) mice were significantly increased compared to that for the control mice (0.044 ± 0.01 $mmHg^{-1}$; $p=0.024$). No differences were distinguished among proximal and middle portions of CKD (0.075 ± 0.02 $mmHg^{-1}$, 0.072 ± 0.02 $mmHg^{-1}$) and control (0.054 ± 0.01 $mmHg^{-1}$, 0.042 ± 0.01 $mmHg^{-1}$) groups. At high pressure ranges (18 to 27 mmHg), overall the

CKD group had decreased compliance values compared to controls. The distal portion of the mouse colon for the CKD (0.003±0.00 $mmHg^{-1}$) group was significantly less compliant compared to that of controls (0.006±0.00 $mmHg^{-1}$; p=0.030). Compliance values for control proximal (0.005±0.00 $mmHg^{-1}$) and middle (0.004±0.00 $mmHg^{-1}$) portions were not different from CKD (0.005±0.00 $mmHg^{-1}$, 0.004±0.00 $mmHg^{-1}$).

From Figure G.3, we also observed peristalsis in response to the intralumenal pressure ranges. Thus, efforts were to analyze any changes in the CKD groups via peristaltic amplitude. Peristaltic amplitude for all three portions of the colon indicated a 0.5 to 1.5 fold increase at low pressure ranges, particularly, 0-3mmHg, for CKD compared to controls. The highest peristaltic amplitudes were observed was at 6mmHg for controls and 3mmHg for CKD. Amplitudes for both groups were progressively diminished from 9-27 mmHg, and an occasional high amplitude variation occurred in animals from both groups (n=3 total) at the highest pressures (24-27mmHg), but no consistent pattern was discerned and these were clearly outlier events. A non-significant proximal to distal gradient for peristaltic amplitude was observed at 3mmHg for CKD colons (median values: 31% for proximal, 27% for middle, and 13% for distal). Additionally, peristaltic amplitudes attained significantly greater magnitudes at lower pressures in CKD (median=3mmHg) compared to controls (median=6mmHg).

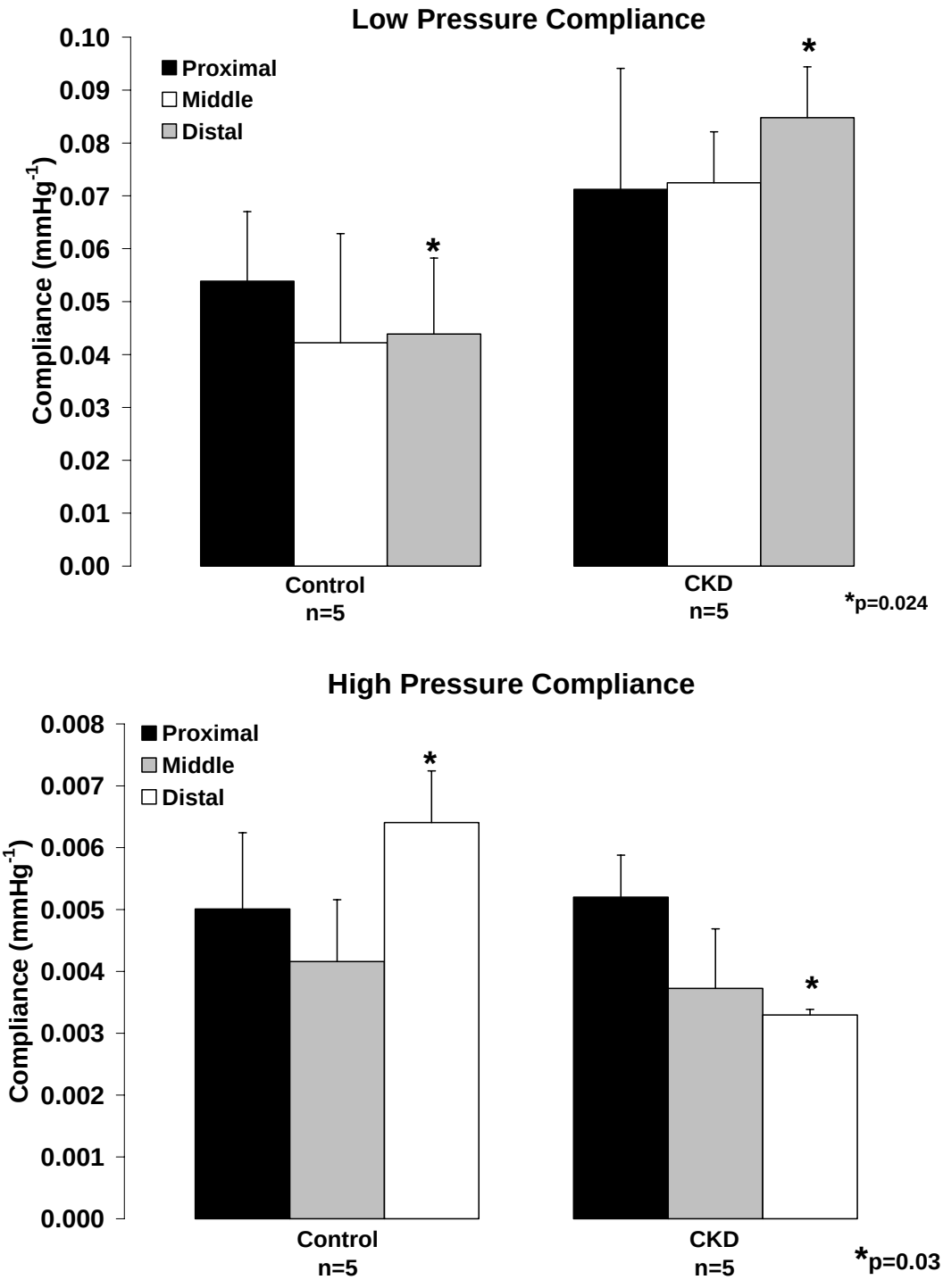

Figure G. 2 Compliance values for low (0-9 mmHg) and high (18-27 mmHg) pressures calculated for control and CKD groups; error bars represent standard error.

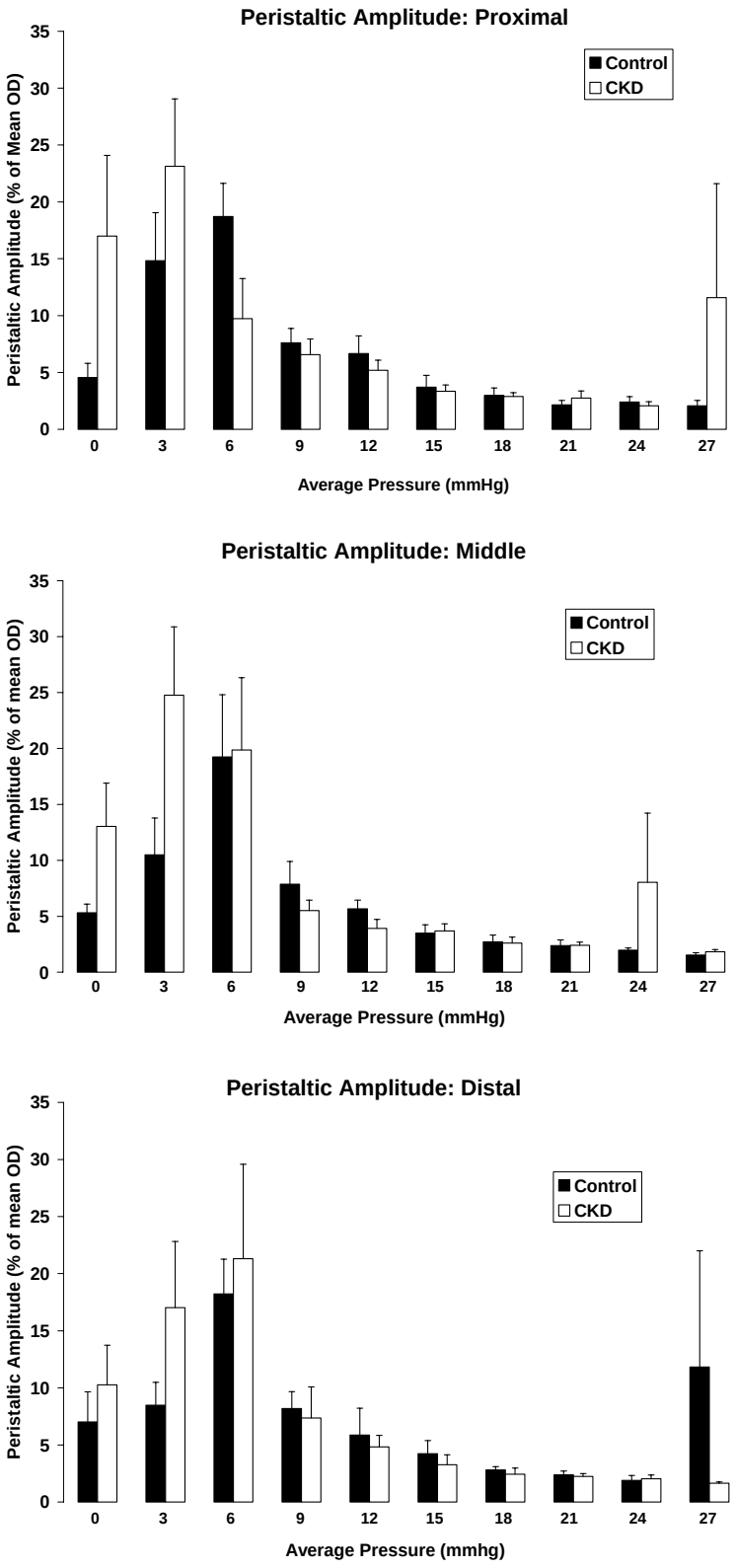

Figure G.3 Average peristaltic amplitude expressed as % of mean outer diameter (OD) for each 3 mmHg increment in the proximal (top), middle (middle), and distal (bottom) portions of the mouse colon

BIBLIOGRAPHY

1. Fultz, N.H., et al., *Burden of stress urinary incontinence for community-dwelling women.* Am J Obstet Gynecol, 2003. **189**(5): p. 1275-82.

2. Diokno, A.C., et al., *Prevalence of urinary incontinence and other urological symptoms in the noninstitutionalized elderly.* J Urol, 1986. **136**(5): p. 1022-5.

3. Meyer, S., et al., *Birth trauma: its effect on the urine continence mechanisms.* Gynakol Geburtshilfliche Rundsch, 1993. **33**(4): p. 236-42.

4. Elbadawi, A., *Functional anatomy of the organs of micturition.* Urol Clin North Am, 1996. **23**(2): p. 177-210.

5. Sugaya, K., et al., *Central nervous control of micturition and urine storage.* J Smooth Muscle Res, 2005. **41**(3): p. 117-32.

6. Yoshimura, N., *Bladder afferent pathway and spinal cord injury: possible mechanisms inducing hyperreflexia of the urinary bladder.* Prog Neurobiol, 1999. **57**(6): p. 583-606.

7. Brading, A.F., et al., *Morphological and physiological characteristics of urethral circular and longitudinal smooth muscle.* Scand J Urol Nephrol Suppl, 2001(207): p. 12-8; discussion 106-25.

8. Brading, A.F., et al., *Blood supply to the bladder during filling.* Scand J Urol Nephrol Suppl, 1999. **201**: p. 25-31.

9. Brading, A.F., *The physiology of the mammalian urinary outflow tract.* Exp Physiol, 1999. **84**(1): p. 215-21.

10. Andersson, P.O., A. Malmgren, and B. Uvelius, *Functional responses of different muscle types of the female rat urethra in vitro.* Acta Physiol Scand, 1990. **140**(3): p. 365-72.

11. Thor, K.B. and C. Donatucci, *Central nervous system control of the lower urinary tract: new pharmacological approaches to stress urinary incontinence in women.* J Urol, 2004. **172**(1): p. 27-33.

12. de Groat, W.C., *Integrative control of the lower urinary tract: preclinical perspective.* Br J Pharmacol, 2006. **147 Suppl 2**: p. S25-40.

13. Schafer, W., *Some biomechanical aspects of continence function.* Scand J Urol Nephrol Suppl, 2001(207): p. 44-60; discussion 106-25.

14. Augsburger, H.R., *Elastic fibre system of the female canine urethra. Histochemical identification of elastic, elaunin and oxytalan fibres.* Anat Histol Embryol, 1997. **26**(4): p. 297-302.

15. Dass, N., G. McMurray, and A.F. Brading, *Elastic fibres in the vesicourethral junction and urethra of the guinea pig: quantification with computerised image analysis.* J Anat, 1999. **195 (Pt 3)**: p. 447-53.

16. Walters, R.D., G. McMurray, and A.F. Brading, *Pudendal nerve stimulation of a preparation of isolated guinea-pig urethra.* BJU Int, 2006. **98**(6): p. 1302-9.

17. Kamo, I., et al., *The role of bladder-to-urethral reflexes in urinary continence mechanisms in rats.* Am J Physiol Renal Physiol, 2004. **287**(3): p. F434-41.

18. Kamo, I., et al., *Functional analysis of active urethral closure mechanisms under sneeze induced stress condition in a rat model of birth trauma.* J Urol, 2006. **176**(6 Pt 1): p. 2711-5.

19. Mattiasson, A., et al., *Nerve-mediated functions in the circular and longitudinal muscle layers of the proximal female rabbit urethra.* J Urol, 1990. **143**(1): p. 155-60.

20. Arner, A., et al., *Shortening velocity is different in longitudinal and circular muscle layers of the rabbit urethra.* Urol Res, 1998. **26**(6): p. 423-6.

21. Creed, K.E. and B.A. Van der Werf, *The innervation and properties of the urethral striated muscle.* Scand J Urol Nephrol Suppl, 2001(207): p. 8-11; discussion 106-25.

22. Garcia-Pascual, A., et al., *Partial nicotinic receptor blockade unmasks a modulatory role of nitric oxide on urethral striated neuromuscular transmission.* Nitric Oxide, 2005. **13**(2): p. 98-110.

23. Webb, R.C., *Smooth muscle contraction and relaxation.* Adv Physiol Educ, 2003. **27**(1-4): p. 201-6.

24. Tomita, T. and H. Watanabe, *Factors controlling myogenic activity in smooth muscle.* Philos Trans R Soc Lond B Biol Sci, 1973. **265**(867): p. 73-85.

25. Brading, A.F., *Spontaneous activity of lower urinary tract smooth muscles: correlation between ion channels and tissue function.* J Physiol, 2006. **570**(Pt 1): p. 13-22.

26. Malmqvist, U., et al., *Female pig urethral tone is dependent on Rho guanosine triphosphatases and Rho-associated kinase.* J Urol, 2004. **171**(5): p. 1955-8.

27. Sergeant, G.P., et al., *Specialised pacemaking cells in the rabbit urethra.* J Physiol, 2000. **526 Pt 2**: p. 359-66.

28. Sergeant, G.P., et al., *Interstitial cells of Cajal in the urethra.* J Cell Mol Med, 2006. **10**(2): p. 280-91.

29. Fowler, C.J., *Integrated control of lower urinary tract--clinical perspective.* Br J Pharmacol, 2006. **147 Suppl 2**: p. S14-24.

30. Miller, K.L., *Stress urinary incontinence in women: review and update on neurological control.* J Womens Health (Larchmt), 2005. **14**(7): p. 595-608.

31. Norton, P. and L. Brubaker, *Urinary incontinence in women.* Lancet, 2006. **367**(9504): p. 57-67.

32. Heesakkers, J.P. and R.R. Gerretsen, *Urinary incontinence: sphincter functioning from a urological perspective.* Digestion, 2004. **69**(2): p. 93-101.

33. Kirby, M., *A review of the role of primary care in the diagnosis and management of stress urinary incontinence.* Health Serv J, 2004. **114**(5923): p. suppl 3-7 following 54.

34. Melton, L., *Targeted treatment for incontinence beckons.* Lancet, 2002. **359**(9303): p. 326.

35. Cardozo, L., *Neurobiology of stress urinary incontinence: new insights and implications for treatment.* J Obstet Gynaecol, 2005. **25**(6): p. 539-43.

36. Smith, P.P., R.J. McCrery, and R.A. Appell, *Current trends in the evaluation and management of female urinary incontinence.* Cmaj, 2006. **175**(10): p. 1233-40.

37. Moreland, R.B., J.D. Brioni, and J.P. Sullivan, *Emerging pharmacologic approaches for the treatment of lower urinary tract disorders.* J Pharmacol Exp Ther, 2004. **308**(3): p. 797-804.

38. Thor, K.B., *Serotonin and norepinephrine involvement in efferent pathways to the urethral rhabdosphincter: implications for treating stress urinary incontinence.* Urology, 2003. **62**(4 Suppl 1): p. 3-9.

39. Steers, W.D., *Rat: overview and innervation.* Neurourol Urodyn, 1994. **13**(2): p. 97-118.

40. de Groat, W.C., et al., *Neural control of the urethra.* Scand J Urol Nephrol Suppl, 2001(207): p. 35-43; discussion 106-25.

41. Kamo, I., et al., *Urethral closure mechanisms under sneeze-induced stress condition in rats: a new animal model for evaluation of stress urinary incontinence.* Am J Physiol Regul Integr Comp Physiol, 2003. **285**(2): p. R356-65.

42. Kerns, J.M., et al., *Effects of pudendal nerve injury in the female rat.* Neurourol Urodyn, 2000. **19**(1): p. 53-69.

43. Peng, C.W., et al., *External urethral sphincter activity in a rat model of pudendal nerve injury.* Neurourol Urodyn, 2006. **25**(4): p. 388-96.

44. Heidkamp, M.C., et al., *Pudendal denervation affects the structure and function of the striated, urethral sphincter in female rats.* Int Urogynecol J Pelvic Floor Dysfunct, 1998. **9**(2): p. 88-93.

45. Lin, A.S., et al., *Effect of simulated birth trauma on the urinary continence mechanism in the rat.* Urology, 1998. **52**(1): p. 143-51.

46. Sievert, K.D., et al., *The effect of labor and/or ovariectomy on rodent continence mechanism--the neuronal changes.* World J Urol, 2004. **22**(4): p. 244-50.

47. Cannon, T.W., et al., *Effects of vaginal distension on urethral anatomy and function.* BJU Int, 2002. **90**(4): p. 403-7.

48. Chermansky, C.J., et al., *A model of intrinsic sphincteric deficiency in the rat: electrocauterization.* Neurourol Urodyn, 2004. **23**(2): p. 166-71.

49. Rodriguez, L.V., et al., *New objective measures to quantify stress urinary incontinence in a novel durable animal model of intrinsic sphincter deficiency.* Am J Physiol Regul Integr Comp Physiol, 2005. **288**(5): p. R1332-8.

50. Falconer, C., et al., *Paraurethral connective tissue in stress-incontinent women after menopause.* Acta Obstet Gynecol Scand, 1998. **77**(1): p. 95-100.

51. Keane, D.P., et al., *Analysis of collagen status in premenopausal nulliparous women with genuine stress incontinence.* Br J Obstet Gynaecol, 1997. **104**(9): p. 994-8.

52. Rocha, M.A., et al., *The impact of pregnancy and childbirth in the urethra of female rats.* Int Urogynecol J Pelvic Floor Dysfunct, 2006.

53. Yalla, S.V. and H.M. Burros, *Conduit and compliance responses of female canine urethra. Experimental study of effects of varying amounts of instrumental dilation and urethral myotomy.* Urology, 1974. **3**(5): p. 598-603.

54. Mayo, M.E. and F. Hinman, *The effect of urethral lengthening.* Br J Urol, 1973. **45**(6): p. 621-30.

55. Thind, P., G. Lose, and H. Colstrup, *How to measure urethral elastance in a simple way. Elastance: definition, determination and implications.* Urol Res, 1991. **19**(4): p. 241-4.

56. Thind, P., et al., *The effect of pharmacological stimulation and blockade of autonomic receptors and of pudendal blockade on urethral stress relaxation in healthy women.* Br J Urol, 1994. **74**(1): p. 86-92.

57. Thind, P., G. Lose, and H. Colstrup, *Pressure response to rapid dilation of resting urethra in healthy women.* Urology, 1992. **40**(1): p. 44-9.

58. Colstrup, H., *Rigidity of the resting female urethra. Part I. Static measurements.* J Urol, 1984. **132**(1): p. 78-81.

59. Colstrup, H., *Rigidity of the resting female urethra. Part II. Dynamic measurements.* J Urol, 1984. **132**(1): p. 82-6.

60. Vorp, D.A., et al., *Wall strength and stiffness of aneurysmal and nonaneurysmal abdominal aorta.* Ann N Y Acad Sci, 1996. **800**: p. 274-6.

61. Thind, P. and G. Lose, *Urethral stress relaxation phenomenon in healthy and stress incontinent women.* Br J Urol, 1992. **69**(1): p. 75-8.

62. Thind, P., et al., *The urethral resistance to rapid dilation: an analysis of the effect of autonomic receptor stimulation and blockade and of pudendal nerve blockade in healthy females.* Scand J Urol Nephrol, 1995. **29**(1): p. 83-91.

63. Yalla, S.V., H.M. Burros, and M.I. Ivker, *Physical properties of female urethral wall. Experimental method for determining relative degree of urethral wall stiffness.* Urology, 1973. **2**(3): p. 269-75.

64. Jankowski, R.J., et al., *Development of an experimental system for the study of urethral biomechanical function.* Am J Physiol Renal Physiol, 2004. **286**(2): p. F225-32.

65. Jankowski, R.J., et al., *Biomechanical characterization of the urethral musculature.* Am J Physiol Renal Physiol, 2006. **290**(5): p. F1127-34.

66. Van der Werf, B.A., T. Hidaka, and K.E. Creed, *Continence and some properties of the urethral striated muscle of male greyhounds.* BJU Int, 2000. **85**(3): p. 341-9.

67. Awad, S.A. and J.W. Downie, *Relative contributions of smooth and striated muscles to the canine urethral pressure profile.* Br J Urol, 1976. **48**(5): p. 347-54.

68. Brant, A.M., G.J. Rodgers, and H.S. Borovetz, *Measurement in vitro of pulsatile arterial diameter using a helium-neon laser.* J Appl Physiol, 1987. **62**(2): p. 679-83.

69. Streng, T., R. Santti, and A. Talo, *Similarities and differences in female and male rat voiding.* Neurourol Urodyn, 2002. **21**(2): p. 136-41.

70. Labadie, R.F., et al., *Pulsatile perfusion system for ex vivo investigation of biochemical pathways in intact vascular tissue.* Am J Physiol, 1996. **270**(2 Pt 2): p. H760-8.

71. Ligush, J., Jr., et al., *Evaluation of endothelium-derived nitric oxide mediated vasodilation utilizing ex vivo perfusion of an intact vessel.* J Surg Res, 1992. **52**(5): p. 416-21.

72. Brant, A.M., et al., *Biomechanics of the arterial wall under simulated flow conditions.* J Biomech, 1988. **21**(2): p. 107-13.

73. Vorp, D.A., et al., *A device for the application of cyclic twist and extension on perfused vascular segments.* Am J Physiol, 1996. **270**(2 Pt 2): p. H787-95.

74. Hughes, J.M. and S.J. Bund, *Arterial myogenic properties of the spontaneously hypertensive rat.* Exp Physiol, 2002. **87**(5): p. 527-34.

75. Fung, Y.C., *Biomechanics: Mechanical Properties of Living Tissues*. Second ed. 1993, New York: Springer-Vlag.

76. Raghavan, M.L., M.W. Webster, and D.A. Vorp, *Ex vivo biomechanical behavior of abdominal aortic aneurysm: assessment using a new mathematical model.* Ann Biomed Eng, 1996. **24**(5): p. 573-82.

77. Sumner, D.S., D.E. Hokanson, and D.E. Strandness, Jr., *Stress-strain characteristics and collagen-elastin content of abdominal aortic aneurysms.* Surg Gynecol Obstet, 1970. **130**(3): p. 459-66.

78. Hayashi, K., *Experimental approaches on measuring the mechanical properties and constitutive laws of arterial walls.* J Biomech Eng, 1993. **115**(4B): p. 481-8.

79. Hudetz, A.G., *Incremental elastic modulus for orthotropic incompressible arteries.* J Biomech, 1979. **12**(9): p. 651-5.

80. Junqueira, L.C., G. Bignolas, and R.R. Brentani, *Picrosirius staining plus polarization microscopy, a specific method for collagen detection in tissue sections.* Histochem J, 1979. **11**(4): p. 447-55.

81. Dolber, P.C. and M.S. Spach, *Conventional and confocal fluorescence microscopy of collagen fibers in the heart.* J Histochem Cytochem, 1993. **41**(3): p. 465-9.

82. Dayan, D., et al., *Are the polarization colors of picrosirius red-stained collagen determined only by the diameter of the fibers?* Histochemistry, 1989. **93**(1): p. 27-9.

83. Prantil, R.L., et al., *Ex vivo biomechanical properties of the female urethra in a rat model of birth trauma.* Am J Physiol Renal Physiol, 2007. **292**(4): p. F1229-37.

84. Vorp, D.A., et al., *Identification of elastic properties of homogeneous, orthotropic vascular segments in distension.* J Biomech, 1995. **28**(5): p. 501-12.

85. Roach, M.R. and A.C. Burton, *The reason for the shape of the distensibility curves of arteries.* Can J Biochem Physiol, 1957. **35**(8): p. 681-90.

86. Cox, R.H., *Viscoelastic properties of canine pulmonary arteries.* Am J Physiol, 1984. **246**(1 Pt 2): p. H90-6.

87. Goepel, C. and C. Thomssen, *Changes in the extracellular matrix in periurethral tissue of women with stress urinary incontinence.* Acta Histochem, 2006. **108**(6): p. 441-5.

88. Liapis, A., et al., *Changes of collagen type III in female patients with genuine stress incontinence and pelvic floor prolapse.* Eur J Obstet Gynecol Reprod Biol, 2001. **97**(1): p. 76-9.

89. Goepel, C., et al., *Periurethral connective tissue status of postmenopausal women with genital prolapse with and without stress incontinence.* Acta Obstet Gynecol Scand, 2003. **82**(7): p. 659-64.

90. Barbic, M., B. Kralj, and A. Cor, *Compliance of the bladder neck supporting structures: importance of activity pattern of levator ani muscle and content of elastic fibers of endopelvic fascia.* Neurourol Urodyn, 2003. **22**(4): p. 269-76.

91. Damaser, M.S., et al., *Effect of vaginal distension on blood flow and hypoxia of urogenital organs of the female rat.* J Appl Physiol, 2005. **98**(5): p. 1884-90.

92. Huang, W.C. and J.M. Yang, *Bladder neck funneling on ultrasound cystourethrography in primary stress urinary incontinence: a sign associated with urethral hypermobility and intrinsic sphincter deficiency.* Urology, 2003. **61**(5): p. 936-41.

93. Conway, D.A., et al., *Comparison of leak point pressure methods in an animal model of stress urinary incontinence.* Int Urogynecol J Pelvic Floor Dysfunct, 2005. **16**(5): p. 359-63.

94. Thind, P. and G. Lose, *The effect of bilateral pudendal blockade on the static urethral closure function in healthy females.* Obstet Gynecol, 1992. **80**(6): p. 906-11.

95. Henrion, D., *Pressure and flow-dependent tone in resistance arteries. Role of myogenic tone.* Arch Mal Coeur Vaiss, 2005. **98**(9): p. 913-21.

96. Smith, P.G. and S. Bradshaw, *Innervation of the proximal urethra of ovariectomized and estrogen-treated female rats.* Histol Histopathol, 2004. **19**(4): p. 1109-16.

97. Lee, J.G., A.J. Wein, and R.M. Levin, *Effects of pregnancy on urethral and bladder neck function.* Urology, 1993. **42**(6): p. 747-52.

98. Schaer, G.N., et al., *Sonographic evaluation of the bladder neck in continent and stress-incontinent women.* Obstet Gynecol, 1999. **93**(3): p. 412-6.

99. Yalla, S.V., et al., *Striated sphincter participation in distal passive urinary continence mechanisms: studies in male subjects deprived of proximal sphincter mechanism.* J Urol, 1979. **122**(5): p. 655-60.

100. Boutouyrie, P., et al., *Smooth muscle tone and arterial wall viscosity: an in vivo/in vitro study.* Hypertension, 1998. **32**(2): p. 360-4.

101. Siegman, M.J., et al., *Calcium-dependent resistance to stretch and stress relaxation in resting smooth muscles.* Am J Physiol, 1976. **231**(5 Pt. 1): p. 1501-8.

102. Lose, G., *Urethral pressure measurement--problems and clinical value.* Scand J Urol Nephrol Suppl, 2001(207): p. 61-6; discussion 106-25.

103. Hickey, D.S., J.I. Phillips, and D.W. Hukins, *Arrangements of collagen fibrils and muscle fibres in the female urethra and their implications for the control of micturition.* Br J Urol, 1982. **54**(5): p. 556-61.

104. Briones, A.M., et al., *Alterations in structure and mechanics of resistance arteries from ouabain-induced hypertensive rats.* Am J Physiol Heart Circ Physiol, 2006. **291**(1): p. H193-201.

105. Scott, M. and I. Vesely, *Aortic valve cusp microstructure: the role of elastin.* Ann Thorac Surg, 1995. **60**(2 Suppl): p. S391-4.

106. Bagot, K. and R. Chess-Williams, *Alpha(1A/L)-adrenoceptors mediate contraction of the circular smooth muscle of the pig urethra.* Auton Autacoid Pharmacol, 2006. **26**(4): p. 345-53.

107. Werkstrom, V., et al., *Neurotransmitter release evoked by alpha-latrotoxin in the smooth muscle of the female pig urethra.* Naunyn Schmiedebergs Arch Pharmacol, 1997. **356**(2): p. 151-8.

108. Teramoto, N., G. McMurray, and A.F. Brading, *Effects of levcromakalim and nucleoside diphosphates on glibenclamide-sensitive K+ channels in pig urethral myocytes.* Br J Pharmacol, 1997. **120**(7): p. 1229-40.

109. Pagani, M., et al., *Effects of age on aortic pressure-diameter and elastic stiffness-stress relationships in unanesthetized sheep.* Circ Res, 1979. **44**(3): p. 420-9.

110. Fridez, P., et al., *Short-Term biomechanical adaptation of the rat carotid to acute hypertension: contribution of smooth muscle.* Ann Biomed Eng, 2001. **29**(1): p. 26-34.

111. Kuo, H.C., *Effects of vaginal trauma and oophorectomy on the continence mechanism in rats.* Urol Int, 2002. **69**(1): p. 36-41.

112. Chang, S., et al., *Increased contractility of diabetic rabbit corpora smooth muscle in response to endothelin is mediated via Rho-kinase beta.* Int J Impot Res, 2003. **15**(1): p. 53-62.

113. Azadzoi, K.M., et al., *Alteration of urothelial-mediated tone in the ischemic bladder: role of eicosanoids.* Neurourol Urodyn, 2004. **23**(3): p. 258-64.

114. Fleming, W.W., *Mechanisms of adaptive supersensitivity in smooth muscles vs cardiac muscle: a brief review.* Clin Exp Pharmacol Physiol, 1989. **16**(6): p. 447-50.

115. Lindsey, M.L., et al., *Extracellular matrix remodeling following myocardial injury.* Ann Med, 2003. **35**(5): p. 316-26.

116. Drake, M.J., et al., *Structural and functional denervation of human detrusor after spinal cord injury.* Lab Invest, 2000. **80**(10): p. 1491-9.

117. Persson, K., et al., *Morphological and functional evidence against a sensory and sympathetic origin of nitric oxide synthase-containing nerves in the rat lower urinary tract.* Neuroscience, 1997. **77**(1): p. 271-81.

118. Deplanne, V., S. Palea, and I. Angel, *The adrenergic, cholinergic and NANC nerve-mediated contractions of the female rabbit bladder neck and proximal, medial and distal urethra.* Br J Pharmacol, 1998. **123**(8): p. 1517-24.

119. Kakizaki, H. and W.C. de Groat, *Reorganization of somato-urethral reflexes following spinal cord injury in the rat.* J Urol, 1997. **158**(4): p. 1562-7.

120. Bridgewater, M., J.R. Davies, and A.F. Brading, *Regional variations in the neural control of the female pig urethra.* Br J Urol, 1995. **76**(6): p. 730-40.

121. Andersson, K.E. and A.J. Wein, *Pharmacology of the lower urinary tract: basis for current and future treatments of urinary incontinence.* Pharmacol Rev, 2004. **56**(4): p. 581-631.

122. Taki, N., et al., *Evidence for predominant mediation of alpha1-adrenoceptor in the tonus of entire urethra of women.* J Urol, 1999. **162**(5): p. 1829-32.

123. Andersson, K.E., *The importance of the cholinergic system in neurourology.* Eur Urol, 1998. **34 Suppl 1**: p. 6-9.

124. Masuda, H., et al., *Role of a central muscarinic cholinergic pathway for relaxation of the proximal urethra during the voiding phase in rats.* J Urol, 2001. **165**(3): p. 999-1003.

125. Mangiarua, E.I., E.H. Joyce, and R.D. Bevan, *Denervation increases myogenic tone in a resistance artery in the growing rabbit ear.* Am J Physiol, 1986. **250**(5 Pt 2): p. H889-91.

126. Yokoyama, O., et al., *The influence of pelvic nerve transection on the neuromuscular system of the canine urinary bladder.* Urol Res, 1992. **20**(1): p. 45-8.

127. Kane, D.D., et al., *Motor pudendal nerve characterization in the female rat.* Anat Rec, 2002. **266**(1): p. 21-9.

128. Rocha, M.A., et al., *Impact of pregnancy and childbirth on female rats' urethral nerve fibers.* Int Urogynecol J Pelvic Floor Dysfunct, 2007.

129. Kwon, H.Y., A.J. Wein, and R.M. Levin, *Effect of anoxia on the urethral response to phenylephrine.* J Urol, 1995. **154**(4): p. 1527-31.

130. Kakizaki, H., M.O. Fraser, and W.C. De Groat, *Reflex pathways controlling urethral striated and smooth muscle function in the male rat.* Am J Physiol, 1997. **272**(5 Pt 2): p. R1647-56.

131. Persson, C.G. and K.E. Andersson, *Adrenoceptor and cholinoceptor mediated effects in the isolated urethra of cat and guinea-pig.* Clin Exp Pharmacol Physiol, 1976. **3**(5): p. 415-26.

132. Gilletti, A. and J. Muthuswamy, *Brain micromotion around implants in the rodent somatosensory cortex.* J Neural Eng, 2006. **3**(3): p. 189-95.

133. Chambler, A.F., et al., *Coracoacromial ligament tension in vivo.* J Shoulder Elbow Surg, 2003. **12**(4): p. 365-7.

134. Takamizawa, K., K. Hayashi, and T. Matsuda, *Isometric biaxial tension of smooth muscle in isolated cylindrical segments of rabbit arteries.* Am J Physiol, 1992. **263**(1 Pt 2): p. H30-4.

135. Dou, Y., et al., *Longitudinal residual strain and stress-strain relationship in rat small intestine.* Biomed Eng Online, 2006. **5**: p. 37.

136. Patel, D.J.a.V., R.N., *Basic Hemodynamics and Its Role in Disease Processes*. 1980, Baltimore: University Park Press.

137. Greenland, J.E., N. Dass, and A.F. Brading, *Intrinsic urethral closure mechanisms in the female pig.* Scand J Urol Nephrol Suppl, 1996. **179**: p. 75-80.

138. Tracey, K.J., *Physiology and immunology of the cholinergic antiinflammatory pathway.* J Clin Invest, 2007. **117**(2): p. 289-96.

139. Osinski, M.A. and P. Bass, *Chronic denervation of rat jejunum results in cholinergic supersensitivity due to reduction of cholinesterase activity.* J Pharmacol Exp Ther, 1993. **266**(3): p. 1684-90.

140. Kim, R.J., et al., *Striated muscle and nerve fascicle distribution in the female rat urethral sphincter.* Anat Rec (Hoboken), 2007. **290**(2): p. 145-54.

141. Lien, K.C., et al., *Pudendal nerve stretch during vaginal birth: a 3D computer simulation.* Am J Obstet Gynecol, 2005. **192**(5): p. 1669-76.

142. Almeida, F.G., H. Bruschini, and M. Srougi, *Urodynamic and clinical evaluation of 91 female patients with urinary incontinence treated with perineal magnetic stimulation: 1-year followup.* J Urol, 2004. **171**(4): p. 1571-4; discussion 1574-5.

143. Nager, C.W., et al., *Correlation of urethral closure pressure, leak-point pressure and incontinence severity measures.* Int Urogynecol J Pelvic Floor Dysfunct, 2001. **12**(6): p. 395-400.

144. Weinberger, M.W., *Conservative treatment of urinary incontinence.* Clin Obstet Gynecol, 1995. **38**(1): p. 175-88.

145. Fitzgerald, M.P., et al., *Urethral collagen morphologic characteristics among women with genuine stress incontinence.* Am J Obstet Gynecol, 2000. **182**(6): p. 1565-74.

146. Wagenseil, J.E., et al., *One-dimensional viscoelastic behavior of fibroblast populated collagen matrices.* J Biomech Eng, 2003. **125**(5): p. 719-25.

147. Gusic, R.J., et al., *Mechanical properties of native and ex vivo remodeled porcine saphenous veins.* J Biomech, 2005. **38**(9): p. 1770-9.

148. Roy, S., P. Silacci, and N. Stergiopulos, *Biomechanical properties of decellularized porcine common carotid arteries.* Am J Physiol Heart Circ Physiol, 2005. **289**(4): p. H1567-76.

149. Coulson, R.J., et al., *Effects of ischemia and myogenic activity on active and passive mechanical properties of rat cerebral arteries.* Am J Physiol Heart Circ Physiol, 2002. **283**(6): p. H2268-75.

150. Kinchen, K.S., et al., *Factors associated with women's decisions to seek treatment for urinary incontinence.* J Womens Health (Larchmt), 2003. **12**(7): p. 687-98.

151. Parente, M.P., et al., *Deformation of the pelvic floor muscles during a vaginal delivery.* Int Urogynecol J Pelvic Floor Dysfunct, 2007.

152. Brant, A.M., *Hemodynamics and mass transfer aspects of arterial disease*, in *Bioengineering*. 1986, University of Pittsburgh: Pittsburgh. p. 300.

153. Thomas, G.B.a.J.H.L.V., *Chapter 3. Assessing and Presenting Experimental Data*, in *Mechanical Measurements*. 1995, Addison-Wesley Publishing Co.: Reading, MA. p. 45-98.

154. College, S.C. [cited; Available from: http://www.shelfieldpeonline.co.uk/html/motor_units_and_motor_neurone_.html.

155. Freschi, J.E., A.G. Parfitt, and W.G. Shain, *Electrophysiology and pharmacology of striated muscle fibres cultured from dissociated neonatal rat pineal glands.* J Physiol, 1979. **293**: p. 1-10.

156. von Heyden, B., et al., *Response of guinea pig smooth and striated urethral sphincter to cromakalim, prazosin, nifedipine, nitroprusside, and electrical stimulation.* Neurourol Urodyn, 1995. **14**(2): p. 153-68.